

THE POZZOLANIC REACTION OF
MECHANICALLY TREATED COAL BOTTOM
ASH IN A CEMENTITIOUS ENVIRONMENT
OF SELF-COMPACTING CONCRETE



MOHAMMAD ISMAIL YOUSEF ALBIAJAWI

اونيفورسيتي مليسيا قهغ السلطان عبدالله
UNIVERSITI MALAYSIA PAHANG
AL-SULTAN ABDULLAH

DOCTOR OF PHILOSOPHY

UNIVERSITI MALAYSIA PAHANG
AL-SULTAN ABDULLAH

UNIVERSITI MALAYSIA PAHANG AL-SULTAN ABDULLAH

DECLARATION OF THESIS AND COPYRIGHT

Author's Full Name : MOHAMMAD ISMAIL YOUSEF ALBIAJAWI

Date of Birth : 14/1/1994

Title : THE POZZOLANIC REACTION OF MECHANICALLY TREATED COAL BOTTOM ASH IN A CEMENTITIOUS ENVIRONMENT OF SELF-COMPACTING CONCRETE

Academic Session : SEMESTER II 2023/2024

I declare that this thesis is classified as:

- CONFIDENTIAL (Contains confidential information under the Official Secret Act 1997)*
- RESTRICTED (Contains restricted information as specified by the organization where research was done)*
- OPEN ACCESS I agree that my thesis to be published as online open access (Full Text)

I acknowledge that Universiti Malaysia Pahang Al-Sultan Abdullah reserves the following rights:

1. The Thesis is the Property of Universiti Malaysia Pahang Al-Sultan Abdullah
2. The Library of Universiti Malaysia Pahang Al-Sultan Abdullah has the right to make copies of the thesis for the purpose of research only.
3. The Library has the right to make copies of the thesis for academic exchange.

Certified by:

Mohammad

(Student's Signature)



(Supervisor's Signature)

TS. DR. RAHIMAH BINTI EMBONG

New IC/Passport Number

Date: 22 / 7 / 2024

Name of Supervisor

Date: 01 August 2024

NOTE : * If the thesis is CONFIDENTIAL or RESTRICTED, please attach a thesis declaration letter.



اونيورسيتي مليسيا قهغ السلطان عبد الله
UNIVERSITI MALAYSIA PAHANG
AL-SULTAN ABDULLAH

SUPERVISOR'S DECLARATION

I hereby declare that I have checked this thesis and in my opinion, this thesis is adequate in terms of scope and quality for the award of the degree of Doctor of Philosophy.

(Supervisor's Signature)

Full Name : TS. DR. RAHIMAH BINTI EMBONG
Position : Senior Lecturer
Date : 01 August 2024



اونيورسيتي مليسيا قهغ السلطان عبد الله
UNIVERSITI MALAYSIA PAHANG
AL-SULTAN ABDULLAH

(Co-supervisor's Signature)

Full Name : TS. DR. KHAIRUNISA BINTI MUTHUSAMY
Position : Associate Professor
Date : 01 August 2024



STUDENT'S DECLARATION

I hereby declare that the work in this thesis is based on my original work except for quotations and citations which have been duly acknowledged. I also declare that it has not been previously or concurrently submitted for any other degree at Universiti Malaysia Pahang Al-Sultan Abdullah or any other institutions.

Mohammad

(Student's Signature)

Full Name : MOHAMMAD ISMAIL YOUSEF ALBIAJAWI
ID Number : PAH20001
Date : 22/7/2024



اونيورسيتي مليسيا قهغ السلطان عبدالله
UNIVERSITI MALAYSIA PAHANG
AL-SULTAN ABDULLAH

THE POZZOLANIC REACTION OF MECHANICALLY TREATED COAL
BOTTOM ASH IN A CEMENTITIOUS ENVIRONMENT OF SELF-
COMPACTING CONCRETE

MOHAMMAD ISMAIL YOUSEF ALBIAJAWI



Thesis submitted in fulfillment of the requirements

for the award of the degree of

Doctor of Philosophy

اونيورسيتي مليسيا فاهم السلطان عبدالله
UNIVERSITI MALAYSIA PAHANG
AL-SULTAN ABDULLAH

Faculty of Civil Engineering Technology

UNIVERSITI MALAYSIA PAHANG AL-SULTAN ABDULLAH

AUGUST 2024

ACKNOWLEDGEMENTS

Gratefulness is expressed to Allah, the Almighty, for bestowing His favour upon the accomplishment of this study endeavor. I express gratitude to the divine for endowing me with a sound physical state, robustness, and aptitude to successfully complete the composition of my thesis. Without the benevolence of His favour, this study project will not come to fruition. Furthermore, I express my utmost gratitude to the revered Blessed Prophet Muhammad (Peace be upon him).

Initially, I would want to convey my sincere appreciation to my supervisor, Ts. Dr. Rahimah Embong, for granting me the chance to pursue my PhD under her guidance and for providing me with assistance during the duration of my studies. She offered me insightful ideas and recommendations. I am very grateful to her for always motivating me to publish my research in journals with high impact factors, so enhancing the quality of my study. I would like to extend my heartfelt appreciation to my co-supervisor Prof. Madya Ts. Dr. Khairunisa binti Muthusamy for her invaluable expertise and guidance, which has been instrumental in supporting and inspiring me throughout my study.

Additionally, I would like to extend my sincere appreciation to all my family supporters, particularly to the parents who gave me life, bestowed upon me boundless affection and care, and wholeheartedly encouraged and supported the road I have chosen with unwavering optimism. All my family provides invaluable assistance and affection, which has been crucial in helping me navigate the most challenging period of my life. Additionally, they have provided me with unlimited financial support during my whole academic journey.

Finally, I would like to express my gratitude to UMPSA for awarding me the scholarship, which greatly facilitated the successful completion of my PhD programme. I really appreciate the assistance provided by laboratory staff and faculty members of civil engineering technology in granting me full access to the resources in the civil engineering laboratory.

ABSTRAK

Penggunaan bahan buangan industri seperti abu dasar arang batu (CBA) dalam penghasilan konkrit merupakan alternatif ekologi yang boleh digunakan sebagai sumber utama dalam industri pembinaan. Disebabkan oleh faktor ekonomi dan alam sekitar daripada penghasilan CBA, para penyelidik semakin berminat menjalankan kajian menggunakan sisa industri untuk digunapakai sebagai bahan binaan baharu seperti penggunaan CBA dalam konkrit pemampatan sendiri (SCC). Kebanyakan kajian membincangkan penggunaan CBA sebagai agregat halus dalam konkrit, namun begitu, hasil kajian penggunaan CBA sebagai bahan gantian simen dalam SCC adalah terhad. Sejajar dengan itu, kajian ini dijalankan bagi menilai keberkesanan penggunaan CBA dengan pelbagai nisbah sebagai bahan gantian simen dalam penghasilan SCC. Di antara ciri unik CBA sebagai salah satu produk sampingan industri adalah ianya mempunyai sifat pozzolanik yang tinggi untuk digunakan sebagai bahan gantian separa kepada simen dalam SCC. Oleh itu, kajian ini bertujuan untuk mengkaji kesan CBA sebagai bahan gantian separa bagi simen terhadap sifat-sifat SCC. Kandungan CBA yang digunakan dalam kajian ini sebagai bahan gantian separa bagi simen adalah sebanyak 10% hingga 50%. Manakala bahan SCC lain (iaitu air, agregat kasar, agregat halus dan kandungan super-plasticizer) dikekalkan malar dalam semua campuran SCC. Tujuan kajian ini adalah untuk menilai sifat fizikal, kimia, dan mikrostruktur CBA yang dirawat secara mekanikal sebagai bahan pozzolanik untuk menentukan kesesuaian penggunaannya dalam penghasilan SCC. Pengaruh sifat pozzolanik CBA dengan saiz yang berbeza (3000, 5000, 7000 kitaran) dinilai melalui analisis termogravimetrik (TGA), indeks aktiviti kekuatan (SAI), ujian Chapelle dan ujian Frattini. Melalui ujian tersebut, saiz CBA yang optimum dengan prestasi yang lebih baik telah digunakan untuk menyediakan campuran SCC. Tambahan pula, CBA juga telah diuji terhadap sifat segar SCC yang mengandungi CBA melalui Flow slump, L-Box, V-funnel, J-Ring, dan dibandingkan dengan SCC tanpa kandungan CBA. Pengaruh SCC yang mengandungi CBA terhadap sifat mekanikal seperti kekuatan mampatan, halaju nadi ultrasonik (UPV), kekuatan lentur dan kekuatan tegangan telah dikaji selepas 7, 14, 28, 56, 90, dan 180 hari pengawetan berbanding kepada SCC tanpa kandungan CBA. Selain itu, sifat ketahanan SCC seperti penyerapan air, rintangan asid, dan rintangan sulfat juga telah dikaji untuk menentukan ketahanan SCC. Ujikaji kesan SCC yang mengandungi CBA juga telah dijalankan terhadap pelbagai ujian bersuhu tinggi. Dapatan kajian ini mendapati nilai optimum sebanyak 20% CBA sebagai bahan gantian bagi simen menunjukkan peningkatan ketara terhadap sifat segar dan mekanikal SCC berbanding dengan SCC kawalan pada tempoh pengawetan selepas 28 hari. Walau bagaimanapun, penggunaan CBA dalam menambahbaik ciri-ciri spesimen SCC adalah disebabkan oleh kesan pozzolanik dan jumlah silika CBA dapat dikesan terutamanya semasa tempoh pengawetan selepas 28 hari. Sebaliknya, untuk sifat ketahanan, CBA mempamerkan penyerapan air yang lebih tinggi disebabkan oleh liang dan lompong yang tinggi berbanding dengan sampel kawalan SCC. Dari segi asid, specimen SCC yang mengandungi CBA mengalami lebih banyak kemerosotan berbanding dengan sampel kawalan SCC setelah direndam dalam larutan asid sulfurik. Dari segi rintangan sulfat, hasil kajian menunjukkan bahawa kandungan CBA sebanyak 10% dalam SCC mempamerkan ketahanan yang lebih baik apabila terdedah kepada larutan sulfat. SCC yang mempunyai kandungan CBA sebanyak 10% juga menunjukkan rintangan yang lebih baik apabila terdedah kepada suhu tinggi. Kesimpulannya, kajian ini telah berjaya dilaksanakan dengan penilaian dan penghasilan SCC yang mesra alam dengan campuran CBA yang boleh membawa kelebihan kepada persekitaran dan menggalakkan amalan bangunan mampan.

ABSTRACT

The use of industrial waste such as coal bottom ash (CBA) in the production of concrete is an ecological alternative would be able to minimize the amount of main resources consumed in the construction industry and reduce CBA waste disposal. Due to the economic and environmental benefits of CBA, the attention of researchers has taken to use of industrial waste to introduce new building materials such as CBA in self-compacting concrete (SCC). Most of the literature discussed the utilization of CBA as fine aggregate in concrete but using ground CBA as cement replacement in SCC has not been investigated yet. Furthermore, this study is to use ground CBA with various replacements ratios for cement in the production of SCC. Unique characteristic of CBA as one of the industrial by-products that has high pozzolanic properties, which is highly recommended to be used as partial cement replacement in SCC. Therefore, this study aims to investigate the effect of ground CBA as partial cement replacement on the properties of SCC. The ground CBA was used as partial replacement of cement from 10% to 50%. While other SCC materials (water, coarse aggregate, fine aggregate, and super-plasticizer content) were kept constant in all SCC mixes. First, this study aims to evaluate the physical, chemical, and microstructural properties of mechanically treated CBA as pozzolanic materials to determine its suitability for use in the production of SCC. Thereafter, the influence of pozzolanic properties of different sizes by various grinding cycles (3000, 5000, 7000 cycles) of ground CBA is investigated by thermogravimetric analysis (TGA), strength activity index (SAI), Chapelle test and Frattini test. After that, the optimum grinding size with better performance has been used to prepare the SCC mixture. Furthermore, the ground CBA was tested in the fresh properties of SCC containing CBA such as Flow slump, L-Box, V-funnel, J-Ring, and compared to SCC without ground CBA in the mixture. Then, the influence of SCC containing ground CBA on the mechanical properties such as the compressive strength, ultrasonic pulse velocity (UPV), flexural strength and tensile strength were conducted after 7, 14, 28, 56, 90, and 180 days of curing compared to SCC without ground CBA in the mixture. Other than that, the durability properties of SCC such as water absorption, acid resistance, and sulphate resistance were conducted to determine the durability of SCC. Apart from that, the effect of SCC containing ground CBA subjected to various elevated temperature test was conducted. The findings of this study were found up to CBA 20% the optimum as cement replacement that observed significant improvements in fresh and mechanical properties of SCC compared to those of control SCC at later curing ages after 28 days. However, the inclusion of ground CBA improves the characteristics of the SCC specimens due to the pozzolanic impact of the siliceous nature of ground CBA, particularly during the later curing ages after 28 days. On the other hand, For the durability properties incorporation ground CBA exhibiting to higher water absorption due to high porous and void compared to SCC control samples. In terms of acid the SCC specimens containing ground CBA experience more deterioration as compared to control SCC after immersed in sulfuric acid solution. In terms of sulphate resistance showed that ground CBA10% of SCC exhibited better durability when exposed to sulphate solution. SCC containing ground CBA10% also exhibits better resistance upon subjected to elevated temperature. From this study, achieving success in the production of eco-friendly SCC with ground CBA could lead to a more pristine environment and promote sustainable building practices.

TABLE OF CONTENT

DECLARATION	
TITLE PAGE	
ACKNOWLEDGEMENTS	ii
ABSTRAK	iii
ABSTRACT	iv
TABLE OF CONTENT	v
LIST OF TABLES	xi
LIST OF FIGURES	xii
LIST OF SYMBOLS	xviii
LIST OF ABBREVIATIONS	xxi
CHAPTER 1 INTRODUCTION	1
1.1 Background of Study	1
1.2 Problem Statement	4
1.3 Objectives of the Research	7
1.4 Scope of the Research	7
1.5 Significance of Research	10
1.6 Thesis Outline	11
CHAPTER 2 LITERATURE REVIEW	13
2.1 Introduction	13
2.2 Self-Compacting Concrete (SCC)	13
2.2.1 Background	13
2.2.2 Advantages and Disadvantages of SCC	16
2.2.3 Mixture design of SCC	17
2.2.4 Application of SCC	20

2.3	Coal Bottom Ash (CBA)	22
2.3.1	Background	22
2.3.2	Production of CBA	24
2.3.3	Environmental Issues of CBA	26
2.3.4	Pre-Treatment of CBA	27
2.3.5	Properties of Coal Bottom Ash (CBA)	35
2.3.6	Microstructure	42
2.3.7	Utilization of CBA in Concrete	47
2.4	Properties of Concrete Containing CBA in SCC	51
2.4.1	Fresh Properties of SCC Incorporating CBA	51
2.4.2	Mechanical Properties of SCC Incorporating CBA	57
2.4.3	Durability Properties	67
2.4.4	Elevated Temperatures	74
2.5	Summary of Research Gap	76
CHAPTER 3 METHODOLOGY		82
3.1	Introduction	82
3.2	Flow-Chart of Experimental Work	83
3.3	Materials Preparation	84
3.3.1	Tap Water	84
3.3.2	Ordinary Portland Cement (OPC)	84
3.3.3	Coal bottom ash (CBA)	86
3.3.4	Fine Aggregate	87
3.3.5	Coarse Aggregate	88
3.3.6	Superplasticizer (SP)	88
3.4	Characteristics and Testing of Materials used in SCC	90

3.4.1	Sieve Analysis Test	90
3.4.2	Particles Size Analysis	90
3.4.3	Moisture Content of Aggregate and CBA	91
3.4.4	Fineness Modulus (FM) of Aggregates and CBA	92
3.4.5	Absorption and Specific Gravity of CBA and SCC Ingredient	93
3.5	Experimental program	93
3.5.1	Designing of Mix for SCC	94
3.5.2	Preparation and Casting of Samples	95
3.5.3	Curing Method for the Samples	97
3.5.4	Mechanical Grinding Process for CBA	98
3.6	Testing of samples	99
3.6.1	Fresh Properties of SCC	99
3.6.2	Mechanical Properties of SCC	104
3.6.3	Durability Properties	108
3.6.4	Microstructural Properties	112
3.6.5	Pozzolanic Properties Test	119
3.6.6	Elevated Temperature	124
3.7	Statistical Analysis for the Results	125
3.8	Summary	126
 CHAPTER 4 PHYSICAL, CHEMICAL, MICROSTRUCTURE AND POZZOLANIC CHARACTERISTICS OF CBA		127
4.1	Introduction	127
4.2	Properties and Characterization of CBA as Supplementary Cementitious Materials	127
4.2.1	Physical Properties of Original CBA and Ground CBA with Various sizes Compared to Cement	127

4.2.2	Chemical Oxides Composition of Original CBA and CBA with Various Sizes Compared to Cement	129
4.2.3	Microstructural Characteristics of Original CBA and Ground CBA with Various sizes Compared to Cement	132
4.2.4	Pozzolanic Characteristics of Original CBA and Ground CBA Compared to Cement	142
4.3	Statistical Analysis Pearson Correlation Analysis	153
4.4	Summary of Key Findings	155

CHAPTER 5 FRESH, MECHANICAL, DURABILITY, AND ELEVATED TEMPERATURE PROPERTIES OF COAL BOTTOM ASH IN SELF COMPACTING CONCRETE **158**

5.1	Introduction	158
5.2	Fresh Properties of Optimum Mechanically Treated Ground CBA Based on SCC	159
5.2.1	Slump Flow of Optimum Mechanically Treated Ground CBA Based on SCC	159
5.2.2	L-Box of Optimum Mechanically Treated Ground CBA Based on SCC	161
5.2.3	V-Funnel of Optimum Mechanically Treated Ground CBA Based on SCC	162
5.2.4	J-Ring of Optimum Mechanically Treated Ground CBA Based on SCC	163
5.3	Mechanical Properties of Optimum Mechanically Treated Ground CBA Based on SCC	165
5.3.1	Compressive Strength of Optimum Mechanically Treated Ground CBA Based on SCC	165
5.3.2	Flexural Strength of Optimum Mechanically Treated Ground CBA Based on SCC	168

5.3.3	Splitting Tensile Strength of Optimum Mechanically Treated Ground CBA Based on SCC	170
5.3.4	Ultrasonic Pulse Velocity of Optimum Mechanically Treated Ground CBA Based on SCC	173
5.4	Co-Relationships Between Mechanical Properties of Self-Compacting Concrete	175
5.5	Thermogravimetry Analysis (TGA) on Cement Pastes Samples and optimum mechanically treated Ground CBA	183
5.6	FESEM of Hardened SCC Samples and those made of optimum mechanically treated Ground CBA (ITZ)	186
5.7	Durability Properties of optimum mechanically treated Ground CBA Based on SCC	188
5.7.1	Water Absorption of optimum mechanically treated Ground CBA Based on SCC	189
5.7.2	Acid Resistance of Optimum Mechanically Treated Ground CBA SCC	192
5.7.3	Sulphate Resistance of optimum mechanically treated Ground CBA Based on SCC	199
5.8	Elevated Temperature of Optimum Mechanically Treated Ground CBA Based on SCC	206
5.8.1	Visual Observations	206
5.8.2	Mass Loss	209
5.8.3	Strength loss	211
5.9	Summary of Key Findings	213
CHAPTER 6		215
CONCLUSION AND RECOMMENDATIONS		215
6.1	Introduction	215

6.2	Conclusions	215
6.2.1	Characteristics of Ground CBA in Physical and Chemical and Microstructure Properties as Pozzolanic Materials	215
6.2.2	Pozzolanic Characteristics of Ground CBA in Cementitious Composite Particles as Pozzolanic Materials	216
6.2.3	Fresh and Mechanical Properties of Optimum Mechanically Treated Ground CBA Based on SCC	217
6.2.4	Durability Properties of SCC Containing Ground CBA and Subjected to Elevated Temperatures	217
6.3	Recommendations For Future Studies	218
	REFERENCES	219
	LIST OF PUBLICATIONS	249
	AWARDS	251
	APPENDICES	252
	APPENDIX A: NUMBER OF SAMPLES USED IN THE EXPERIMENTAL WORK	253
	APPENDIX B: STRENGTH ACTIVITY INDEX FOR VARIOUS SIZES OF GROUND CBA	254
	APPENDIX C: MICROSTRUCTURE IMAGES FOR SCC CONTROL AND SCC WITH VARIOUS RATIOS OF GROUND CBA	257



اونيورسيتي مليسيا قهغ السلطان عبدالله
UNIVERSITI MALAYSIA PAHANG
AL-SULTAN ABDULLAH

LIST OF TABLES

Table 1.1	Stages of the experimental work of this study	9
Table 2.1	Recommended values of SCC fresh properties	18
Table 2.2	Presents an overview of the various mixture design methods for SCC that have been reported in previous studies.	19
Table 2.3	CBA production in various countries	26
Table 2.4	Summary of chemical pre-treatment of materials in mortar and concrete	30
Table 2.5	Summary of mechanical pre-treatment of CBA in mortar and concrete	33
Table 2.6	Physical characteristics of CBA	37
Table 2.7	Chemical composition properties of CBA	40
Table 2.8	Fresh properties of SCC containing CBA as sand replacement reported by previous researchers	51
Table 2.9	Summary of mechanical properties of CBA as sand replacement in SCC mixe	59
Table 2.10	Effect of CBA as a cement replacement on the UPV of concrete	66
Table 2.11	Summarized of the research gap as reported by several researchers	77
Table 3.1	Chemical composition of cement (OPC)	85
Table 3.2	Physical properties of cement (OPC)	85
Table 3.3	Particle size distribution and physical properties of fine aggregate	87
Table 3.4	Particle size distribution and physical properties of coarse aggregat	88
Table 3.5	Characteristics of SP brand Sika Visco Crete -2044	89
Table 3.6	Moisture content (%) of the materials used in the experimental wor	92
Table 3.7	Fineness modulus of the materials used in the experimental work	92
Table 3.8	Absorption and specific gravity of the materials used in the experimental work	93
Table 3.9	Mixture design proportion for 1 m ³ SCC mixture in (kg/m ³)	95
Table 3.10	Categories of fresh properties for SCC in accordance with (EFNARC, 2005) standard.	100
Table 4.1	Physical properties of cement, original CBA and ground CBA with various grinding sizes	129
Table 4.2	Chemical composition in oxide content (%) of cement, original CBA and CBA with various grinding sizes	131
Table 4.3	Pearson correlation analysis for various grinding sizes in comparison to Original CBA	154

LIST OF FIGURES

Figure 1.1	Cement production in Malaysia from 2014 to 2023	5
Figure 2.1	Benefits of use application of SCC	16
Figure 2.2	CBA industry waste. (a) waste of CBA in the landfill (b) Process of clean CBA in the landfill	24
Figure 2.3	The exemplary thermal power plant of coal-fired	25
Figure 2.4	Coal ash waste impact on the earth, water, and groundwater resources	27
Figure 2.5	CBA collected from thermal power plant was classified as A1) and A2) Original CBA and A3), A4) various sizes after grinding process	36
Figure 2.6	A1 and A2 SEM images of grinding CBA and dried before used, B1 and B2 CBA after used in mortar and concrete with magnification 1000x	43
Figure 2.7	SEM images CBA shape grinded and dried before curing	45
Figure 2.8	Samples contain CBA in concrete after hydration and curing 28 days	45
Figure 2.9	FESEM images for CBA with magnification range up to 20 μm	46
Figure 2.10	SEM photomicrographs for CBA categories	47
Figure 2.11	XRD for CBA element composition	47
Figure 2.12	Compressive strength of CBA in concrete at various curing period	49
Figure 2.13	Summary of advantages and disadvantages of CBA in concrete application as investigated by researchers	51
Figure 2.14	Variation of slump values in SCC with varying CBA substitution ratios for sand	54
Figure 2.15	L-box values' variation in SCC using varying CBA replacement ratios for sand	56
Figure 2.16	The samples' compressive strength with varying replacement percentages for aggregate with CBA in SCC	63
Figure 2.17	Flexural strength of samples with various replacement for fine aggregate ratios of in SCC at different curing ages	64
Figure 2.18	CBA samples' splitting tensile strength with varying replacement percentages of fine aggregate in SCC at different curing ages	65
Figure 2.19	Percentage of loss by weight of CBA in concrete mixes at various curing ages	70
Figure 2.20	Influence of the Sulfuric acid of concrete samples at 7 days and 28days	70
Figure 2.21	Weight loss when used CBA as partial cement replacement and immersed in sulfate for various curing	72

Figure 2.22	Variation of water absorption with different percentages of CBA	73
Figure 3.1	Flow chart of research methodology	83
Figure 3.2	Cement binder used in this experimental study	85
Figure 3.3	Particles of CBA a) Original CBA, b) Micro-fine ground CBA	86
Figure 3.4	Fine aggregate used in this experimental work	87
Figure 3.5	Coarse aggregate used in this experimental work	88
Figure 3.6	SP used in the experimental work for SCC mixture production a) is the total SP collect for experimental work b) SP amount used in each mix	89
Figure 3.7	Sieve shaker apparatus to sieve particles of CBA and ingredient of SCC	90
Figure 3.8	Particle Size instrument (Malvern Hydro 2000MU)	91
Figure 3.9	Preparation of the SCC specimens at the laboratory (a Materials for mixing, b) concrete inside drum mixer, c) concrete after put in cubes moulds, and c) concrete after put in beam moulds	96
Figure 3.10	Preparation process for SCC samples containing micro fine CBA	97
Figure 3.11	Curing method for the SCC samples a) all samples for experimental work (b Prism samples for flexural strength	98
Figure 3.12	Mechanical grinding process for original CBA to micro-fine ground CBA to be used in SCC	99
Figure 3.13	Slump flow test apparatus (a test flow SCC b) Slump flow apparatus	101
Figure 3.14	Apparatus of the L-box test (a L-box flow test b) L-box apparatus	102
Figure 3.15	V-funnel test apparatus a) V-funnel flow test b) V-funnel apparatus	103
Figure 3.16	J-Ring test apparatus a) J-Ring flow test b) J-Ring apparatus	103
Figure 3.17	Automatic compressive strength machine	104
Figure 3.18	Automatic Splitting tensile strength machine	105
Figure 3.19	Flexural strength test machine	106
Figure 3.20	UPV device used in the experimental study	107
Figure 3.21	Electric oven used for water absorption in this experimental work	109
Figure 3.22	Sulphuric acid preparation and samples immered in acidic solution	110
Figure 3.23	Sodium sulphate preparation and samples immered sulphate solution	111
Figure 3.24	FESEM instrument used in this experimental work	112
Figure 3.25	XRF used in this experimental work	113
Figure 3.26	XRD instrument used in the present experimental work	114
Figure 3.27	BET instrument used in the present experimental work	115
Figure 3.28	SEM used in the present experimental work	116

Figure 3.29	TGA device used in the present experimental work	117
Figure 3.30	FTIR device used in this experimental work	118
Figure 3.31	EDX device used in the present experimental work	119
Figure 3.32	Experimental process of the Chapelle test for CBA to check the pozzolanic reactivity	121
Figure 3.33	Graphical process of the Frattini test to check the pozzolanic reactivity of CBA	122
Figure 3.34	Preparation process and filtration for various samples	123
Figure 3.35	Determination of $[\text{OH}^-]$ and $[\text{Ca}]^{+2}$ concentration	123
Figure 3.36	Samples exposure to elevated temperature in the electric furnace	125
Figure 4.1	Particle size distribution of cement, original CBA and ground CBA with various grinding sizes	129
Figure 4.2	XRD Diffractogram pattern of cement OPC binder	133
Figure 4.3	XRD Diffractogram analysis result for raw CBA, CBA-3000, CBA-5000, and CBA-7000	134
Figure 4.4	SEM morphology of cement at low and high magnification 1000x and 5000x	135
Figure 4.5	Scanning electron microscope (SEM) with Energy Dispersive X-ray (EDX) images with magnification of 1000x for (a)Original CBA, (b) CBA-3000, (c) CBA-5000, (d) CBA-7000	137
Figure 4.6	Fourier-Transform Infrared Spectroscopy (FTIR) analysis for cement	138
Figure 4.7	Fourier-Transform Infrared Spectroscopy (FTIR) results analysis for original CBA and ground CBA (CBA-3000, CBA-5000, CBA-7000)	140
Figure 4.8	Thermogravimetric (TGA) analysis result for Cement OPC binder	141
Figure 4.9	Thermogravimetric (TGA) analysis result for original CBA, CBA-3000, CBA-5000, and CBA-7000	142
Figure 4.10	Pozzolanic activity of ground CBA with various sizes using Chapelle test	144
Figure 4.11	Results of the Frattini test for control and various sizes of ground CBA samples at 8 days	146
Figure 4.12	Results of the Frattini test for control and various sizes of ground CBA samples at 15 days	147
Figure 4.13	Compressive strength results of CBA-3000 as cement replacement in mortar mixture	150
Figure 4.14	Compressive strength results of CBA-5000 as cement replacement in mortar mixture	151
Figure 4.15	Compressive strength results of CBA-7000 as cement replacement in mortar mixture	152

Figure 5.1	Slump flow of SCC mixes containing different replacement levels of ground CBA	160
Figure 5.2	L-box of SCC mix containing different replacement levels of ground CBA	162
Figure 5.3	V-Funnel of SCC mix containing different replacement levels of ground CBA	163
Figure 5.4	J-Ring of SCC mix containing different replacement levels of ground CBA	165
Figure 5.5	Compressive strength results of SCC containing ground CBA-7000 with various replacement ratios at different curing ages	168
Figure 5.6	Flexural strength results of SCC containing ground CBA-7000 with various replacement ratios at different curing ages	170
Figure 5.7	Splitting tensile strength results of SCC containing ground CBA-7000 with various replacement ratios at different curing ages	172
Figure 5.8	Failure occurs through coarse aggregate of SCC mixes containing ground CBA with various replacement ratios	173
Figure 5.9	UPV results of SCC containing ground CBA-7000 with various replacement ratios at different curing ages	174
Figure 5.10	Co-relation compressive strength vs flexural strength of SCC containing ground CBA at 7 days	176
Figure 5.11	Co-relation compressive strength vs flexural strength of SCC containing ground CBA at 180 day	176
Figure 5.12	Co-relation Compressive strength vs Tensile strength of SCC containing ground CBA at 7 days	177
Figure 5.13	Co-relation Compressive strength vs Tensile strength of SCC containing ground CBA at 180 days	177
Figure 5.14	Co-relation Compressive strength vs UPV of SCC containing ground CBA at 7 days	178
Figure 5.15	Co-relation Compressive strength vs UPV of SCC containing ground CBA at 180 days	179
Figure 5.16	Co-relation Flexural strength vs UPV of SCC containing ground CBA at 7 days	180
Figure 5.17	Co-relation Flexural strength vs UPV of SCC containing ground CBA at 180 days	180
Figure 5.18	Co-relation Flexural strength vs Tensile strength of SCC containing ground CBA at 7 days	181
Figure 5.19	Co-relation Flexural strength vs Tensile strength of SCC containing ground CBA at 180 days	181
Figure 5.20	Co-relation UPV vs Tensile strength of of SCC containing ground CBA at 7 days	182

Figure 5.21	Co-relation UPV vs Tensile strength of SCC containing ground CBA at 180 days	183
Figure 5.22	Thermogravimetry analysis at 7 days for control cement paste and those contained various replacement ratios of ground CBA	184
Figure 5.23	Thermogravimetric analysis at 28 days for control cement paste and those contained various replacement ratios of ground CBA	185
Figure 5.24	Thermogravimetry analysis at 56 days for control cement paste and those contained various replacement ratios of ground CBA	186
Figure 5.25	FESEM micrographs of SCC specimens at a) 7 days, b) 28 days, and c)56 days for control and ground CBA 10%, 20%, 50 % of SCC samples at X5000 magnification	188
Figure 5.26	Water absorption ratio results of ground CBA with various replacement ratios at different curing ages	191
Figure 5.27	FESEM images of a) control, b) ground CBA 10%, c) ground CBA20%, and d) ground CBA50% in SCC at 3000x magnification	191
Figure 5.28	SCC specimens containing CBA after being immersed in (H ₂ SO ₄) solution for 7 days	193
Figure 5.29	SCC specimens containing CBA after being immersed in (H ₂ SO ₄) solution for 28 days.	194
Figure 5.30	SCC specimens containing CBA after being immersed in (H ₂ SO ₄) solution for 56 days.	194
Figure 5.31	SCC specimens containing CBA after being immersed in (H ₂ SO ₄) solution for 90 days	195
Figure 5.32	Mass loss of SCC containing ground CBA as cement replacement immersed in H ₂ SO ₄ for various curing ages	197
Figure 5.33	Strength deterioration of SCC containing ground CBA as cement replacement immersed in H ₂ SO ₄ for various curing ages	199
Figure 5.34	SCC specimens containing CBA after being immersed in Sodium sulphate (Na ₂ SO ₄) solution for 7 days.	201
Figure 5.35	SCC specimens containing CBA after being immersed in Sodium sulphate (Na ₂ SO ₄) solution for 28 days	201
Figure 5.36	SCC specimens containing CBA after being immersed in Sodium sulphate (Na ₂ SO ₄) solution for 56 days	201
Figure 5.37	SCC specimens containing CBA after being immersed in Sodium sulphate (Na ₂ SO ₄) solution for 90 days	202
Figure 5.38	Mass loss of SCC containing ground CBA as cement replacement immersed in Na ₂ SO ₄ for various curing ages	204
Figure 5.39	Strength deterioration of SCC containing ground CBA as cement replacement immersed in Na ₂ SO ₄ for various curing ages	206
Figure 5.40	Visual observation for surface texture of the SCC specimens exposed to 200°C.	208

Figure 5.41	Visual observation for surface texture of the SCC specimens exposed to 400°C.	208
Figure 5.42	Visual observation for surface texture of the SCC specimens exposed to 600°C	209
Figure 5.43	Visual observation for surface texture of the SCC specimens exposed to 800°C	209
Figure 5.44	Mass loss of SCC specimens containing ground CBA and control exposed to elevated temperatures	211
Figure 5.45	Effect of temperature towards strength loss of SCC containing ground CBA when subjected to elevated temperature	212

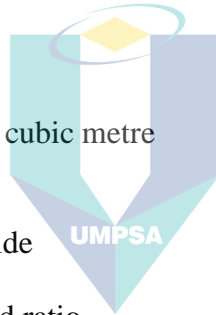


اونيورسيتي مليسيا قهغ السلطان عبدالله
UNIVERSITI MALAYSIA PAHANG
AL-SULTAN ABDULLAH

LIST OF SYMBOLS

A	Mass of SSD sample in air
Al ₂ O ₃	Aluminium oxide
Al	Aluminum
Al ₆ Si ₂ O ₁₃	Mullite
B	Mass of basket in water containing saturated aggregate sample
C ₃ A	Tricalcium aluminate
C	Carbon
Ca	Calcium
C ₂ S	Dicalcium silicate
C ₄ AF	Tetracalcium aluminoferrite
CBA-3000	Mechanical pretreatment for prepare CBA with 3000 cycle grinding
CBA-5000,	Mechanical pretreatment for prepare CBA with 5000 cycle grinding
CBA-7000	Mechanical pretreatment for prepare CBA with 7000 cycle grinding
CBA10%	Replacement ratio for ground CBA 10% for cement
CBA20%	Replacement ratio for ground CBA 20% for cement
CBA30%	Replacement ratio for ground CBA 30% for cement
CBA40%	Replacement ratio for ground CBA 40% for cement
CBA50%	Replacement ratio for ground CBA 50% for cement
C-O	Carbon–oxygen bond
cm ³ /g	Cubic centimetre per gram
cm ⁻¹	Reciprocal centimetre (or wavenumber)
C–H	Carbon–Hydrogen bond
CaO	Calcium Oxide
CaCl ₂	Calcium Chloride
[Ca] ²⁺	Calcium Cation ions
C-H	Calcium Hydroxide
C-S-H	Calcium Silicate Hydrate
CH	Calcium Hydroxide or Portlandite
CO ₂	Carbon dioxide
C ₃ S	Tricalcium Silicate
Ca(OH) ₂	Calcium Hydroxide
d ₁ , d ₂	Lateral dimensions of the samples
D10	Diameter at which 10% of a sample's mass
D50	Diameter at which 50% of a sample's mass
D90	Diameter at which 90% of a sample's mass
D _{UPV}	Distance(km)
D	Design of cross-sectional dimension
d	Mass of the oven-dried aggregate in air
EDTA	Ethylenediaminetetraacetic acid
ft	Feet
Fe	Iron
Fe-S	Iron(II) Sulfide or Iron-Sulfur bond
Fe-O	Iron(II) oxide

F_{wc}	Average compressive strength of samples before exposure to elevated temperature
F_h	Average compressive strength of samples after exposure to elevated temperature
F_{t1}	Average compressive strength of SCC samples after curing in water at various ages of test
F_{t2}	Average compressive strength of SCC samples after immersion in acid or sulfate solution
FM	Fineness modulus
F_{ct}	Spilt tensile strength
g	Gram
F_{cf}	Flexural strength
g/L	Grams per liter
Fe_2O_3	Ferric oxide
H_2SO_4	Sulfuric acid
H-O-H	Hydrogen oxide bond
HCl	Hydrochloric acid
h_1	Vertical Section
h_2	Horizontal Section
HNO_3	Nitric Acid
H	Hight
H_2O	Water
Kg/m^3	Kilogram per cubic metre
K	Potassium
Km	Kilometre
K_2O	Pottasium oxide
kg	Kilogram
L/S	Liquid to solid ratio
L	length
mol/L	Moles per liter
m^2/g	Square meter per gram
m	meters
mm	Millimetre
M1	Weight of samples before heated
M2	Weight of samples after heated
mmol/l	Millimoles per litre
M_2	Weight of CBA in grams
M_3	Weight of CaO mixed with CBA in grams
M_4	Weight of CaO in the blank sample in grams
mL	Millilitre
m_1	Mass of specimens before immersion
m_2	Mass of specimens after immersion
m^2	Square meters
m^3	Cubic metre
Mn_2O_3	Manganese (III) oxide
mol	Molar concentration
M	Molar
MgO	Magnesium oxide
MPa	Megapascal
NO _x	Nitrous oxide



اونيورسيتي مليسيا فهغ السلطان
 UNIVERSITI MALAYSIA PAHANG
 AL-SULTAN ABDULLAH

N/mm ²	Newton/square millimetre
Na ₂ O	Sodium oxide
Na ₂ SO ₄	Sodium sulphate
NaCl	Sodium chloride
NaOH	Sodium hydroxide
O-H	Hydroxide
O	Oxygen
[OH] ⁻	Hydroxyl ions
P	Maximum load
P ₂ O ₅	Phosphorus pentoxide
PA	Passing ability
PM	Particulate matter
SG	Specific gravity
Si-C	Silicon carbide
Si-O-Si	Siloxanes or oxygen–silicon backbone
Si-O-Fe	Silicon dioxide or silicon- oxygen–Iron bond
Si-O	Silicon–oxygen bond
S-O	Sulphur-oxygen bond
Si	Silicon
SiO ₃	Silicates
SF	Slump flow
SO ₃	Sulphur trioxide
SP	Superplasticizer
SiO ₂	Silicon dioxide
s	Second
S	sulphur
t	Tonnes
TiO ₂	Titanium oxide
V	Velocity
V ₂	Amount of 0.1 M HCl consumed by the sample solution, measured in millilitres
V ₃	Amount of 0.1 M HCl consumed by the blank solution, measured in millilitres
VF	Viscosity Flow
W _{t1}	Weight of air-dried samples for the materials
W _{t2}	Weight of electric oven dried samples for the material
W _w	Weight of saturated specimen in water
W _d	Weight of specimen in dry condition after drying in the oven
w/b	Water to powder ratio
w/c	Water to cement ratio
ZnO	zinc oxide
µm	Micrometre
%	Percent
°C	Degree Celcius
&	And



اونيورسيتي مليسيا قهغ السلطان عبدالرحمن
 UNIVERSITI MALAYSIA PAHANG
 AL-SULTAN ABDULLAH

LIST OF ABBREVIATIONS

AAMs	Alkali-activated materials
ACI	American Concrete Institute
ASTM	American Society for Testing and Materials
BS EN	European standard
BET	Brunauer-Emmett-Teller
BS EN	British Standard European Norm
BJH	Barrett-Joyner-Halenda
CBA	Coal bottom ash
EFNARC	European Federation of Specialist Construction Chemicals and Concrete Systems
EDS	Energy Dispersion Spectroscopy
FA	Fly ash
FESEM	Field emission scanning electron microscopy analysis
FTIR	Fourier transform infrared
ITZ	Interfacial transition zone
i.e.	id est
KEV	Kapar Energy Ventures
LA	Los Angeles
LOI	Loss of ignition
MS EN	Malaysian Standard European Norm
NC	Normal Concrete
OPC	Ordinary Portland cement
SAI	Strength Activity Index
SBC	Sugarcane bagasse ash
SEM	Scanning Electron Microscope
SCC	Self-Compacting Concrete
SSD	Saturated surface dry
SPSS	Statistical Package for the Social Sciences
TGA	Thermogravimetric analysis
UPV	Ultrasonic pulse velocity
VSI	Visual stability index
XRD	X-Ray diffraction analysis
XRF	X-ray Fluorescence

CHAPTER 1

INTRODUCTION

1.1 Background of Study

Concrete is an essential component in the field of construction and is recognised as one of the most popular building materials for civil engineering structures on a worldwide basis. The prevalence of concrete can be attributed to the fact that it is not only cost effective, but also possesses adequate strength and serviceability throughout its anticipated design duration (Kumar & Singh, 2020). A new and innovative in construction is called self-compacting concrete (SCC). SCC is a unique type of concrete that represents an upgraded version of traditional concrete. The concept of SCC was introduced by Prof. Okamura in 1986 and further advanced by Ozawa, Maekawa, and their research team at the University of Tokyo in Japan. The primary objective of SCC is to improve the building quality and address the challenges associated with insufficient skilled labour (Maekawa & Ozawa, 1999; Okamura et al., 1993). Its development has signified a major technological improvement that has resulted to good quality concrete, improved productivity as well as enhanced on site working environment (Shetty & Jain, 2019). It may be described as a kind of concrete that can be easily poured and compacted by its own weight, with little or no need for vibration, and without separating or bleeding (Promsawat et al., 2020). Furthermore, using SCC offers several benefits, such as decreased construction time and labor expenses, elimination of mechanical vibrators to minimize consumption of energy and noise pollution, and enhanced filling ability for pouring into densely packed structures, ensuring optimal structural performance (Promsawat et al., 2020).

To be classified as effective, SCC must fulfil many different types of critical factors, including the ability to fill and pass, the strength of its anti-segregation ability, the volume stability of the material, and the mechanical properties required for durability. The properties of SCC in a fresh state are its most critical attributes. The properties and quality of the substances comprising SCC have a substantial influence on the final properties of SCC, including its strength, durability, and serviceability. The composition

of SCC involves the precise measurement of the various components such as ordinary portland cement (OPC), fine aggregate, coarse aggregate, water, and admixtures. To achieve the desired fresh concrete properties of SCC, such as the ability to fill compacted areas around steel reinforcement and prevent segregation, a significant amount of binder, primarily OPC is required. However, SCC with high OPC content is more expensive and less environmentally friendly. The emission of a significant amount of greenhouse gases is a consequence of the negative environmental impact of OPC consumption. The consumption of cement for concrete production continues to rise, indicating a growing demand. The production of cement results in greater emissions of carbon dioxide (CO₂) (Mansour & Al Biajawi, 2022; Pisciotta et al., 2023). The production of one tonne of cement releases an estimated 900 kg of CO₂ into the environment (M. I. Al Biajawi, Johari, et al., 2023; Sousa et al., 2022). This means that the cement sector is responsible for up to 6% of the total CO₂ emissions that are generated by cement plants worldwide (M. I. Y. Al Biajawi & Embong, 2023; Talaei et al., 2019).

Despite this, the manufacture of cement has a negative effect on the surrounding ecosystem. According to a study by (Lehne & Preston, 2018) more than 4 billion tonnes of cement are produced annually. Given the present circumstances, this problem requires considerable attention to achieve the United Nations Sustainable Development Goals, and additional efforts must be made to address both natural resource management and waste utilization problems. As an eco-friendly option, SCC can be produced from industrial waste as a sustainable alternative, by reducing building expenses and preserving natural resources. Utilizing industrial waste as supplementary cementitious materials SCM in SCC might improve the properties of the concrete mixture, both in terms of its fresh state and mechanical strength. Furthermore, the worldwide initiative to enhance the properties of SCC and reduce its cement content and carbon footprint has included the integration of SCM at larger quantities.

Therefore, using substitute substances to reduce the demand for cement is a successful approach to producing building materials with a reduced carbon footprint. Simultaneously, the thermal power plant that relies on coal generates two noteworthy forms of waste: Fly ash (FA) and CBA. In Malaysia, about 6.8 million tonnes of FA and 1.7 million tonnes of CBA are generated each year, resulting in significant environmental concerns at both the local, national, and international levels (Balakrishnan et al., 2017;

Rafieizonooz et al., 2016). Other researchers and organizations had previously analysed the utilization of CBA as alternative materials in construction. Nowadays, recycling ashes generated from thermal power plant has been used as building materials has met industry standards and guidelines with significant environmental benefits. It will minimize the quarrying of natural aggregates and reduce the volume of waste disposed of at the landfill (Khaskheli et al., 2020). CBA is disposed of as a landfilling material, which poses an environmental danger to living beings due to some toxic metals embedded in the particles (Mangi et al., 2018). It is now a global concern to find environmentally friendly solutions for industrial waste's safe disposal to sustain a cleaner and greener environment (Dou et al., 2017). Large amounts of CBA waste annually increased in various countries worldwide. Studies (Abdulmatin et al., 2018) show that CBA has potential as partial alternative binder with cement in concrete production due to its pozzolanic property and high silica percentage; hence, CBA can be utilized as a pozzolanic material to improve concrete strength and transport properties.

According to American Society for Testing and Materials (ASTM) the key reference that provides comprehensive details on the physical and chemical characteristics of FA or pozzolanic material in concrete, which promotes the reuse of this material in concrete (ASTM C618, 2019). It considers the specifications given in the international standard. Pozzolanic activity describes the capacity of active SiO_2 and Al_2O_3 in coal ashes to react with lime and contribute to the development of strength. In addition, coal ashes include several additional active oxides, but their concentrations are generally little or insignificant (Shi & Day, 2000). Hence, the pozzolanic reactivity of coal ashes may be approximately determined by the reactivity of active SiO_2 , and Al_2O_3 . The high concentration of silica in CBA makes it a promising candidate for use as a pozzolanic materials (Thomas et al., 2017). Approach of utilizing industrial waste such as CBA as incorporation mixing materials would contribute to reduction of wastes in the environment and minimize the main resources. The present study investigates the significance of utilizing CBA as alternative cement materials in SCC and new pre-treatment mechanisms (mechanical pretreatment) to produce ground CBA can be use in the SCC production. The inclusion of ground CBA is expected to improve the strength of the samples on the SCC with the benefit of reducing the waste from the industries.

1.2 Problem Statement

Waste management has emerged as a prominent ecological problem in the 21st century. It encompasses several types of wastes, such as industrial waste, building waste, and residential garbage. The excessive accumulation of waste is growing into a significant concern, since it not only presents threats to human activities but also has detrimental effects on the ecosystem. On the other hand, the recent spurt in the progressing of modern life activities, especially in the construction and building industries, has increased cement demand worldwide (Mangi et al., 2018). Thus, reducing cement consumption could help lessen construction costs. However, increments in cement manufacturing cause harmful impacts on the environment pollution due to the exhaustion of carbon dioxide during its production (Bakhtyar et al., 2017; Pipilikaki & Beazi-Katsioti, 2009).

The outcome of OPC is expected to continue growing, reaching 4 billion tons per year by 2040. This significant increase has raised significant concerns about the environmental impact due to the excessive use of energy and resources. In accordance with the 2022 report of the International Energy Agency (IEA-2022), the cement industry is responsible for approximately 7% of the global total CO₂ emissions. It also emits approximately 0.66–0.82 kg of CO₂ per kilogram of cement produced. The construction sector's demand for cement is an important component of production; and it is expected that cement production will grow in the future. During this era, there was a consistent and gradual growth in cement output, with the total yearly production fluctuating at around 1 billion tons each year. Figure 1.1 depicts the cement output in Malaysia spanning from 2014 to 2023. In general, the increase in cement manufacturing not only requires a higher number of natural non-renewable resources but also results in a growing amount of waste.

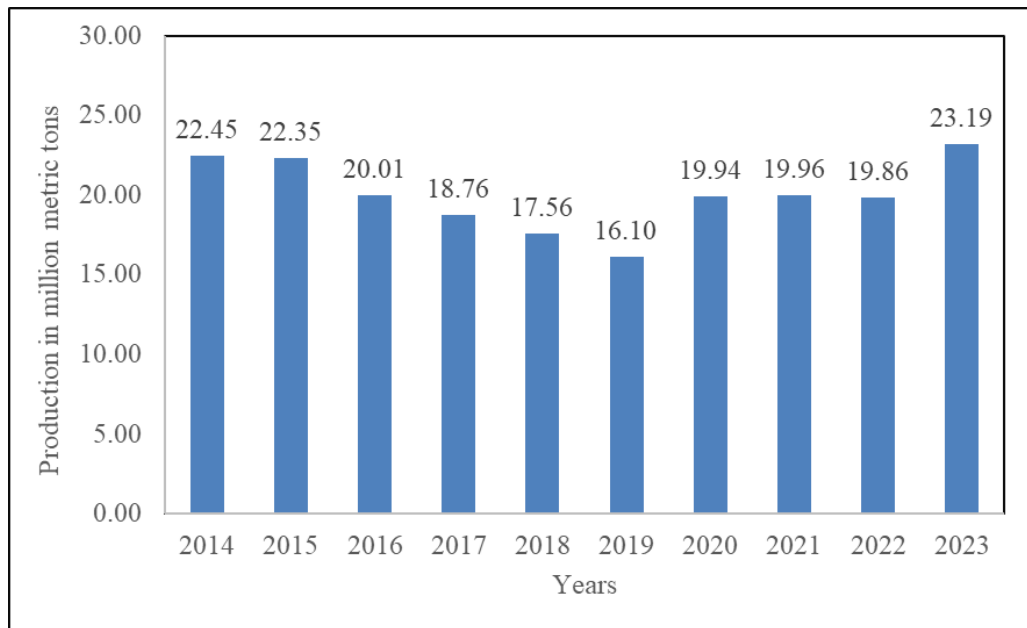


Figure 1.1 Cement production in Malaysia from 2014 to 2023
Source: Statista (2023)

Therefore, attempts are conducted to reduce cement consumption, which could help protect the environment. This need is particularly crucial in the development of SCC, which requires materials that can enhance its properties without compromising its unique ability to flow under its own weight and fill formwork completely. Research indicates that incorporating materials such as fly ash, slag, and silica fume can not only reduce the environmental impact but also improve the workability, durability, and strength of SCC. These materials offer additional benefits by increasing the sustainability and overall performance of SCC, thus contributing to more eco-friendly and efficient construction practices.

Subsequently, the upward direction of coal use is going to continue predominantly due to a strong need for electricity. Consequently, the growing need for coal production has led to a rise in industrial waste. CBA is among the largest form of industrial waste generated by coal-fired thermal power plants. hence potentially constituting a threat to the environment. The yearly CBA produced in Malaysia is around 1.7 million tonnes (Mangi et al., 2019). The appropriate disposal of such wastes is a formidable task and represents a significant environmental problem for the worldwide community. Hence, it is crucial to use CBA in order to mitigate environmental concerns (Silva et al., 2019). The disposal of unneeded CBA incurs significant costs and imposes a substantial demand

on the power sector, ultimately shifting the responsibility to the energy user. Furthermore, the deposition of CBA ash in landfills exacerbates the persistent issue of depleting landfill capacity in Malaysia (Mangi et al., 2018). Moreover, CBA, a common local material in Malaysia, to reduce the influence of CBA waste it could be used as a partial replacement material with cement in concrete production to help that promoting to help in lower construction cost, intensive energy use and environmental harm, enhancing concrete performance. Moreover, widely utilizing by-product-based pozzolanic material CBA could support the sustainability of concrete manufacturing. Moreover, using CBA will decrease abundant waste presence from coal-based energy in the production industry (Deonarine et al., 2023).

However, CBA is the favourable pozzolanic materials in the production of cement composite. The influence of CBA inclusion on hydration was reported by many researchers and the results shows improvement the properties of the concrete such strength mechanical, and durability properties (Hakeem et al., 2023; Ho & Huynh, 2023). Generally, pozzolanic materials are added to PC to increase its performance. The enhancement in quality occurs as a result of the pozzolanic reaction between calcium $(OH)_2$ and silica in the presence of water, to the formation of calcium silicate hydrate (C-S-H). However, according to Massazza et al. (2003), the total quantity of calcium hydroxide involved in the pozzolanic reactions depends on various aspects like curing length, ratio of the $Ca(OH)_2$ to pozzolan, silica content in the reactive phase, and pozzolan content in the reactive phase. The reaction's inactivity of the pozzolanic material of the $Ca(OH)_2$ is high. Many factors have been attributed to this, such as the pozzolan's surface area, content of cement alkaline, temperature, as well as water/solid ratios. Often, the material's pozzolanic action can be calculated by physical, chemical, and mechanical techniques. CBA retains a higher reactive fraction with extra pozzolanic characteristics.

Moreover, several previous studies Chindasiriphan et al., (2023); (Mousa, 2023) focus on the performance of the CBA in cementitious framework without any researches focusing in the mechanical treatment process works and any approaches in SCC. A few issues emerged when CBA was used as sand or aggregate replacement. One of it was directly related to the reduction of mechanical strength performance. While it was currently identified as a pozzolanic substance and encouraged to use CBA as alternative materials with cement in the concrete mixture. Nevertheless, SCC has been enhanced to

comply with the need for SCC with improved fresh, mechanical, and durability characteristics. Therefore, the use of SCC can minimize or even eliminate the harmful effect of negative building practices. In aggressive environments, the integration of CBA and SCC could give possibility advantages for engineering properties for concrete structures. In its characteristics related to SCC behaviour, many issues are lack of knowledge fundamentally in SCC. Further research on SCC is thus practical to expose aggressive environments, characterize SCC using laboratory testing methods, and building problems with SCC are workable.

1.3 Objectives of the Research

This research aims to study the response for pozzolanic reaction in cementitious environment and the impact of mechanical treatment of CBA in SCC. To achieve the aim of the research, several specific objectives were defined as follows:

- I. To evaluate the physical, chemical, and microstructural properties of original CBA and mechanically treated CBA as alternative cementitious materials.
- II. To analyse the influence of mechanically treated CBA on its pozzolanic properties based on Thermogravimetric analysis (TGA), strength activity index (SAI), Chapelle test, and Frattini test in cementitious binder.
- III. To analyse the effect of mechanically treated CBA as partial cement replacement in the fresh properties of SCC based on slump flow, L-box, V-funnel, J-Ring, and mechanical properties of SCC based on compressive strength, flexural strength, Ultrasonic pulse velocity (UPV), splitting tensile strength.
- IV. To evaluate the influence of mechanically treated CBA as partial cement replacement on the durability properties based on (water absorption, sulphate attack, acid attack) and influence of elevated temperature (200°C, 400°C, 600°C, and 800°C).

1.4 Scope of the Research

The main objective in this research study is to produce sustainable CBA by replacing partials cement amount in the SCC which is suitable to the environment and

comply with the engineering properties. The scope of study covers several important elements such as preparation and characterization of materials and determination of mechanical treatment process of CBA. Firstly, CBA was sieved passing 300 μm then grinding using Los Angeles machine for 3000 cycles, 5000 cycles, and 7000 cycles to be passed sieve 75 μm and retained sieve 45 μm with in accordance ASTM C618. In this study micro fine CBA particles were analysed in terms of physical, chemical, and microstructural properties as pozzolanic materials. For the analysis of the pozzolanic properties of ground micro-CBA for various particles sizes was tested in Fourier transform infrared (FTIR), X-ray Fluorescence (XRF), X-Ray diffraction analysis (XRD), Scanning Electron Microscope (SEM), Barrett-Joyner-Halenda (BJH) and Brunauer-Emmett-Teller (BET). Furthermore, ground micro-CBA were also analysed to select the optimum replacement ratio of ground CBA and tested in various areas such as Thermogravimetric analysis (TGA), Chapelle test, Frattini test, and strength activity index (SAI). This study was selected the best mix design of SCC containing ground CBA as cement replacement in accordance with the European Federation of Specialist Construction Chemicals and Concrete Systems (EFNARC). In addition, the adapted mix design of this study was used to evaluate the fresh mechanical properties of the SCC mix. The selected mix design by different mixing ingredients such as cement and, river sand aggregate, coarse aggregate, and various ground CBA content with target strength of SCC was selected to be 35 MPa. In this study various ground micro-CBA was used as partial cement replacement in SCC. The scope of experimental work was carried in several stages out as shown in Table 1.1. The details of experimental work for as the following:

- ❖ Characterizations of the original and various sizes of mechanically ground CBA are determined by measuring the particle size, surface area, and fineness. The mineralogy of mechanically treated CBA was also verified by using various devices such as X-Ray Diffraction (XRD), X-Ray Fluorescence, and Scanning Electron Microscopy (SEM).
- ❖ The mechanically treated CBA were also analysed to evaluate the influence of CBA with replacement ratio of CBA and tested in various such as Thermogravimetric analysis (TGA), Chapelle test, Frattini test and strength activity index (SAI).
- ❖ The design mix was made to achieve the target strength after adding mechanically treated CBA to the concrete in different amounts (10%, 20%, 30%, 40%, and 50%).

The optimal mix proportion was used in the SCC that had ground CBA and was compared to the SCC without CBA (control samples). Various tests of SCC were conducted at this stage: flow slump, L-Box, V-Funnel, and J-Ring.

- ❖ The specimens are tested in the mechanical and durability at an early age and long curing ages (56, 90, and 180 days). The performance of SCC containing mechanically treated CBA exposed to different temperatures (200°C, 400°C, 600°C and 800°C) for one hour. In addition, all samples were visually observed and tested for mass loss and compressive strength after 28 days of curing.
- ❖ Finally, the results related to the different properties: mechanical, durability, microstructural properties, and elevated temperatures of SCC with ground CBA were analysed.

Table 1.1 Stages of the experimental work of this study

Stage	Experimental work activity
Stage 1	Collected and prepared and characterized for original CBA and mechanically treated CBA compared with cement particles (Objective 1 and 2). The limitations are time and energy consuming to obtain ultra fine particles of CBA.
Stage 2	The optimum size of mechanically treated CBA was used to design the mixture in SCC for control samples and SCC with ground CBA to evaluate the fresh, and mechanical properties (Objective 2). The limitation in this stage for the fresh properties has been set to achieve the EFNARC standard with target strength 35MPa.
Stage 3	The mechanical properties of SCC containing mechanically treated CBA as cement replacement and select the optimum compared to control samples was analysed (Objective 3). Durability properties of SCC in terms of (water absorption, sulphate attack, acid attack,) and select the optimum level of replacement for CBA (Objective 4). The effect of SCC containing mechanically treated CBA subjected to various temperature (200°C, 400°C, 600°C, and 800°C) for one hours and select the optimum level of replacement was carried out (objective 4).
Stage 4	Analysis the data of the study.
Stage 5	Conclusion of the study and Recommendation for the future research.

1.5 Significance of Research

The development of concrete with more complicated geometries and dense reinforcing has been growing progressively. Moreover, the demand increased for improving the current practices of concrete technology has led to create an approach of concrete with better qualities, which encouraged scholars to advance further investigations in this area of research. Consequently, an innovative type of concrete called SCC has been improved. Simultaneously, one key challenge, confronted by the civil engineering sector, is how to go more environmentally friendly. Using waste materials, e.g., CBA, is one of the carefully utilized techniques in construction and building applications. The main aim of this study is to evaluate the performance of SCC production using supplementary cementitious materials CBA as cement replacement and to provide a approach with a strong base for the use of binders in sustainable practices. The outcomes of this research can contribute to enhancing the implementation of construction applications by reducing the costs associated with the main materials used in SCC mixtures and reducing the utilization of non-renewable materials, while enhancing the characteristics of SCC. The results of this study will provide valuable insight into the use of CBA as cement substitute in SCC production.

Nevertheless, the results of this study showed that the behaviour of SCC containing CBA as a partial cement replacement under aggressive conditions such as acid and sulphate resistance. Furthermore, the present research also would provide the influence of SCC containing CBA subjected to elevated temperatures. Overall, the use of an industrial by-product produced from thermal power plants such as CBA plays a crucial role in maintaining the ecological balance and sustainable development of a country as a whole and in the building sector in particular. In addition, the use of industrial by-products as supplementary cementitious materials has the potential to mitigate the greenhouse gas emissions (carbon dioxide), reduce the waste pollution, and promote environmentally friendly construction.

1.6 Thesis Outline

This thesis is structured into six chapters.

Chapter 1 provides a description the introduction, which clarifies the research objectives, the study area, identify the research gaps and problems, research objectives, research significant, and scope of study.

Chapter 2 characterizes the literature review relative with this study; a comprehensive present of earlier and recent studies related to the behavior of utilizing cementitious material CBA in concrete and the properties of CBA. Primarily this chapter is divided into two core parts: fresh properties, and mechanical properties of CBA in SCC. Whereas the second part focuses on the effect of mechanically treated CBA, and focuses on the utilization of SCC, and application of SCC. This chapter ended with the influence of elevated temperatures for concrete containing various recycled waste as cement replacement.

Chapter 3 shows the experimental program and procedures. It is comprised of the methodology utilized in this research to realize the specified objectives. This chapter describes the materials characteristics and mixtures design for SCC following the methods and specific standards. Moreover, the mixing procedures, steps of casting and, curing process and periods are explained. Details of the materials used in the experimental work such as cement and river sand aggregate, coarse aggregate, superplasticizer, and water are also described. The description of the experimental methods and standards adopted to evaluate various testing performed in the fresh properties based on (Flow slump, L-Box, V-Funnel, U-Box, J-Ring) and mechanical properties based on (compressive strength, flexural strength, Ultrasonic pulse velocity (UPV), splitting tensile strength). Furthermore, experimental producers investigate the performance of SCC in terms of durability resistance such as (water absorption sulfate attack and acid attack) are provided in this chapter. Finally in this section methods used to investigate the SCC when exposed to elevated temperatures are provided.

Chapter 4 presents the results of characterization of mechanically treated CBA by mechanical grinding in this study, the chemical and physical properties and the analysis of microstructure and select the optimum parameter in the mechanical grinding method with various grinding sizes for mechanically treated CBA. The chemical

composition, Fourier transform infrared (FTIR), X-ray Fluorescence (XRF), X-Ray diffraction analysis (XRD), Scanning Electron Microscope (SEM), Barrett-Joyner-Halenda (BJH) and Brunauer-Emmett-Teller (BET), and particle sizes of mechanically treated CBA are also presented in this chapter. Also, in this chapter discussed the influence of CBA as pozzolanic materials and testing in various test including strength activity index (SAI), Thermogravimetric analysis (TGA), Chapelle test, and Frattini test.

Chapter 5 shows the results performed from the fresh, mechanical, and durability properties of SCC containing ground CBA as partial cement replacement. Furthermore, in this chapter present the influence of CBA as partial cement replacement in SCC subjected to various elevated temperature (200°C, 400°C, 600°C, and 800°C).

Chapter 6 Conclusion and Recommendations. This chapter conclude and summarizes based on the main research outcome and reviews the objectives. Recommendations for future experimental work and research opportunities are also elaborated on in this chapter.



اونيورسيتي مليسيا قهغ السلطان عبدالله
UNIVERSITI MALAYSIA PAHANG
AL-SULTAN ABDULLAH

CHAPTER 2

LITERATURE REVIEW

2.1 Introduction

This chapter aims to review the relevant research related to the topic of this study “The influence of pozzolanic reactivity of CBA in SCC”. This chapter discusses in the light of the available literature, the properties of SCC. Also, this chapter provides an overview on the CBA characteristics, properties of SCC, and concrete containing CBA as fine aggregate or cement replacement based on waste by-products. The durability and elevated temperatures proportions in the concrete or SCC also has been discussed in this chapter. Therefore, this chapter provided an overview on the using of CBA and the various properties (fresh, strengths, and durability) in concrete. Moreover, this study described the CBA used in the applications of civil engineering projects. Furthermore, in this chapter highlighted the new approach in utilizing CBA as SCC and present the possibility to utilized CBA as SCC; advantages and disadvantages of using this method. Finally, a review on the testing of the properties of CBA in concrete as reported by other researchers is presented.

2.2 Self-Compacting Concrete (SCC)

The next sub-sections discuss the SCC based on the standards and previous studies. The discussion includes background, advantages and disadvantages mixtures design, and the application that can applied SCC based on previous studies.

2.2.1 Background

Concrete is a significant component in construction. Concrete has been developed from a material, which mainly incorporates cement, aggregate, water, in addition to a few admixtures to a specifically engineered material, which is made of various additional ingredients that enhance performance in a range of exposure circumstances (Kanyal et al., 2021; P. Li et al., 2021). Concrete is a frequently utilized building material due to its beneficial characteristics (Miraldo et al., 2021). However, conventional concrete has

some flaws in the commercial use of ordinary concrete. To tackle the issue of limited construction such as Intricate designs, the density of reinforcing steel in structural components, a shortage of skilled labor, the construction industry's fast development, and the poor quality of construction have altogether prompted the adoption of SCC to address these issues (J. Li et al., 2021; Z. Ma et al., 2021; Siddique, 2019). In 1988, Okamura was the first to introduce the utilization of SCC, which has been developed to tackle the problem of building extremely overcrowded reinforced concrete components (Alexandra et al., 2018; Ashish & Verma, 2019; Shi et al., 2015; Yankun et al., 2021). The aim of developing SCC primarily involves creating a new type of concrete, which enjoys the capability of flowing through and filling mold corners and reinforcing spaces without using vibrations or compacting through the casting process (Adesina & Awoyera, 2019; Chandru et al., 2018).

The primary concept of SCC in the fresh state revolves around its rheological properties, which are crucial for ensuring its workability and stability. Rheology, the study of the flow and deformation of materials, is the main design factor for SCC because it directly influences the concrete's ability to flow, fill intricate formwork, pass through dense reinforcement, and maintain homogeneity without segregation or bleeding (Okamura & Ouchi, 2003). Viscosity control is a critical aspect of SCC's rheology. Proper viscosity ensures that the concrete can flow smoothly while resisting segregation of the aggregates. A well-designed SCC mix achieves a balance between fluidity and stability, allowing it to spread into place under its own weight while maintaining uniformity (EFNARC, 2002). This balance is typically achieved by using a combination of superplasticizers to enhance flow and viscosity-modifying agents to maintain cohesiveness (EFNARC, 2002).

Temperature also plays a significant role in the rheology of SCC. Higher temperatures can accelerate the hydration process, reducing the working time and increasing the risk of early setting, which can compromise the concrete's flowability and lead to defects. Conversely, lower temperatures can slow down the hydration process, affecting the early strength development and workability. Therefore, controlling the temperature and understanding its effects on the rheological properties of SCC are vital for ensuring consistent performance (Abed, 2019). In summary, the importance of

rheology in SCC design lies in its direct impact on the concrete's fresh state properties, which determine the ease of placement, compaction, and overall quality of the finished structure. Proper control of viscosity, attention to temperature effects, and the use of appropriate admixtures are essential to achieving the desired performance characteristics of SCC.

Generally, SCC is realized by using recently developed generation superplasticizers to decrease the water-binder ratio. Furthermore, supplementary cementation or tranquil substances materials such as powdered calcareous plants, natural pozzolanic, FA and ground CBA would be used. In order to improve viscosity and reduce the expense of compressive concrete. Exclude for the use of non-vibrators, the similar trend is realized in regular vibrated concretes with the same components are utilized with finer content and using very strong superplasticizers in the application. Several previous studies have carried out SCC experiments using additives such as FA and CBA. Both ashes are appropriating additive for SCC works as well as minimize circumferential pollution reasoned by this waste. The CBA is a by-product of coal combustion, which is commonly not properly used. In most developing countries, such as Malaysia, the by-product of thermal power stations has been commonly used in the concrete industry as a cement substitute material this is due to despite its important benefits in terms of workability and durability (Kasemchaisiri & Tangtermsirikul, 2008; Mangi et al., 2019; Zainal Abidin et al., 2014).

CBA due to its strong and light weight characteristics, it is a good substitute for sand and is appropriate for fine aggregate use as reported by several studies (Kasemchaisiri & Tangtermsirikul, 2008; Mangi et al., 2019; Zainal Abidin et al., 2014). Furthermore, Mohd Sani et al. (2010) reported that CBA is used for production of lightweight concrete masonry as a thin aggregate and as a cement substitute for structural and masonry aims. The utilize of CBA as pozzolanic extension in cement replacement would revolutionize the cement manufacture (Sani et al., 2010). There are many advantages of using SCC, including reducing construction time and labor cost, giving up a mechanical vibrator (which helps reduce the energy consumption, noise pollution, and safe), and improving filling ability when pouring in a highly congested structure, which ensures good structural performance as shown in the Figure 2.1.

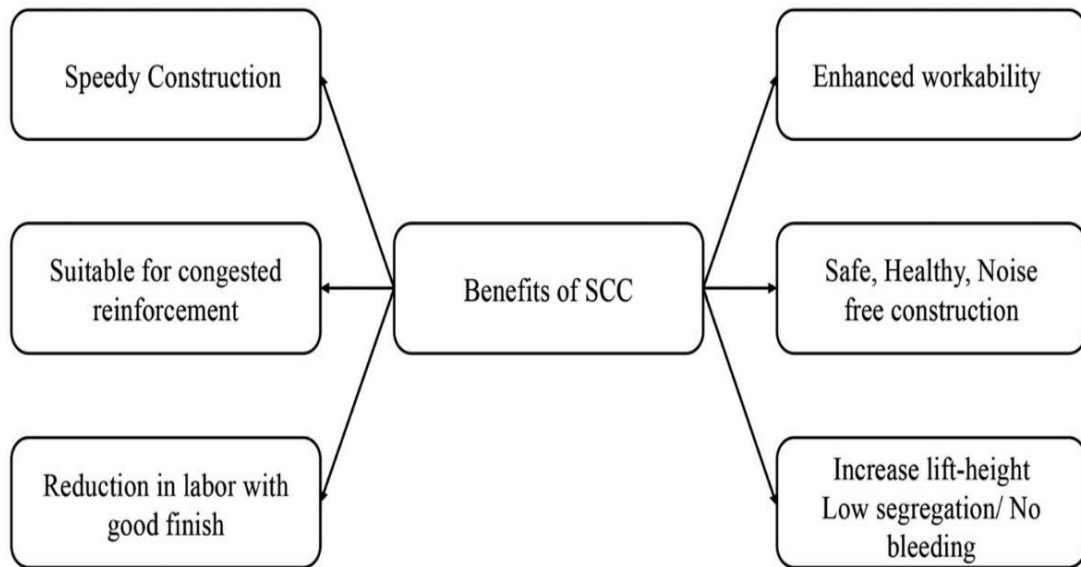


Figure 2.1 Benefits of use application of SCC

Source: Sani et al., (2010)

2.2.2 Advantages and Disadvantages of SCC

The invention of SCC has significantly benefited the construction industry with a wide range of advantages due to its unique features in quality and economy. Elimination of the need for vibration reduces the number of workers and machinery requirements which reduce construction costs. Okamura and Ouchi et al. (2003) reported that the number of workers can be decreased by 30% from those required if normal concrete is used in large applications. SCC has good deformability and passing ability with high resistance to segregation which can be placed in heavily reinforced applications and compacted under its self-weight. With no vibration, it accelerates the process of casting concrete and reduces the mixer truck movement and pump operations, which decreases the construction time (Okamura & Ouchi, 2003). Okamura and Ouchi et al. (2003) also stated that the construction period may reduce by 20% in huge scale projects where SCC is applied (Okamura & Ouchi, 2003).

Recently, a considerable significance has been directed towards SCC due to the benefits it provides, such as minimizing building time, lowering labour costs, and improving structural compaction for reinforced complicated shapes (Adesina & Awoyera, 2019; Elemam et al., 2020; Hamzah et al., 2015). The SCC containing CBA has fresh characteristics to guarantee that it functions very well in the mixture (Kumar & Singh,

2020; Pathak & Siddique, 2012). The SCC fresh characteristics, including mobility, filling capability, passing capability, and segregation resistance, are critical criteria that influence the effectiveness of SCC with the CBA use (Ibrahim et al., 2021a; Singh et al., 2018). In general, SCC can be obtained by utilizing a new superplasticizer generation by reducing the ratio of water/binder (w/b) in concrete. SCC has one downside, which involves the increased costs due to using chemical admixtures like superplasticizers (Ibrahim et al., 2015). Additionally, supplementary material ingredients, such as CBA are utilized to enhance the SCC viscosity and lower its cost (Hamzah, Jamaluddin, et al., 2020). Moreover, previous scholars examined SCC, utilizing various additives, namely CBA. They found that CBA is an effective ingredient for SCC because of its lightweight and hard nature in reducing environmental contamination caused by this waste. Furthermore, the utilization of natural resources linked with main materials production causes severe environmental impacts (Singh et al., 2019; Sua-Iam & Makul, 2015; Zainal Abidin et al., 2015).

SCC has been applied in several applications. Moreover, besides its advantages there are some disadvantages to using SCC that should be considered. It demands designers with high levels of experience to produce and control the SCC mix to achieve the fresh properties required. SCC is designed with high amounts of chemical admixtures and cementitious materials which may delayed the setting time (Okamura & Ouchi, 2003). In addition, the low content and small size of coarse aggregates in SCC compared to normal concrete lead to improve the properties (Turcry et al., 2002). Moreover, SCC is higher than that of normal concrete (NC) due to high volumes of paste, large quantities of mineral fillers, low coarse aggregates content and high range of water reducing admixture (Heirman & Vandewalle, 2003; S.-D. Hwang & Khayat, 2008). Finally, there are no standard methods or specifications for proportioning self-compacting concrete materials. However, SCC has been successfully used in many applications, and these disadvantages can be decreased or eliminated.

2.2.3 Mixture design of SCC

In 1995, Okamura introduced the first recommended SCC mixture design, dubbed as the Japanese or rational technique at that time. SCC can flow under its weight for filling gaps in the piece of work, flowing freely all through the reinforcing bars without external vibrator support. Also, it allows further concrete's accurate levelling when placed without

any segregation (Li et al., 2005; Nagamoto & Ozawa, 1999; Okamura, 1997). Therefore, when the SCC mixture design was developed, various assessments were conducted, such as V-Funnel, slump flow, and L-Box to evaluate fresh state properties and the SCC limitation according to EFNARC guidelines as illustrated in Table 2.1 (EFNARC, 2005). This method is referred to as an empirical design (EFNARC, 2005). Su et al., (2001) presented the conventionalized empirical design approach's simple application for implementation and stated that this method may significantly decrease the amount of time, binders, and expense involved. This approach primarily aims to enhance workability via the utilization of a specified amount of paste material for keeping every aggregate material in place, thus increasing the freshness and strength of the concrete. This is often referred to as the technique of packing aggregates closely (Shi et al., 2015). This means that SCC should use a minimum coarse aggregate amount volume, an increased paste volume, an increased powder volume, a lowering water-to-powder ratio, a higher superplasticizer dose, and an infrequently necessary viscosity modifying agent (Su et al., 2001). Recent studies have summarized the SCC mixture design (Danish & Ganesh, 2020) and, in 2015, it was found that the SCC mixture design is determined by five factors. These include 1) an empirical design method, 2) a close aggregate packing technique, 3) paste rheology, 4) a method of compressive strength, and 5) a statistical factorial approach (EFNARC, 2005). Previous research has shown that the SCC compressive strength ranged between 20 and 100 MPa at 28 curing days, with 40 MPa as a mean compressive strength (Aggarwal et al., 2008; Jawahar et al., 2012; Sedran et al., 2004). SCC has a high resilience degree. Also, no extraordinary mix design is required if it achieves real applicability, economy, practicability, and high quality in both its fresh and hardened states. General exhibits are determined as a part by the basic materials used in the mix design (P. L. Domone, 2007).

Table 2.1 Recommended values of SCC fresh properties

Slump flow		V-funnel test		L-box test	
Slump flow classes	Slump flow (mm)	Viscosity classes	V-funnel times (s)	Passing ability classes	Blocking ratio (H2/H1)
SF1	550–650	VF1	≤8	PA1	≥ 0.8 with 2 bars
SF2	660–750	VF2	9-25	PA2	≤ 0.8 with 3 bars
SF3	760–850	-	-	-	-

Source: EFNARC, (2005)

On the other hand, several mixture design methods for SCC. Domone, (2009); Petersson et al., 2004) each introduced an approach in 1996. In 1999, the Laboratory Central (Sedran & De Larrard, 1999) established a methodology using the BTRHEOM rheometer and RENE-LCPC applications. Su et al., (2001) established a parameter known as the packing factor to modify the proportion of aggregate and paste in a material. Hwang & Tsai, (2005) was introduced a concentrated mixture design approach that was based on the optimum density theory and excess paste theory. Saak et al., (2001) was used rheology of a paste model to develop fiber-reinforced self-compacting concrete (SCC). Kheder & Al Jadiri, (2010) was designed a novel technique that enables the precise rationing of self-compacting concrete (SCC) mixes with determined compressive strength. Sonebi, et al. (2004) was introduced a novel mixture design approach that combines the European standard (EN206-1), the Chinese technique, and the optimization of granular packing. Additionally, there are other adapted mixture design approaches that are derived from existing methods(Choi et al., 2006; Dinakar et al., 2013; Wu & An, 2014). The approaches could be categorized into five groups based on design principles: empirical design method, compressive strength method, close aggregate packing method, methods based on statistical factorial model, and rheology of paste model. The available mixture methods for designing SCC in the existing literature are compiled and presented in Table 2.2

Table 2.2 Presents an overview of the various mixture design methods for SCC that have been reported in previous studies.

Classification	Main features	References
Empirical design method	Fix coarse and fine aggregate first, and then obtain self-compactability by adjusting W/B and superplasticizer dosage	(Okamura & Ouchi, 2003)
	Use mortar flow and mortar V-funnel testing to select the fine aggregate volume, volumetric water-to-powder ratio and superplasticizer dosage	(EDAMATSU et al., 1999)
	For a given set of required properties, make the best estimation of the mixture proportions, and then carry out trial mixes to prove	(P. Domone, 2009)
	Conduct in three phases, i.e. paste, mortar and concrete	(Khaleel & Razak, 2014)
Compressive strength method	Based on the ACI 211.1 method for proportioning conventional concrete and the EFNARC method for proportioning SCC.	(Kheder & Al Jadiri, 2010)

Table 2.2 Continued

Classification	Main features	References
Compressive strength method	Use GGBS in SCC based on the strength requirements and consider the efficiency of GGBS.	(Dinakar et al., 2013)
Close aggregate packing method	Use Densified Mixture Design Algorithm (DMDA), derived from the maximum density theory and excess paste theory. Use packing factor (PF) to control the content of fine and coarse aggregate in mixture proportion. Use software to design SCC based on the compressible packing model (CPM). Use a combination of the excessive paste theory and ACI guidelines to design self-consolidating lightweight concretes. Based on FN EN 206-1 standard, compressible packing mode (CPM) and packing factor (PF)	(C. Hwang & Tsai, 2005) (Su et al., 2001) (Sedran & De Larrard, 1999) (Shi & Yang, 2005) (Sebaibi et al., 2013)
Statistical factorial model	Obtain a statistical relationship between five mixture parameters and the properties of concrete Design in a L18 orthogonal array with six factors, namely, W/C ratio, water content (W), fine aggregate to total aggregate (<i>S/a</i>) percent, fly ash content (FA), air entraining agent (AE) content, and superplasticizer content (SP). Useful to evaluate the effect of three types of sand proportions (river sand, crushed sand and dune sand), in binary and ternary systems, on fresh and hardened properties of SCC	(Khayat et al., 1999) (Ozbay et al., 2009) (Bouziani, 2013)
Rheology of paste model	Avoid segregation of the aggregates as a critical design parameter, then a new segregation-controlled design methodology is introduced for SCC. Expand Saak's concepts to include the effects of aggregate (and paste) volume ratio, particle size distribution of the aggregates and fine to coarse aggregate ratio, to propose a new paste rheology model. Steel fiber-reinforced SCC based on the paste rheology model.	(Saak et al., 2001) (Bui et al., 2002) (Ferrara et al., 2007)

2.2.4 Application of SCC

Following its success in Japan with more than 400,000 m³ of annual production for bridges and buildings in SCC, other areas of the world have adopted SCC. The following described several applications was utilized SCC.

- i. With more than 828m height (2716.5ft) and 166 floors, Burj Khalifa (2010) in Dubai holds the distinction as the tallest building and self-contained tower in the world with the highest number of floors. SCC plays a larger role in high-rise construction to solve the issue of congested reinforcement and ease of positioning. The groundwater in under construction of the Burj Dubai substructure is especially high, with chloride concentrations of up to 4.5 % and sulphate concentrations of up to 0.6%. The amounts of chloride and sulphate present in groundwater are much greater than those found in seawater. Consequently, the key concern in designing of the piles and the raft base foundation was durability. The concrete mixture for the piles which are 1.5m in diameter and 43 m long with design capacity of 3000 tonnes (t) each was a 60MPa mix based on a triple blend with 25% FA, 7% silica fume, and a (water to cement ratio) w/c equal 0.32. A viscosity modifying admixture was utilized to gain a slump flow of 675 +/- 75mm to limit the possibility of defects during construction. The construction of the Burj Khalifa, the world's tallest building, required innovative solutions for pumping concrete to unprecedented heights. The rheological parameters of the concrete mix were meticulously designed to ensure a balance between flowability and stability, crucial for high-pressure pumping. A high-performance concrete mix with low viscosity and controlled yield stress was developed to minimize friction and avoid segregation during pumping, allowing it to reach heights of over 600 meters. The pumping rate and pressure were carefully monitored and adjusted to maintain the mix's integrity throughout the ascent (Esmailkhanian et al., 2014). Similarly, the design of SCC for long bridge spans and tunnel linings hinges on achieving optimal rheological properties to ensure ease of placement and durability. For bridges, the SCC mix is designed to have high flowability to fill formworks and encapsulate dense reinforcement without mechanical vibration. This requires precise control of viscosity and yield stress to prevent segregation and bleeding, ensuring a uniform and durable structure (Feys, 2009). In tunnel linings, SCC must flow over long distances and into complex geometries while maintaining stability. The mix design for tunnel linings often includes viscosity-modifying admixtures and high powder content to enhance flowability and prevent segregation, ensuring a consistent and homogenous concrete lining (P. L. Domone, 2006).

- ii. Dragon Bridge (2012), Alcalá De Guadaira, Seville, Spain. This impressive 124m long bridge, split into four parts, stands out due to its unusual form. The concrete structure performs is a dragon that appears to protrude from the Guadaira River in the province of Seville. The dragon’s body is made up of an egg-shape section, 4 meters high and 2 meters wide of SCC reinforced. Its shape was clad in “trancadis” using more than 4,500 m² of mosaic tiles.
- iii. The 800 million-dollar Sodra Lanken (1997) Project in Sweden. In particular, it was one of the biggest building infrastructure projects that used SCC. The 6 Km long four-lane highway in Stockholm involved seven main intersections, and rock tunnels totalling over 16 km partly lined with concrete and over 225,000 m³ of concrete. Incorporating SCC was ideal to cope with the density of reinforcement required and the highly uneven rock surfaces. Another example can be found in the UK at St George Wharf (2004), London Docklands where SCC has been utilized to save time and manpower. SCC was utilized in limited areas on two floors in lift shaft walls, up stand beams and columns and for stairs precast on site.

2.3 Coal Bottom Ash (CBA)

The following sub-sections discussed about the production, environmental issue, pretreatment technique as well as the potential use of CBA in concrete production that is associated with the aggregate or cement replacement and its application in structural elements. Consequently, CBA has received a lot of interest in the construction industry in recent years and its physical properties, chemical properties and potential utilization of CBA from the previous research were briefly discussed in the following subsections.

2.3.1 Background

Throughout the world, coal is a highly recommended natural resource that has been utilized to generate electricity and steam for more than a decade and a half. The requirement for coal for power generation has increased dramatically in both emerging and developed nations (Singh & Siddique, 2016). Approximately two-thirds of coal mined today is being used to generate electricity (Morse, E., Turgeon, 2012). According to a study by Pei, (1993), coal was described as black in colour and composed mostly of carbon. As coal is burnt, carbon goes together in the air with oxygen, much as when oil

is burnt to make carbon dioxide. Coal ash is mainly released when coal is burned in coal-fired thermal plants. Several by-products of coal combustion from thermal power plants, such as boiler slag and CBA, are included in coal ash.

Boiler slag is another type of waste produced in thermal power plants. It is an inorganic substance produced during the combustion of coal in boilers at temperatures ranging from 1500°C to 1700°C and is obtained by wet ash removal from wet bottom boilers. Moreover, it is commonly found in two forms of wet-bottom boilers, sludge tap boiler and cyclone boiler. Boiler slag is obtained from both the surface of the molten iron and the bottom of the furnaces. Similarly, in FA, SiO₂ (25-45%), Al₂O₃ (5-30%), MgO (0-20%) and CaO (35-55%) are the main constituents. Nevertheless, boiler slags usually have one single size and vary in diameter from 0.5 mm to 5 mm. Typically, boiler slags have a smooth surface structure, but when gases are trapped in the slag during removal from the burner, the quenched slag becomes vesicular or porous. Boiler slag produced from burning lignite or sub-bituminous coal is much more porous than slag produced by the combustion of coals (Hannan et al., 2017; Heidrich et al., 2013; Robl et al., 2017).

CBA is the term used to refer to the ash accumulated in the furnace's bottom part. It is the unburned residue from coal combustion in thermal power plants. It is founded in the boiler and amounts for up to 20% of total coal ash (Singh, 2018). Chemically, CBA is a complicated combination of metal carbonates and oxides (Muthusamy et al., 2020). Physically, CBA is often larger in size, pores, lighter and glassy in origin, granular in form, and comparable in color to cement (Embong, 2019). The usage of CBA is likely to sustain the overall economy in the forthcoming construction phase and can help reduce the consumption of natural resources. CBA is a significant source for production wastes generated by thermal power plants. Recycling CBA has various benefits, including environmental, economic, as well as product benefits. The numerous features in the development and implementation method for CBA had been examined extensively in earlier researches (Embong et al., 2021; Kim & Lee, 2015).

Additionally, several researchers have utilized materials such as pumice powder (Ardalan et al., 2017), nano-silica (Bernal et al., 2018; Mastali & Dalvand, 2018), FA (Ardalan et al., 2017; Guo et al., 2020; Rantung et al., 2019), metakaolin (Ghoddousi & Saadabadi, 2017), rice husk ash (Raisi et al., 2018), and palm oil fuel ash (Ranjbar et al., 2016) as a partial of replacement for cement in (SCC). In addition, the majority of researchers worldwide are currently working for a sustainable environment.

Consequently, several studies are focused on obtaining benefits from waste materials causing environmental problems instead of burying such materials (Tang et al., 2020). For example, CBA industries are considered major by-product industries in some countries, such as Malaysia, Thailand and Indonesia. These manufactories produce a substantial amount of waste in the form of CBA, which are used for electricity generation in coal fired power plants (Abdullah et al., 2019; Cleaner Coal Ash Disposal Gets Bipartisan Support in Virginia - Circle of Blue, 2019), as shown in Figure 2.2.



Figure 2.2 CBA industry waste. (a) waste of CBA in the landfill (b) Process of clean CBA in the landfill

Source: Cleaner Coal Ash Disposal Gets Bipartisan Support in Virginia - Circle of Blue, (2019)

2.3.2 Production of CBA

CBA is a raw material that can be collected from coal plants, warehouses, manufacturing industries and energy plants. Coal incineration produces huge amounts of air pollution, as well as waste materials. A sequence of filters works on regulating the air pollutants emission, which is then emitted through the stacks pollution chimneys of the air pollutants like nitrous oxide (NO_x), particulate matter (PM), and sulphur (S). Figure 2.3 shows the generation process of CBA with by-product residues generated in coal-fired thermal power plants and describes the main processes in an exemplary coal-fired power plant. Around 15 million tons of ground CBA are produced yearly in the US, where in the range of 10% to 15% are recycled as useful byproducts. In certain cases, CBA can be used as a road base, snow and ice control, and structural fills (Coal Combustion By

products, 2018; Eliche-Quesada et al., 2021). Table 2.3 presents CBA production from various countries among the fossil power resources. Many factors can influence CBA production, which includes the different types and sources of coal. Coal utilized in energy plants, hugely affects CBA's chemical composition, containing sub-bituminous, lignite, humidity, as well as other levels of compounds, coal, and anthracite coal variable carbon. Anthracite coal, however, possesses the highest level of carbon, range from 86% to 97%, followed by bituminous coal with a carbon amount of around 40% to 80% (Kopp, 2018; Morse & Turgeon, 2012). The specifications for each coal grade vary among countries, but the key components are organized by (ASTM D388-18a, 2018; ASTM D4326-13, 2013). This variation in the types of coal results in differences in alumina (Al_2O_3), silica (SiO_2), loss on ignition (LOI) levels of CBA, and ferric oxide (Fe_2O_3), with bituminous coal waste containing fewer carbon amounts compared with the sub-bituminous or lignite coal waste. However, coal's chemical composition utilized for different purposes in the industry can be identified by their mineral's geological formations (Morse, E., Turgeon, 2012).

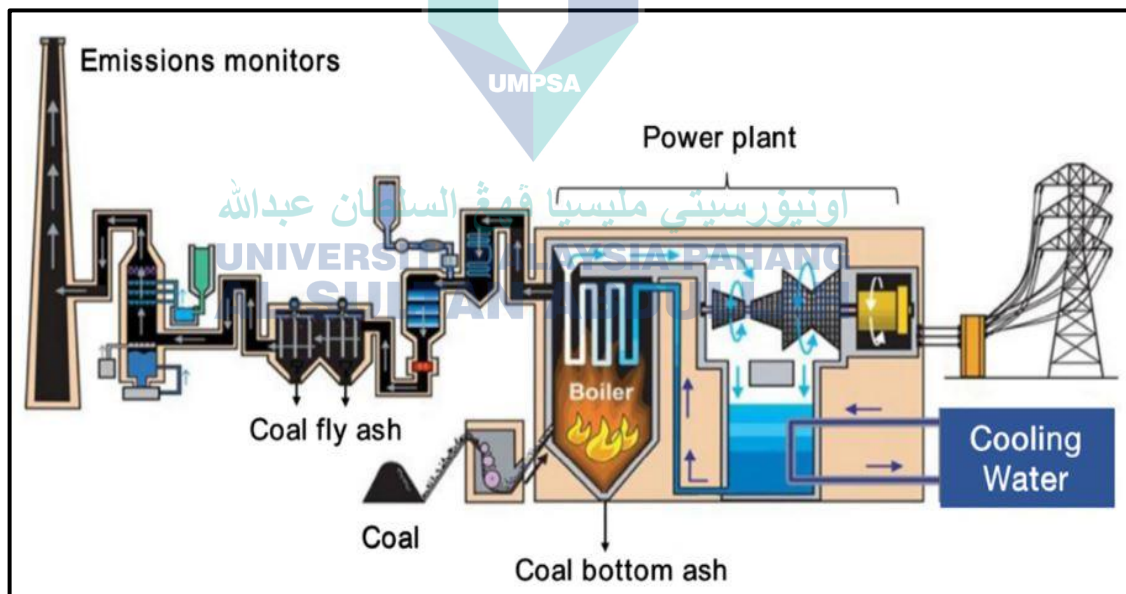


Figure 2.3 The exemplary thermal power plant of coal-fired
 Source: Coal combustion by products, (2018)

Table 2.3 CBA production in various countries

Country	CBA Production (tons/year)	References
USA	10 million	(American Coal Ash Association, 2018)
Malaysia	1.7 million	(Mangi et al., 2018)
Europe	18 million	(Cewep, 2017)
China	~ 60 million	(Ma et al., 2017)
India	100 million	(Singh et al., 2017)

2.3.3 Environmental Issues of CBA

In our world, one of the key goals of society is to achieve a better quality of life. However, the increased consumption of services and goods has exerted a huge effect. The production of large amounts of wastes and increased pollution is the result of this growing consumption. From the production of goods to the elimination of wastes, and in every phase of the system, maximizing the efficiency of energy utilization should be the aim of any sustainable growth. To address this problem, each step should be related to other phases or steps of the entire system (Caviglia et al., 2020; Viet et al., 2020). Nowadays, recycling and management of coal waste are considered one of the main tasks of environmental protection. Coal occupies the bulk of the whole world's waste, which has polluted the Earth as shown in Figure 2.4. For many years, coal has been left for decomposition in natural conditions (Das et al., 2019). The main coal contaminants that are the most widely used, such as thermal coal and metallurgical coal, should be taken into consideration for recycling. Coal waste has a low recycling rate, which contributes significantly to environmental contamination (Glushkov et al., 2019). However, the open dumping of CBA from numerous industries and thermal power stations has resulted in significant environmental contamination and a variety of health concerns. Furthermore, the way of disposal of CBA waste constituents may move into surface water or groundwater, posing a threat to living organisms. Also, a spillage risk remains, which fills the surrounding areas with CBA (J. Li & Wang, 2019). CBA's effect is toxic, heavy metals that dissolve and percolate in a leachate shape. This can be a source of groundwater pollution. According to an experimental study by Ruhl et al., (2009), the chemical composition of CBA was investigated to determine the ratio of the concentration of

various element composition in metals such as copper, zinc, arsenic, barium, nickel and mercury. The obtained concentrations of the aforementioned elements were contrasted to those recommended by different standards. The desirable percentage of copper, zinc, arsenic, barium, and nickel in CBA was determined to be up to four times that of the allowed range. Similarly, several previous studies (Kravchenko & Lysterly, 2018; Ruhl et al., 2012) had reported comparable findings for heavy metal contents. Therefore, when CBA is utilized to replace cement in concrete, it will mitigate harmful leachate. Furthermore, the accumulation of heavy metals makes CBA hazardous than fine aggregate as it is present in higher amounts. The existence of acidic conditions in the CBA dumps increases leachability compared to fine aggregate (Amran et al., 2021). This has necessitated the utilization of coal waste for different applications, such as aggregates and other uses in concrete and renewable energy (Hannan et al., 2020). This has necessitated the utilization of coal waste for different applications, such as aggregates and other uses in concrete and renewable energy (Hannan et al., 2020).



Figure 2.4 Coal ash waste impact on the earth, water, and groundwater resources
Source: Das et al., (2019)

2.3.4 Pre-Treatment of CBA

Different type of process for pretreatment of CBA have been used to produce CBA from the industrial wastes. The incorporation of CBA elements into concrete mixture raises concerns about the environmental impacts such as the possibility of heavy metals leaching into the under-ground water or in the soil. Leaching is defined as the process

whereby a waste of CBA component is removed mechanically or chemically into a solution from a solidified matrix by the passage of solvent such as water. The pre-treatment process can be divided into two phases. The first phase the chemical pretreatment method such as alkali metal removal and hydraulic acid treatment and reflux chemical treatment and other etc. The second phase is mechanical pretreatment include grinding size, sieving and incineration process in various temperatures. The following sub-section presented the review of the CBA and other materials treatment process as reported by various researchers.

2.3.4.1 Chemical pretreatment

The chemical treatment process was investigated by several researchers (Kusbiantoro et al., 2019; Hammoud et al., 2017c Jarusiripot, 2014; Mangi et al., 2019). Kusbiantoro et al., (2019) reported that the aim of the study to enhance the pozzolanic reactivity of CBA through chemical pre-treatment process. The results showed chemical oxide composition of ashes that were pre-treated with various acid concentration showed an optimum peak at 0.5 mol of H_2SO_4 . The inclusion of this CBA as a partial cement replacement material provide superior performance on the compressive strength of hardened mortar (Kusbiantoro et al., 2019). Furthermore, Hammoud et al. (2017) was investigated the effect of HCl solution in various concentrations of CBA in concrete. Also identified heating temperature, time and acidic treatment of CBA pretreatment. The results show that the pretreatment protocol defined is effective for most elements. There is a good coherence between experimental and simulated data for elements such as calcium and sulphur these elements have been well described in the mineralogical assemblage. Results are less convincing for other elements (e.g. antimony) for which not enough data exists yet, in order to correctly define their geochemical speciation in the CBA (Hammoud et al., 2017).

In the study by Feng et al., (2004) investigated the influence of hydrochloric acid pretreatment on the pozzolanic activity and chemical properties of rice husk ash. It was observed significant increase in the strength of the rice husk ash (pretreated) specimen. The pozzolanic activity of rice husk ash by pretreatment is not only stabilized but also enhanced obviously. It is shown the sensitivity of pozzolanic activity of the rice husk ash heated hydrochloric acid (HCl) pretreatment rice husk to burning conditions is reduced. The above explained and discussion for the chemical treatment of CBA is reported by

several researchers as seen in the Table 2.4. Also demonstrates in Table 2.4 the solution used with various percentages of CBA and various solutions used for treatment in concrete mix, also observation of used this solution as is shown in the Table 2.4.



اونيورسيتي مليسيا قهغ السلطان عبدالله
UNIVERSITI MALAYSIA PAHANG
AL-SULTAN ABDULLAH

Table 2.4 Summary of chemical pre-treatment of materials in mortar and concrete

Author /year	Source of CBA	Materials used and percentages	Solution used for treatment and amount	Observation
(Kusbiantoro et al., 2019)	Malaysia	CBA as cement replacement in mortar (0,5%, 10,15,20%)	H ₂ SO ₄ solution, (0.1 M, 0.5 M, and 1.0 M).	The optimum percentage is 5% can be improved the compressive strength, also increased the compressive strength when increased the ages.
(Mangi et al., 2019)	Malaysia	CBA as cement replacement in concrete	Sodium sulphate 5% (Na ₂ SO ₄) and 5% Sodium Chloride (NaCl).	The concrete doesn't change in weight when used curing in NaCl and Na ₂ SO ₄ compared to normal curing in water.
(Tayeh et al., 2019)	Iraq	CBA as cement replacement (10%, 20% and 30%)	4% of calcium chloride solution (CaCl ₂ .2H ₂ O)	Improved the strength properties when used solution of CaCl ₂ .2H ₂ O with CBA in concrete mixture.
(Liu et al., 2018)	Singapore	CBA as cement replacement in mortar.	Alkali solutions such as (sodium hydroxide (NaOH) or calcium hydroxide (Ca(OH) ₂) used at pre-determined alkalinity (pH = 12 or 14) to react with incineration CBA at specific temperatures (25°C or 70°C) at 120 minutes	Alkali treatment enhanced the pozzolanic properties and removes the metallic aluminum and minimizes aeration in incineration CBA blended cement mortars.
(Hammoud et al., 2017)	France	CBA as fine replacement in concrete	HCl (0.18M, 0.5M, 1M, 1.5M)	It has been observed that a low Liquid to solid ratio (L/S) increases the efficiency of the pre-treatment process, reducing the production of effluents.

Table 2.4 Continued

Author /year	Source of CBA	Materials used and percentages	Solution used for treatment and amount	Observation
(Embong et al., 2016)	Malaysia	Sugarcane bagasse ash (SBC) as cement replacement in mortar (10%,20 %, 30%,50%)	HCl solutions (0.1M,0.5M ,1.0M)	The mechanical properties of SBC are gradually decreased when increased the percentages of replacement.
(Wongkeo et al., 2012)	Thailand	CBA as cement replacement in concrete (0%, 10%, 20%, 30%)	Calcium hydroxide 4:5 by weight, aluminum powder was added at 0.2% by weigh of mix.	The mechanical and other properties was increased when with CBA content due to tobermorite formation.
(Feng et al., 2004)	Japan	Rice husk ash as cement replacement in mortar 30%	1 N HCl	Reduce the range of pore and enhance the pozzolanic reactivity of treated rice husk ash mortar compared to cement in normal mortar.

2.3.4.2 Mechanical pretreatment

In order to use CBA and minimize the environmental influence, mechanical treatment method such as grinding size was investigated by several researchers Abubakar & Baharudin, (2012); Khongpermgoon et al., (2020); Tayeh et al., (2019). Burhanudin et al. (2018) was reported the influence of CBA as cement replacement in concrete, the particles were used in this research retained particles on a no. 325 μm sieve and the percentages of this particles was 3% in the mixture concrete. The results showed a low fineness of CBA would result in a low compressive strength of concrete. Furthermore, the grinding time change the physical properties and the fineness particles size reduced the workability of CBA. In similarity, Mangi et al. (2018) was observed the grinding process is necessary for the CBA to make it useful as a supplementary cementitious material. The grinding size was passed sieve no 300 μm . The results showed decreased when increased the percent of replacement in all properties such as compressive and tensile and density.

In reference Khongpermgoon et al. (2020), the author studied the effect of CBA in various range of particle size 3.65 to 50.45 μm as cement replacement in concrete. The CBA was collected from the thermal power station in Selangor, Malaysia known as Kapar Energy Ventures (KEV). The CBA was dried in the oven at a temperature of $110\pm 5^\circ\text{C}$ for 24 hours. Then, was used to grinding by Los Angeles (LA) grinder machine for 2hours, the process of grinding of CBA done in two stages. First stage grinding process, it was sieved using 300-micron sieve. The ground CBA which passed through the 300micron sieve was then proceeded for the second stage grinding in a ball mill for 20hours until fine CBA was achieved where almost 75% passed through 63-micron sieve. it was found the influence of particles size that led to decrease the properties of concrete contain CBA such as compressive strength, workability, and spilt tensile strength. This is due to need more grinding to be fineness and the low pozzolanic activity at the early age of 28 days. In similarly, the above explained and discussion for the mechanical treatment of CBA is reported by several researcher, as seen in the Table 2.5. Also demonstrates in Table 2.5 the grinding size of CBA and influence of various ratio of replacement for CBA in concrete mix, also optimum percentage and the benefit of this as shown in Table 2.5.

Table 2.5 Summary of mechanical pre-treatment of CBA in mortar and concrete

Author /year	Source of CBA	Materials used and percentages	Particle grinding size	Key research findings		Observations
				Recommend level	Benefits	
(Khongpermgoson et al., 2020)	Thailand	CBA as cement replacement (0, 15%, 25%, 35%, and 45%)	Retained on a sieve No. 325, passed sieve no. 600 μm	15%		Improve the pozzolanic reactivity when used CBA as cement replacement CBA is a suitable material for use as a pozzolan in high strength concrete and, maintaining a favourable mechanical strength.
(Khongpermgoson et al., 2019)	Thailand	CBA as cement replacement 10% with various w/c (0.15, 0.35) and water to binder ratio W/b (0.3, 0.7)	Retained sieve no. 45 μm	10% (w/b)	with	Increased the strength at 28 days when used CBA as cement replacement 10% with w/b 10% with w/b ratio give good strength properties and chloride resistance. Also, reduced the permeability of the samples
(Tayeh et al., 2019)	Iraq	CBA as cement replacement (10%, 20%, and 30%)	Passed sieve No. 200 mm	10%		Achieve strength properties almost the same of the normal concrete compared to other percentages was decreased 10% and 20% of CBA replacement was gave the same results compared to normal concrete in the strength properties. And 30% of CBA replacement decreased in all properties

Table 2.5 Continued

Author /year	Source of CBA	Materials used and percentages	Particle grinding size	Key research findings		Observations
				Recommend level	Benefits	
(Burhanudin et al., 2018)	Malaysia	CBA as cement replacement (10%, 20%, and 30%)	Passed sieve no 150µm	20%	The additional fineness particle of CBA in concrete increased packing factor which helps minimize the voids and continues pozzolanic activity in cement matrix.	The grinding time change the physical properties and also the fines reduced the workability and in the 20% of CBA increased the strength compared the others percentages.
(Mangi et al., 2018)	Malaysia	CBA as cement replacement (10%, 20%, and 30%)	passed sieve no 300 µm	10%	Achieve acceptable strength properties compared to normal concrete and the target	The CBA was decreased when increased the percent of replacement in all properties such as compressive and tensile and density.
(Jamaluddin et al., 2016)	Malaysia	CBA as fine replacement (0, 10%, 15%, 20%, 25%, 30%)	Sieved into sieve passing 5 mm and 600µm.	10%	CBA with 10% replacement have highest strength properties compare to normal concrete	The water cement ratio gives the major impact of the SCC with CBA due to characteristically absorbing water during mixing process. Also, the optimum 10% of CBA due to pore refinery influence by pozzolanic reactivity of CBA

2.3.5 Properties of Coal Bottom Ash (CBA)

The CBA contains various size distributions that depend on the rate of combustion at the power plant. Generally, the particle size of CBA is in the range of fine to coarse and categorized as lightweight material. Thus, the most crucial part of utilizing CBA as aggregate or cement replacement in the concrete. The improperly conducted replacement may not archive the desired strength criteria under the relevance standard. Therefore, The following sub-sections discussed the physical and chemical properties of CBA as reported by previous researches.

2.3.5.1 Physical Properties

From the laboratory investigations, the physical characteristics of CBA rely on the behaviour and size of particles. Furthermore, the characteristics of CBA draw upon parent rock fragments' changeability, collected from different sources (Mangi et al., 2019). Additionally, the rate of pulverization and combustion temperatures has an effect on the physical characteristics of CBA. In general, the characteristics of CBA particles show that they are angular and irregular in shape as demonstrated in Figure 2.5 (A1, A2) (Ankur & Singh, 2021; Rafieizonooz et al., 2016). CBA is lighter and brittle in concrete when compared to fine aggregate due to its porous inner structure. Earlier researches Aydin, (2016); Khongpermgoson et al., (2019) on CBA demonstrated that its specific gravity ranges from 0.8 to 2.9. The low values can be attributed to voids, depending on the grinding size of CBA. This pore condition of CBA contributes to an increased water absorption of about 4.1 to 25.8%. The fineness modulus of CBA has a range of 1.5 to 5.6 within the range of standard fine aggregate in concrete (Ahn et al., 2016a; Sanjuán et al., 2019). The CBA particles' display suggests that they are much coarser compared to the fine aggregate particles (Mangi, et al., 2019). The CBA's unit weight or density falls within the range of 1200 to 1620 kg/m³, whereas fine density has a range of 1900 to 2800 kg/m³ (Aali et al., 2019). However, they are heavier in comparison to the fine aggregate particles. The larger proportion of fine particles and a smaller proportion of medium and coarse sand make CBA differ somewhat from the fine aggregate. The large diversity in the characteristics of CBA is due to variations in sources, combustibles, the kind of fuels utilized, and the duration of the burning. The physical properties of CBA can be varied by pulverization or grinding CBA particles through different grinding processes as demonstrated in Figure 2.5 (A3, A4) (Ankur & Singh, 2021; Rafieizonooz et al., 2016).

The physical properties of CBA can be varied by pulverization or grinding CBA particles through different grinding processes. With increasing grinding time, the specific gravity and specific surface area of CBA particles increase (Hannan et al., 2017). Likewise, another study by Mangi, et al. (2019) reported a continuous change in the properties of the specific surface area and specific gravity can be seen when the grinding period is increased. After up to 40 hours of grinding, the specific gravity and specific surface recorded values of (2.36–3.10), (2347–4870 cm²/g), respectively. Notwithstanding the increment in the specific surface area and specific gravity of the CBA particles after grinding, the value of sum alumina, active silica, and ferric oxide improved to be 70 to 80%, indicating a considerable increase in the pozzolanic reactivity of CBA particles.

Overall, the lower specific gravity of CBA compared to cement is primarily due to the differences in their chemical compositions and physical structures. CBA is a by-product of coal combustion in thermal power plants, and it typically contains a significant amount of porous, lightweight particles. This porosity results from the combustion process, where inorganic components of coal melt and solidify into porous structures. The specific gravity of CBA typically ranges from 1.8 to 2.9, whereas the specific gravity of cement is around 3.15. In contrast, cement is a manufactured product composed mainly of calcium silicates, aluminates, and ferrites, which are denser and have a more uniform, solid structure. The higher density of these compounds results in a higher specific gravity for cement. Additionally, the production process of cement involves high-temperature kilning, which leads to the formation of dense clinker minerals that further contribute to its higher specific gravity. In Table 2.6 the widely tested physical characteristics of CBA are included, which are specific gravity (SG), fineness modulus (FM), and water absorption (%). The application had been implemented according to different authors.

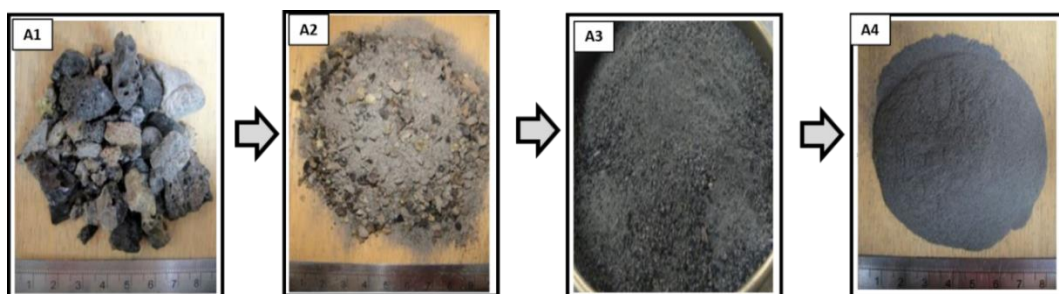


Figure 2.5 CBA collected from thermal power plant was classified as A1) and A2) Original CBA and A3), A4) various sizes after grinding process

Source: Ankur & Singh, (2021)

Table 2.6 Physical characteristics of CBA

Authors	Specific Gravity (SG)	Water Absorption (%)	Fineness Modulus (FM)	Application of CBA
(Mangi et al., 2019)	2.4	-	-	Substitute for cement in concrete
(Mangi et al., 2019)	2.5	-	-	Substitute for cement in concrete
(Khongpermgoson et al., 2019)	2.9	-	-	Substitute for cement in concrete
(Sanjuán et al., 2019)	2.1-2.5	6.8	1.5	Substitute for cement in concrete
(Mangi et al., 2018)	2.2	-	-	Substitute for cement in concrete
(Brake et al., 2018)	2.8	-	-	Substitute for cement in concrete
(Argiz et al., 2018)	2.7	-	-	Substitute for cement in concrete
(Nghopok et al., 2018)	2.2	-	2.8	Substitute for cement in concrete
(Abdulmatin et al., 2018)	2.1	--	2.3	Substitute for cement in bricks
(Vinai et al., 2017)	2.2	-	-	Substitute for cement in blocks
(Kim et al., 2017)	1.7	-	-	Substitute for cement in concrete
(Oruji et al., 2017)	2.8	-	-	Substitute for cement in mortar
(Hanjitsuwan et al., 2017)	2.1	-	-	Substitute for cement in mortar
(Aydin, 2016)	1.4	-	-	Substitute for cement in brick
(Jang et al., 2016)	1.9	-	-	Substitute for cement in mortar
(Ahn et al., 2016b)	1.9	4.1	5.6	Substitute for cement in mortar
(Kim et al., 2015)	1.8	5.4	2.1	Substitute for cement in concrete
(Ibrahim et al., 2015)	2.6	1.0	2.9	Substitute for cement in mortar
(Naganathan et al., 2015)	2.1-2.7	-	-	Substitute for cement in bricks
(Luna et al., 2014)	2.0	-	-	Substitute for cement in ceramic bricks
(Topçu et al., 2014)	2.2	-	-	Substitute for cement in mortar

2.3.5.2 Chemical Composition

The chemical composition of CBA in previous studies are illustrated in Table 2.7. The chemical composition of the CBA samples were investigated by different researchers using X-ray fluorescence (XRF) and X-ray diffraction (XRD) analysis, respectively, to determine the pozzolanic materials containing $\text{SiO}_2 + \text{Al}_2\text{O}_3 + \text{Fe}_2\text{O}_3$ content. According to several previous research Al-Amoudi et al., (2022); Becerra-Duitama & Rojas-Avellaneda, (2022), pozzolanic is composed of siliceous and aluminous components that react with calcium hydroxide in the existence of water to form cementitious materials. The amount of pozzolanic activity is assessed in terms of its reaction with $\text{Ca}(\text{OH})_2$. The reaction occurred mostly due to pozzolanic which contains silica, alumina, and ferric iron. The sum of silica or alumina and ferric iron should be higher than 70% in accordance with ASTM C618, (2019). Generally, pozzolanic materials are added to portland cement (PC) to increase its performance. The enhancement in quality occurs as a result of the pozzolanic reaction between calcium $(\text{OH})_2$ and silica in the presence of water, to the formation of calcium silicate hydrate (C-S-H) (Wu et al., 2017). However, according to (Massazza, 2003), the total quantity of calcium hydroxide involved in the pozzolanic reactions depends on various aspects like curing length, ratio of the $\text{Ca}(\text{OH})_2$ to pozzolan, silica content in the reactive phase, and pozzolan content in the reactive phase. The reaction's inactivity of the pozzolanic material of the $\text{Ca}(\text{OH})_2$ is high. Many factors have been attributed to this, such as the pozzolan's surface area, content of cement alkaline, temperature, as well as water/solid ratios. Often, the material's pozzolanic action can be calculated by physical, chemical, and mechanical techniques. CBA retains a higher reactive fraction with extra pozzolanic characteristics (Yin et al., 2018). CBA particles consist of silica, alumina, and iron and are categorized as a pozzolanic material according to (ASTM C618, 2019). The CBA particles contain a higher amount of SiO_2 and are naturally hydrophilic (Ahmad et al., 2010; Arickx et al., 2010; Sadon et al., 2017). In general, the SiO_2 content of CBA can greatly affect the forming of (C-S-H) gels in cement, as well as concrete after hydration (Oruji et al., 2017). On the other hand, the large particle size of CBA results in a low level of pozzolanic reactivity (Kim & Lee, 2016). Hence, grinding CBA to a smaller particle size would enhance the reactivity of the silica. It is thought that earlier studies attempted to use CBA in its natural condition without processing it, emphasizing on energy savings and simplicity of usage to increase its appeal to concrete producers. In CBA, carbon is produced due to ineffective

combustion in incinerators or boilers (Kadir et al., 2016). However, this varies based on the coal exporter, as well as the conditions of processing and operation, which mainly contains alumina, silica, and ferric oxide. These are the key chemical components in a calcined, natural pozzolanic that is used in concrete by standard guidelines (ASTM C618, 2019). Based on the literature, the sum of the three compounds is in the range of 56.10% to 95.4% of the total chemical composition, with a maximum of 0.3 to 11.86% LOI content. (Mangi et al., 2018; Rafieizonooz et al., 2016). Data based on previous studies showed that CBA is a pozzolanic substance for a specified class 'C' or specified class 'F' according to (ASTM C618,2019).



اونيورسيتي مليسيا قهغ السلطان عبدالله
UNIVERSITI MALAYSIA PAHANG
AL-SULTAN ABDULLAH

Table 2.7 Chemical composition properties of CBA

Authors	Chemical Composition (%)												
	SiO ₂	Al ₂ O ₃	Fe ₂ O ₃	CaO	Na ₂ O	MgO	SO ₃	K ₂ O	Mn ₂ O ₃	TiO ₂	P ₂ O ₅	LOI	Sum of SiO ₂ , Al ₂ O ₃ , and Fe ₂ O ₃
(Mangi et al., 2019)	52.50	17.65	8.30	4.72	-	0.58	0.84	-	-	2.17	-	4.01	78.450
(Aydin, 2016)	55.1	28.1	8.3	1.1	-	0.3	0.3	1.5	-	-	-	3.9	91.50
(Khongpermgonson et al., 2019)	35.6	19.6	14.9	18.7	-	2.4	1.7	2.3	-	-	-	3.6	71.10
(Ghafoori & Bucholc, 1996)	41.70	17.10	6.63	22.5	1.38	4.91	0.42	0.40	1.27	1.27	1.27	1.13	65.43
(Luna et al., 2014)	64.45	15.89	7.77	3.92	0.89	2.45	< 0.01	1.60	-	-	< 0.01	11.86	88.31
(Ibrahim et al., 2015)	34.10	9.31	12.39	-	0.12	5.28	0.91	0.51	-	-	-	-	55.80
(Naganathan et al., 2015)	56.0	26.7	5.80	0.80	0.20	0.60	0.10	2.60	-	1.30	-	4.60	88.50
(Mangi et al., 2018)	53.80	18.10	8.70	5.30	-	0.58	0.90	-	-	1.20	-	4.02	80.60
(Ahn et al., 2016b)	49.90	29.30	10.50	1.64	-	-	-	4.69	-	2.83	-	-	89.70
(Jang et al., 2016)	44.20	31.50	8.9	2.0	-	2.6	-	-	-	2.4	-	-	84.60
(Yoon et al., 2019)	54.0	23.4	8.9	7.8	0.8	1.3	0.3	0.6	-	-	-	-	86.30
(Argiz et al., 2018)	52.4	27.5	6.6	2.4	0.36	1.83	-	3.48	-	0.97	0.12	42.7	86.50

Table 2.7 Continued

Authors	Chemical Composition (%)												
	SiO ₂	Al ₂ O ₃	Fe ₂ O ₃	CaO	Na ₂ O	MgO	SO ₃	K ₂ O	Mn ₂ O ₃	TiO ₂	P ₂ O ₅	LOI	Sum of SiO ₂ , Al ₂ O ₃ , and Fe ₂ O ₃
(Hanjitsuwan et al., 2017)	26.17	15.79	14.21	28.51	1.05	2.98	1.50	1.43	-	0.31	0.25	7.68	56.10
(Abdulmatin et al., 2018)	35.6	19.6	14.9	18.7	1.2	2.4	1.7	2.3	-	-	-	3.6	70.10
(Topçu et al., 2014)	51.51	18.76	9.57	5.08	0.52	0.93	0.007	2.56	-	-	0.07	10.85	79.84
(Oruji et al., 2017)	58.7	20.1	6.2	9.5	0.1	1.6	0.4	1.0	-	-	-	0.8	86
(Sanjuán et al., 2019)	54.60	28.80	5.30	1.40	0.37	1.89	-	3.72	-	1.03	0.17	2.30	88.70
(Wongkeo et al., 2012)	44.56	22.48	14.93	10.54	0.77	2.54	0.65	1.76	0.12	0.46	0.19	1	81.97
(Jaturapitakkul & Cheerarot, 2003)	48.12	23.47	10.55	11.65	0.07	3.45	1.76	3.45	0.07	-	-	4.02	82.14
(Hopkins & Oates, 1998)	79.8	11	4.6	2.5	0.34	0.8	0.05	0.67	0.08	-	-	0.3	95.40
(Menéndez et al., 2014)	49.97	26.95	8.34	8.28	0.14	1.12	0.11	0.78	0.05	2.25	0.95	1.85	85.26
(Kizgut et al., 2010)	61.36	21.86	6.78	2.55	0.44	2.1	-	3.5	-	1.03	-	1.75	90

2.3.6 Microstructure

The microstructure of CBA in applications such as cement, concrete or mortar can be observed by scanning electron microscopy (SEM) and field emission scanning electron microscope (FESEM). An observation of the morphology produced changes from the shape of the raw material into the shape of a hydrated calcium silicate hydrates (C-S-H) gel. In addition, cracking and various shape changes were observed in the samples. Furthermore, the pozzolanic reaction degree draws upon pozzolanic characteristics, including chemical composition, surface area, as well as active phase materials (Embong et al., 2016; Mertens et al., 2009). Several previous (Singh & Bhardwaj, 2020; Zhou & Shen, 2020) investigations have demonstrated that silicon dioxide (SiO_2) and aluminium oxide (Al_2O_3) are the major elements in CBA due to their additional pozzolanic characteristic, which is identical to that of FA generated in a thermal power plant. These elements compound interact with calcium hydroxide during the hydration process of cement to create further C-S-H as displayed in Figure 2.6 (A1 and A2) by (Mangi et al., 2019; Rafieizonooz et al., 2016), the morphology of sharp, irregular, porous, and spherical CBA particles are shown in Figure 2.6. The CBA was collected and dried in the oven at a temperature of $110 \pm 5^\circ\text{C}$ and ground using a ball mill grinder machine to make it finer. The chemical properties showed that CBA predominantly contains $\text{SiO}_2 + \text{Al}_2\text{O}_3 + \text{Fe}_2\text{O}_3$. Moreover, the grinding of CBA to a lower size resulted in increasing the specific surface area lead to improve the pozzolanic reaction (Mangi et al., 2019).

The grinding CBA mix has finer particles and a more densely packed C-S-H gel compared to the samples without CBA based in concrete and mortar. Based on the microstructure analysis by (Mangi et al., 2019; Oruji et al., 2017), the influence of CBA was observed after being used as a substitute substance for cement in concrete, and mortar. (Oruji et al., 2017) performed a microstructural analysis to evaluate the chemical composition of C-S-H compound contained in CBA in the cement mixture. The findings identified that hydrated CBA samples at 28 days had a lower and more densely packed C-S-H compared to conventional mix samples. It was also observed that the pore size was lower in the samples containing CBA in the blended cement mixture. This is due to the incomplete pozzolanic reaction that led to lower calcium to silica ratios of the C-S-H compound in the hydration process at 28 days of curing as shown in Figure 2.6 (B1). Moreover, this incomplete pozzolanic reaction decreased the strength in this curing age. According to a study by Mangi et al. (2019), SEM analysis was carried out for concrete containing CBA at 56 days of curing. The findings showed that the pozzolanic reaction started at the late age of curing at 56 days. Nevertheless, it was observed that the

pozzolanic reaction of CBA with calcium hydroxide led to a good form of C-S-H. The formation of C-S-H gel was discovered in the concrete containing ground CBA, which could substantially fill the voids in the concrete and lead to the strength development as shown in Figure 2.6 (B2).

Additionally, CBA contains fractions of mullite vitreous (Massazza, 2003). Kurama & Kaya, (2008) showed CBA-based in concrete containing CBA microstructural characterization. A microstructural analysis was conducted via XRD and SEM analysis to examine various combinations of concrete which contain CBA as a replacement (0 to 25%) of cement replacement. The microstructural analysis of various incorporation exhibited the existence of further reactive silica in CBA, thereby resulting in additional C-S-H gel formation. The improved dissolvability of CBA has been proven beneficial for cement-based composites, according to the estimate of reactive silica obtained by the XRD analysis (Kurama & Kaya, 2008).

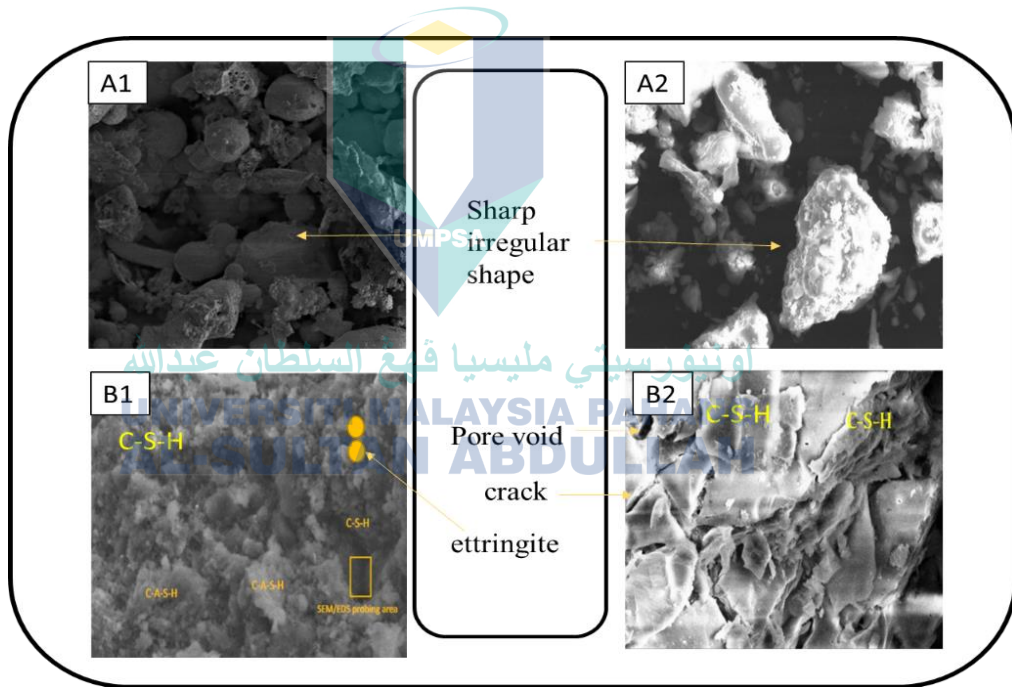


Figure 2.6 A1 and A2 SEM images of grinding CBA and dried before used, B1 and B2 CBA after used in mortar and concrete with magnification 1000x

Source: Mangi et al., (2019)

2.3.6.1 Pozzolanic Reactivity of CBA

Generally, the ability of the pozzolanic reaction of materials is the capability to act with $\text{Ca}(\text{OH})_2$. Also can be defined as a measure of the degree of time or reaction rate between pozzolan and Ca^2 or calcium hydroxide ($\text{Ca}(\text{OH})_2$) in the presence of water. The level of pozzolanic reaction depends on the pozzolan's specific properties, such as specific surface area, chemical composition and active phase materials (Mertens et al., 2009). According to past studies by Rafieizonooz et al., (2016); Mangi et al., (2019c) were observed that the irregular, sharp, spherical and porous particles morphology of CBA as shown in Figure 2.7. The CBA was collected and dried in the oven at 110 ± 5 and grinded by using ball mill grinder machine to make it finer. Moreover, the chemical properties indicated that CBA mainly contained $\text{SiO}_2 + \text{Al}_2\text{O}_3 + \text{Fe}_2\text{O}_3$ (Mangi et al., 2019f). Furthermore, the smaller size particles of CBA lead to increases the specific surface area necessary to improves pozzolanic reaction (Mangi et al., 2019d). The microstructure results of the utilization of CBA to replaces cement in concrete. Also, it was observed when increase the percentages of CBA in concrete shows increase the size and number of pores in concrete mixture as shown in Figure 2.8 (Oruji et al., 2017; Mangi et al., 2019b). However according to Massazza et al. (2003) it was reported the total quantity of calcium hydroxide associated with pozzolanic scanning includes various aspects such as length of curing, silica content of reactive phases, ratio of $\text{Ca}(\text{OH})_2$ to pozzolan and reactive phase content of pozzolan. The hesitation of reaction for pozzolanic materials with $\text{Ca}(\text{OH})_2$ is also highly due to many factors affect such as the surface area of pozzolan, cement alkaline content, temperature and water to solid ratio. The pozzolanic action of material is usually calculated by chemical, physical and mechanical methods (Massazza, 2003).

It has been mentioned that CBA has a high reactive fraction along with additional pozzolanic characteristics. Additionally, CBA contains fractions mullite vitreous fractions. Kurama et al. (2008) CBA-based concrete microstructural characterization. The microstructural analysis was performed using SEM and XRD analysis on various concrete combinations containing CBA as a substitution (0 to up to 25%) of cement replacement, the microstructural analysis result of various incorporation shows the presence of more reactive silica in CBA, resulting in more C-S-H gel forming. Also stated that the estimation of reactive silica obtained by XRD analysis specifies the improved dissolvability of CBA, which later proved beneficial for cement-based composites (Kurama & Kaya, 2008).

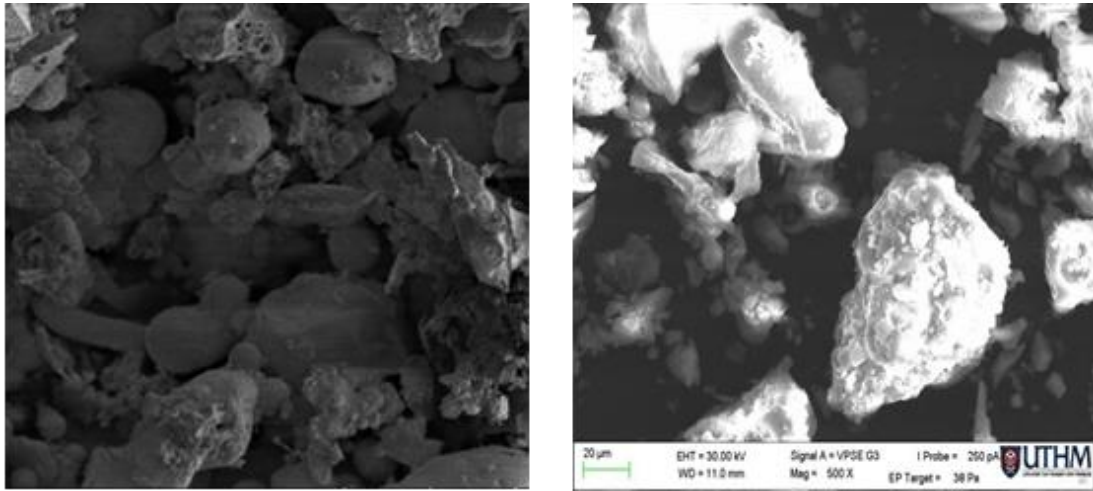


Figure 2.7 SEM images CBA shape grinded and dried before curing
 Source: Rafieizonooz et al., (2016)

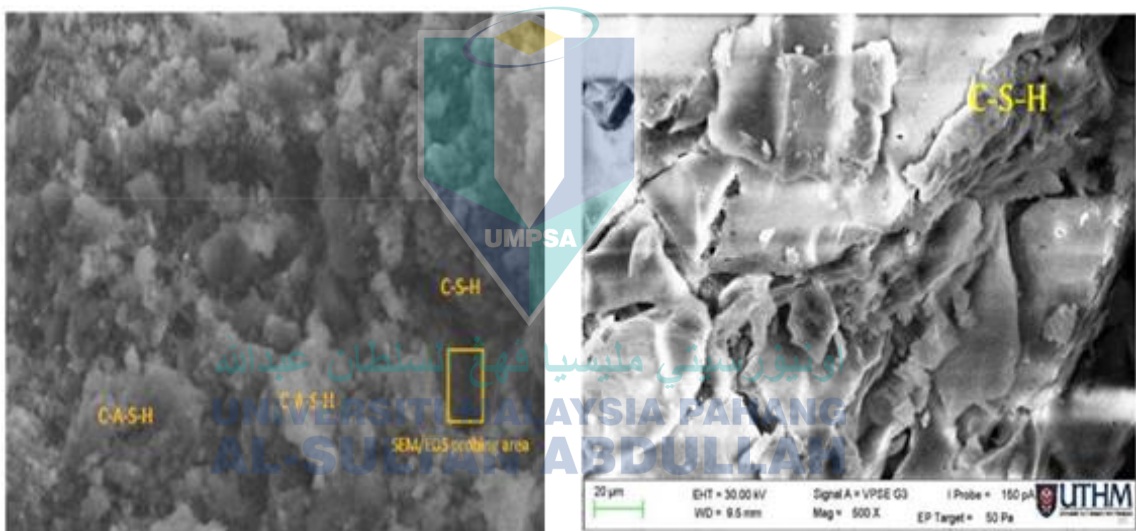


Figure 2.8 Samples contain CBA in concrete after hydration and curing 28 days
 Source: Oruji et al., (2017)

2.3.6.2 Mineralogical characteristics

The burn temperature and cooling rate are critical parameters in the incineration phase that greatly affected the CBA microstructure. From the Figure 2.9 it can be observed the SEM images obtained when increased magnification of the samples for the different magnification range from up to 20 um (Asokbunyarat et al., 2015). The SEM image as can be shown in Figure 2.10 can be categorized the particles of CBA into three categories such as Fine parts of crushed bottom CBA, huge spherical as FA particle, and

FA classes. The popular particles, though, look like the first form. The particular part of CBA the same joint with FA particles in which the larger particles were observed unevenly on the outside surface (Marto et al., 2010).

Kurama & Kaya, (2008) examined the CBA mineralogical analyses. X-Ray Diffraction (XRD), model S 5000 diffractometer, recorded crystalline mineral phases with nickel-filtered. Also, the result shows CBA had a relatively natural mineralogy comprising such as alumina, glass and crystalline phases of quartz, ferrite spinel, and calcite as can be seen in the Figure 11 (Kurama & Kaya, 2008). Furthermore, another pervious study was reported endorsed by Gorme et al. (2010) the microstructural analysis for CBA. The results show subsistence of mullite silicon oxide and silicon phosphates are essential crystalline forms which can be existent in CBA. The aforementioned examination also reported that silica was found partially in the crystalline quartz shapes and in Al as mullite mixture (Gorme et al., 2010). The existence of iron was observed in the form of oxide magnetite and hematite, encountered similar results by (Marto et al., 2010).

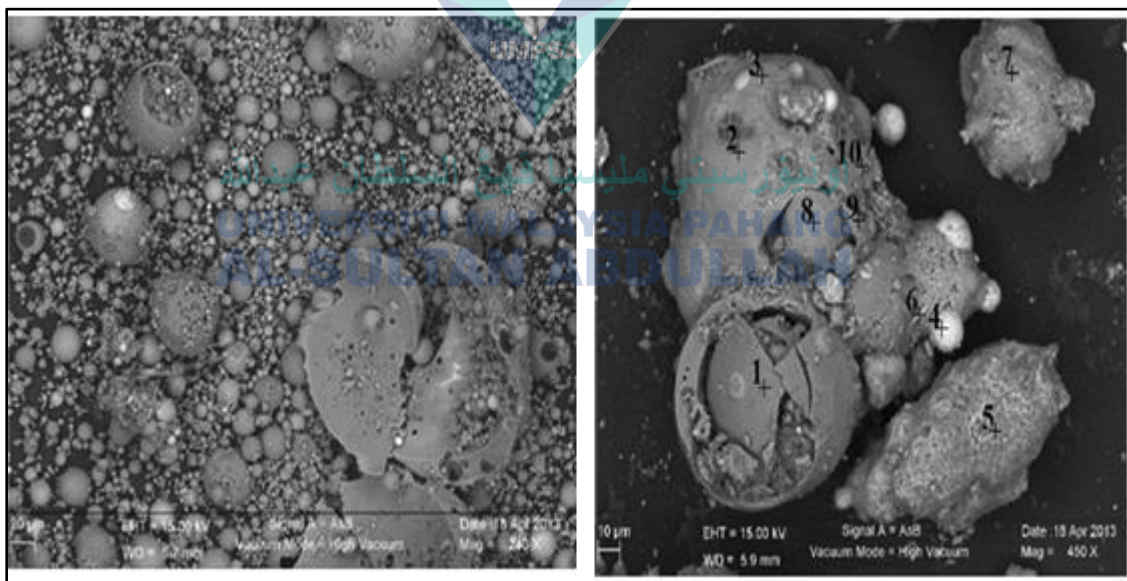


Figure 2.9 FESEM images for CBA with magnification range up to 20 µm

Source: Asokbunyarat et al., (2015)

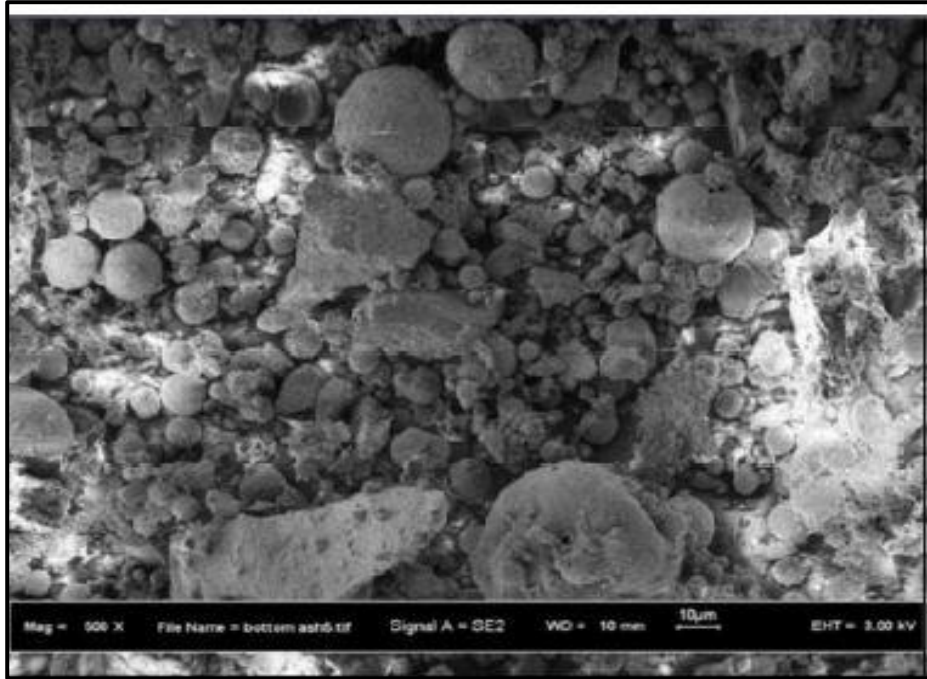


Figure 2.10 SEM photomicrographs for CBA categories
 Source: Marto et al., (2010)

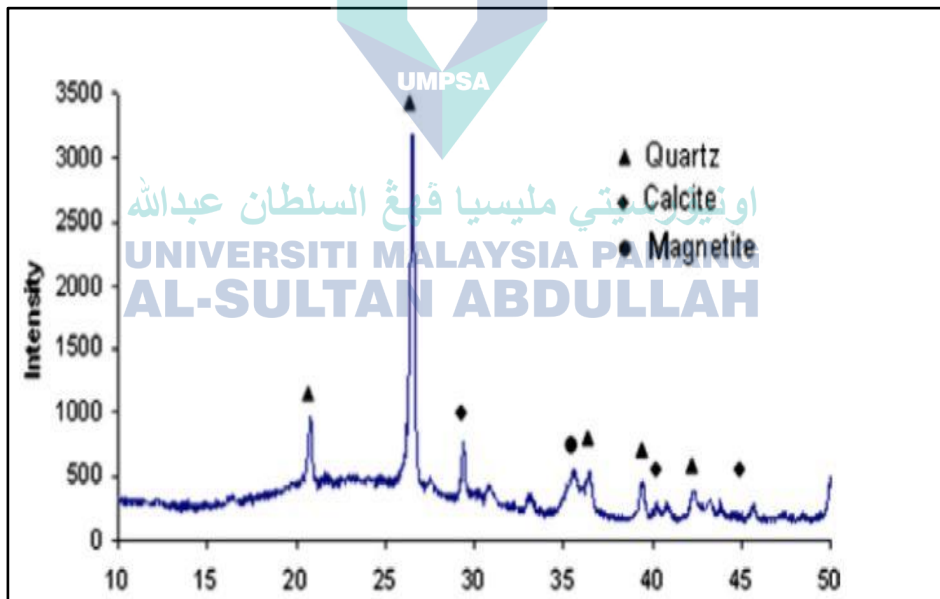


Figure 2.11 XRD for CBA element composition
 Source: Kurama & Kaya, (2008)

2.3.7 Utilization of CBA in Concrete

The following sub-sections discussed the potential use of CBA in concrete production that is associated with the aggregate or cement replacement.

2.3.7.1 CBA as Cement Replacement Materials in Concrete

CBA is used in concrete admixtures to enhance the performance of concrete. Portland cement contains about 65% lime. Some of this lime becomes free and available during the hydration process. When CBA is present with free lime, it reacts chemically to form additional cementations materials, improving many of the properties of the concrete (Siddique, 2014). Several researchers have investigated the CBA as cement replacement in concrete in their studies (Mangi et al., 2018; Abubakar & Baharudin, 2012; Khan & Ganesh, 2016) carried out experimental research in concrete on the effects of original and grinded of CBA. They based on the compressive strength efficiency of concrete cubes (150mm x 150mm x 150mm) including original BA (OBA) and ground (GBA) replacing cement for 7, 14, 28, 56 and 90 days. Where M1 is the control specimen, M2, M3 & M4 represent CBA and M5, M6 & M7 represent a GBA substitution of 10%, 20%, and 30% respectively for cement. After 28 days, concrete containing bottom ash (BA) gains more strength compared to the control mix due to the pozzolanic reaction between the BA and calcium hydroxide. Ground bottom ash (GBA) concrete gains more strength than ordinary bottom ash (OBA) concrete because GBA has a higher pozzolanic activity. At 56 days, the strength of GBA concrete with 10% replacement (M5) surpasses the control mix (M1) due to the ongoing pozzolanic reaction. However, at the same 10% replacement level, OBA concrete (M2) has less strength because it is coarser, with more voids, and therefore a lower pozzolanic reaction. Mixes M6 and M7, as well as M3 and M4, have lower strength compared to M5 and M2 respectively, because these mixes contain less cement and more BA, resulting in less available calcium hydroxide for the pozzolanic reaction, leading to reduced strength. The compressive strength of CBA-containing concrete as compared to control specimen was given in Figure 2.12.

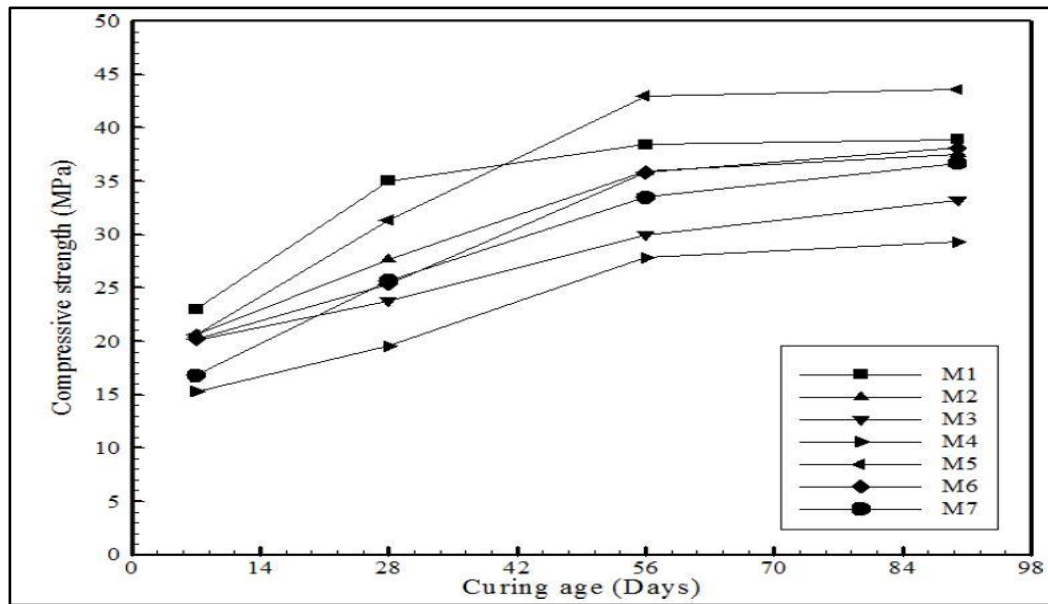


Figure 2.12 Compressive strength of CBA in concrete at various curing period

Source: Khan & Ganesh, (2016)

2.3.7.2 CBA as aggregate replacement materials in concrete

Based on previous researchers, studies several waste materials such as FA, silica fume, and cement may be used in the building industry. Concrete is one of the most frequently used building materials. The main materials that constitute such as cement, aggregates (gravel, and sand). Natural of river sand resources are becoming minimize gradually limited. The shortage of river sand has caused the cost of concrete production to rise. In Malaysia the building industry is plagued because finite availability and high prices for river sand production. On the other hand, thermal power plants have been accumulating an enormous quantity of CBA from decades. Deposits of CBA wastes are charming a severe environmental hazard for the surrounding community. According to the environmental problems posed by CBA. So, several previous researchers have been reported encouraging results on use of CBA either as partial or as total alternative of river sand in concrete.

Cherief et al. (1999) in the experimental work noticed the strength activity index of CBA with Ordinary Portland cement after 28 and 90 days of hydration was 0.88 and 0.97 respectively. These values are higher than 0.75 at 28 days and 0.85 at 90 days, required by the European standard BS EN 450-1, (2012). The larger value of strength activity index points out that the pozzolanic activity of CBA is a suitable in reaction in

concrete mixture. They also reported that pozzolanic activity of CBA starts at 14 days and consumption of calcium hydroxide was significant after 90 days of hydration (Cheriat et al., 1999).

Furthermore, Kim et al. (2016) reported that CBA could be utilized as aggregates in high-strength concrete. They examined high concrete's workability and mechanical properties and observed that CBA would have more impact on flexural strength than compressive strength. And also, and in their research, CBA is a possible replacement material for sand in concrete (Kim et al., 2016). In similarly, Singh & Siddique, (2016); Aggarwal & Siddique, (2014) reported that concrete properties incorporating high amounts of CBA as sand replacement were also examined. They found that CBA utilized in concrete at 28 days of curing, ultra-pulse speed and compressive strength were not affected (Singh & Siddique, 2016). According to several previous studies by (Aggarwal & Siddique, 2014; Singh & Siddique, 2016) examined the microstructure and properties of concrete incorporating CBA have been examined as a substitute for natural concrete sand. Singh and Siddique et al. (2016) studied the drying shrinkage and compressive strength of concrete containing CBA as total or partial replacement of fine aggregate. They reported that after 90 days of curing period, the compressive strength of CBA concrete outstripped that of normal concrete. Moreover, they found that drying shrinkage of CBA concrete mixtures reduced with increase in CBA content in concrete (Aggarwal & Siddique, 2014; Singh & Siddique, 2016).

The use of CBA in concrete also involves some advantages and disadvantages, which also have been summarized and provided in Figure 2.13. The fact that the CBA can be used in two ways either in original or powder (after careful grinding) was well known. The original coal base ash was commonly used in the concrete construction as a substitute for natural sand. However, the powdered form of CBA is very limited. Since the conversion of original coal base ash into ground CBA is needed by the CBA systemic grinding process. So, few studies of CBA as a partial cement substitute have been published. It can therefore be summarized, from available literature that CBA provides major advantages over the initial CBA. The key benefit is that applying ground CBA in concrete will substantially reduce chloride penetration and decreased environmental burden. In addition to for instance, some slight drawbacks, it decreases early strength and absorbs more water during the preparation of concrete mixtures.

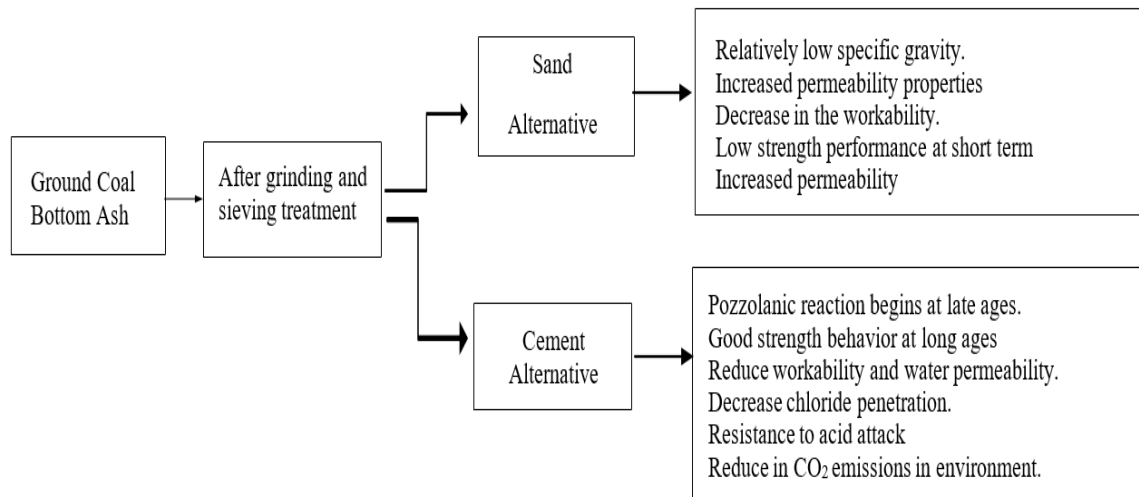


Figure 2.13 Summary of advantages and disadvantages of CBA in concrete application as investigated by researchers

Source: Aggarwal & Siddique, (2014); Singh & Siddique, (2016)

2.4 Properties of Concrete Containing CBA in SCC

The next sub-sections discuss the fresh and mechanical properties of self-compacting concrete (SCC) incorporating CBA as fine aggregate.

2.4.1 Fresh Properties of SCC Incorporating CBA

As displayed in Table 2.8, previous studies reported the results of fresh properties tests of CBA as fine aggregate replacement in the SCC, showing the range of fresh properties and the impact of adding varying ratios of CBA substitution in SCC.

Table 2.8 Fresh properties of SCC containing CBA as sand replacement reported by previous researchers

References	CBA replacement (%)	w/b	Superplasticizer (%)	Fresh concrete properties			
				Slump flow (mm)	L-box (H2/H1)	V-funnel (s)	J-ring (h2-h1 mm)
(EFNARC, 2005)	–	–	–	650–800	0.8–1	–	–

Table 2.8 Continued

References	CBA replacement (%)	w/b	Superplasticizer (%)	Fresh concrete properties			
				Slump flow (mm)	L-box (H2/H1)	V-funnel (s)	J-ring (h2-h1 mm)
(Ibrahim et al., 2015)	0	0.4	0.16 - 0.36	730	0.94	—	—
	10			710	0.859	—	—
	20			640	0.80	—	—
	30			570	0.74	—	—
(Hamzah et al., 2015)	0	0.35	0.16-0.30	730	0.70	—	—
	10	0.40		710	0.8	—	—
	15	0.45		690	0.82	—	—
	20			640	0.85	—	—
	25			600	0.9	—	—
	30			560	0.95	—	—
(Keerio et al., 2021)	0	0.38	1.7- 2.0	740	0.83	7.4	2.5
	10			735	0.85	11.2	4.5
	20			760	0.92	11.89	7.4
	30			755	0.87	10.22	8.7
	40			750	0.89	12	6.8
(Jamaluddin et al., 2016)	0	0.35	0.16-0.32	745	0.90	—	—
	10	0.40		725	0.81	—	—
	15	0.45		708	0.80	—	—
	20			685	0.77	—	—
	25			648	0.70	—	—
	30			625	0.66	—	—
(Kasemchaisiri & Tangtermsirikul, 2008)	0	0.31	1,200 cc/m ³	700	0.83	—	—
	10			680	0.80	—	—
	20			670	0.60	—	—
	30			560	0.50	—	—

Table 2.8 Continued

References	CBA replacement (%)	w/b	Superplasticizer (%)	Fresh concrete properties			
				Slump flow (mm)	L-box (H2/H1)	V-funnel (s)	J-ring (h2-h1 mm)
(Siddique & Kunal, 2015)	0	0.41	1.88 - 2.0	673	0.89	7.50	2.3
	10	-		673	0.80	6.60	4.6
	20	0.55		591	0.95	6.20	4.7
	30			627	0.82	4.0	11.6
(Aswathy & Paul, 2015)	0	0.68	5.16	702	0.99	8	—
	5%			696	0.97	8	—
	10%			676	0.96	10	—
	15%			670	0.9	11	—
	20%			660	0.89	12	—
	30%			640	0.88	12	—
(Zainal Abidin et al., 2014)	0	0.4	0.20	715	0.92	—	—
	5%			705	0.89	—	—
	10%			700	0.84	—	—
	15%			615	0.79	—	—
	20%			560	0.75	—	—
	30%			550	0.65	—	—

2.4.1.1 Slump Flow Test

The slump flow test involves an average diameter of a concrete volume after releasing the conventional slump cone. It can be assessed on a couple of perpendicular sides (EFNARC, 2005). As shown in Figure 2.14, previous research identified the CBA quantity impact on the SCC passing ability. Siddique & Kunal, (2015) studied the SCC fresh properties with the use of CBA at 10%, 20%, 30%, and superplasticizer amount (1.88-2.0%). The results showed that slump flow increased for all the replacement percentages, excluding the one containing 20% CBA and 1.90% of superplasticizer (591mm) (Siddique & Kunal, 2015), as per the guidelines outlined by the standard EFNARC, ranging between (650-800 mm) of SCC (EFNARC, 2005). Increases in the

superplasticizer amount resulted in a higher flow, while increases in the CBA amount resulted in a reduction of slump flow (Siddique & Kunal, 2015). In their study, (Ibrahim et al., 2015) studied the slump flow for SCC and the results revealed a 740-540 mm range and reported a relative difference between various mixes because the flow characteristics of self SCC mixtures contain CBA, which have a higher viscosity than control specimens (Ibrahim et al., 2015). Another study by Keerio et al., (2021) produced various SCC mixes using CBA (10-40%) as a fine aggregate substitute and found that CBA content increased and the slump flow decreased due to the CBA porosity, which, compared with fine aggregate, absorbed more water. The findings of another study, conducted by Hamzah et al. (2015) revealed that the time of slump flow increased with an increase in the CBA replacement content in SCC. Mixtures containing 0-30% CBA content showed slump flow time, ranging between 2 and 5 seconds, i.e., in line with the range outlined by (EFNARC, 2005). The reason is that the CBA's irregular shape lowered interparticle friction with the addition of CBA, which decreased the SCC mixes' viscosity.

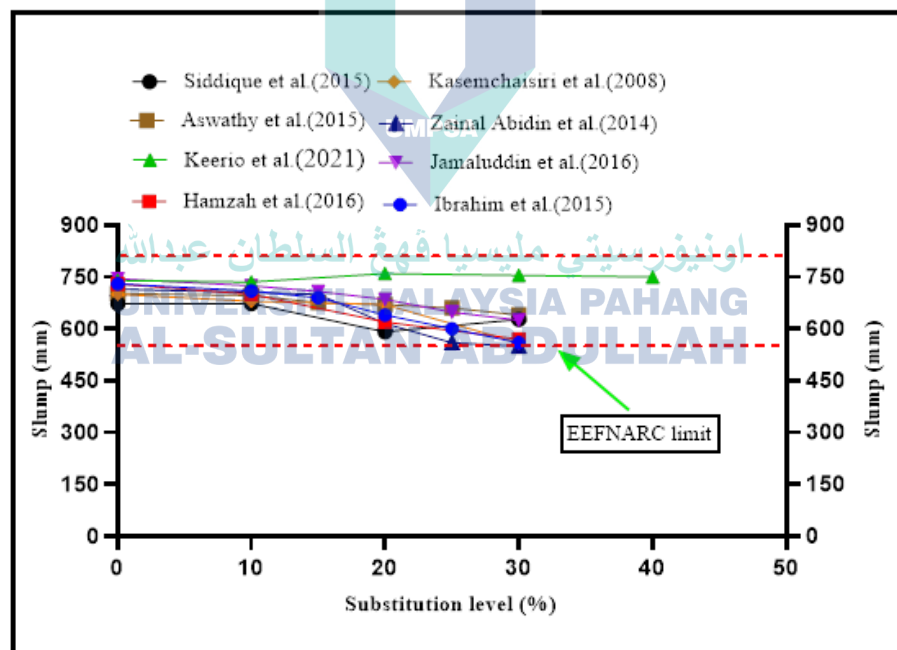


Figure 2.14 Variation of slump values in SCC with varying CBA substitution ratios for sand

Source: Al Biajawi et al. (2023)

2.4.1.2 L-Box Test

The percentage of L-box elevation can be used in tandem with the H2/H1 ratio to define the self-compacting concrete's passing abilities (EFNARC, 2005). Several previous studies examined the effect of CBA quantity on the SCC L-box test, as shown in Figure 2.15. According to study by Kasemchaisiri & Tangtermsirikul, (2008) reported that the L-box passage ratio was between 0.83 and 0.05 and that the value decreased in all mixtures as the CBA percentage in SCC increased. A reduction in the L-box ratio due to the presence of aggregate blockage in a mixture of SCC, containing CBA, was detected and a greater level of inter-particle friction was produced by the CBA particles (Kasemchaisiri & Tangtermsirikul, 2008). Similarly, another study by Jamaluddin et al. (2016) reported a decrease in the L-box test results with increasing the replacement proportion of CBA incorporated into the SCC mixture. Nevertheless, when the w/b proportion increases, the value of the L-box decreases. The results varied between 0.9 and 0.66, indicating that the concrete mixture without CBA had a higher passing ability (Jamaluddin et al., 2016). This is due to the aggregate clogging up in front of apertures, which made it difficult for particles to flow freely without occlusion (Jamaluddin et al., 2016).

Hamzah, et al. (2015) observed that the L-box flow results improved with increasing the CBA proportion in concrete. The ranges of L-box results is between 0.7 and 0.95 (Hamzah et al., 2015). According to Singh, Mithulraj, et al., (2019), an increase was observed in the L-box ratio, thereby increasing the replacement proportion of CBA in the SCC mixture. The value reached up to 1.0 in a 30% of CBA, with a greater value, which showed an improved passing ability (Singh, Mithulraj, et al., 2019). EFNARC standard guideline (EFNARC, 2005) categorized L-box passing ratios as (passing ability 1 (PA1) with two rebars) or (passing ability 2 (PA2) with three rebars). The findings provided by each researcher indicated that the L-box passing ratio is within the acceptable range (EFNARC, 2005).

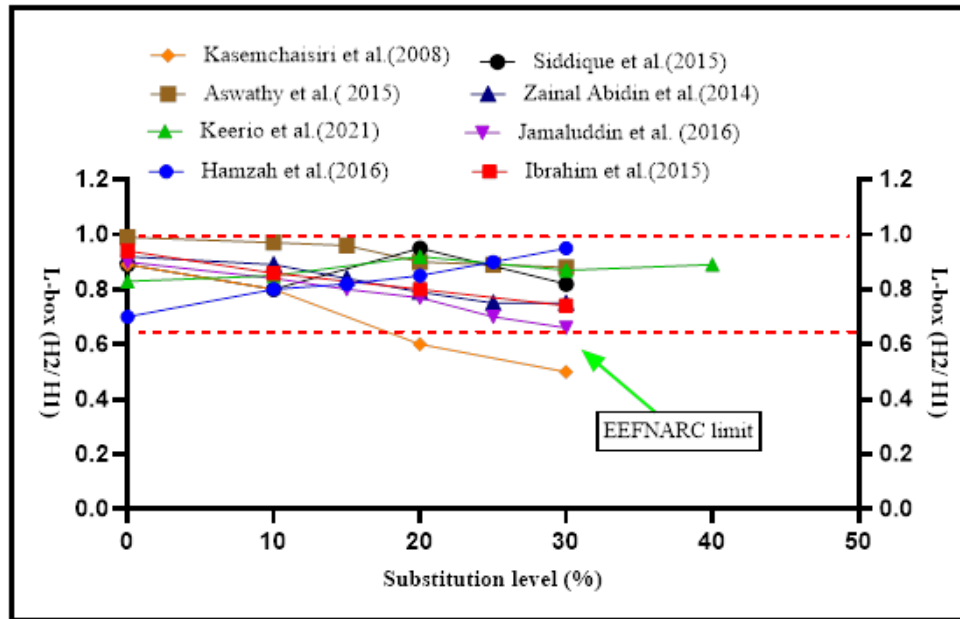


Figure 2.15 L-box values' variation in SCC using varying CBA replacement ratios for sand

Source: Al Biajawi et al., (2023)

2.4.1.3 V-Funnel Test

This conducted test verifies the SCC mixtures' viscosity and flowability. A mixture's better flowability denotes a very short flow time and, as per EFNARC, the V-funnel test's duration ranges between 6 and 12 seconds (EFNARC, 2005). It was established in another previous study that the V-funnel flow time for several types of SCC ranged between 2.5 to 4.6 seconds according to Keerio et al. (2021). They found that the V-funnel flow time of SCC increases as the replacement ratio of CBA increases. They also confirmed that a high quantity of superplasticizer is required for producing SCC when CBA is combined with metakaolin, as compared to SCC made without any replacement materials (Keerio et al., 2021). Likewise, Aswathy & Paul, (2015) observed an increment in the V-funnel value as the percentage content of CBA increased due to increase the duration. The finding of V-funnel value between 8 and 12 seconds, signifying an enhanced passing ability (Aswathy & Paul, 2015). The EFNARC standard guideline (EFNARC, 2005) categorized V-funnel flow time into two categories: VF1 (8s), and VF2 (9–25s) (EFNARC, 2005). According to the findings obtained by each researcher, the V-funnel flow time of certain results falls into the VF1 category, while others fall into the VF2 category (EFNARC, 2005).

2.4.1.4 J-ring Test

The J-ring test, in parallel to the L-box test, can be applied in conjunction with the test of slump flow to ascertain that concrete can pass-through bars, as per (EFNARC, 2005). According to ASTM C1621, (2014), J-ring can be defined as a method of testing concrete's capacity of passing through under its weight, thereby filling spaces, and getting a blocking evaluation ASTM C1621, (2014). The J-ring flow results were reported by Siddique & Kunal, (2015) which ranged between 2.3 and 11.6 mm for various SCC. The results of the J-ring flow of SCC containing CBA rose as the CBA amount increased for all the mixtures (Siddique & Kunal, 2015). Also, based on another study by Keerio et al. (2021) the values of the J-ring ranged between 2.5 to 8.7 mm. As observed, the values increased with an increase in the CBA replacement ratios in the SCC mixture (Keerio et al., 2021).

2.4.1.5 Discussion of finding from fresh Properties

Existing research indicates that the ideal content of CBA is between 10% and 20% to meet the criteria of "filling and passing ability" and "segregation resistance". The dependence of the result depends on the water-binder ratio and the amount of superplasticizer used. An increase in the CBA content has been observed to have a negative effect on processability and segregation. CBA has the potential to be used at 10% to 20% in SCC, meeting standards set by the (EFNARC). Based on the above-mentioned previous studies, it was observed that the key properties of CBA in SCC, namely slump and L-box ratio, show a decrease, while J-ring and V-funnel values increase with increasing substitution ratio of CBA in the concrete mix. The reduction in the freshness properties of the mixture can be attributed to the absorption of moisture content by the CBA particles, resulting in increased friction between the aggregate particles generated by the CBA particles. The conclusions from all of the previous studies support the criteria and limitations established in the SCC standards and recommendations, including the requirements of (EFNARC, 2005).

2.4.2 Mechanical Properties of SCC Incorporating CBA

The next sub-sections discuss the mechanical properties of SCC incorporating CBA as fine aggregate in mixture. The discussion includes compressive strength, flexural tensile

strength, and splitting tensile strength. Table 2.9 presents a summary of the CBA effect on the SCC mechanical properties based on previous studies.



اونيفرسيتي مليسيا قهغ السلطان عبدالله
UNIVERSITI MALAYSIA PAHANG
AL-SULTAN ABDULLAH

Table 2.9 Summary of mechanical properties of CBA as sand replacement in SCC mixes

Reference	Particles of CBA	CBA replacement ratio (%)	Findings		
			Compressive Strength	Flexural Strength	Split Tensile strength
(Siddique et al., 2012a)	Passing through 4.75 mm	0, 10%, 20%, 30%	Decreased for all replacement percentages	-	Decreased for all replacement percentages
(Siddique, 2013)	Passing through 4.75 mm	0, 10%, 20%, and 30%	Reduction for all replacement percentages	-	Decreased for all replacement percentages
(Kumar & Singh, 2020)	Passing through 4.75 mm	0, 10% CBA mixed with 25%, 50%, 75% and 100% recycled coarse aggregate	Decreased for all mixes and all replacement percentages for early age for long term increased in each percentage.	-	Decreased for all mixes and all replacement percentages for early age for long term increased in each percentage.
(N. Singh, Mithulraj, et al., 2019)	Passing through 4.75 mm	0, 10% of CBA mixed with 20% and 30% of FA, and 10% of MK	Increased in all percentages of CBA replacement with RCA up to 50 after that drop in higher percentages	-	A drop in all percentages of replacement expect at 50% of RCA
(Siddique & Kunal, 2015)	Passing through 4.75 mm	0, 10%, 20, and 30%	Decreased in all replacement-percentages at all curing ages	-	Decreased in all replacement percentages at all curing ages
(Jamaluddin et al., 2016)	Passing through 4.75 mm	0,10%,15%,20%, 25%, and 30%	-	Increased by 10% replacement other percentages was decreased as CBA increased	-

Table 2.9 Continued

Reference	Particles size of CBA	CBA replacement ratio (%)	Findings		
			Compressive Strength	Flexural Strength	Split Tensile strength
(Aswathy & Paul, 2015)	Passing through 4.75 mm	5%, 10%, 15%, 20%, 25% , and 30%	Increased by 5% and 10 %, while other percentages were decreased as CBA increased	Increased by 5% and 10%, while the other percentages were decreased as CBA increased.	Increased by 5% and other percentages were decreased as CBA increased.
(Hamzah et al., 2016)	0.075 mm and 20mm	0,10%,15%,20%,25% , and 30%	Increased by up to 10% CBA and other percentages was decreased as CBA increased.	Increased by up to 10% CBA and other percentages were decreased as CBA increased.	Increased by up to 10% CBA and other percentages were decreased as CBA increased.
(Zainal Abidin et al., 2015)	Bigger than 5 mm	0,10%,15%,20%,25% , and30%	Increased by up to 15%, and other percentages were decreased as CBA increased.	Increased by up to 15%, and other percentages were decreased as CBA increased.	Increased by up to 15%, and other percentages were decreased as CBA increased.

Table 2.9 Continued

Reference	Particles of CBA	CBA replacement ratio (%)	Findings		
			Compressive Strength	Flexural Strength	Split Tensile strength
(Keerio et al., 2021)	Passing through 4.75mm	10%,20%,30%, and 40%	Increased in all replacement percentages	Increased in all replacement percentages	Increased in all replacement percentages
(N.Singh, Arya, et al., 2019)	Passing through 4.75mm	10 % CBA, 30 % FA, and 25% to 100 % RCA.	Increased by 10 % CBA with RCA up 50%, and other percentages of RCA with CBA were decreased.	-	-
(Hamzah, Ibrahim, et al., 2020)	Passing through 4.75mm	0,10%,15%,20%,25%, and 30%	Increased by 10% and other replacement percentages were decreased as CBA increased	-	-
(Kasemchaisiri & Tangtermsirikul, 2008)	Passing through 4.75 mm	0 %, 10 %, 20 %, and 30 %	increased by 10% CBA and other percentages were decreased as CBA increased	-	-

2.4.2.1 Compressive strength

Compressive strength along with fresh characteristics are regarded as the significant valuable features of SCC, providing a complete picture of the condition of concrete as they are closely associated with the cement paste structure (Siddique, 2019). Furthermore, the concrete's compressive strength at room temperature is influenced by ambient curing, water-to-cement ratio, aggregate particles size and category, aggregate-paste interface transition zone, categories of admixture, and stress applied (Neville, 2011). Previous researchers Hamzah, Ibrahim, et al., (2020); Hamzah, Jamaluddin, et al., (2020); Kasemchaisiri & Tangtermsirikul, (2008) confirmed the CBA suitable percentages of use in the SCC mix, i.e., 10%-20%; such a percentage improved compressive strength properties. According to study by Siddique et al., (2012a) examined how the compressive strength of the SCC containing CBA and FA can be affected by the utilizing water to powder ratio (w/p). The results showed a comparable behavior with regular SCC when strength was increased by lowering the w/p ratio. SCC showed enhanced strength properties as the w/p ratio decreased, i.e., 0.439 to 0.414 for the 0% CBA, a decrease from 0.50 to 0.47 for the 10% CBA, with a decrease from 0.58 to 0.51 for the 20% CBA, and from 0.620 to 0.546 for the 30% CBA. SCC can be produced at 40-50 MPa compressive strength using various percentages of CBA merged with coal FA between 15% and 30%.

As reported by Kasemchaisiri & Tangtermsirikul, (2008) the SCC compressive strength with CBA is 10%-30%, compared with the control samples without CBA. It was found that 10 % of CBA obtained higher values of compressive strength. The one with percentages were decreased, which can be attributed to delayed pozzolanic reaction, which dominated over the raised porosity. Similar observations were also made by Hamzah, Ibrahim, et al.,(2020), whereby increasing replacement amounts of CBA ranging from 10% to 30% decreased the compressive strength. The decrease was between 54 MPa and 42 MPa at 180 curing days, as demonstrated in Figure 2.16. Another study by Zainal Abidin et al.,(2014) recorded an increased compressive strength up to 15% CBA in the SCC mix. These increased properties of strength revealed that there was a pozzolanic reactivity in SCC containing CBA particles. Compressive strength obtained these increases: 44.30MPa, 50.33MPa, 54.05MPa, 37.90MPa, 36.65MPa for CBA0%, CBA10%, CBA15%, and CBA20%, CBA25%, respectively.

A reduction in concrete strength was obtained by Siddique & Kunal, (2015) throughout the curing initial stages due to CBA's delayed pozzolanic reactivity. However, the concrete strength improved significantly during the long period of curing. The compressive strength in SCC decreased with increasing the water-to-binder ratio and the proportion of CBA replacement. According to the conducted review of previous studies, the behavior of SCC containing CBA can be affected by the percentages of CBA, the superplasticizer inclusion, and the utilized w/c ratio. Therefore, adding a finer size of CBA using appropriate proportions encourages the formation of pozzolanic reactions.

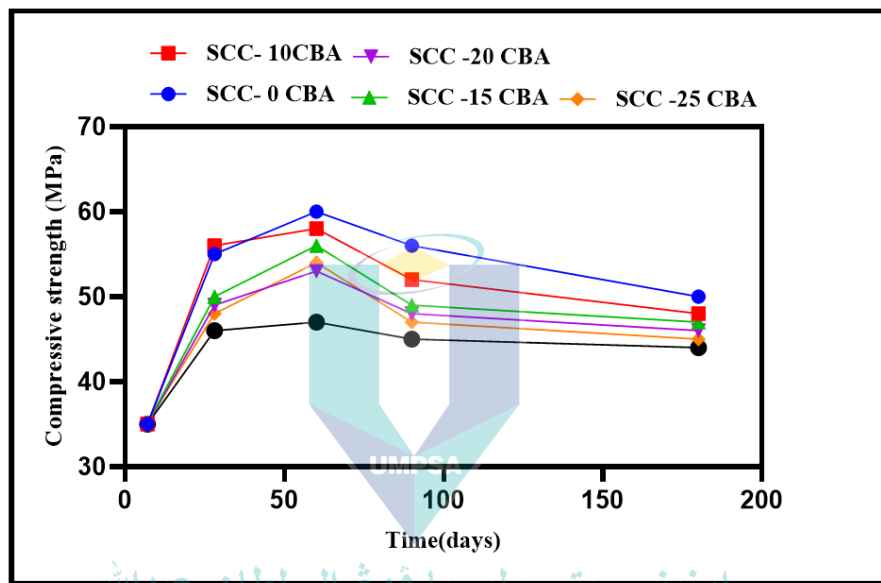


Figure 2.16 The samples' compressive strength with varying replacement percentages for aggregate with CBA in SCC

Source: Hamzah et al., (2020)

2.4.2.2 Flexural strength

According to Jamaluddin et al., (2016), a reduced flexural strength for SCC incorporating CBA was observed at different ages, as exhibited in Figure 2.17. Fine aggregate was substituted with CBA at varying ratios of replacement up to 30%. Furthermore, the optimal percentage of 10% CBA is higher when compared with control samples. The authors reported an increased flexural strength with a higher value of 8.2 MPa with 0.35 w/c during the lengthy time of curing ages. Conversely, the flexural strength was decreased for all water-cement ratios when 15%, 20%, 25%, and 30% alternative of CBA is utilized in SCC (Jamaluddin et al., 2016). Another study by Zainal Abidin et al. (2015) reported that CBA's flexural strength in self-compacting concrete

with 10% and 15% alternative of CBA is greater compared to SCC without the addition of CBA at 7-28 days ages of curing. Furthermore, flexural strength for other replacement percentages was decreased.

Another study by Siddique et al. (2012a) reported that the flexural strength of SCC was decreased as CBA increased. They showed that when the CBA replacement ratio increases, flexural strength drops because of a weaker contact between the cement paste and ashes. According to study by Keerio et al. (2021) the SCC mixes' flexural strength with CBA from (10% to 30%) decreased as the replacement percentages increased at various ages starting from 3 to 180 days of curing in contrast to regular concrete without CBA. The reduction occurred due to low inter-particle abrasion between the aggregate particles, as the CBA particles have spheres formed.

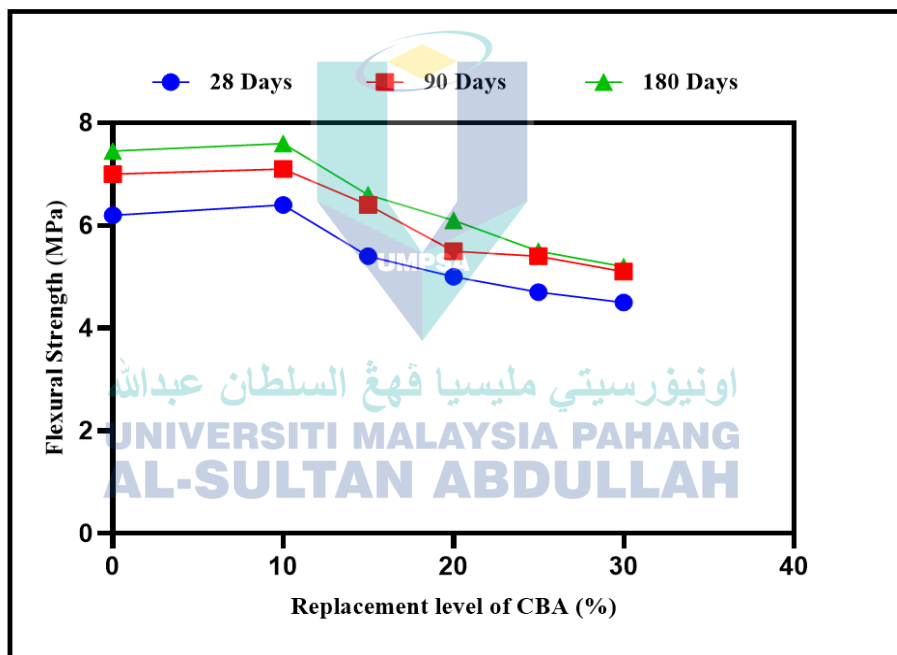


Figure 2.17 Flexural strength of samples with various replacement for fine aggregate ratios of in SCC at different curing ages

Source: Jamaluddin et al., (2016)

2.4.2.3 Splitting tensile strength

Various mechanical characteristics of concrete can be assessed using one of the fundamental and significant characteristics (Ibrahim et al., 2015). The splitting tensile strength of the concrete structures significantly affects the cracking development and size (Ibrahim et al., 2015). Concrete is weak under tension and, therefore, it is essential to

conduct a preliminary assessment of the concrete's splitting tensile strength (Ibrahim et al., 2015). Another study by Siddique & Kunal, (2015) examined the splitting tensile strength of SCC containing 10%, 15%, 20%, 25%, 30% of CBA as a partial replacement for fine aggregate in concrete. There was a decrease in the concrete's splitting tensile strength with increased amounts of CBA at the entire ages of curing due to insufficient interlocking of the fine aggregate particles replacing the fine aggregate with CBA. Similar trend observations were also made by Sandhya & Reshma, (2013), who reported a decrease in the SCC splitting tensile strength with increased CBA replacement percentages, while strength increased with curing ages.

Another study by Zainal Abidin et al. (2015) recorded splitting tensile strengths of 3.6 MPa, 3.75 MPa, 3.9 MPa, 3.5 MPa, 3.4 MPa, and 3.1 MPa at 28 days, in the examined SCC mixture containing CBA 0%, 10%, 15%, 20%, 25%, 30%, respectively. An increase was reported in the splitting tensile strength of the samples as the CBA replacement ratio reached 15%, as shown in Figure 2.18. Similarly, another study by Aswathy & Paul, (2015) reported an increase in the splitting tensile strength as the replacement ratio of CBA reached 10% using a fixed 0.45 w/c ratio. This increased CBA replacement resulted in more porous concrete, having larger pores, which were scattered across the CBA aggregate surface, thereby decreasing its tensile strength (Aswathy & Paul, 2015).

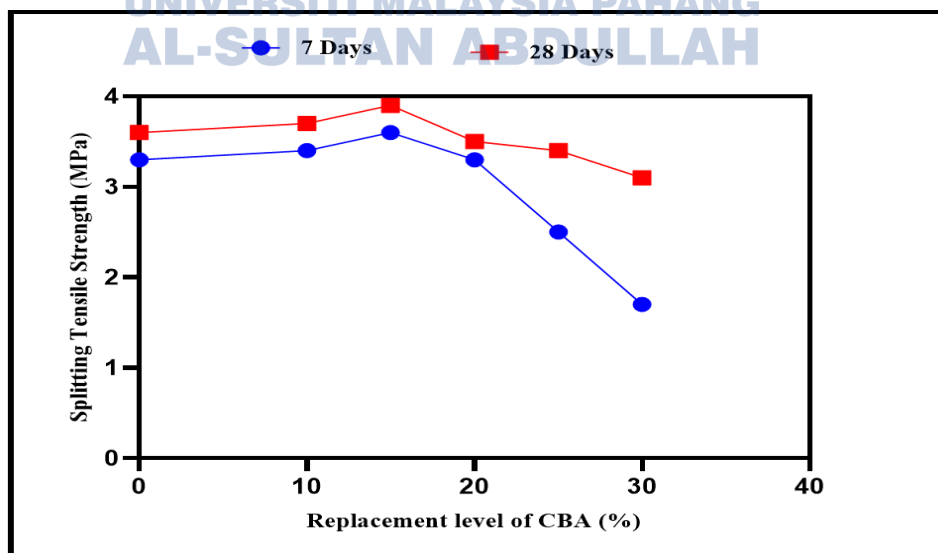


Figure 2.18 CBA samples' splitting tensile strength with varying replacement percentages of fine aggregate in SCC at different curing ages

Source: Zainal Abidin et al.,(2015)

2.4.2.4 Ultrasonic Pulse Velocity (UPV)

The ultrasonic pulse velocity (UPV) test involves the impulse method. It has been utilized for a non-destructive test, which determines the calibers of concrete and selects an appropriate structure survey to determine the degree of cracking or degradation and to evaluate any change in the concrete properties. It is also applied to demonstrate the presence of cracks and voids, evaluate the efficacy of crack repairs, and demonstrate the relative quality and uniformity of concrete. Pulse velocity can be measured by dividing the length by transit time of the samples as mentioned by ASTM C597, (2016). A few studies (Rafieizonooz et al., 2016, 2017) are currently available for assessing the UPV of concrete containing CBA. The study by (Rafieizonooz et al., 2016, 2017) reported that using CBA as a different percentage of cement substitute influenced the ultrasonic pulse velocity of concrete. According to study by Rafieizonooz et al. (2016) reported that pulse velocity decreased with the increasing percentage of CBA as a cement alternative material in the concrete mix. The ranges of quality were from medium to excellent and the ranges of UPV were 3000 to 4300 m/s. The reduction was due to a decrease in permeable pore space. Another previous work Rafieizonooz et al. (2017) reported that ultrasonic UPV decreased with increasing percentages of replacement. The results showed that the UPV values were drastically decreased when the temperature increased. Thus, further research needs to be carried out to generate an adequate ultrasonic pulse velocity of concrete when using CBA as a cement alternative material in the concrete mix. Table 2.10 illustrates CBA percentages and the influence of CBA at varied ratios of substitution in the concrete mix.

Table 2.10 Effect of CBA as a cement replacement on the UPV of concrete

Authors	CBA replacement level (%)	Influence on the UPV with the replacement ratio
(Rafieizonooz et al., 2016)	0, 20	The UPV of CBA as a cement alternative decreased at an early age, but in the long term, it increased with the range from 3900 to 4300 m/s and the range of quality was from medium to excellent.
(Rafieizonooz et al., 2017)	0, 20, 50, 75	The UPV of CBA as a cement alternative material decreased with increased substitution percentages at 91 days of curing; different elevated

Table 2.10 Continued

Authors	CBA replacement level (%)	Influence on the UPV with the replacement ratio
(Rafieizonooz et al., 2017)	0, 20, 50, 75	temperatures led to a drastic reduction in UPV values.
(Naganathan et al., 2015)	0,55, 65,75	The UPV of CBA as a cement alternative increased with the increase of CBA mixed with FA. This is because finer particles filled the porous in concrete mixture.

2.4.2.5 Discussion of finding from Mechanical Properties

The investigation of the influence of the CBA volume in SCC on its strength characteristics revealed that the incorporation of CBA as sand replacement material at levels of up to 10% yielded a significant improvement relative to traditional concrete. Previous research has shown that the incorporation of a modest amount of CBA as sand replacement in SCC has resulted in notable improvements in mechanical parameters, including compressive strength, split tensile strength, and flexural strength. These enhancements have been seen that reach up to 10% in the majority of the results. The increase in strength may be ascribed to the pore refinement effect resulting from the pozzolanic activity of CBA. The use of CBA as sand replacement material leads to an enhanced level of porosity. However, it is worth noting that the presence of silica in CBA particles plays a crucial role in facilitating the synthesis of C-S-H, a gel-like substance that significantly contributes to the development of strength in materials. The observed increase in strength may be attributed to the higher concentration of C-S-H in the SCC samples mixed with CBA. This increase in C-S-H is a consequence of the reaction between the calcium hydroxide produced during cement hydration and the reactive silica present in the CBA.

2.4.3 Durability Properties

Durability of concrete may be defined as the ability of concrete to resist weathering action, chemical attack, and abrasion while maintaining its desired engineering properties (Alexander et al., 2017; Bijen, 2003). Durability refers to a structure's capacity to retain essentially its original performance, strength, and soundness over an extended period of time (Page & Page, 2007). In the construction industries,

durability is one of the most important properties of concrete structure. It is important to produce the concrete with good durability to ensure the concrete structure performs satisfactorily throughout its lifetime (Richardson, 2002; Tayeh et al., 2022). Concrete samples' durability is affected by a variety of parameters, some of which are external and are linked to service circumstances that are beyond the designer's control and should be considered throughout the design process (Bijen, 2003). The following sub-sections present a review on the durability properties of concrete in terms of acid attack, sulphate attack.

2.4.3.1 Acid Attack

Sulfuric acid is one of the most corrosive acids for concrete and, depending on its content and the way it is produced, can cause significant deterioration and damage to concrete structures that come into contact with it. This acid is formed in concrete by the oxidation of iron sulphide minerals such as pyrite or marcasite. Furthermore, acids attack concrete by dissolving the hydrated and un-hydrated compounds of cement paste and removing part of it, leaving soft and weak mass. The intensity of the attack depends on the acidity level. Usually, pH less than 4.5 leads to a severe damage. Concrete permeability, cementitious material content and water to cement ratio are the major factors that influence the resistance to acid attack. This action results in an increase in capillary porosity, loss of cohesiveness and eventually loss of strength. The formation of ettringite leads to an increase in solid volume, resulting in expansion, cracking, and mass loss, particularly when restrained. Concretes are also affected by acid attack due to the exposure to the rain that contains sulphuric acid and nitric acid with pH between 4.0 – 4.5 (Neville, 2011). Due to the alkalinity of cement paste, the acid has the chance to attack the cement and decomposes the cementitious matrix by decalcifying (C–S–H), thus causing strength loss. According to studies Aiken et al. (2022); Zivica & Bajza, (2002), there are several acidic resistance factors of cement-based materials such as kind of acidic, concentration ratio, type of cement, cement content, water cement-ratio, curing condition, pore structure and protective measures. It can be measured based on the alkalinity level in the concrete. For the reaction to occur, the acid reacts with calcium hydroxide (C-H) exists in concrete and produces gypsum. Corrosion of concrete due to sulphuric acid can generally be characterized by the following reactions namely chemical, microbiological, and specific sulphuric acid environment.

Sulfuric acid (H_2SO_4) one of the most acidic can deteriorate the properties of concrete. According to Khan & Ganesh, (2016) reported the influence of CBA as cement replacement at varying percentages of 10%, 20%, and 30% and different ages of curing was investigated. The findings for the effect of CBA when immersed in 1% acid solution are as illustrated in Figure 2.19. Also, it was observed that the grinding CBA had more resistance to acid attacks and sulphate resistance than original CBA as cement replacement in the concrete mixture. According to study by Muthusamy et al., (2021) reported that the influence of concrete containing CBA as partial sand replacement in concrete subjected to H_2SO_4 with 5% concentration solution in the concrete samples at 7 days and 28 days. Figure 2.20 shows the influence of H_2SO_4 exhibit to physical appearance change in the concrete samples at early and late age.

Based on previous works by Khongpermgonson et al. (2019); Menéndez et al. (2019), the incorporation of CBA as an alternative material has led to a reduction in interconnected pores in concrete because of the grinding of CBA to fine particle sizes. This is because of the positive effect of both chemical and physical performance of ground bottom ash and dense of the concrete structure when CBA was ground to increase the fineness. The existence of CBA, regardless of the process treatment, tends to enhance the resistance of sulfuric acid, as well as chloride attacks in concrete and mortar. Consequently, concrete and mortar containing CBA can be safely utilized in acid rain or other chemically hazardous environmental conditions.

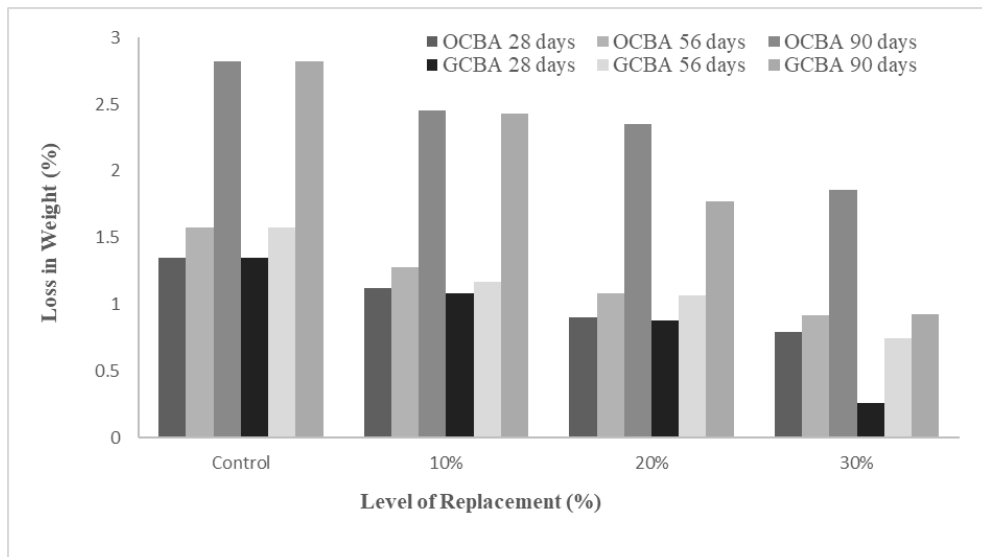


Figure 2.19 Percentage of loss by weight of CBA in concrete mixes at various curing ages

Source: Khan & Ganesh (2016)



Figure 2.20 Influence of the Sulfuric acid of concrete samples at 7 days and 28 days

Source: Muthusamy et al. (2021)

2.4.3.2 Sulphate Attack

Sulfate attack of concrete is a complex process, which includes physical salt attack due to salt crystallization and chemical sulfate attack by sulfates from seawater or any chemical containing sulphate ions. Sulfate attack can lead to expansion, cracking, strength loss, and disintegration of the concrete (Kanaan et al., 2022; Ting & Yi, 2023). Sulfate attack is generally attributed to the reaction of sulfate ions with calcium hydroxide and

calcium aluminate hydrate to form ettringite. This mechanism is also one of the important factors influencing the durability of concrete (Akhshah et al., 2023; Rahman & Bassuoni, 2014). Sulphate can react with hydrated calcium aluminate and produce expansive products, such as ettringite and gypsum. As a result, the concrete becomes more compact, and its strength is slightly increased in the initial stage of the reaction process (Abba et al., 2017; Diaz Caselles et al., 2021). However, with the gradual formation of an expansive stress on concrete through continuous accumulation of expansive products, tensile stress is developed in the concrete. Once the stress exceeds the tensile strength of the concrete, cracks are formed that finally result in the reduction of the bearing capacity. This causes the concrete to crack, further damaging the concrete. In addition to the formation of ettringite and gypsum and its subsequent expansion, the deterioration due to sulfate attack is partially caused by the degradation of the calcium silicate hydrate through leaching calcium compounds (Tang et al., 2021; Whittaker & Black, 2015). This process leads to loss in calcium silicate hydrate gel stiffness and an overall deterioration of the concrete mixture.

In terms of prevention, the use of sulphate resisting cements would provide additional safety against sulphate attack. Consequently, protecting against sulphate attack requires appropriate cementitious materials to reduce the ingress of sulphates into concrete mixture (Elahi et al., 2021; Nadir & Ahmed, 2022). In terms of pozzolans materials helps to increase concrete resistance and deterioration towards sulphate attack (Aragón et al., 2020). According to several previous studies Gagatek & Hooton, (2019; Lawrence, (1990) have shown that some pozzolans increase the life expectancy of concrete exposed to sulphate. The sulphate resistance may be improved by limiting tricalcium aluminate (C_3A) content in cement by restricting the amount of $Ca(OH)_2$ formed in the hydrated cement paste, or by converting the $Ca(OH)_2$ to more stable form such as C-S-H. The use of blended cement decreases the total amount of $Ca(OH)_2$ in cement and thus inhibits the reaction between sulphate and $Ca(OH)_2$ which lead to ettringite formation.

Several previous studies Cohen & Mather, (1991); Hodhod & Salama, (2013); Khan & Siddique, 2011) stated that the strength properties of concrete that was exposed to sulphate solution which showed reduction in the strength with the utilization of CBA in concrete mixture. The occurs due to C-S-H gel deprivation, and volumetric expansion leading to cracking. This attack also triggers the gypsum precipitation and deformation

of C-S-H. The deformation of C-S-H destroys the bonding ability of C-S-H and due to that strength loss in concrete. Consequently, sulphate reaction leads towards volumetric expansion and develops internal stresses which create interruption in concrete. According to study by Mangi et al. (2019) used CBA as partial cement replacement subjected to 5% Na_2SO_4 solution for concrete samples. The finding showed that loss in weight when immersed to sulphate solution compared to water curing and acid curing as shown in Figure 2.21.

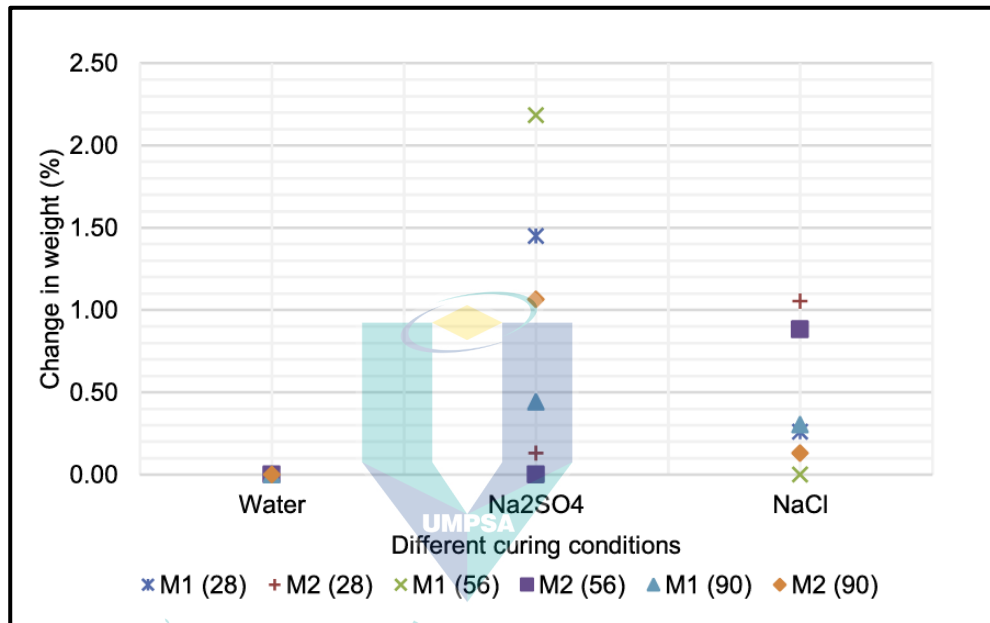


Figure 2.21 Weight loss when used CBA as partial cement replacement and immersed in sulfate for various curing

Source: Mangi et al., (2019)

On the other hand, several previous studies Durgun & Sevinç, (2022); Kasaniya et al., (2021); Wan Ibrahim et al., (2021a) reported that the strength of concrete that was exposed to sulphate solution can be enhanced with the utilization of CBA in the concrete mix. This is due to CBA that has less calcium but high in silica content. When pozzolanic reaction takes place, $\text{Ca}(\text{OH})_2$ will react with silica from CBA thus resulting in formation of the secondary C-S-H gel (Ganesan et al., 2023; Wan Ibrahim et al., 2021b). The formation of this secondary C-S-H gel has been significantly producing concrete with high resistance to sulphate attack and increase the durability of the concrete. The internal structure of the concrete will become denser with the formation of C-S-H gel, which will reduce the porosity and permeability of the concrete making it unavailable for sulphate,

ettringite or gypsum to form, thus the chances for sulphate ion penetrating the concrete will be lower (Chambua et al., 2021; Zhou et al., 2022). The result was supported by researches done by Kaminskis et al., (2020); Mangi et al., (2019) which shown that the addition of CBA in concrete mixture will improve the resistance to sulphate attacks.

2.4.3.3 Water Absorption

Water absorption is one of the essential tests that assess concrete durability. Also, this test is used to evaluate the percentage of water absorption in the concrete mix. This test was performed on hardened samples at 28 days of curing according to (EN, 2013). Mangi et al., (2018) presented that the percentage of water absorption decreased due to increased CBA replacement level in the concrete mixture. The reduction in water absorption due to water demand driven by the rise specific surface area of CBA. The percentages alternative level of CBA was 10%, 20%, 30%, and 40% by total cement weight in concrete. The water absorption result was 5.40% ,5.37%, 5.32,5.24%, respectively as shown in Figure 2.22 (Mangi et al., 2018).

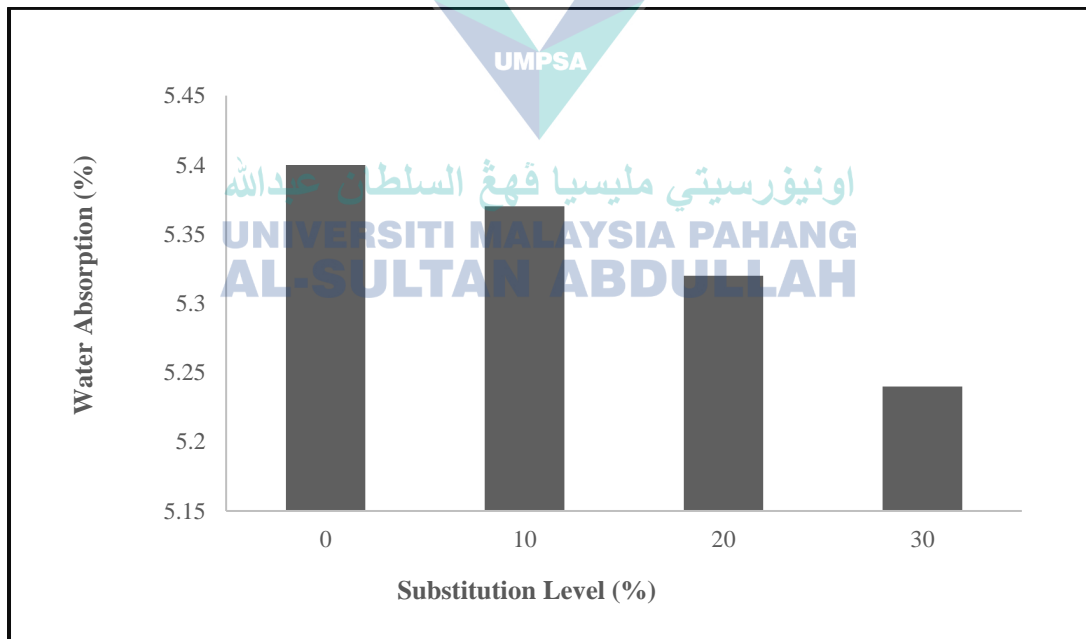


Figure 2.22 Variation of water absorption with different percentages of CBA
Source: Mangi et al., (2018)

Khan et al. (2016) studied the effect of CBA on concrete properties, especially water absorption. The water absorption was found the water absorption was increased

when increased the percentages of CBA as cement replacement in various level (0%, 10%, 20%, and 30%). The increased due to fineness of CBA and the porosity of the particles that allow for the samples to be more absorbed (Khan & Ganesh, 2016). Similarly, another study was reported by Mangi et al., (2019) was found the increased in the water absorption when increased the CBA replacement level in concrete. The increased in the water absorption due to increased fineness of CBA and the porosity of the particles (Mangi et al., 2019). Furthermore, several studies were reported that the influence of CBA in water absorption of the concrete mixture depending on the percentages of replacement. This is due to the higher water demand driven by the rise specific surface area of CBA (Aydin, 2016; Balasubramaniam & Thirugnanam, 2015). Moreover, the concrete containing CBA could be an influence for water absorption and porosity due to the rates of chloride entry into the concrete (Kim et al., 2014). It was recorded the highest water absorption 32%, and the lowest water absorption is 1.20% respectively (Aydin, 2016; Balasubramaniam & Thirugnanam, 2015). Besides, (Kalaw et al., 2015). has reported the influence of CBA's water absorption level. They found that the mixture containing CBA has a significant effect through the increased water absorption of concrete more than that of the control specimen. This is due to amount of CBA, which usually has larger particle sizes and a smaller specific surface area, increasing water absorption capacity. In this study was used CBA as fine aggregate replacement in concrete production. The water absorption lead to increased with increase the replacement ratios of CBA due to large particles of CBA.

Overall, incorporating CBA as an alternative material in the concrete mix has increased concrete water absorption. The samples with rising replacement ratios showed rising absorption levels. At the same time, those with lower replacement ratios were less porous and, therefore, absorbed fewer quantities of water.

2.4.4 Elevated Temperatures

An elevated temperature is one of the most severe as well as unpredictable hazards that may affect the functioning of a structural system in its lifetime. Exposure to high temperatures may be caused by unintentional or intentional fires, which can result in damage to both the afflicted building and its surrounding structures (Kodur et al., 2020; Malik et al., 2021). Temperature increase can lead to changes in the microstructure (the physical and chemical characteristics) of concrete, and therefore certain qualities of the

concrete may be damaged. Different temperatures and exposure times have different effects on the properties of concrete (Qian et al., 2023; Tawfik et al., 2023). SCC mixing ingredients also influence the strength properties when exposed to high temperatures. In high-temperature settings, the internal composition experiences a range of physical transformations followed by chemical reactions, resulting in irreversible changes affecting efficiency and, in the worst-case scenario, leading to the material's total loss (Amran et al., 2022; Saif et al., 2023). There are several factors influence in the performance of concrete when exposed to elevated temperatures (Shah et al., 2019). According to previous study by Babalola et al., (2021) reported that there are two factor influence the concrete behavior when exposed to high temperatures such as material and environmental factors. The materials factors such as types of aggregate, properties of cement paste, the adhesion of aggregate and cement paste and thermal incompatibility between components of the composite influence the strength of SCC at high temperatures (Mathews et al., 2021). Moreover, environmental factors including heating rate, duration of exposure to maximum temperature, cooling rate, loading conditions and moisture regime, which are also important for the behaviour of concrete composites at high temperatures (Aslani & Samali, 2015).

According to several previous studies Ahn et al., (2016b); Nadeem et al., (2014) reported that moisture loss, evaporation, and chemical structure decomposition may change for those specimens as temperatures rise, potentially leading to more cracks. The rise in temperature leads in the evaporation of water, the dehydration of C-S-H gel, the breakdown of calcium hydroxide and calcium aluminates, and, changes in the aggregate occur, as a result of these changes, the strengths (Martín-Garrido et al., 2020; Song et al., 2022). In practice, 300°C is considered a critical temperature, and temperatures beyond this point may result in serious damage to concrete. The compressive strength of concrete drastically declines between 300°C and 500°C, and concrete heated beyond 600°C to 800°C is no longer structurally useful (Khan et al., 2023; Zaid et al., 2024). According to study by Malik et al. (2021) mass loss that occurs between 20°C and 400°C is due to the loss of physically bound water in the aggregate and cement matrix, as well as thermal swelling of the physically bound water, which results in an increase in capillary porosity. CBA when subjected to elevated temperature (200°C to 800°C) exhibit higher mass loss due to the larger pores produced (Nathe & Patil, 2022). However, the compressive strength of CBA in concrete after exposed to the elevated temperature is greater than that

of control because the CBA particles present in the sample enhances its microstructure by filling voids, hence increasing its compressive strength (Singh et al., 2023).

2.5 Summary of Research Gap

Several researchers investigated the effect of potential application of CBA as alternative materials in concrete. Furthermore, the investigation of ground CBA as partial cement replacement on SCC has not yet been investigated. Nevertheless, identification of suitable method that can be used to provided CBA with micro fine particles that can be used as partial cement replacement in SCC. However, the details are merely focus on the performance of using various sizes of CBA in cementitious framework without any pretreatment process. According to summary in literature review listed in the Table 2.11. There are a few gaps that could be completed to contribute to obtaining novel knowledge on the production and application of micro fine CBA based in the pozzolanic with a new method in concrete is SCC. As can be seen from the Table 2.11, the pretreatment process such as mechanical pretreatments and utilization of used those materials in SCC. Finally, the aims of this study is to thoroughly investigate its feasibility as a see component and its influence on the fresh and hardened, durability and microstructural properties of the produced mixtures in concrete. Also, conducted to further embrace the possible extensive work on CBA to improving the pozzolanic reactivity by the mechanically pretreatment and produced new materials that can be applied in various application of civil engineering and safe the environment from any waste disposed to landfill.

Table 2.11 Summarized of the research gap as reported by several researchers

Author/Year	Materials used in concrete	Mechanical pretreatment	Utilization in SCC	Limitation
(Meena et al., 2023)	CBA as fine aggregate replacement (0, 10%, 20%, and 30%).	Passing sieve no. 4.75mm	1.Slump flow 2.Vfunnel 3.T ₅₀₀ (s) 4.J-Ring 5. L-box	In this study, the compressive strength was increased with increased CBA up to 20% content at late curing ages. This is due to late pozzolanic rection and developed at late ages.
(Keerio et al., 2021)	CBA as fine aggregate replacement (0, 10%, 20%, and 30%).	Passing sieve 4.75 mm	1.Slump flow 2.Vfunnel 3.T ₅₀₀ (s) 4.J-Ring 5. L-box	In this study, SCC properties such as slump flow, L-box shows increased while increasing the alternative percentages of coal bottom ash. This is due to high viscosity, different value of water cement ratio SP.
(Cabrera et al., 2021)	CBA as fine aggregate replacement (0, 10%, 20%, 30%,)	Passing sieve 5mm and retained 0.25mm	1.Slump flow 2.V Funnel 3.J-Ring 4.L-box	In this study, the mechanical properties decreased with increased the replacement ratios of CBA. This could be mainly attributed to the pozzolanicity of the CBA.

Table 2.10 Continued

Author/Year	Materials used in concrete	Mechanical pretreatment	Utilization in SCC	Limitation
(Simões et al., 2021)	CBA as fine aggregate replacement (0, 20%, 30%, 40% and 50%)	Passing sieve 4.75 mm	1.Slump flow 2.V-funnel 3. L-box	In this study, the mechanical properties of coal bottom ash in self-compacting concrete have decreased with increased the percentages of replacement. This is due to no binding ability upon hydration process.
(Hamzah et al., 2020)	CBA as fine replacement (0%, 10%, 15%, 20%, 25%, and 30%).	Passing sieve 4.75 mm	1.Slump flow	In this study, the compressive strength with 10% CBA was recorded highest as compared to other mixes at curing age after 28 days.
(Hamzah et al., 2015)	CBA as fine replacement (0%, 10%, 15%, 20%, 25% , and 30%)	CBA within the range size of 0.075 mm	1.Slump flow 2.V Funnel 3.T ₅₀₀ (s) 4. L-box	The fresh properties of CBA in SCC shows decreased when the percentages of CBA content increased. Also, the compressive strength was decreased when increased the CBA content. This is due to increase of water cement ratio and due to more pore effect from CBA.

Table 2.10 Continued

Author/Year	Materials used in concrete	Mechanical pretreatment	Utilization in SCC	Limitation
(Ibrahim et al., 2015)	CBA as aggregate replacement (0, 10%, 20, 30)	fine Passing sieve size 5 mm.	1. Slump flow test. 2. L-box	SCC properties such as slump flow, L-box shows reduced while increasing the alternative percentages of CBA. This is due to high viscosity, different value of water cement ratio, and CBA has more absorbing compared to normal concrete.
(Aswathy & Paul, 2015)	CBA as replacement (10%, 15%, 20%, 25%, and 30%)	fine Passing sieve no. 4.75 mm	1. Slump flow 2. V Funnel 3. T ₅₀₀ (s) 4. L-box	The mechanical properties of CBA in SCC has decreased with increased the percentages of replacement. The results shows for slump flow and the L-box were decreased with increased the percentages of replacement. Furthermore, for V-funnel and T500 was increased with increased the percentages of replacement. This is due to porosity of CBA, and more absorb, and cohesiveness and lack in paste volume.
(Siddique, 2013)	CBA as aggregate replacement (10%, 20, 30)	fine Retained on sieve no 90 (0, µm)	1. Slump flow, 2. J-ring, 3. V Funnel, 4. L-box and 5. U box	In this study the compressive strength was increased with increased CBA content. Also, indicated low chloride permeability resistance with CBA content in SCC. This is due to higher CBA content in the mixture.

Table 2.10 Continued

Author/Year	Materials used in concrete	Mechanical pretreatment	Utilization in SCC	Limitation
(Kasemchaisiri & Tangtermsirikul, 2008)	CBA as fine aggregate replacement (0, 10%,20, and 30)	Passing sieve no 4.75mm	1. Slump flow test. 2. L-box	Slump flow and L-box of the self-compacting concrete with CBA was decreased compared to normal concrete. This is due increase of inter-particle frictions between aggregate particles produced from CBA particles. The resistance against sodium sulfate (Na ₂ SO ₄) was enhanced with the increase of CBA content.
(Lin & Lin, 2006)	CBA cement replacement in mortar (10%, and 20%)	Passing sieve no 200 mm	No Utilization as SCC	In this research, examined the pozzolanic reactions and engineering properties of CBA mixed with cement in mortar. The results shows decreased in early age strength when increase the percentages of replacement. This is due to late of hydration for CBA compared to cement. Finally, the pozzolanic reactivity in the CBA can be used as cement replacement

Table 2.10 Continued

Author/Year	Materials used in concrete	Mechanical pretreatment	Utilization in SCC	Limitation
(Mohammad, 2024)	Ground CBA as partial cement replacement (10%, 20%,30%,40%,50%)	particles passing 75 μm retained in 45 μm	1.Flow slump 2.L-box 3. V-funnel 4.J-Ring	<p>1. To evaluate the physical, chemical, and microstructural properties of original CBA and mechanically treated CBA as alternative cementitious materials.</p> <p>2. To analyze the influence of mechanically treated CBA on its pozzolanic properties based on Thermogravimetric analysis (TGA), strength activity index (SAI), Chapelle test, and Frattini test in cementitious binder.</p> <p>3. To analyse the effect of mechanically treated CBA as partial cement replacement in the fresh properties of (SCC) based on slump flow, L-box, V-funnel, J-Ring, and mechanical properties of SCC based on compressive strength, flexural strength, Ultrasonic pulse velocity (UPV), splitting tensile strength.</p> <p>4. To evaluate the influence of mechanically treated CBA as partial cement replacement on the durability properties based on (water absorption, sulphate attack, acid attack) and influence of elevated temperature (200°C, 400°C, 600°C, and 800°C).</p>



UNIVERSITI MALAYSIA PAHANG
AL-SULTAN ABDULLAH

CHAPTER 3

METHODOLOGY

3.1 Introduction

This chapter elaborates the methodology that has been applied in this research. In this study, it is focused on the use of one of supplementary cementitious materials in order to evaluate the pozzolanic reaction of micro-fine ground CBA as cement replacement in SCC. Furthermore, pretreatment processes of mechanically grinding of CBA was explored in various SCC tests. In addition, the mechanical properties and durability of the SCC mixture were tested at various curing ages. After that, the influence of micro-fine ground CBA under different elevated temperatures of SCC were investigated in this study. Subsequently, the mix design process used for SCC mixture is presented. Finally, the testing procedures essential to accomplish the study's objectives are described. The methodology used in this research that has been applied comprises the four stages as the following:

- Stage 1: Review and collect the materials.
- Stage 2: Pre-treatment process for CBA using mechanical treatment grinding process (Objective 1).
- Stage 3: Test the raw and various sizes of mechanically treated CBA in the chemical, physical, and microstructural properties at different pozzolanic tests (Objective 2).
- Stage 4: Cementitious framework evaluation and test of optimum sizes by mechanically treated CBA in various SCC fresh, mechanical, and durability properties and influence under various elevated temperatures (Objectives 3 and 4).
- Stage 5: Analysis the results and presentation of data.

3.2 Flow-Chart of Experimental Work

Figure 3.1 shows the applied flowchart of research methodology in this study. The methodology of this research is expected to be feasible as the standard method that could be used for production of micro fine ground CBA. The experimental methods and procedures adopted in this study are based on earlier works and directives from different international standards. The experimental work in this research was carried out in detail in the following sections.

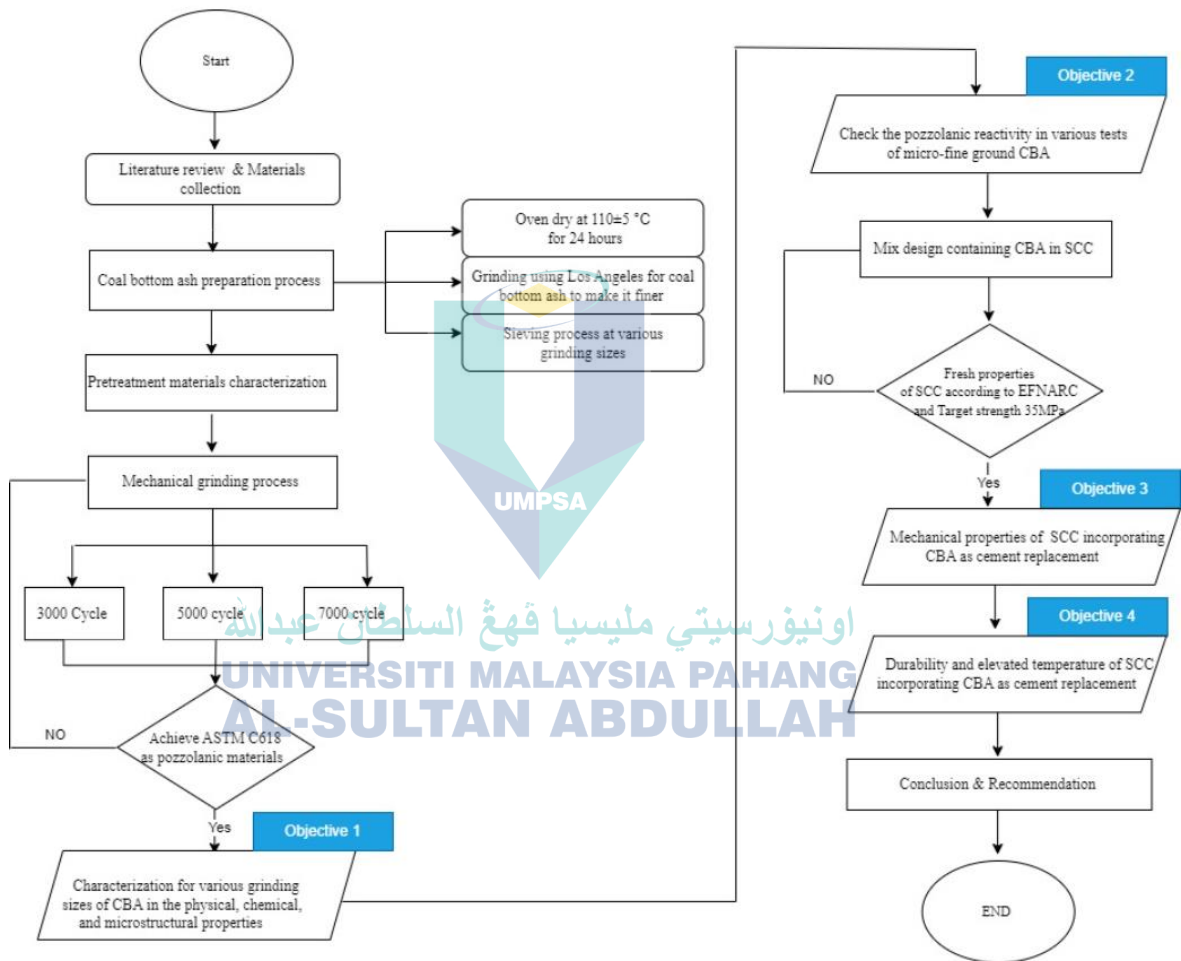


Figure 3.1 Flow chart of research methodology

3.3 Materials Preparation

In the experimental work the materials used include ordinary portland cement (OPC), river sand as fine aggregate, coarse aggregate, superplasticizer, and micro fine ground CBA. The CBA was collected from the Department of Environment in coal thermal power plant Tanjung Bin, Johor, Malaysia, which is a by-product of coal combustion, and the Portland cement was used in this research according to ASTM C150/C150M. The following details about the materials used in this research and specification for the materials:

3.3.1 Tap Water

In this research, the water used for SCC mixing was obtained from the domestic water supply in the structure and concrete laboratory at faculty of civil engineering technology. Water used in SCC mixing is clean and free from harmful quantities of oils, acids, alkalis, salts, organic materials, or other substances that may be harmful to concrete.

3.3.2 Ordinary Portland Cement (OPC)

OPC was used in this research as a main binder for all concrete mixture mixing with CBA production. The OPC used was produced by PANDA Corporation Berhad, Malaysia, and followed with ASTM C150, (2016) specifications as shown in Figure 3.2. The OPC was utilized for the preparation of control and modified SCC samples with a specific gravity equal 3.15. The chemical oxides composition and physical properties of OPC illustrated in Table 3.1 and Table 3.2.



Figure 3.2 Cement binder used in this experimental study

Table 3.1 Chemical composition of cement (OPC)

Chemical / Oxide Composition	Percentages (%)
Calcium Oxide (CaO)	76.6
Silicon Dioxide (SiO ₂)	11.5
Sulphur trioxide (SO ₃)	2.86
Iron Oxide (Fe ₂ O ₃)	4.00
Aluminum Oxide (Al ₂ O ₃)	2.39
Potassium Oxide (K ₂ O)	0.937
Magnesium Oxide (MgO)	0.397
Phosphorus Pentoxide (P ₂ O ₅)	0.578
Loss of Ignition (LOI)	2.20

Table 3.2 Physical properties of cement (OPC)

Physical Properties (Units)	Values
Blaine Fineness (m ² /g)	0.867
Initial Setting Time (mins)	95
Soundness (mm)	1.0
BET Surface Area (m ² /g)	0.563

3.3.3 Coal bottom ash (CBA)

CBA particles are angular, irregular and porous, with a rough surface texture. The particle size ranges from coarse size to fine sand as shown in Figure 3.3. The CBA particles range of the size from coarse (gravel) to fine (sand). Furthermore, the particles of CBA are interlocking characteristics. The particle size of original CBA fall within the range of 0.1 mm to 10 mm as shown in the Figure 3.3 a). CBA is lighter and brittle than natural sand. In this study, the CBA was used at with grinding size passing 75 μ m retained in 45 μ m. Then, the CBA was dried in the oven. The CBA were dried in the electric oven at 105°C for 24 hours to remove the moisture. The next step was sieving CBA at 300 μ m to remove coarse particles. Then, the original CBA was placed into Los Angeles machine until get the required fineness. The size of steel ball was used is 50mm and the number of steel balls was 20. Afterward, the ground CBA was sieved in order to reach a residue less than 35% in sieve 45 μ m in accordance with ASTM C618, (2019), and this study classified as class F ash type as shown in Figure 3.3 b). According to ASTM C618, (2019) to be considered as pozzolanic properties should retained less than 35% with sieve 45 μ m of total weight of the powder sample. The CBA was screened to remove the oversized particles to be more fineness and used as cement replacement. The original CBA and ground CBA have average particles size ranges less than 4.75mm to passing sieve less than 45 μ m respectively. The particles size of CBA can be reduced by increasing the grinding duration.

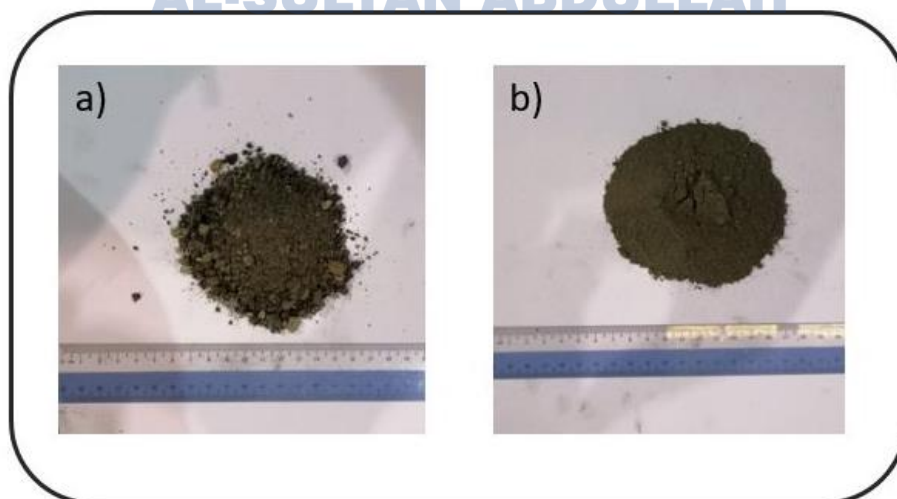


Figure 3.3 Particles of CBA a) Original CBA, b) Micro-fine ground CBA

3.3.4 Fine Aggregate

River sand neutrally occurs as granular materials composed of finely divided from the rock and mineral particles. The river sand as fine aggregate was used in this experimental work. The aggregate was obtained from Gambang, Kuantan in Pahang. The fine aggregate was sieved using the mechanical electric shaker to perform the grading of particles distribution. The aggregate was cleaned by washing to remove the clay and organic materials, after that dried in the laboratory oven at $100 \pm 5^\circ\text{C}$ for 24 hours before using and sieving according to ASTM C136, (2003). Furthermore, in this research, the particle size of fine aggregate was used less than or passes through the sieve size 4.75mm in accordance with guidelines in the ASTM C136 standard as shown in Figure 3.4. Table 3.3 showed the particle size distribution.

Table 3.3 Particle size distribution and physical properties of fine aggregate

Sieve size (mm)	10	4.75	2.36	1.18	0.600	0.300	0.150	Specific gravity	Moisture content	Absorption (%)
Passing %	100	97.4	93.9	73.9	45.7	15.1	3.4	2.62	0.50	0.90



Figure 3.4 Fine aggregate used in this experimental work

3.3.5 Coarse Aggregate

In this research crushed stone granite was used as coarse aggregate in the concrete mixture as shown in Figure 3.5. The particle size of the coarse aggregate was used in this research passing 20 mm and retained in the size 10 mm were used in accordance with EFNARC, (2005). The coarse aggregate has been cleaned by washing to remove the clay and organic materials, after that dried in the laboratory oven at $100 \pm 5^\circ\text{C}$ for 24 hours before using and sieving according to ASTM C33, (2003). Table 3.4 shows the particle size distribution of coarse aggregate.

Table 3.4 Particle size distribution and physical properties of coarse aggregate

Sieve size (mm)	20	16	14	12.5	10	4.75	Specific gravity	Moisture content	Absorption (%)
Passing %	100	97.2	65.4	15.6	2.30	0	2.61	0.25	0.78

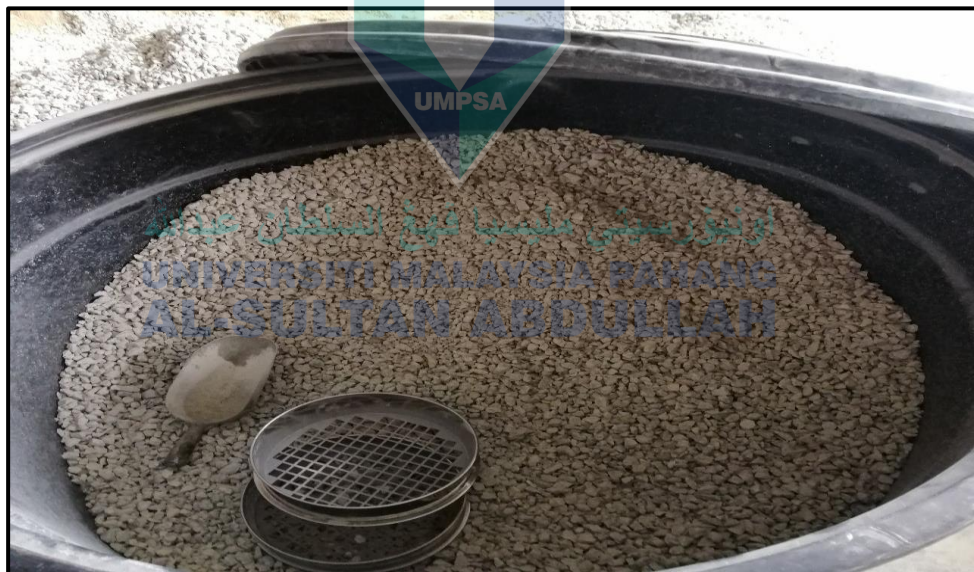


Figure 3.5 Coarse aggregate used in this experimental work

3.3.6 Superplasticizer (SP)

A Superplasticizer (SP) type Sika Visco Crete -2044 PC provided from branch of Sika Company in Kuantan, Pahang, Malaysia was utilized as shown in Figure 3.6. In this experimental work the SP used in accordance with guideline in the standard ASTM C494-86, (2009). Superplasticizer an important component of most modern SCC mixes, water

reducers, enhance the flowability of mixture while reducing the water utilized in the mix. Composed of more advanced, the SP offering advantages such as lower segregation and bleeding, enhanced bond strength, increased sample density. Superplasticizer used in the current experimental work as shown in Figure 3.6, to achieve superior and improve flowability at low water/binder (w/b) ratio. Sika Visco Crete -2044 PC does not contain any chloride or other components which promote steel corrosion. Table 3.5 shows the characteristics of Sika Visco Crete -2044 was used in the experimental work.



Figure 3.6 SP used in the experimental work for SCC mixture production a) is the total SP collect for experimental work b) SP amount used in each mix

Table 3.5 Characteristics of SP brand Sika Visco Crete -2044

Properties	Description in accordance to ASTM C494 and BS-EN5075 Part3
Type	Sika Visco Crete -2044 PC
Color	Brownish liquid
Strong Condition	Stored properly in original, unopened and undamaged packaging in dry conditions and protected from direct sunlight at temperatures between +5 °C and +35 °C.
Chemical Base	Aqueous solution of modified polycarboxylates
Dosage use	1.0–2.0% by weight of cement.

3.4 Characteristics and Testing of Materials used in SCC

The materials used in this study such as cement, fine aggregate, coarse aggregate, micro fine CBA. This section is explained the characteristics for the all the materials using various characterization tools that can be explained in the sub sections below.

3.4.1 Sieve Analysis Test

Sieve analysis is a method used to establish particle size distribution of a material such as original and micro fine CBA, fine aggregate, coarse aggregate as shown in Figure 3.7. This method is performed by sifting a particles sample through a stack of wire mesh sieves, separating it into discrete size ranges. A sieve shaker was utilized vibrates the sieve stack for a fixed time. Vibration reorients irregularly formed particles as they fall through sieves. This test is conducted to assess the percentage of various grain sizes contained within. The sieve analysis was used to select finer particle distribution. The size distribution is a crucial factor that significantly influences the selection of materials used. In this experimental work, the standard ASTM C136/C136M was used.



Figure 3.7 Sieve shaker apparatus to sieve particles of CBA and ingredient of SCC

3.4.2 Particles Size Analysis

Particles size analysis was used to evaluate the particles of the original CBA and mechanically pretreatment CBA the results explained in the next chapter. There are two

type of particle size analysers ranges to measure the particles. The first range particles for CBA dynamic light scattering analysers measure particles in solutions in the 0.6 nm to 6 µm range. The second range particles for CBA Laser diffraction analysers are used for particles in a CBA within the range of 10 µm to 1 mm. In this experimental work, the second range to observe the size particles of cement and original CBA and micro-CBA using device as illustrated in Figure 3.8.

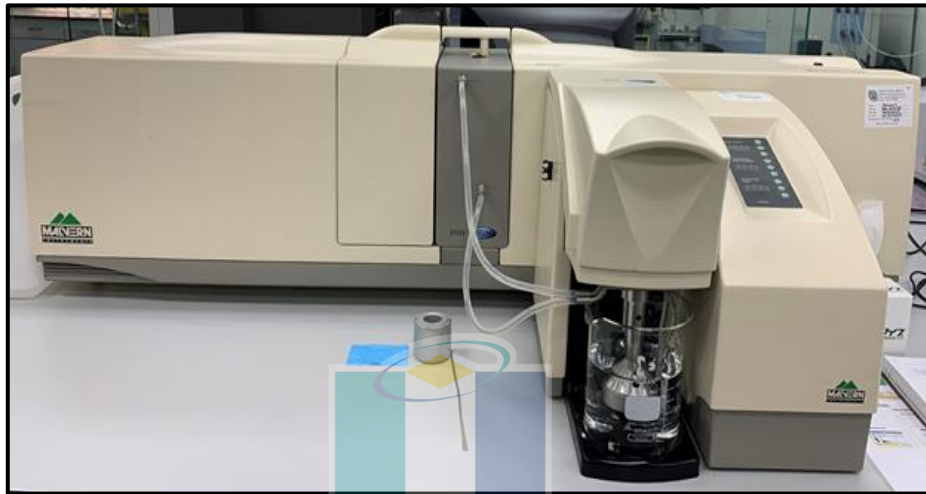


Figure 3.8 Particle Size instrument (Malvern Hydro 2000MU)

3.4.3 Moisture Content of Aggregate and CBA

The moisture content of aggregate, original CBA, and micro ground CBA in accordance with guidelines in the ASTM C566. The test starts with a weight of 2500g of coarse aggregate, and for the fine materials such as fine aggregate, original CBA, and micro-CBA 500g was used before determining the dry weight. After that, the same amount of the materials was put it in the electric oven at temperature rate $110^{\circ}\text{C} \pm 5^{\circ}\text{C}$ for 24 hours. The moisture content is the weight losses of the samples due to dried at electric oven as shown in Table 3.6. It can be calculated according to the following Equation 3.1.

$$\text{Moisture content (\%)} = \left(\frac{W_{t1} - w_{t2}}{w_{t2}} \right) \times 100\% \quad 3.1$$

Where, W_{t1} = weight of air-dried samples for the materials, W_{t2} = weight of electric oven dried samples for the materials.

Table 3.6 Moisture content (%) of the materials used in the experimental work

Properties/ Materials	Coarse aggregate	Fine aggregate	Ground CBA	Original CBA
Moisture content (%)	0.25	0.50	1.07	0.95

3.4.4 Fineness Modulus (FM) of Aggregates and CBA

This test method is used primarily to determine the grading of materials proposed for use as fine materials or coarser materials. The fineness modulus of coarse aggregate and original CBA and micro fine ground CBA in accordance with the guidelines (ASTM C136, 2012). The fineness modulus FM is a single parameter to describe the grading curve; it can be useful in checking the uniformity of grading. A small number of fineness modulus indicates fine grading, while the bigger fineness coarser. In this test, a sample of dry aggregate of known mass is separated through a series of sieves of progressively smaller openings for determination of particle size. The sizes of sieves used in the test were: 20mm, 16mm, 14 mm, 12.5 mm, 10 mm and pan. Where the standard sieves for fine aggregate used were 4.75mm, 2.36mm, 1.18mm, 0.600mm, 0.300mm, 0.150mm, 0.075mm. Table 3.7 showed the fineness modulus of fine, original CBA, and micro fine ground CBA. It can be calculated according to the following Equations 3.2 and 3.3.

For coarse aggregate

$$FM \text{ coarse aggregate} = \left(\frac{\text{Cumulative percent retained on standard}}{100} \right) \quad 3.2$$

For fine aggregates:

$$FM \text{ fine} = \left(\frac{\text{Cumulative percent retained on standard}}{100} \right) \quad 3.3$$

Table 3.7 Fineness modulus of the materials used in the experimental work

Properties/ Materials	Coarse aggregate	Fine aggregate	Ground CBA	Original CBA
Fineness modulus	3.80	2.60	2.65	2.54

3.4.5 Absorption and Specific Gravity of CBA and SCC Ingredient

The specific gravity of aggregate was specified to guarantee the right quantity is utilized during the concrete casting as shown in Table 3.8. This test was conducted according to ASTM C127, (2012). For measuring the water absorption, the aggregate was sunken in water with a depth more than 50mm above the basket top. The aggregates were allowed to be fully immersed in water for 24 hours. The both aggregate and basket under water was labelled as (B) was weighted. After that, the aggregate was placed on a dry cloth. On the other hand, the empty basket was weighed in water, and the value was known as (C). The aggregate weight was taken as (A) when using cloth to dry the surface of aggregate when the water is not visible. To determine the water absorption, the aggregate was oven at $110\pm 10^{\circ}\text{C}$ for 24 hours. It was determined according to the Equations 3.4 and 3.5.

$$\text{Water absorption} = (A-D)/D \times 100\% \quad 3.4$$

$$\text{Specific gravity} = (A)/(A-(B-C)) \times 100\% \quad 3.5$$

where,

A = mass of SSD sample in air (g), B = mass of basket in water containing saturated aggregate sample (g), C = mass of the empty basket in water (g), and D = mass of the oven-dried aggregate in air (g).

Table 3.8 Absorption and specific gravity of the materials used in the experimental work

Properties/ Materials	Coarse aggregate	Fine aggregate	Ground CBA	Original CBA
Absorption	0.78	0.90	6.15	5.30
Specific Gravity	2.61	2.62	2.43	2.21

3.5 Experimental program

In the next subsections, the mixture design of SCC with ground CBA as a partial cement replacement and the sample preparation at different curing ages are discussed. In addition, the mechanical pretreatment to prepare ground CBA for use in the SCC mix is discussed in the following subsection.

3.5.1 Designing of Mix for SCC

The mix design of SCC is very complicated because of different variability and the characteristics of the materials used. Furthermore, the mix design of SCC that influence by the mix proportion of the main ingredients and the proportion of admixture to achieve high flowability. A rational mix-design method for SCC using a variety of materials is necessary. (Okamura et al., 1995) have proposed a simple mix proportioning system assuming general supply from ready-mixed concrete plants.

In this study, mix design of SCC was selected in accordance with standard of (EFNARC, 2005) which was proposed by (Okamura et al., 1995) at University of Tokyo in Japan. Moreover, several series of trial mixes occurred with different calculations according to varying the percentage of superplasticizer content and water -powder ratio, in order to achieve a target strength with high flowability. In accordance with guidelines in the standard (EFNARC, 2005) the fine and coarse aggregate were fixed that can achieve the self-compatibility of SCC mixture. Various superplasticizer dosage was used in the experimental work, the optimal that can achieve SCC mixture with high flowability was chosen. In this experimental work, the mix design was carried out with coarse aggregate ratio 45% and fine aggregate ratio 55% by the volume of concrete mixture this comply with the (EFNARC, 2005) and followed the Japanese method for SCC. The trial mix were designed with content from 1.8 % of SP for all cast samples. Furthermore, the target strength was designed to achieve 35MPa. The selected mix design for SCC is as shown in Table 3.9. After achieving the mix design for control SCC, where replaced the partial cement was replaced with micro fine CBA with ratio 10%, 20%,30%,40%, and 50% in the SCC mixture. After preparation, all the samples were tested for its mechanical, durability properties and under various elevated temperatures.

Table 3.9 Mixture design proportion for 1 m³ SCC mixture in (kg/m³)

Samples ID	Water content (kg/m ³)	Cement (kg/m ³)	Fine aggregate (kg/m ³)	Coarse aggregate (kg/m ³)	CBA content (kg/m ³)	Superplasticizer (% Binder)
Control	185	550	952	620	0	1.8
CBA 10%	185	495	952	620	55	1.8
CBA 20%	185	440	952	620	110	1.8
CBA 30%	185	385	952	620	165	1.8
CBA 40%	185	330	952	620	220	1.8
CBA 50%	185	275	952	620	275	1.8

3.5.2 Preparation and Casting of Samples

In this experimental work, the SCC samples were designed to achieve the target strength of 35MPa with high flowability to achieve the workability of SCC. Before starting to prepare the samples, each of the required main materials and micro fine CBA were measured and weighed with high precision. SCC mixture was performed using drum with medium size mixer. However, to prepare the samples, all the tools were wet to reduce the water loss during mixing and natural evaporation. To ensure, powder materials such as cement and fine and micro fine ground CBA were put it in the drum mixer. First, the drum mixer was started mixing for three minutes to ensure all the materials mix properly and homogeneously. After that, superplasticizer was mixed with water to allow for uniform distribution throughout the concrete mixing process. The mixer was then filled twice with the water. At the beginning of the mixing process, 50% of the water content was added, and the remaining 50% was added two minutes later. After adding the water, the concrete mixing lasted for another three minutes for a consistent mixture to be obtained. Concrete mix was stirred for a further three minutes after adding the given water for a more consistent mixture of concrete. After that, mixing continued for a further three minutes, often pausing for three minutes so that lumped concrete cannot be formed

in the mixer. After testing of the fresh concrete properties, casting was carried out immediately after this process of mixing as shown in Figure 3.9. After twenty-four hours, the specimens were taken out from the moulds under certain laboratory conditions with a $27\pm 3^{\circ}\text{C}$ temperature. These steps were recorded as shown in Figure 3.10.



Figure 3.9 Preparation of the SCC specimens at the laboratory (a Materials for mixing, b) concrete inside drum mixer, c) concrete after put in cubes moulds, and d) concrete after put in beam moulds

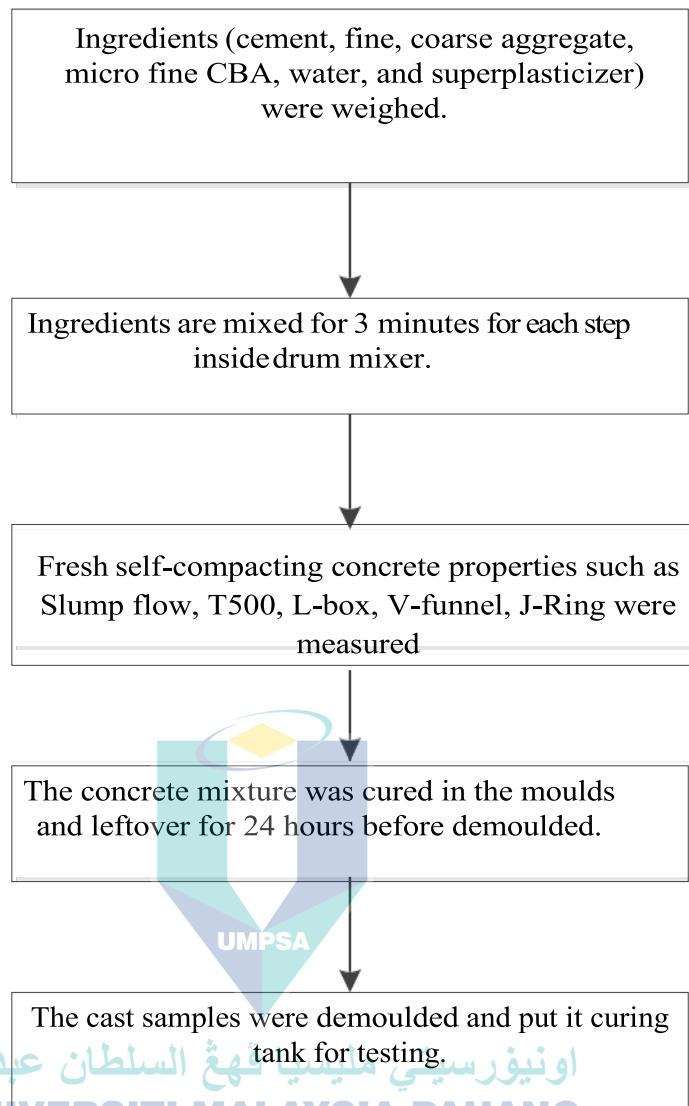


Figure 3.10 Preparation process for SCC samples containing micro fine CBA

3.5.3 Curing Method for the Samples

Appropriate curing of concrete structures is essential in order to ensure that the concrete meets the requirements of performance and durability. The curing method is the final stage in the production of newly placed concrete. When concrete is adequately cured, water in the concrete will make cement particles interact with the water throughout the cement hydration process and develop the strength to resist contraction stress. The type of curing method that is used in this research are among all types of curing techniques such as water curing as shown in Figure 3.11. Curing condition is very important in gaining the strength of samples. Curing of SCC samples was commenced as soon as after adequate hardening of the sample under room temperature for a minimum

period of 18 to 24 hours as recommended by the standard. For this study, SCC samples were cured in a water basin for 7, 14, 28, 56, 90, and 180 days until the testing ages, respectively. This process is known as curing. Adequate curing is vital to quality concrete according to ASTM C31, (2016).

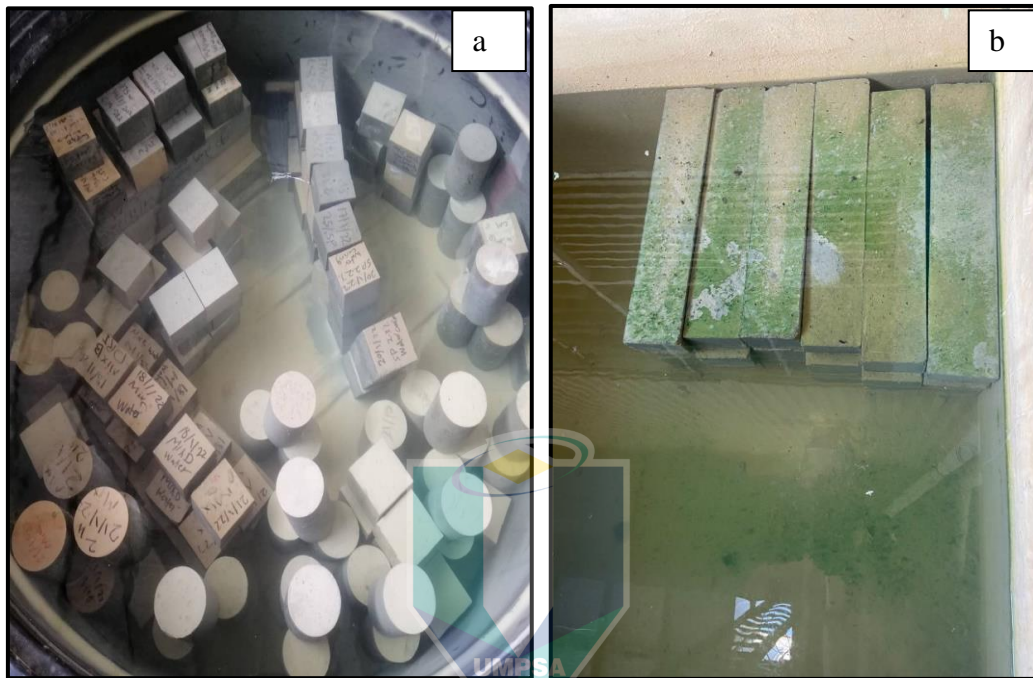


Figure 3.11 Curing method for the SCC samples a) all samples for experimental work (b) Prism samples for flexural strength

3.5.4 Mechanical Grinding Process for CBA

The process of mechanical grinding for CBA to convert it to ground CBA with various sizes to be used as pozzolanic materials as shown in the Figure 3.12. The mechanical grinding process for ground CBA starts with dried in the electric oven at temperature $110\pm 5^{\circ}\text{C}$ to remove all traces of moisture content for 24 hours. Consequently, the CBA was sieved using an electric sieve to separate the coarse particles and fine particles. After that, the fine particles placed in the electric Los Angeles machine and ground for 3000 cycles, 5000 cycles, and 7000 cycles as shown in Figure 3.12. Subsequent, the micro fine particles of CBA sieved with sieve mesh less than $45\ \mu\text{m}$ to achieve the standard guidelines as mentioned in the ASTM C618. Hereafter, the materials were characterized with physical and chemical and microstructure properties.

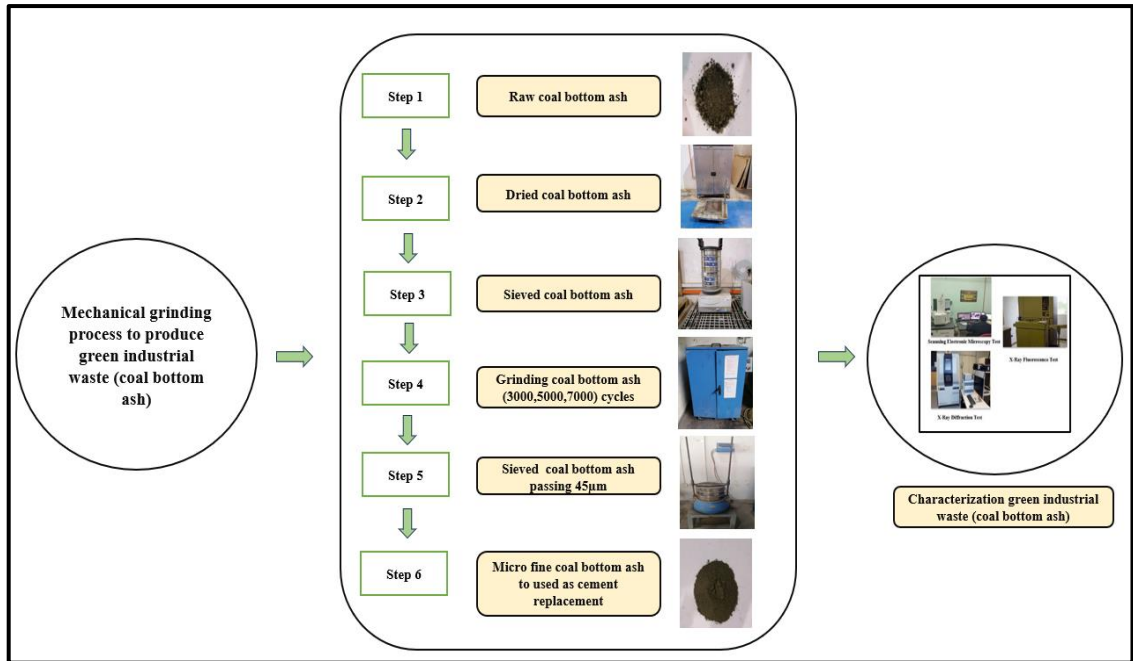


Figure 3.12 Mechanical grinding process for original CBA to micro-fine ground CBA to be used in SCC

3.6 Testing of samples

The testing methods covers the determinations of fresh, mechanical and durability properties of SCC containing ground CBA as partial cement replacement. Furthermore, in the following subsections discussed the tests used for pozzolanic properties and the microstructural characteristics of CBA in SCC samples. All the forms of testing complied with the required standards.

3.6.1 Fresh Properties of SCC

For the purpose of assessing the SCC properties in the concrete's fresh state, the following tests, including slump flow test, V-funnel test, and L-box test were performed. For mitigating the time impact on the test results of SCC, fresh workability tests of SCC were performed immediately after the mixing was completed. The entire tests of fresh SCC were accomplished following the EFNARC, (2005) for producers and processors, who are specialized in SCC mixes. According to EFNARC, (2005), the fresh properties of SCC are typically classified into one of three categories, Table 3.10 lists the classes required for a variety of applications. A detailed description of the fresh properties and the standards is provided as follows:

Table 3.10 Categories of fresh properties for SCC in accordance with (EFNARC, 2005) standard.

Slump flow (SF) categories	Slump flow range (mm)
SF 1 (mm)	550–650
SF2 (mm)	660–750
SF 3 (mm)	760–850
Viscosity Flow (VF) categories	V-funnel time (s)
VF1	≤ 8
VF2	9 to 25
Passing ability (L-box) categories	L-box Range
PA1	≥ 0,80 with 2 rebars
PA2	≥ 0,80 with 3 rebars
J-ring	(Step height in mm)
-	0–10

3.6.1.1 Slump Flow Test

The flow slump test is used to evaluate the horizontal flow of SCC in the absence of obstruction. The slump flow test is a measure of mixture filling ability. This test is performed similarly to the conventional slump test using the standard EFNARC, (2002) slump cone as shown in Figure 3.13, instead of measuring the slumping distance vertically, the mean spread of the resulting concrete patty is measured horizontally. This number is recorded as the slump flow. The visual stability index (VSI) is determined through rating the apparent stability of the slump flow patty. This test is performed according to the standard EFNARC, (2002).

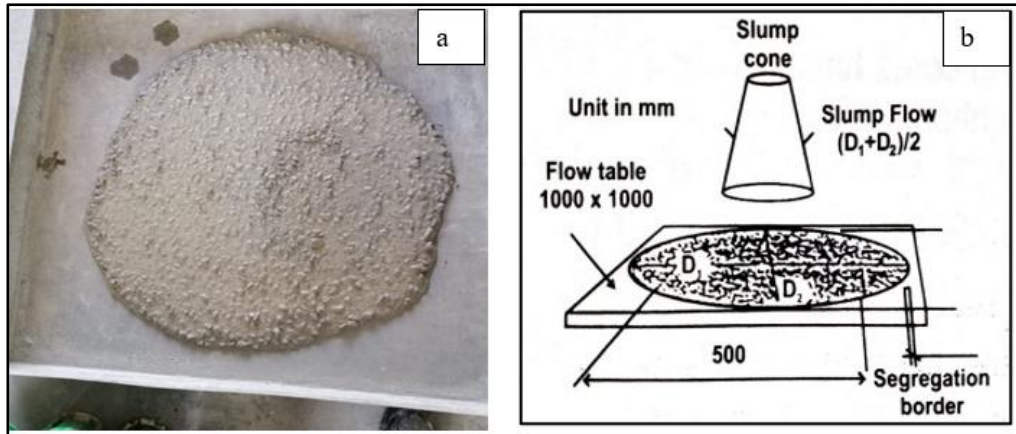


Figure 3.13 Slump flow test apparatus (a test flow SCC b) Slump flow apparatus

3.6.1.2 L-Box Test

The device consists of a rectangular section box in 'L' form, with an upper and lower section divided by a moveable, in front of which vertical lengths of reinforcement bars are fitted as shown in Figure 3.14. The vertical section is filled with concrete, and the gate raised to allow concrete to flow into the horizontal section. When the flow ends, the concrete height at the end of the horizontal segment is expressed as a proportion of that remaining in the vertical section (H_2/H_1 in the diagram). The height of the concrete left in the vertical section (h_1) and at the end of the horizontal section (h_2) is measured. The concrete height remaining in the vertical section (h_1) and the horizontal section (h_2) end is calculated. The ratio of h_2/h_1 is measured as the blocking ratio. It shows the concrete's slope at rest. This is an indicator of passing capacity, or the degree to which concrete passage through the bars is limited. The box's horizontal portion can be marked at 200 mm and 400 mm from the gate and the time taken to calculate these points. This test is performed according to the standard EFNARC, (2002).

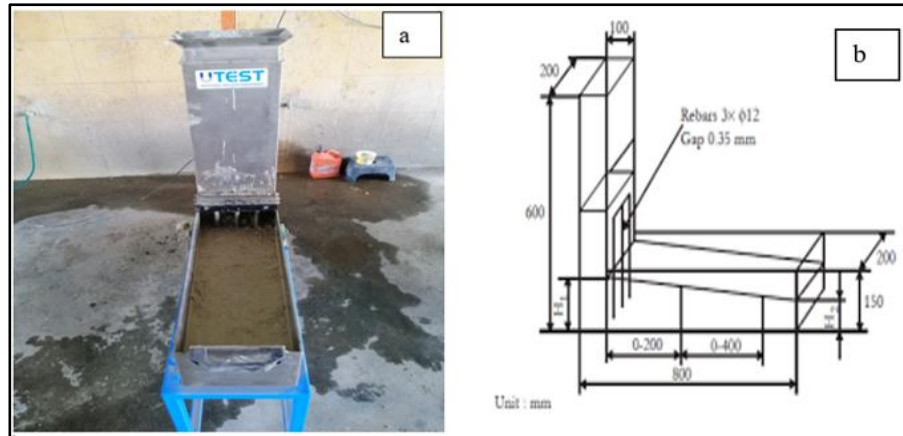


Figure 3.14 Apparatus of the L-box test (a L-box flow test b) L-box apparatus

3.6.1.3 V- Funnel Test

The V-shaped funnel machinery used to calculate concrete self-compacting capacity. The V- funnel has opening slide at the bottom. The filling time is defined as the time necessary for vertical flow from the V-funnel lower opening after it is full with fresh SCC. The specified V-funnel is used to evaluate concrete with maximum aggregate size of 20 mm as shown in Figure 3.15. The funnel is filled about 12 liter of concrete the time take for it to flow through the apparatus was measured. The funnel is filled with about 12 litres of concrete the time to flow through the device calculated. Then, this funnel can be refilled concrete, and left for 5 minutes. If the concrete shows segregation, then the flow time will increase significantly. Therefore, concrete refill the funnel, and left for 5 minutes. If the concrete displays segregation, the flow time increases dramatically. This test is performed according to the standard (EFNARC, 2002).

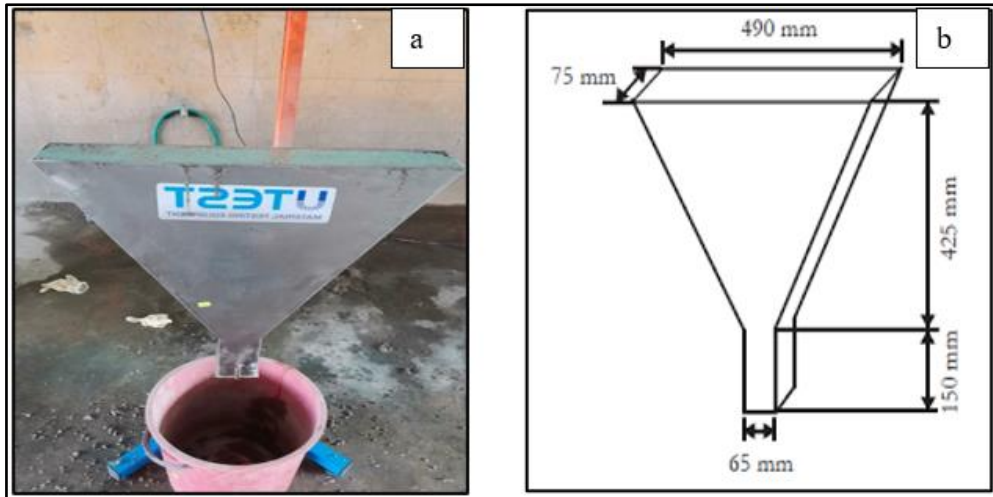


Figure 3.15 V-funnel test apparatus a) V-funnel flow test b) V-funnel apparatus

3.6.1.4 J- Ring Test

The test is utilized to assess the concrete's passing ability. The apparatus requires a rectangular steel ring (width 30mm x length 25mm), drilled vertically with hole to accommodate threaded portions of the reinforcement bar as shown in Figure 3.16. These bar sections may be of various diameters and spaced at various intervals. With usual reinforcement considerations 3x the maximum aggregate size could be sufficient in accordance (EFNARC, 2002). The diameter of the ring of vertical bars is 300 mm, and the height 100 mm as shown in Figure 3.16. This test was evaluated according to the specification as mentioned by standard (EFNARC, 2002).

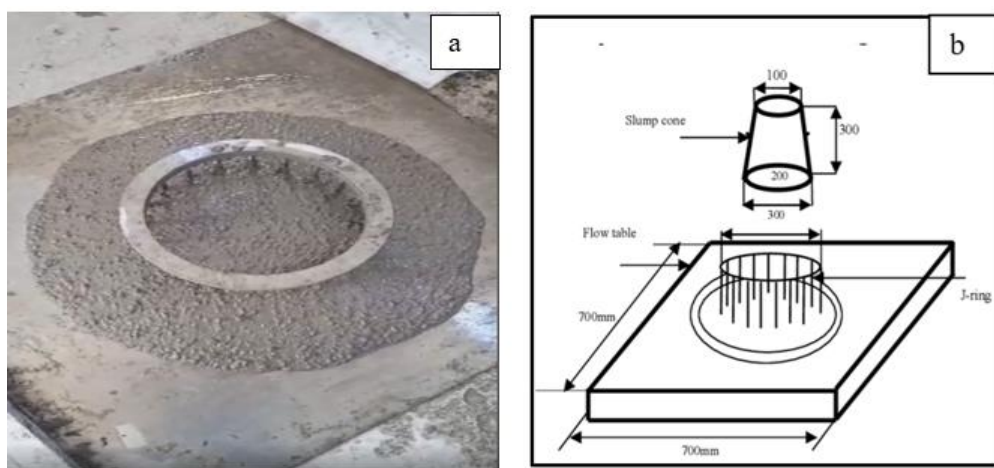


Figure 3.16 J-Ring test apparatus a) J-Ring flow test b) J-Ring apparatus

3.6.2 Mechanical Properties of SCC

Several of mechanical properties has been performed in this experimental work such as compressive strength, splitting tensile strength, flexural strength, and ultrasonic pulse velocity. The following subsections showed each of the producers of properties in details in accordance with standards.

3.6.2.1 Compressive strength Test

The most important property of SCC is compressive strength. In this study for all mixes, three cubes for each percentage of replacement in SCC mixture. The dimensions of the samples (100mm × 100mm × 100mm) were tested at in this research at ages of 7,14, 28,56 90, and 180 days. In this research, the test was carried out using an automated concrete compression machine as shown in Figure 3.17, with 3000 kN strength, to evaluate compressive strength for all samples. The concrete cube samples were tested according to (ASTM C39, 2020). The mean compressive strength was estimated using Equation 3.6 below:

$$\text{Compressive Strength (MPa)} = \frac{\text{Load Failure (N/mm}^2\text{)}}{\text{Surface Area of sample (mm)}} \quad 3.6$$



Figure 3.17 Automatic compressive strength machine

3.6.2.2 Splitting Tensile Strength Test

Splitting tensile strength is indirect technique of assessing concrete tensile strength using a cylinder sample that tensile strength across vertical diameter as shown in Figure 3.18. Moreover, the tensile strength for concrete samples is the tensile stresses developed due to the application of the compressive load at which the concrete samples might crack. as mentioned by ASTM C469, (2011). The splitting tensile test was performed on the cylinder samples with the dimensions of 100 mm diameter and 200 mm of height. The test procedure was adapted by following ASTM C469, (2011). The test was performed at the age of 7, 14, 28, 56, 90, and 180 days on the normal substrate and treated CBA samples. The cylindrical samples were tested by applying the force narrowing the region along the sample length that at the end contributes the samples to fail in tension. The splitting cylinder tensile strength was calculated by Equation 3.7 as following:

$$F_{ct} = \frac{(2 \times P)}{(\pi \times L \times D)} \quad 3.7$$

F_{ct} is the split tensile strength, in Mega Pascal (MPa).

P is the maximum load, in Newton (N).

L is the length of the line of contact of the samples, in millimeters.

D is the design of cross-sectional dimension, in millimeters

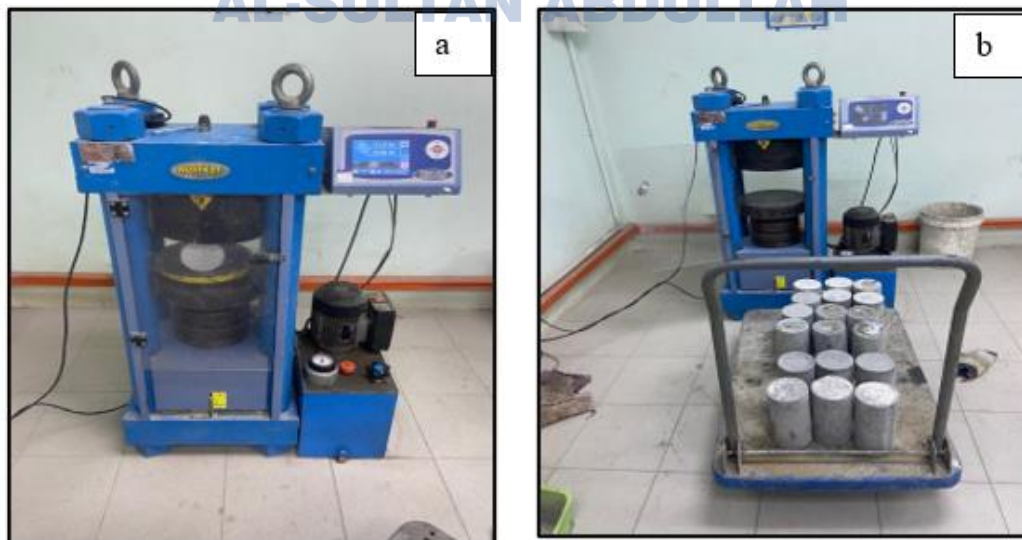


Figure 3.18 Automatic Splitting tensile strength machine

3.6.2.3 Flexural strength Test

In this study, the flexural strength is determined by the maximum bending stress that could be applied for the materials before it yields as shown in Figure 3.19. Flexural strength is evaluated with beam (prismatic) samples those are undergo to a bending moment by application of load through upper and lower rollers as mentioned by (ASTM C78, 2010). At the age of 7, 14, 28, 56, 90 and 180 ages of curing, the flexural strength test was performed with the specimen's size of 100 mm × 100 mm × 500 mm according the procedure from (ASTM C78, 2010). The test was examined in order to investigate the bending tensile strength of the normal SCC and mechanically pre-treated CBA concentrate. The test was carried out by using the 100 kN AG-X Shimadzu Universal Testing Machine at the concrete laboratory with the loading rate of 1 MPa/min. as shown in Figure 3.19. The flexural strength was estimated using Equation 3.8 below:

$$F_{cf} = \frac{(P \times L)}{(d_1 \times d_2^2)} \quad 3.8$$

F_{cf} is the flexural strength, in mega pascals (MPa)

P is the maximum flexural load, in (N)

L is the distance between supporting roller, in millimeters

d_1, d_2 is the lateral dimensions of the samples, in millimeters

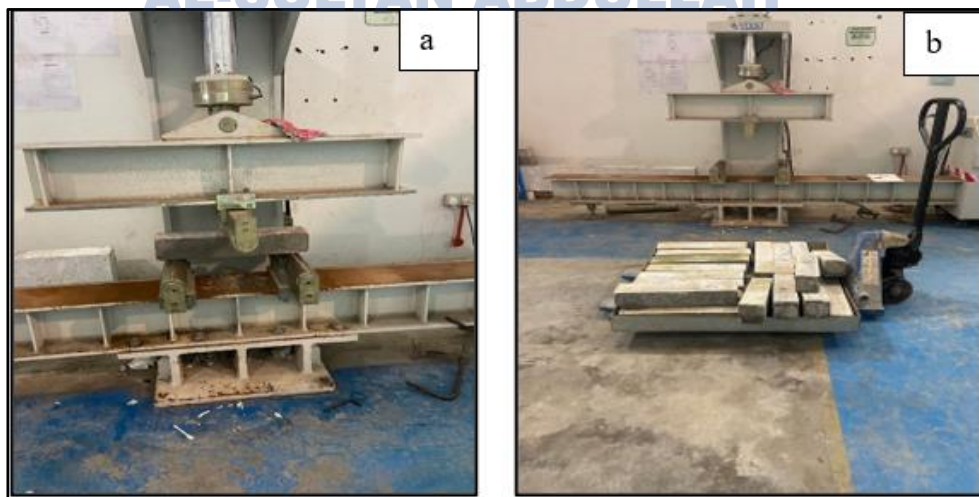


Figure 3.19 Flexural strength test machine

3.6.2.4 Ultrasonic pulse velocity (UPV) Test

The Ultrasonic-Pulse Velocity (UPV) test is used in structural applications to determine the consistency of concrete between or within members, to identify the cracks and voids inside concrete members, that is important in evaluation of concrete properties and realize the microstructure of concrete status in aging or exposure to any severe conditions. Moreover, as a tool for quantifying the quality control through calculating the relationship between velocity and distance over the average time on each point as shown in Figure 3.20. In this study, the UPV test was carried out using SCC cube with 100 mm sides. At least three cubes were used for each mixture. The UPV test was performed in accordance with the requirements of the ASTM C 597, (2016). The UPV test represented the required time of the wave transferred between two opposite faces of the cubes in horizontal directions. The average reading was calculated and the pulse velocity, v (m/s) for all cubes samples was measured using the following Equation 3.9.

$$V_{UPV} = \frac{D_{UPV}}{T_{UPV}} \quad 3.9$$

V_{UPV} : Pulse velocity, D_{UPV} : Distance (m). T : is the average time on each point selected in the test that the pulse needs to travel from two opposing faces (sec).

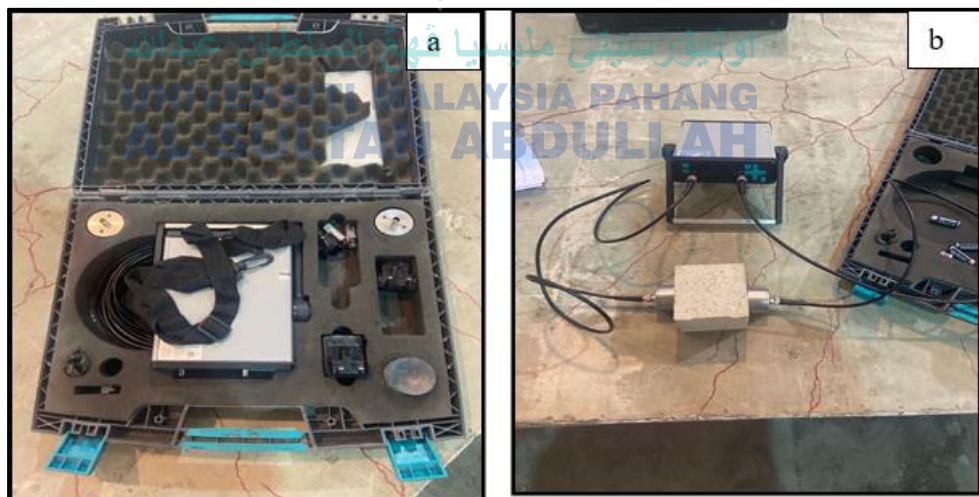


Figure 3.20 UPV device used in the experimental study

3.6.3 Durability Properties

Several of durability properties has been performed in this experimental work such as water absorption, acid resistance, and sulphate resistance. The following subsections showed each of the producers of properties in details in accordance with standards

3.6.3.1 Water absorption Test

This test is used to determine the percentage of water absorption of the concrete mixture as shown in Figure 3.21. This test is performed to determine the effect of micro-fine CBA as a partial replacement of cement towards the water absorption of SCC. The fabricated and modified SCC samples were tested for water absorption under the effect of micro fine CBA. The test was done according to ASTM C642-13, (2013). The samples were cured in the water curing tank for 7, 28, 56, 90, and 180 days. The concrete cubes samples having dimensions of 100mm x 100mm x 100mm were fabricated. The cubes were dried in an electric oven at a temperature of $105 \pm 5^{\circ}\text{C}$ for a period of not less than 24 hours. After drying, and then the samples were weighted by immersing them in the water, about 50 ± 5 mm water was maintained on the surface of the fabricated samples. After that, the surface of the samples was dried using a dried piece of cloth to get saturated condition then the weight was recorded. The water absorption values of the samples containing mechanically micro fine CBA were calculated using Equation 3.10. The obtained results were compared with results obtained from the control samples. Water absorption results are expressed as a percentage of the dry weight of the samples in the Equation 3.10.

$$\text{Water absorption (\%)} = \frac{(W_w - W_d)}{(W_d)} \times 100\% \quad 3.10$$

where, W_w : weight of saturated specimen in water, (g), W_d : weight of specimen in dry condition after drying in the oven, (g).

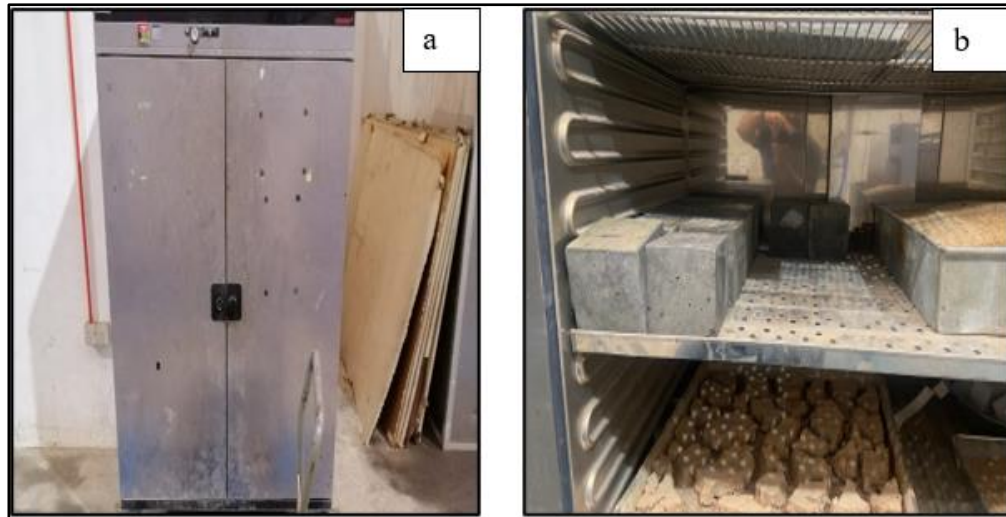


Figure 3.21 Electric oven used for water absorption in this experimental work

3.6.3.2 Acid Resistance Test

This test method provides a means of assessing the acid resistance that determines the durability performance of CBA as cement replacement in SCC samples as shown in Figure 3.22. The acid solution was prepared according to ASTM C1898, (2020). Acid resistance test was conducted to determine the effect of CBA as partial cement replacement towards acid resistance of SCC samples. During this test, the three parameters to be determined are measurement of mass loss, visual assessment, and strength loss. This test was conducted by preparing 72 cubes of 100 mm x 100 mm x 100 mm size containing CBA as partial cement replacement in SCC mixture for this experimental work, it contained 10%, 20%, 30% 40%, and 50% CBA as cement replacement in SCC samples. The samples were cured in water curing until 28 days. After 28 days, the mass of all SCC samples was measured. Then, three samples from each mix were immersed in 5% sulfuric acid (H_2SO_4) solutions for various duration of immersion at 7, 28, 56, 90 days. At every immersion duration the loss in weight of the samples was measured and any changes in terms of specimen's shape and strength were observed. The prepared cubes were cured in water for 28 days after which they were immersed in 5% H_2SO_4 in accordance with ASTM C1898, (2020). The initial mass and the mass of SCC samples after the immersion period of 7, 28, 56, and 90 days were measured for finding the mass loss due to the deterioration of concrete samples. The average value of three samples was considered for assessment. The mass loss and strength loss were determined by using Equations 3.11 and 3.12.

$$\text{Mass loss (\%)} = ((M_1 - M_2) / M_1) \times 100\% \quad 3.11$$

Where,

M_1 mass of samples before immersion

M_2 mass of samples after immersion

$$\text{Change in the compressive strength (\%)} = \left(\frac{F_{t1} - F_{t2}}{F_{t1}} \right) \times 100\% \quad 3.12$$

F_{t1} = Average compressive strength of SCC samples after curing at various ages of test.

F_{t2} = Average compressive strength of SCC samples after immersion in acid solution after curing at various age of test.

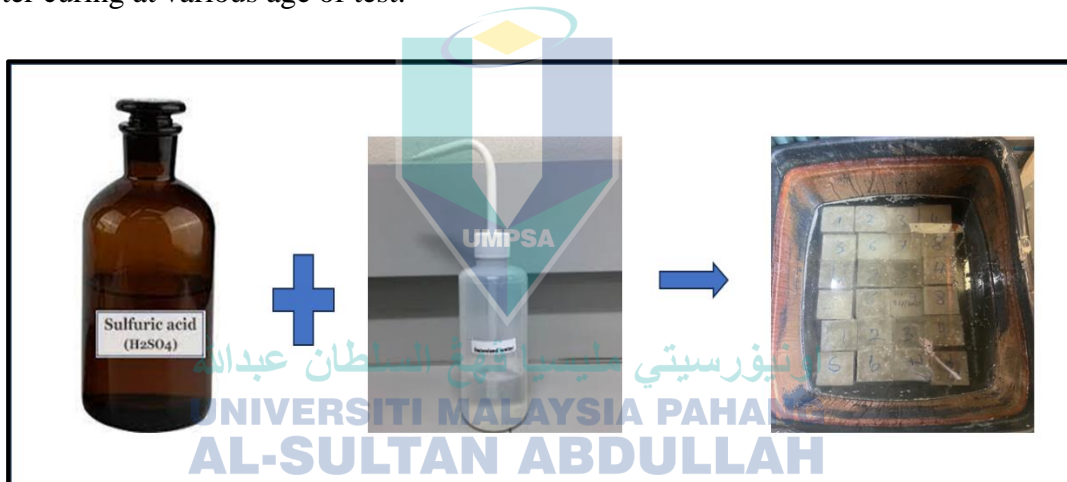


Figure 3.22 Sulphuric acid preparation and samples immered in acidic solution

3.6.3.3 Sulphate Resistance Test

This test method provides a means of assessing the sulphate resistance that determines the durability performance of CBA as cement replacement in SCC samples as shown in Figure 3.23. The sulphate solution was prepared according to (ASTM C1012, (2018). The degree of sulphate attack was evaluated by measuring strength reduction and mass loss of SCC samples. During this test, three parameters to be determined are measurement of mass loss, visual assessment, and strength loss. This test was conducted by preparing 72 concrete cubes of 100 mm x 100 mm x 100 mm size containing CBA as partial cement replacement in SCC mixture. SCC mixture for this experimental work

contains 10%, 20%, 30% 40%, and 50% CBA as cement replacement. The samples were cured in water curing for 28 days. After 28 days, the mass of all SCC samples was measured. Then, three samples from each mix were immersed in 5% sodium sulphate acid (Na_2SO_4) solutions for various ages of curing at 7, 28, 56, and 90 days. At every curing age the loss in weight of the samples was measured and any changes in terms of specimen's shape and strength were observed. The prepared cubes were cured in water for 28 days after which they were immersed in 5% Na_2SO_4 at all times of the immersion period. The initial mass and the mass of SCC samples after the immersion period of 7, 28, 56 and 90 days were measured for finding the mass loss due to the deterioration of SCC samples. The average value of three samples was considered for assessment. The mass loss and strength loss were determined by using Equations 3.13 and 3.14.

where,

$$\text{Mass loss (\%)} = ((m_1 - m_2) / m_1) \times 100\% \quad 3.13$$

M_1 = Mass of samples before immersion
 M_2 = Mass of samples after immersion

$$\text{Change in the compressive strength (\%)} = \left(\frac{F_{t1} - F_{t2}}{F_{t1}} \right) \times 100\% \quad 3.14$$

F_{t1} = Average compressive strength of SCC samples after curing at various age of test.

F_{t2} = Average compressive strength of SCC samples after immersion in acid solution after curing at various age of test.

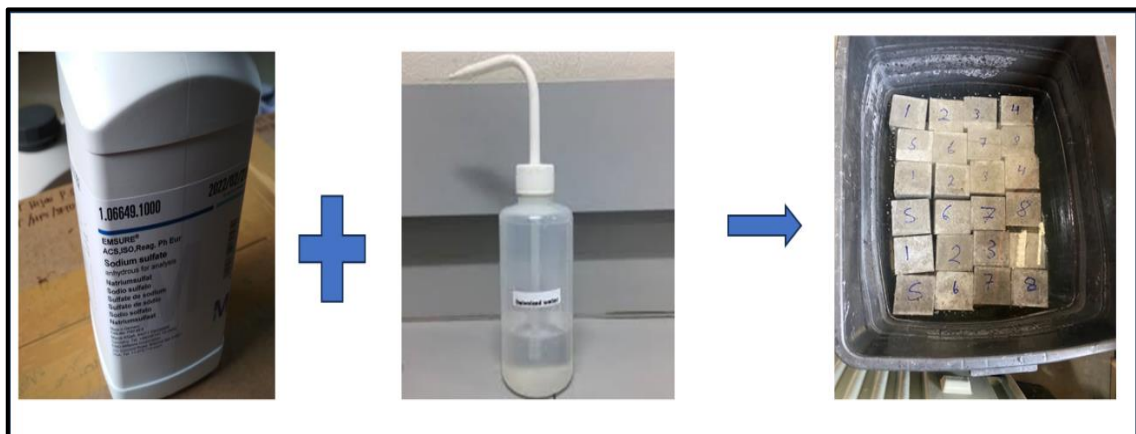


Figure 3.23 Sodium sulphate preparation and samples immersed sulphate solution

3.6.4 Microstructural Properties

For the purpose of assessing the microstructural characteristics for the materials to observe the change in the structure and the chemical composition of SCC control samples and SCC contain CBA as partial cement replacement. Several of microstructure characteristics has been performed in this experimental work such as Field Emission Scanning Electron Microscopy (FESEM), X-ray Fluorescence (XRF), X-Ray diffraction analysis (XRD), Brunauer–Emmett–Teller (BET), Scanning Electron Microscopy (SEM), Thermogravimetric analysis (TGA), Fourier-transform infrared spectroscopy (FTIR), and Energy-dispersive X-ray spectroscopy (EDX). The following subsections describes testing producer performed in the current study.

3.6.4.1 Field Emission Scanning Electron Microscopy (FESEM)

Field Emission Scanning Electron Microscopy analysis (FESEM) was used to investigate the morphologies of CBA particles before and after mechanically pre-treatment process. Supra 55 VP Inca X-Act Oxford FESEM device was used to implement the test. The morphology of the particles obtained from the prepared samples was analyzed with the machine at a +20 kV and under low vacuum conditions. For each sample tested, the working distance (WD) of the lens of the machine and samples were varied in the range from 5 to 9mm to facilitate the observing of the formation of fabricated CBA in SCC. All of the samples were crushed into small pieces, and then polished in order to obtain highly smoothed surfaces as shown in Figure 3.24.

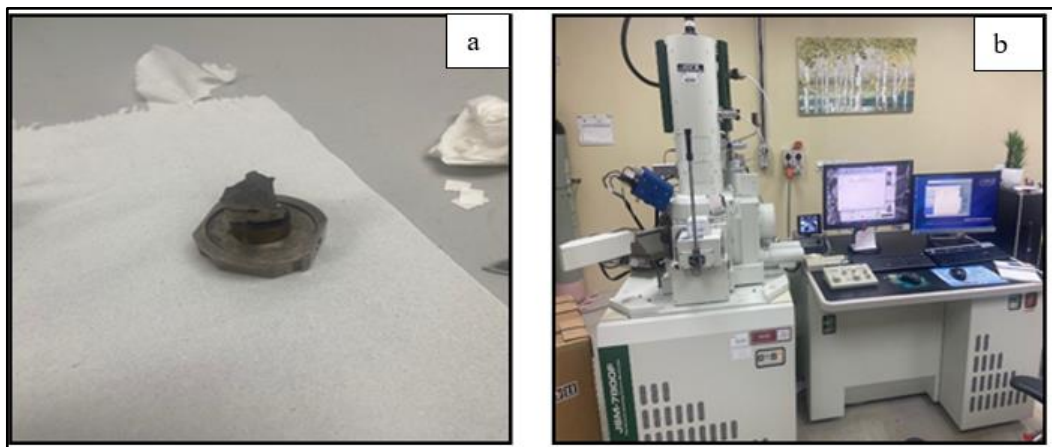


Figure 3.24 FESEM instrument used in this experimental work

3.6.4.2 X-Ray Fluorescence Test (XRF)

X-Ray Fluorescence (XRF) is an analytical technique that used to determine its elemental oxides composition for raw and ground CBA before and after mechanical pretreatment to be used in the SCC mixture as shown in Figure 3.25. The major components of ash content directly affect the chemical composition of CBA. While different category standards could be established in the regions for each coal class ASTM D388-18a, (2018); ASTM D4326-13, (2013) regulate the essential constituents of coal. Analyses of XRF were performed on CBA samples. The chemical composition results of the original CBA, ground CBA with various sizes of grinding. Main chemical compounds such as SiO_2 , Al_2O_3 , and Fe_2O_3 were detected as major components by XRF, as well as a variety of other chemicals in lower proportions. Raw CBA, and ground CBA and cement were analyzed using this XRF test.



Figure 3.25 XRF used in this experimental work

3.6.4.3 X-Ray Diffraction Method (XRD)

X-ray diffraction (XRD) is used to obtain information about the structure, composition and state of polycrystalline materials (Flewitt & Wild, 2017; Zhang et al., 2008). The XRD was used to investigate CBA after mechanical and chemical process by using Rigaku Miniflex X-Ray Diffractometer in a diffraction pattern measurement from

3 to 145 degree, the range for testing 2θ scanning range as shown in Figure 3.26. XRD constructive interference angle calculates for the wavelength and crystalline structural face for the samples. The sample in the form of powder, solid, film or ribbons. The minimum amount of material required is about 10g. However, greater accuracy is achieved if 10g of sample is available. There are restrictions on sample dimensions if the sample is to be mounted in an automatic sample changer (Zhang et al., 2008).



Figure 3.26 XRD instrument used in the present experimental work

3.6.4.4 Brunauer Emmett Teller (BET)

Brunauer -Emmet -Teller (BET) test with the accelerated surface area and porosimetry system were conducted in this study. The BET explains the physical adsorption of gas molecules on a solid surface and serves as the basis for an important analysis technique. This test was used to measure the specific surface area and pore volume and pore size of the original and micro fine ground CBA with various sizes by using nitrogen adsorption isotherm. Specific surface areas of the samples were determined by nitrogen adsorption using the BET analyzer. Furthermore, BET was used to measure the surface area in porous materials such as CBA. First, samples were dried in an oven at 105°C for 24 hours. Then testing was conducted according to (Brunauer et al., 1938). Every sample of CBA was weighed with the range 0.5g and placed in the rod for testing. The device used for BET test as shown in the Figure 3.27.



Figure 3.27 BET instrument used in the present experimental work

3.6.4.5 Scanning Electronic Microscopy (SEM)

The scanning Electron Microscope (SEM) utilizes a condensed beam of high-energy electrons to produce a range of signals on the surface of solid samples as shown in Figure 3.28. The range magnification ranging from 20X to approximately 10,000X, spatial resolution of 50 to 100 nm, and the area ranges around 1 cm to 5 microns of the samples. The SEM in this study was used to identify the impact of before and after mechanical pre-treated of CBA. Furthermore, the test was conducted for various grinding sizes of CBA. The test was accomplished according to guideline of hardened concrete properties described in ASTM C1723-10, (2010).



Figure 3.28 SEM used in the present experimental work

3.6.4.6 Thermogravimetric Analysis (TGA)

Thermogravimetric Analysis (TGA) was used in this study to determine the thermal characterization of cement paste with and without pozzolanic material. STA7000 Hitachi was used to determine the mass loss of material, upon heating the material from room temperature to 1000°C as shown in Figure 3.29. It was conducted in an inert atmosphere using nitrogen gas with a constant flow of 10 ml/min. The mass loss indicated the decomposition of cementitious and pozzolan phase i.e. calcium hydroxide and glassy silica. The test was conducted with full compliant with ASTM E1131,(2020).

To prevent any data misconception, the batch of sample was prepared by mixing cement, CBA, and water. The samples were cured in the water bath with temperature $\pm 30^{\circ}\text{C}$ room temperature until curing aged required. The samples were kept for curing age 7, 28, and 56 days for control and samples contain micro-fine CBA. On the testing day, the specimen was prepared by crushing the hardened specimen and sieve it to pass 300 μm screen. 20 g of this cement paste powder was collected and kept in a sealed lock plastic bag prior to the testing.



Figure 3.29 TGA device used in the present experimental work

3.6.4.7 Fourier transform infrared (FTIR)

The Fourier Transform Infrared Spectrometer (FTIR) model of the device used in this experimental study is the VERTEX 80 as shown in Figure 3.30. The characteristic of FTIR test is to conduct non-destructive analysis of samples to study the composition structure and chemical bond types of molecules. It measures the bond length of molecules, guess the three-dimensional configuration of molecules, and determine the composition of organic functional groups in samples. The Fourier Transform Infrared Spectrometer (FTIR) was used to collect infrared diffuse spectra of CBA samples. Fourier transform infrared (FTIR) spectroscopy was used to identify functional groups by measuring the absorption at characteristic wavelengths of bonds that vibrate independently of one another. The characteristic of FTIR test is to conduct non-destructive analysis of samples to study the composition structure and chemical bond types of molecules. It can measure the bond length of molecules, guess the three-dimensional configuration of molecules, and determine the composition of organic functional groups in samples.



Figure 3.30 FTIR device used in this experimental work

3.6.4.8 Energy Dispersive X-Ray Analysis (EDX)

Energy Dispersive X-ray spectroscopy (EDX) is a method for characterizing materials chemically or analytically. EDX systems are typically affixed to an electron microscope. Furthermore, element spatial distributions of the surface were illustrated using the (EDX) mapping function of the SEM. EDX were carried out in this experimental work to examine the micro-structure of cement, CBA, and for the SCC samples containing CBA as cement replacement. EDX is used for the elemental analysis or chemical characterization of a sample were investigated to understand the physiochemical properties of the cement, original CBA, and ground CBA. It relies on the interaction of some source of X-ray excitation and the sample as shown in Figure 3.31. Its characterization capabilities are due in a large part to the fundamental principle that each element has a unique atomic structure allowing a unique set of peaks on its electromagnetic emission spectrum. The EDX analysis was employed to determine the chemical components and the EDX analysis was used to find the peak formation of C–S–H and C-H for cement and CBA samples. Moreover, EDX is used for chemical identification of elements and their concentration. In EDX, electrons knock out electrons from atoms, producing X-rays of characteristic wavelength.



Figure 3.31 EDX device used in the present experimental work

3.6.5 Pozzolanic Properties Test

In this section, the pozzolanic properties of original CBA and various grinding sizes have discussed. The following sub-sections discuss the influence of the pozzolanic properties of CBA when used as partial cement replacement. Several of pozzolanic properties has been performed in this experimental work such Chapelle, Farttini tests, strength activity index (SAI) in accordance with the standard specifications for each test. Furthermore, the hardened mortar compressive strength and strength activity index were presented in subsequent section to achieve the pozzolanic characteristics in accordance with ASTM C618. For the strength activity index were calculated based on the compressive strength results at various curing ages.

3.6.5.1 Chapelle test

In this experimental study, a Chapelle activity test was used to investigate the pozzolanic reactivity of CBA from a chemical point of view. In the present study, the pozzolanic activity of CBA was investigated in accordance with the guidelines given in NF P18-513, (2012). The procedures for performing the Chappelle activity test of the pozzolanic materials used in this study are shown in the Figure 3.32, according to established standard guidelines. In an Erlenmeyer flask with a capacity of 500 mL, 1.0 g of pozzolan was mixed with 2.0 g of calcium oxide (CaO) in 250 mL of deionized water. The flask was then hermetically sealed and placed in a water bath at a temperature of 80 ± 5 °C for 16 ± 2 hours, while being constantly shaken with small stainless-steel balls

to improve the mixing process. The resulting solution was brought to ambient temperature, then 250 mL of a sucrose-containing solution (240g/L), prepared in deionized water at ambient temperature just before use) was added to the flasks. The flasks were then stirred with a magnetic stirrer for 15 minutes while the solution was agitated. The solution was then passed through the filter paper, and 25 mL of the supernatant was titrated with 0.1 M HCl, using a few drops of phenolphthalein as an indicator. Filtration and piping were done as quickly as possible to prevent the uptake of carbon dioxide from the environment. Equations (3.15) and (3.16) are a representation of the titration process that takes place throughout the procedure.



In addition, the activity at the Chapelle test was determined by applying the formulas in the Equations 3.17 as follows:

$$\text{Pozzolanic activity (mg CaO consumed /g CBA)} = \frac{(28)(2)(2)(V_3M_3 - V_2)}{M_2M_3M_4} \quad 3.17$$

where:

M_2 : Weight of CBA in grams, M_3 : Weight of CaO mixed with CBA in grams. M_4 : Weight of CaO in the blank sample in grams, V_2 : is the amount of 0.1 M HCl consumed by the sample solution, measured in millilitres. V_3 : is the amount of 0.1 M HCl consumed by the blank solution, measured in millilitres.



Figure 3.32 Experimental process of the Chapelle test for CBA to check the pozzolanic reactivity

3.6.5.2 Frattini Test

The Frattini test method is considered as a direct evaluation of the pozzolanic activity according to the European standards BS EN 196-5, (2011). It is a chemical method to determine the presence of calcium oxide which is the active pozzolanic material and hence establish the pozzolanic activity a given sample as shown in Figure 3.33. This test in accordance with the guideline in the standard BS EN 196-5, (2011). Test samples were prepared as a mixture by weight of 80% cement and 20% of ground CBA with various sizes. Blended cements and a control sample prepared with 100% cement (OPC) were mixed with 100 ml of distilled water as shown in Figure 3.34. This sample is then added to 100 mL distilled water at 40°C and vigorously soaked for 20 seconds, after which it is placed in an electric oven at 40°C for four days. After, it is filtered under vacuum conditions and then analyzed via titration to quantify both $[\text{OH}]^-$ and $[\text{Ca}]^{2+}$ ions, the former using 0.1 mol/L HCl solution and five drops of methyl-orange indicator, the latter with 0.03 mol/L EDTA solution and Patton and Reeders indicator. The last titration is performed after a pH correction to achieve a pH value of 12.00 ± 0.5 as shown in Figure 3.35. The same test was carried out for a sample made using cement only and another was replaced with 20% of ground CBA in accordance to standard guideline BS EN 196-5, (2011). Samples were left for 8 days and 15 days in a sealed

plastic bottle in an oven at 40°C. Then, the samples were filtered using (Whatman No. 542 filter paper, nominal pore size diameter ~3 µm) and the filtrate cooled to ambient temperature in a sealed bottle. The following procedure as shown in the Figures 3.34 and 3.35 below. The concentration of hydroxyl ions (OH⁻) in millimoles per liter was determined as:

$$[\text{OH}^-] = (1000 \times 0.1 V_3 \times f_2) / (50) \quad 3.18$$

where V₃ is the volume of 0.1 mol/L HCl consumed during titration in millilitres and f₂ is the HCl factor = 0.1 mol/L.

After the completion of the OH⁻ ion titration, the solution was adjusted to a pH of 12.0 ± 0.5 with NaOH. Subsequently, Calcon was added to the solution as an indicator. Then, titration was performed using an EDTA solution (maintaining the pH value by adding an NaOH solution if necessary) to change the colour from purple to blue. The concentration of Ca²⁺ (expressed as CaO) in millimoles per litre was determined as:

$$[\text{CaO}] = ((1000 \times 0.3 V_4 \times f_1) / (50)) \quad 3.19$$

where, V₄ is the volume of EDTA solution used for the titration, in millilitres;

f₁ is the factor of the EDTA solution.

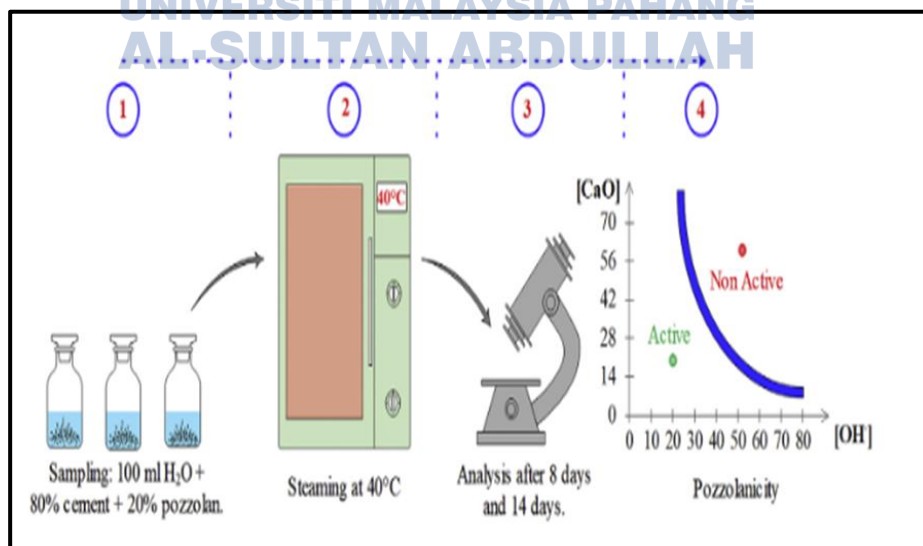


Figure 3.33 Graphical process of the Frattini test to check the pozzolanic reactivity of CBA

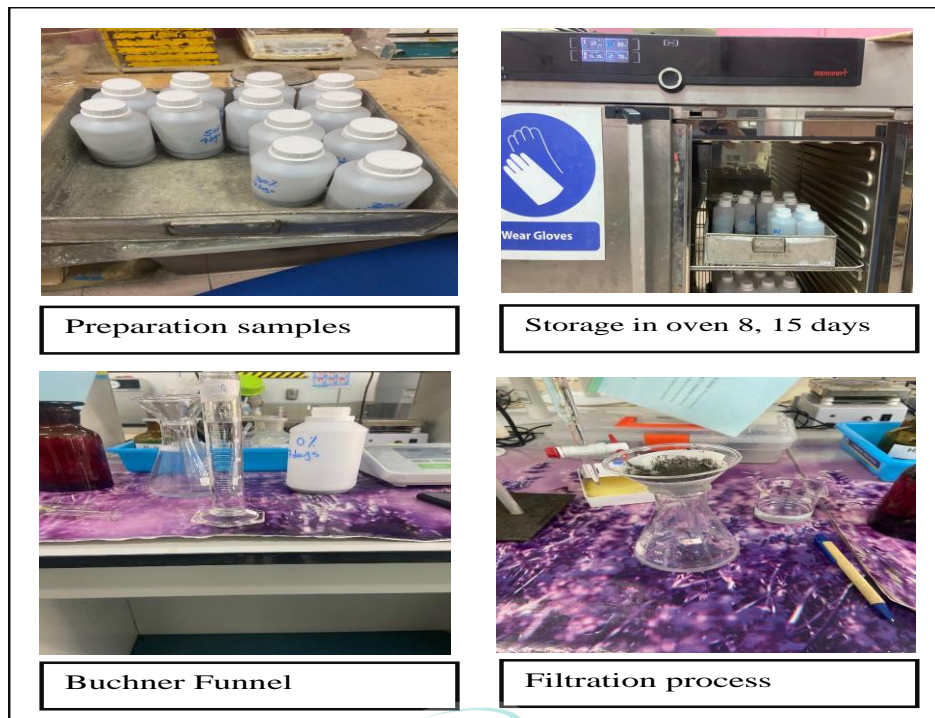


Figure 3.34 Preparation process and filtration for various samples

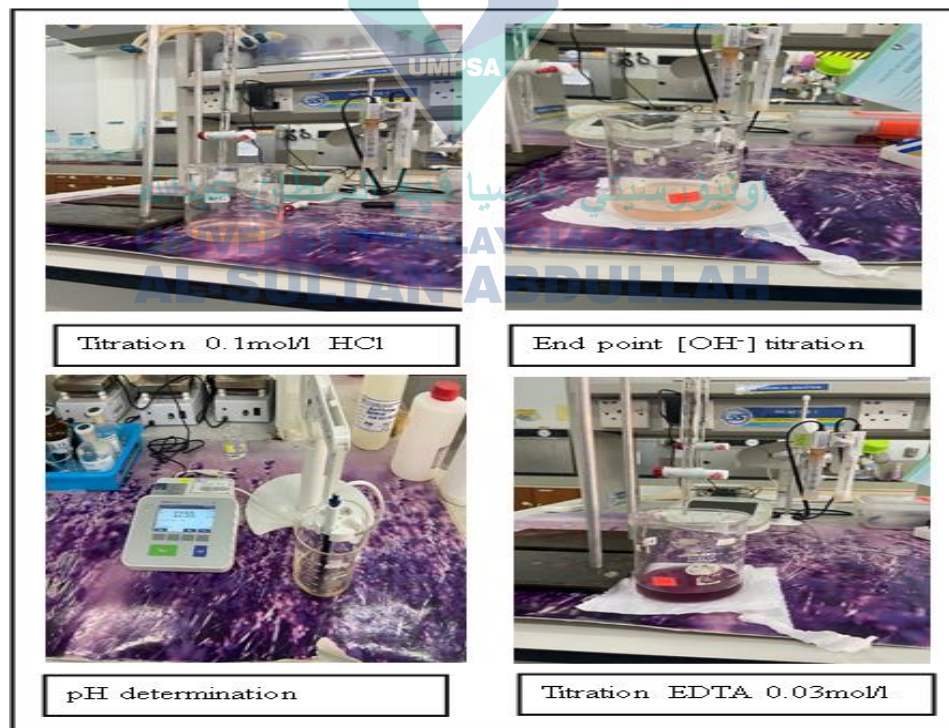


Figure 3.35 Determination of $[\text{OH}^-]$ and $[\text{Ca}]^{+2}$ concentration

3.6.6 Elevated Temperature

Each concrete mixture was cast in moulds to determine the variations in the compressive strength and the weight of the test samples before and after subjected to high temperature as well as to survey the crack patterns on the concrete surface after being exposed to elevated temperature. Furthermore, elevated temperature testing is important to determine the influence of CBA as cement replacement in SCC mixture. In this experimental work, the samples of 100 mm x 100 mm x 100 mm SCC cubes were prepared which consist of 10% to 50% of CBA as cement replacement in the SCC mixture. After 28 days of two stages of water curing, the samples were removed from the tank and dried in an oven for one day at a temperature of 110 ± 5 °C. Next, they were subjected to higher elevated temperatures (200°C, 400°C, 600°C, and 800°C) in an electric muffle furnace to reduce their moisture content by evaporation to lower degree, hence minimizing the possibility of early explosive spalling of samples when exposed to elevated temperatures in the furnace. For exposures to elevated temperatures, an electric furnace was used to elevate the temperature at a heating rate of 10°C/minute. After that, the samples were heated in an electric furnace at different temperatures of 200°C, 400°C, 600°C, and 800°C to simulate the actual environment wherein the concrete is exposed to elevated temperature for one hour as shown in Figure 3.36. To ensure a homogeneous heating environment around the samples, about 20 mm was kept between samples to ensure regular heating rate. After heating, the samples were kept it to cool down until reach to the room temperature. The loss in weight and compressive strength of the samples were examined and calculated using Equations 3.20 and 3.21 respectively.

$$\text{Weight loss (\%)} = \frac{M_1 - M_2}{M_1} \times 100 \quad 3.20$$

where,

M1 = Weight of samples before heated

M2 = Weight of samples after heated

$$\text{Strength loss (\%)} = \frac{f_{wc} - f_h}{f_{wc}} \times 100 \quad 3.21$$

where,

F_{wc} =Average compressive strength of samples before exposure to elevated temperature

F_h =Average compressive strength of samples after exposure to elevated temperature

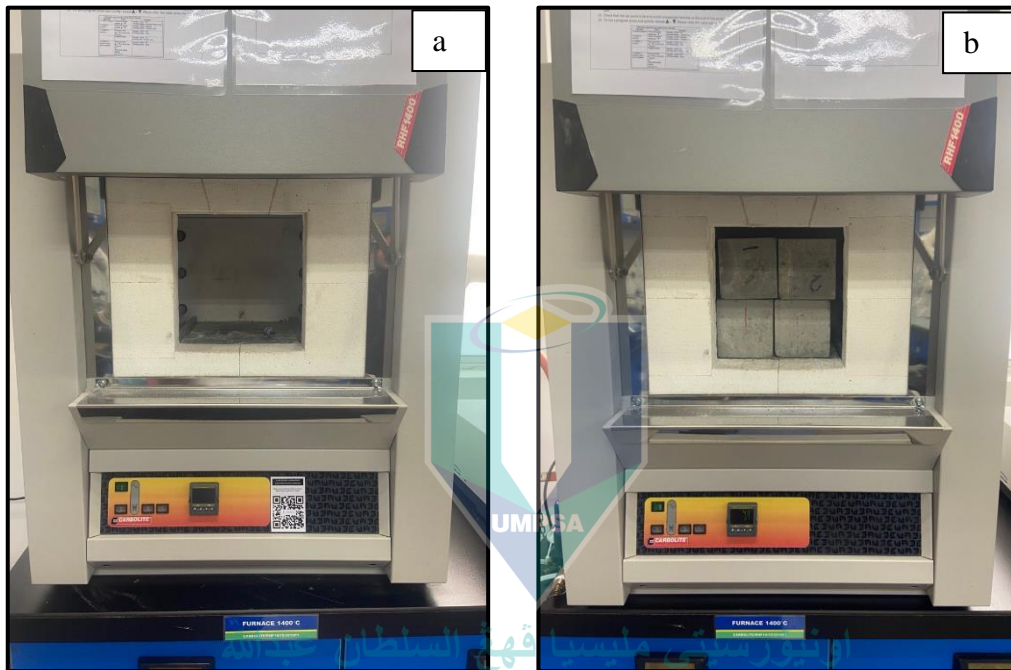


Figure 3.36 Samples exposure to elevated temperature in the electric furnace

3.7 Statistical Analysis for the Results

The statistical analysis used in this experimental work is Pearson correlation. It was used to analyze the experimental results of the physical properties such as Brunauer-Emmett-Teller (BET), Barrett-Joyner-Halenda (BJH), and specific gravity, and to find the correlation among the properties. Hence, evaluation of the engineering properties and comparison between the properties. The main feature in this study, to find the comparison and correlation by using Pearson correlation. The statistical analysis was conducted in various grinding sizes of CBA to choose the most suitable size to produce the SCC mixture. Pearson correlation was performed to obtain the correlation between each variable in all properties and ages of the samples. The limit of Pearson correlation from +1 to -1 where +1 indicates the positive perfect and good relation, -1 indicate the negative

perfect and good relation, 0 that's mean no relation exists. Pearson correlation was divided into various degree of correlation such as perfect, high degree, moderate degree low degree, and no correlation.

3.8 Summary

All experimental testing was conducted in accordance with the research flowchart of the experimental work. Besides that, data was collected to achieve the objectives and justify the result. The industrial waste materials namely CBA were prepared at the concrete laboratory in the Universiti Malaysia Pahang Al-Sultan Abdullah (UMPSA), Malaysia. Characterization of these materials was also conducted. Casting and testing all properties of SCC was conducted. Furthermore, the testing in the experimental work was divided into four main stages including (a) evaluate the physical, chemical, and microstructural properties of mechanically treated CBA as pozzolanic materials (b) analyse the influence of mechanically treated CBA on its pozzolanic properties based on Thermogravimetric analysis (TGA), strength activity index (SAI), Chapelle test, and Frattini test in cementitious binder (c) analyse the effect of mechanically treated CBA as partial cement replacement in the fresh properties of SCC based on slump flow, L-box, V-funnel, J-Ring, and mechanical properties of SCC based on compressive strength, flexural strength, Ultrasonic pulse velocity (UPV), splitting tensile strength (d) evaluate the influence of mechanically treated CBA as partial cement replacement on the durability properties based on (water absorption, sulphate attack, acid attack) and influence of elevated temperature (200°C, 400°C, 600°C, and 800°C). The results of each stage are analysed and discussed in chapter 4 and chapter 5. Then, the results are presented in the form of graphs, and tables in the next chapter.

CHAPTER 4

PHYSICAL, CHEMICAL, MICROSTRUCTURE AND POZZOLANIC CHARACTERISTICS OF CBA

4.1 Introduction

This chapter presents the results of the physical, mechanical and microstructure properties of raw CBA, cement, and various sizes of CBA used as partial cement replacement in SCC mixture. Furthermore, in this chapter, the characteristics of various sizes of micro fine CBA are discussed and the influence of the characteristics in the pozzolanic properties is evaluated. The characteristics of various sizes of ground CBA (CBA-3000, CBA-5000, and CBA-7000) in various testing such as BET, BJH, XRF, FTIR, TGA, and SEM with EDX are discussed in this chapter. Also, the influence of cement pastes in the pozzolanic properties such as strength activity index, Chapelle test, Frattini test were analyzed in this chapter. The optimum value for various sizes of ground CBA were evaluated using the physical, chemical and microstructure properties then will be used in the SCC mixture. Finally, the chapter ends with a summary of the key findings.

4.2 Properties and Characterization of CBA as Supplementary Cementitious Materials

4.2.1 Physical Properties of Original CBA and Ground CBA with Various sizes Compared to Cement

Ordinary Portland Cement (OPC) was used as the main binder. The cement was supplied by local Malaysian manufacture. The average size of cement is $6.920\ \mu\text{m}$ with specific surface area $0.867\ \text{m}^2/\text{g}$. The binder property is important for designing the mixture proportion. This can have a significant effect on the strength. The physical properties of CBA and CBA with various grinding cycles of 3000, 5000, 7000 cycles using electric Los Angeles machine such as moisture content, fineness modulus, specific gravity, and water absorption as illustrated in the Table 4.1. The specific surface area of original CBA $0.179\ \text{m}^2/\text{g}$ and the surface weighted Mean sizes $33.468\ \mu\text{m}$. It was found that the specific gravity for ground CBA is 2.31, 2.35, 2.43 for CBA-3000, CBA-5000,

CBA-7000 cycles respectively. The finding result shows the increment of grinding cycles of CBA increased the specific gravity value. Also, the specific surface area of ground CBA increased with the increase of grinding cycles led to produced higher specific surface area compared to cement. Furthermore, the colour of CBA was observed in this study to be grey after grinding was found to be darker in colour as dark grey or blackish as illustrated in Table 4.1. Generally, the CBA was well graded, and the range of particle size was comparable to cement, the results of range of particle size as shown in the Figure 4.1. Whereas, according to study by (Mangi et al., 2019) it was observed that the particles size for ground CBA less than 45 μm and the colour of CBA was from grey to dark grey after grinding period. The water absorption rate for CBA was found to be 5.30% which was higher absorption due to its porous inner structure (M. I. Al Biajawi et al., 2022). To achieve the high fineness of CBA by using various grinding processes with Los Angeles machine was used and mentioned in the subsequent characterization. This phenomenon is important because combustion can generate different-sized particles in CBA. According to study by Mangi et al., (2019) reported that the grinding time influence on the physical properties of CBA as partial cement replacement in concrete mixture. According to study by Mangi et al., (2019) was observed a continuous change in the properties of the specific surface area and specific gravity can be seen when the grinding period is increased. Nevertheless, the increment in the specific surface area and specific gravity of the CBA particles after grinding, the value of total alumina, active silica, and ferric oxide improved to be 70% to 80%, indicating a considerable increase in the pozzolanic reactivity of CBA particles.

Overall, the original CBA had a particle size ranging from 10 μm to over 1000 μm . Nevertheless, the mechanical pre-treatment effectively decreases the particle sizes with different grinding cycles (CBA-3000, CBA-5000, and CBA-7000) in comparison to the original CBA. Moreover, the CBA mostly consists of carbon particles with a higher LOI value and reactive CBA particles of around 500 μm . According to this findings, grinding CBA would enhance the interparticle reactivity, specifically among cement and CBA pozzolanic particles.

Table 4.1 Physical properties of cement, original CBA and ground CBA with various grinding sizes

Sample ID	Specific Gravity	Color	Volume of pores BJH (cm ³ /g)	Specific Surface Area (m ² /g)	Range of Particle Size (Micron)		
					D10	D50	D90
Cement	3.15	Grey	0.005739	0.867	3.753	20.689	52.420
Original CBA	2.21	Gray, Brownish	0.057857	0.179	22.857	130.820	391.875
CBA-3000	2.31	Dark grey (blackish)	0.010330	0.428	6.983	88.319	422.591
CBA-5000	2.35	Dark grey (blackish)	0.010952	0.392	8.024	88.054	440.504
CBA-7000	2.43	Dark grey (blackish)	0.007822	0.494	5.970	64.683	357.448

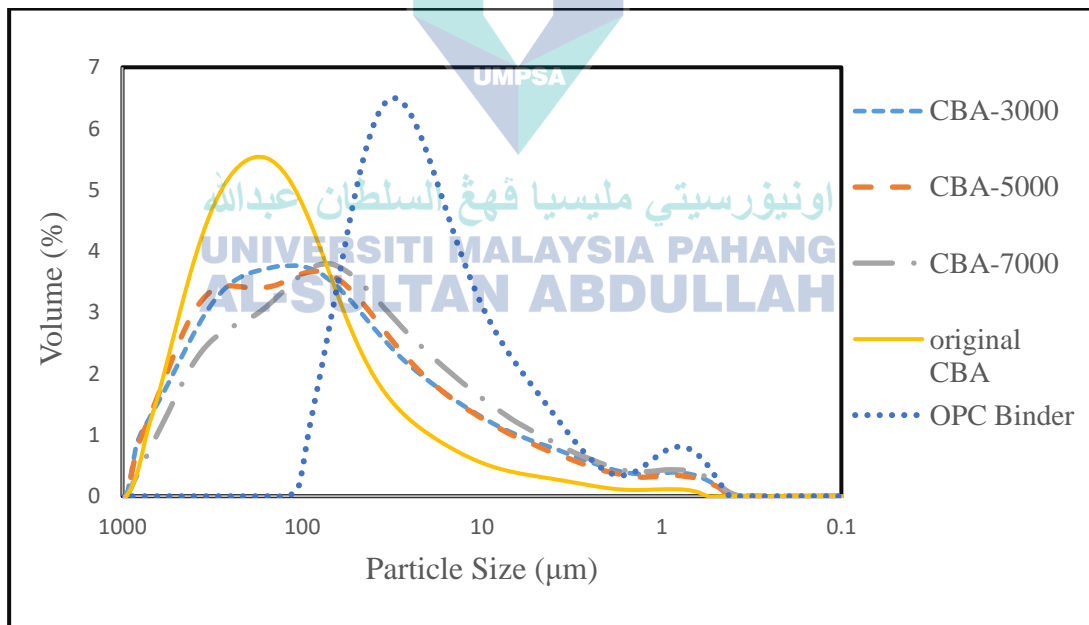


Figure 4.1 Particle size distribution of cement, original CBA and ground CBA with various grinding sizes

4.2.2 Chemical Oxides Composition of Original CBA and CBA with Various Sizes Compared to Cement

The X-ray Fluorescence (XRF) was used in order to obtain the chemical composition of CBA and ground CBA (CBA-3000, CBA-5000, CBA-7000) and cement.

The characterization of cement (OPC) as a main binder was important in the research. It controlled interaction with the chemical bonding of CBA final products. The cement consists mainly of 78.2% composition of $\text{SiO}_2 + \text{CaO}$. The MgO formed 0.693 % of the total oxide and the remaining alkalis are derived in form of K_2O (0.818%), TiO_2 (1.48%) and P_2O_5 (0.0485). The chemical oxide compositions of raw materials (cement, and original CBA) and ground CBA with various sizes CBA-3000, CBA-5000, and CBA-7000 are presented in Table 4.2. From the results of chemical oxides composition, it was observed that CBA and ground CBA are rich in silicon dioxide. CBA has a significantly high composition of ferric oxide of about 18.1% when compared to cement. The chemical composition of composite oxide of $\text{SiO}_2 + \text{Al}_2\text{O}_3 + \text{Fe}_2\text{O}_3$ was at 80.8% for CBA. The LOI value was marginally higher for CBA compared to cement. The major components of ash content directly affect the chemical composition of CBA. While different category standards could be established in the regions for each coal class ASTM D388-18a, (2018); ASTM D4326-13, (2013) regulate the essential constituents of coal. The chemical composition results of the original CBA, CBA-3000, CBA-5000, and CBA-7000 are shown in Table 4.2. The sum of $\text{SiO}_2 + \text{Al}_2\text{O}_3 + \text{SO}_3$ satisfies ASTM C618, (2019) requirement as a natural pozzolana and in the range limit of the standard. Furthermore, the sum of $\text{SiO}_2 + \text{Al}_2\text{O}_3 + \text{SO}_3$ can be classified as class F in accordance with ASTM C618, (2019) standard. Nevertheless, the total sum of silica, alumina and iron is the most important indication of the pozzolanic properties of the material. The analysis result shows, this ground CBA with various grinding sizes can be classified as pozzolanic material Class F –FA base on total amount (%) of SiO_2 , Al_2O_3 , and Fe_2O_3 for CBA-3000, CBA-5000, and CBA-7000 cycles is 81.930%, 81.60% and 79.70% respectively. Similar result has been reported by Mangi et al. (2019) was found the ground CBA after grinding achieve the pozzolanic properties in accordance with (ASTM C618, 2019). However, CBA is to be used as a pozzolanic material, several aspects must be considered, including the chemical composition, the size of the CBA particles, the amount of water required, and the SAI of the mortar. The CBA obtained from different sources had different chemical compositions. Moreover, previous (Duxson et al., 2005; Steveson & Sagoe-Crentsil, 2005) studies have shown that when the average particle size of CBA is less than 10 μm fineness plays a greater role in inhibiting alkali-silica reaction (ASR) mitigation. Consequently, it has been shown that $\text{SiO}_2/\text{Al}_2\text{O}_3$ (SA) ratios with compositions in the range up to 3.9 exhibit higher strength (De Silva et al., 2007; Latifi

et al., 2015). While changes in SA ratio above this range are associated with weak strength for the structural element. Therefore, the original CBA and the ground CBA (CBA-3000, CBA-5000, and CBA-7000) were evaluated based on the elemental composition of the oxides for the samples as shown in the Equation 4.1 below. The results show that the SA ratios for the original CBA and the ground CBA (CBA-3000, CBA-5000, and CBA-7000) as 3.827, 3.577, and 3.98 respectively, which is the range as reported in the previous studies.

$$\text{SA ratios} = \frac{\text{SiO}_2}{\text{Al}_2\text{O}_3} \quad 4.1$$

$$\text{SA ratios of (CBA - 3000)} = \frac{50.90}{13.30} = 3.827$$

$$\text{SA ratios of (CBA - 5000)} = \frac{50.80}{14.20} = 3.577$$

$$\text{SA ratios of (CBA - 7000)} = \frac{50.20}{12.60} = 3.98$$

Table 4.2 Chemical composition in oxide content (%) of cement, original CBA and CBA with various grinding sizes

Chemical elements (%)	Cement OPC	Original CBA	CBA-3000	CBA-5000	CBA-7000	Class of pozzolanic materials ASTM C-618		
						Class N	Class F	Class C
Silicon Dioxide (SiO ₂)	11.5	49.1	50.90	50.80	50.20	Minimum 70%	Minimum 70%	Minimum 50%
Aluminium Oxide (Al ₂ O ₃)	2.39	13.6	13.30	14.20	12.6			
Ferric Oxide (Fe ₂ O ₃)	4.00	18.1	17.30	16.60	16.90			
Sulphur Trioxide (SO ₃)	2.86	0.621	0.534	0.460	0.573	Maximum 4%	Maximum 5%	Maximum 5%
Calcium Oxide (CaO)	76.6	11.8	11.20	11.20	11.6	-	-	-
Magnesium oxide (MgO)	0.397	1.49	1.520	0.251	1.69	Maximum 4.0 %	Maximum 5.0 %	Maximum 5.0%
Potassium Oxide (K ₂ O)	0.937	1.51	2.070	1.66	2.63	-	-	-
Titanium Dioxide (TiO ₂)	-	1.48	1.320	1.30	1.45	-	-	-
Phosphorus pentoxide (P ₂ O ₅)	0.578	1.23	1.310	1.04	1.53	-	-	-
SiO ₂ +Al ₂ O ₃ +Fe ₂ O ₃	17.89	80.8	81.93	81.60	79.70	-	-	-

4.2.3 Microstructural Characteristics of Original CBA and Ground CBA with Various sizes Compared to Cement

This section discusses the microstructure properties from the experimental work of various sizes of CBA and ground CBA (CBA-3000, CBA-5000, CBA-7000) and compared to cement characteristics. The microstructure characteristics includes such as X-ray diffraction (XRD), Scanning Electron Microscope (SEM), Fourier-transform infrared spectroscopy (FTIR), and Thermogravimetric Analysis (TGA). The SEM, XRD, FTIR and TGA analysis of CBA, ground CBA (CBA-3000, CBA-5000, CBA-7000) and cement analysed and reported in the following subsections.

4.2.3.1 X-ray Diffraction (XRD)

The X-ray diffraction (XRD) analysis of OPC as the main binder is presented in Figure 4.2. XRD analysis was performed with the diffraction angle 2θ ranging from 10° to 70° . Phases were identified from the diffraction peaks and the main peak intensities showed various peaks formation for cement and CBA. The formation of the cement consists of main chemical compound such as Silicate (C_3S), dicalcium silicate (C_2S), tricalcium aluminate (C_3A), and Tetracalcium aluminoferrite (C_4AF). Throughout every instance, the cement phases appeared to be highly crystallised, with the major calcium silicate phases (C_3S , C_2S) showing maximum at the values that correlate to 2θ as shown in Figure 4.2. The strong correlation of significant peak intensity of all the major phases of cement components in the angular range for two values of 30° to 35° is one of the main obstacles experienced in the qualitative and quantitative evaluation of cement. This necessitates the identification of the individual elements is extremely difficult.

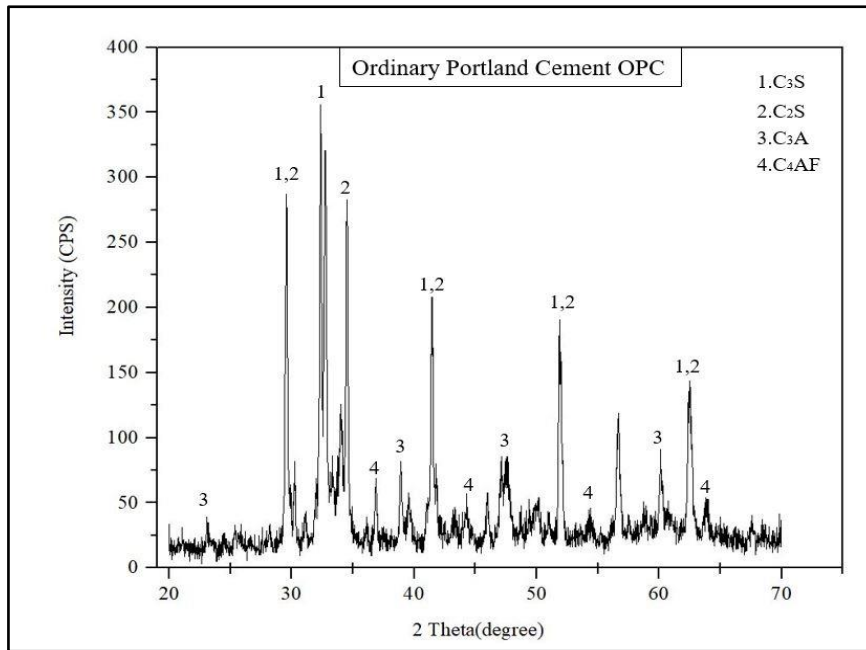


Figure 4.2 XRD Diffractogram pattern of cement OPC binder

The XRD was utilized to investigate the different phases present in the original CBA and ground CBA (CBA-3000, CBA-5000, CBA-7000). Figure 4.3 depicts an XRD diffraction pattern with a succession of peaks that correlate to certain planes in the mineral crystalline phase of original CBA sample. The XRD of CBA formed silica is in perfect accordance to result of the experimental work, in agreement with a number of prior results which reveal that peaks demonstrate the existence of silicon dioxide (Abbas et al., 2020; Zhu et al., 2018). According to Figure 4.3 of the XRD findings, the key components in CBA were found include such as quartz (SiO_2), mullite ($\text{Al}_6\text{Si}_2\text{O}_{13}$), and iron oxide (Fe_2O_3). This finding was consistent with the findings of the chemical properties. The chemical evaluation conducted by the CBA demonstrated that these materials could be utilized as building alternatives. These patterns differ from X-Rays of a certain wavelength at a specific angle, often represented in degrees. Consequently, the diffraction peaks of each peaks are unique and can be utilized to classify minerals or calculate component quantities. With an increased in the grinding sizes which is lead to amorphous material content develops, causing diffraction peaks to spread and vanish while backgrounds intensity rise. A considerable quantity of quartz (SiO_2) and mullite ($\text{Al}_6\text{Si}_2\text{O}_{13}$) was detected by XRD analysis in both the original specimens. CBA has been demonstrated to have a crystalline structure. Consisting of quartz, hematite, and mullite. The findings have further established the existence of SiO_2 and Fe_2O_3 phases in

CBA using XRD test. In addition, the high crystallinity of each component is shown by a peaks structure that is tight and distinctive (Z. Khan et al., 2014; Rafieizonooz et al., 2022).

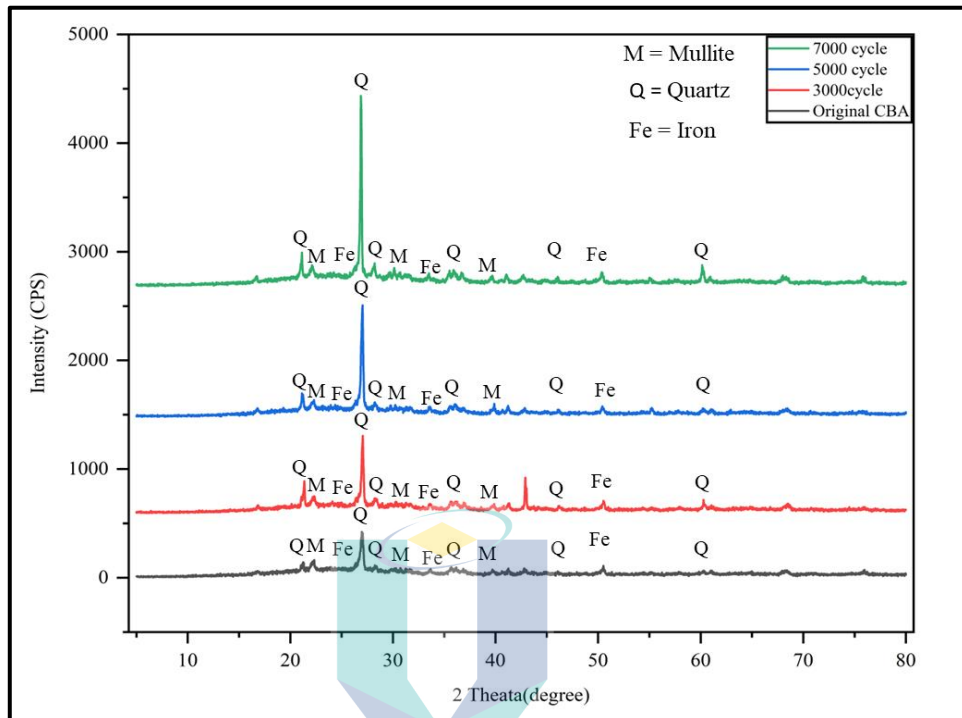


Figure 4.3 XRD Diffractogram analysis result for raw CBA, CBA-3000, CBA-5000, and CBA-7000

4.2.3.2 Scanning Electron Microscope (SEM) with Energy Dispersive X-ray (EDX)

SEM test assists in analysing the sample's structure and shape which is known as morphological investigation. The SEM investigation and study of the morphological properties of solid objects includes the characterization of micro particles. Through morphology investigation, it was observed from the SEM image of the cement particles at low magnification 1000x and high magnification 5000x as shown in Figure 4.4. At low magnification 1000x it was observed the cement particles have irregular shape and dense structure. It also shows fine particles and the most of particles small angular in shape as shown in Figure 4.4 a). Furthermore, it was observed that for cement particles at high magnification 5000x has needle-like structure is visible, needle-like crystals and angular as shown in Figure 4.4 b). According to study by Mangi et al., (2019) stated that the cement particles fine and dense structure from the SEM observations.

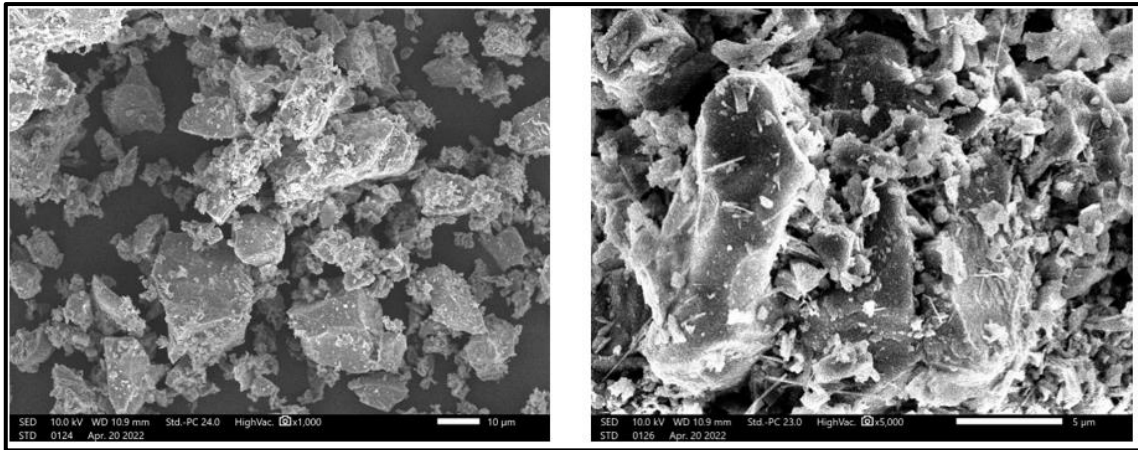


Figure 4.4 SEM morphology of cement at low and high magnification 1000x and 5000x

Figure 4.5 shows the (SEM) micrograph of the morphological properties of solid objects includes the characterization of micro particles. The surface morphology and mapping of the original CBA and ground CBA with various grinding sizes (CBA-3000, CBA-5000, CBA-7000) are presented in Figure 4.5. Meanwhile, the elemental composition analysis of the original CBA and ground CBA with various grinding sizes (CBA-3000, CBA-5000, CBA-7000) are shown in Figure 4.5. Through morphology investigation, it was observed from the (SEM) image of the original CBA, and ground CBA (CBA-3000, CBA-5000, CBA-7000) that the particles had a porous, irregular, and sharp shape. In addition, the composite has an extremely dense structure. In these examples, the pore sizes have been reduced. This is due to the mechanical grinding process of CBA in the types (CBA-3000, CBA-5000, CBA-7000), which causes the material to expand and some voids to gradually fill. When use CBA with increase the grinding cycle led to fill the voids are shown 4.5. The porous particles indicated that the CBA experienced melting and volatile was released during the combustion of the coal. The irregular and porous structure shows that it could provide surfaces for better contact of biomass gasification agent. Similar observation has also been noticed by Reddy et al. (2018) it was observed that CBA is of coarser, irregular, large size with rough surface texture in dark grey color because of the presence of unburnt carbon. Different glassy spheres, spheroids and aggregate with improper form are predominant in the CBA.

On the other hand, elemental composition of original CBA and ground CBA with various grinding sizes (CBA-3000, CBA-5000, CBA-7000) were analyzed by using the Energy Dispersive X-ray (EDX) and illustrated in the Figure 4.5. It can be noticed that

from EDX analysis for original CBA and ground CBA samples contain main element composition such as silicon (Si), aluminum (Al), carbon (C), calcium (Ca), potassium (K), oxygen (O), and iron (Fe). Based on the analysis of the EDX spectrum, it can be inferred that the particles primarily comprise of Calcium-aluminosilicate. The EDX results were a mean value derived from the image's three marked locations. These remarks are consistent with previous studies (Abbas et al., 2020; Bai et al., 2008; McLennan et al., 2000). As the temperatures surpass 1000°C, the mineral predominantly found in coal ash, namely kaolinite, experiences a process of recrystallization. This results in the formation of mullite and the release of supplementary SiO₂. Analysis of the CBA and iron-rich particles revealed the presence of carbon on their surfaces. This implies that un-combusted carbon exhibits a tendency to preferentially amalgamate with constituents of coal ash. The reaction between unburned carbon and SiO₂ is anticipated to yield the formation of Si-C at elevated temperatures. During the process of quenching, there exists a possibility of the Si-C compound undergoing a reaction on the surface of particles that are rich in iron (Abbas et al., 2020; Jaturapitakkul & Cheerarot, 2003).



اونيورسيتي مليسيا فهغ السلطان عبدالله
UNIVERSITI MALAYSIA PAHANG
AL-SULTAN ABDULLAH

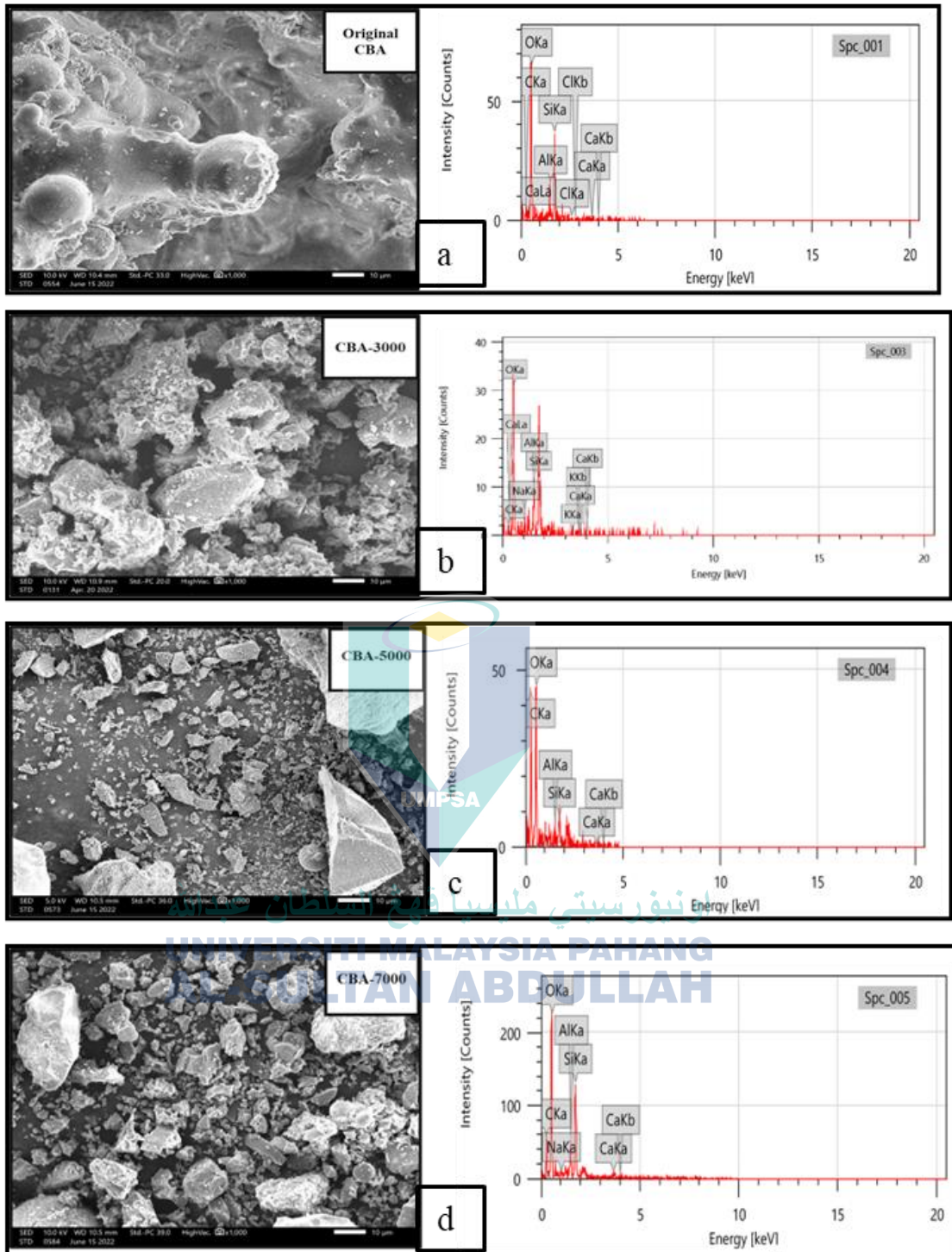


Figure 4.5 Scanning electron microscope (SEM) with Energy Dispersive X-ray (EDX) images with magnification of 1000x for (a)Original CBA, (b) CBA-3000, (c) CBA-5000, (d) CBA-7000

4.2.3.3 Fourier-transform infrared spectroscopy (FTIR)

Another important analysis to provide evidence on the formation chemical structures of functional groups of original CBA, and ground CBA (CBA-3000, CBA-5000, and CBA-700), and cement networks were further analyzed by Fourier Transform Infrared Spectroscopy (FTIR) analysis for all the specimens. To observe the changes in FTIR spectra of these four regions namely, O-H stretching, O-H bending, C-O stretching, and Si-O/S-O stretching vibrations are considered. The waves for the cement at 1000 cm^{-1} started stretching are observed. From the FTIR results in the Figure 4.6 for the cement was found that the peaks above 1000 cm^{-1} become more to straight line and the waves was reduced. This is due to the presence of quartz in cement. Nevertheless, a sharp FTIR for cement at the range of 2000 cm^{-1} to 4000 cm^{-1} is mostly due to the present of C_3S , C_2S , and C_4AF in the compounds of the cement particles. This finding in the agreement of the previous studies by (Danchuwa et al., 2022; Shrestha, 2018)

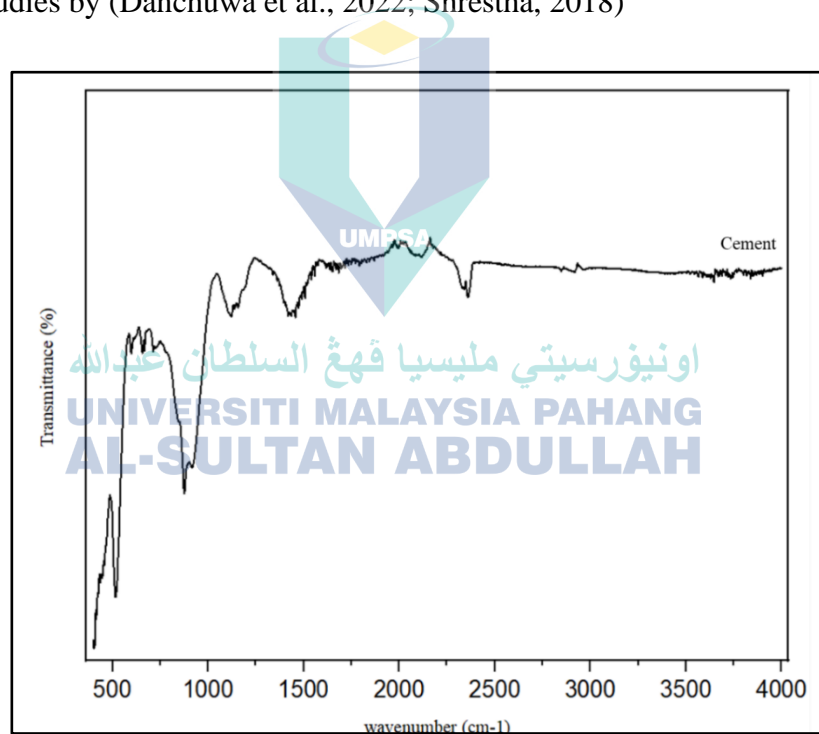


Figure 4.6 Fourier-Transform Infrared Spectroscopy (FTIR) analysis for cement

On the other hand, Figure 4.7 displays the FTIR spectra for original CBA, and ground CBA-3000, CBA-5000, and CBA-7000. For original CBA, it was observed less wavelength and the most characteristics band or the most peak value is located in the range of 500 cm^{-1} to 1000 cm^{-1} . For the waves were observed associated with C-H aromatic (Huda et al., 2021; Zhu et al., 2018). Furthermore, from Figure 4.7 shows

vibrational peaks of the functional groups appeared at wave number of 2250, 2800, 2900 cm^{-1} associated with C–H aromatic O–H, respectively. For the ground CBA (CBA-3000, CBA-5000, CBA-7000) it shows the most peaks 1000 to 1500 cm^{-1} which is due to two reasons. First reason the Si–O–Si bending mode for ground CBA (CBA-3000, CBA-5000, CBA-7000) due to high percentage of silica compared to cement. Also, Si–O–Si for ground CBA (CBA-3000, CBA-5000, CBA-7000) position is shifted to the right position or lower frequency compared with the original CBA, implying a chemical change and different particles size. The second reason is due to larger particle size for the original CBA, and ground CBA (CBA-3000, CBA-5000, CBA-7000) compared to cement particles. Overall, the CBA was observed that high waves number indicate that higher absorbed moisture as collected from their sources, which indicates that the main components of CBA particles are SiO_2 and Al_2O_3 . According to previous research conducted by (Kalaw et al., 2016) it was reported that the influence CBA in geopolymer using FTIR spectroscopy method, and the finding showed that FTIR spectroscopy results the most band for CBA is H-O-H, Si-O-Si, and Si-O-Fe in various wavelength and this indicated that the CBA highly amorphous of silica and higher absorbed moisture as collected from their sources. Similarly, another studies by (Criado et al., 2007; Zhu et al., 2018) used FTIR spectroscopy to investigate the gel composition in Alkali-activated materials (AAMs). The findings showed that the range of wavelength 800-1100 cm^{-1} is assigned to stretching vibrations of Si-O and reflecting that SiO_2 is the main chemical constituent of both the CBA and the alkaline solution.

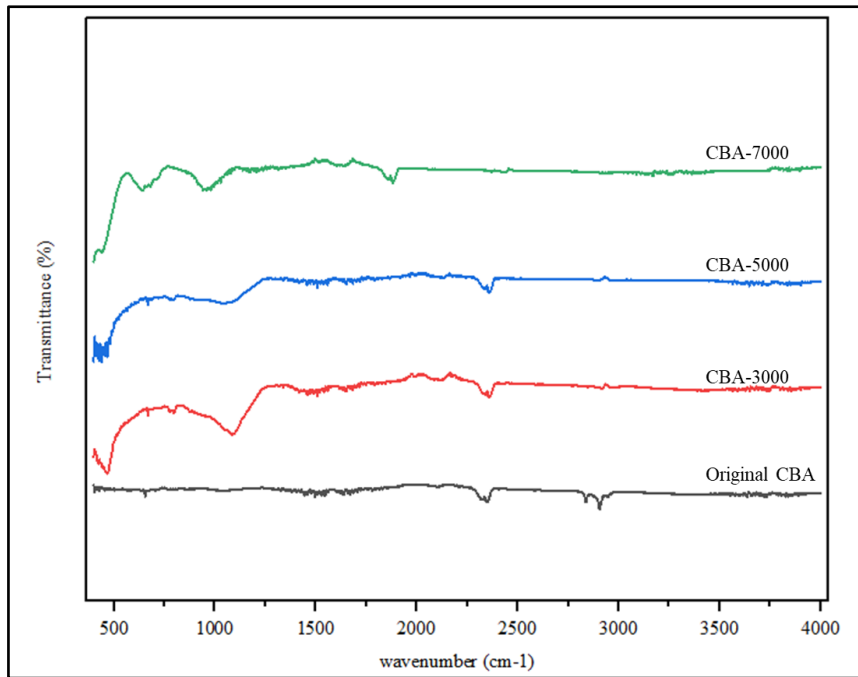


Figure 4.7 Fourier-Transform Infrared Spectroscopy (FTIR) results analysis for original CBA and ground CBA (CBA-3000, CBA-5000, CBA-7000)

4.2.3.4 Thermogravimetric Analysis (TGA)

Thermogravimetric Analysis (TGA) is a modern analytical technique that is easy to operate, as it offers a comprehensive account of both mass and thermal transformations that occur simultaneously during heating. During thermal treatment, the sample undergoes degradation in three successive stages, namely drying, combustion reaction, and end of combustion. In the drying phase, a small amount of water is released, and the overall decomposition is negligible. The combustion reaction phase is bifurcated into two phases: the first phase involves volatile combustion, while the second phase deals with char combustion. The final phase is the end of combustion, where decomposition ceases, and the heat flow reaches zero. TGA is a widely employed technique for exploring physical and chemical processes that lead to changes in mass, encompassing gas adsorption (e.g., Nitrogen), thermal degradation, sample moisture uptake, and other heterogeneous reactions (Tian et al., 2023). This technique permitted continuous weighing of the sample as a function of temperature at a desired temperature from room temperature (28°C) to 1000°C using the device (TGA Q500). The TGA of the cement is as shown in Figure 4.8. For cement, the total weight loss around 5.0 wt% corresponds to the weight loss due to the evaporation of surface adsorbed water. The adsorbed water was extracted by cement from the atmospheric air while it was kept in storage.

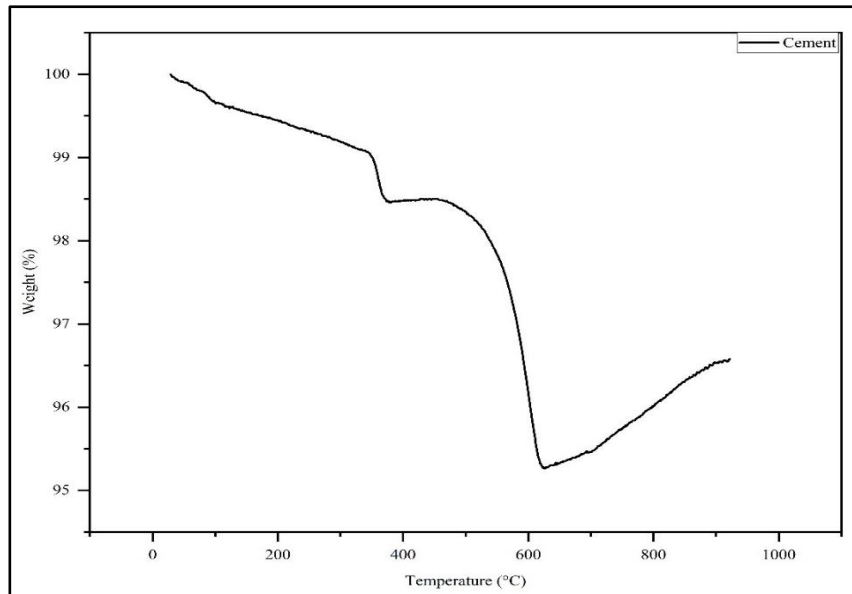


Figure 4.8 Thermogravimetric (TGA) analysis result for Cement OPC binder

For the original CBA, the total weight loss around 16wt% corresponds to the water loss physically adsorbed or contained inside the pore structure in the case of original CBA. The curve of original CBA shows three major weight losses at room temperature 28°C to 200°C, and 200°C to 400°C, and 400°C to 1000°C as shown in Figure 4.9. For the ground CBA (CBA-3000, CBA-5000, CBA-7000), the total weight loss of around 25 % corresponds to the moisture absorbed during preparation and grinding process of ground CBA (CBA-3000, CBA-5000, CBA-7000). The curve of ground CBA (CBA-3000, CBA-5000, CBA-7000) gradual weight loss from room temperature (28°C) to 400°C because of absorbed moisture during grinding process which is oven dried before starting the grinding process. A major weight loss is observed from 400°C to 750°C attributed to oxidation and burning of the organic particles entrapped inside the ground CBA (CBA-3000, CBA-5000, CBA-7000). From 750°C onward, weight loss is reduced although it continues to decrease up to 1000°C and beyond. Consequently, TGA of ground CBA shows different thermal behaviour compared to cement, original CBA. This is due to the original CBA presence of excess of water; absorbed during cooling with water at power plant (ul Haq et al., 2014). Furthermore, cement contains surface moisture particles due to storage process. Overall, the main weight loss for CBA is due to the removal of moisture from the samples. Moreover, the weight loss of CBA at a higher temperature after burning carbon is very low. This showed that CBA was thermally stable and can be used in thermal applications. Apart from that, this finding in

the agreement of the previous studies by (Hashemi et al., 2018; Phutthananon et al., 2023).

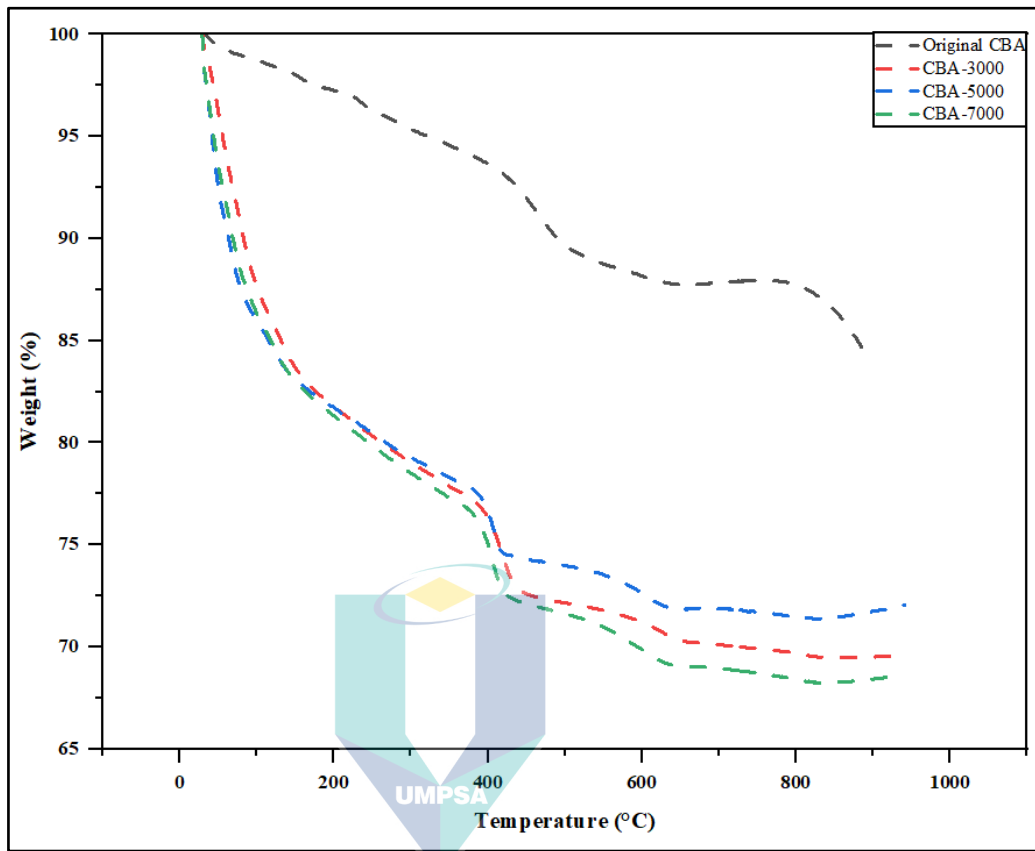


Figure 4.9 Thermogravimetric (TGA) analysis result for original CBA, CBA-3000, CBA-5000, and CBA-7000

4.2.4 Pozzolanic Characteristics of Original CBA and Ground CBA Compared to Cement

In this section, the pozzolanic properties from the experimental work of CBA with different grinding sizes are discussed to understand that CBA was used as an alternative for cement in the preparation of mixtures for hardened mortar samples. The pozzolanic properties characteristics includes such as Chapelle, Fartini tests, strength activity index (SAI) in accordance with the standard specifications for each test. Furthermore, the hardened mortar compressive strength and strength activity index were presented in subsequent section to achieve the pozzolanic characteristics in accordance with ASTM C618. For the strength activity index, it was calculated based on the compressive strength results at various curing ages. The following subsection elaborate each test for determining the pozzolanic properties.

4.2.4.1 Chapelle Test of Original CBA and Ground CBA with Various Sizes Compared to Cement

The Chapelle test is another direct method to assess the pozzolanic reactivity of pozzolans. In literatures, it is very commonly used for testing the pozzolanic materials such as metakaolin (Ferraz et al., 2015; Quarcioni et al., 2015). In this study, pozzolanic reactivity of ground CBA (CBA-3000, CBA-5000, CBA-5000) was investigated using modified Chapelle method NF P18-513, (2012) to evaluate the reactivity of pozzolanic material based on the consumption of Ca(OH)_2 . From the results, the pozzolanic activity by Chapelle analysis of CBA would be determined in an indirect manner by measuring Ca(OH)_2 consumption. Higher utilization of Ca(OH)_2 by activated silica from ground CBA (CBA-3000, CBA-5000, CBA-5000) would be associated with the presence of secondary C–S–H structures in cementitious materials. This structure would facilitate the filling of micro-voids and increase the strength properties of the cementitious substance. In addition, Chapelle activity is a method of measuring the amount of CaO consumed by pozzolans; the higher the value of Chapelle reactivity, the higher the pozzolanic reactivity of the sample. Figure 4.10 shows the CaO values of the different sizes constitutes based on the modified Chapelle test and calculated according to Equations in the standard NF P18-513, (2012).

The result is as expected based on the higher proportion of SiO_2 in ground CBA (CBA-3000, CBA-5000, and CBA-5000) with increase the fineness compared to original CBA. However, the reduction of grinding cycle led to bigger particles of ground CBA which provided less significant impact to the rate of CaO consumption. Based on the results of the Chapelle test shown in the Figure 4.10, the CBA with CBA-5000 consumed the most CaO. The expected result is consistent with the higher silica content of this powder. However, the influence of the low strength and delayed pozzolanic activity of the original CBA on the amount of CaO consumption was comparatively insignificant. For the other fineness sizes of ground CBA (CBA-3000, CBA-5000, CBA-7000), the pozzolanic reactivity is increased, resulting in a higher proportion of silica in the samples. Based on the previously conducted in this study of chemical oxides and pozzolanic reactivity, the different sizes of CBA showed the optimum and recommended CBA-5000 with high pozzolanic activity. However, the improvement due to additional C-S-H product in the sample, which lead to the improvement in terms of mechanical performance of the sample.

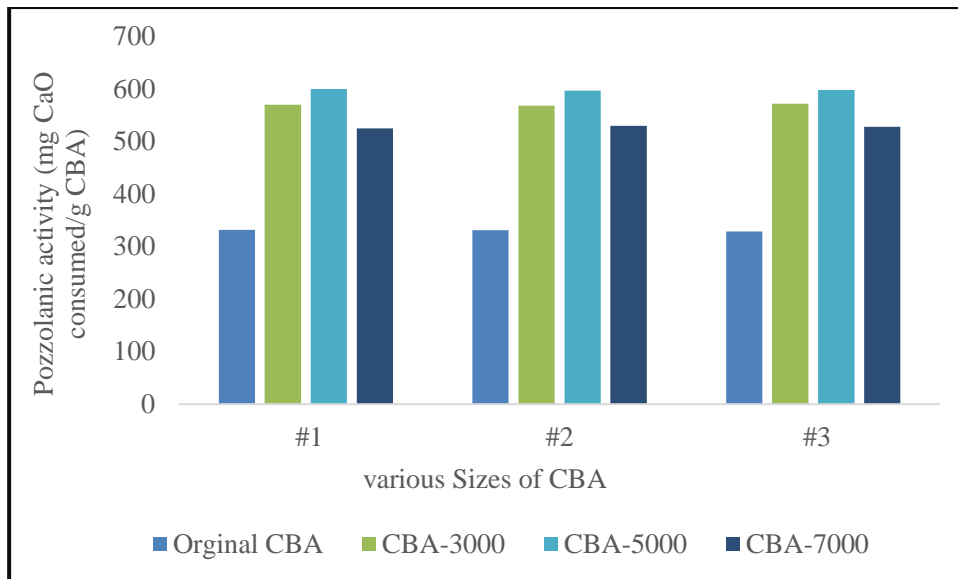


Figure 4.10 Pozzolanic activity of ground CBA with various sizes using Chapelle test

4.2.4.2 Frattini Test of original CBA and Ground CBA with Various Sizes Compared to Cement

The results of the Frattini test are presented in Figures 4.11 and 4.12 in accordance with EN 196-5 as an x/y-chart, with CaO [mmol/l] on the y-axis versus OH⁻ [mmol/l] on the x-axis, and the solubility curve of Ca(OH)₂. Results appearing below the solubility curve indicate the removal of Ca²⁺ from the solution which is attributed to pozzolanic activity, and results above the solubility curve indicate saturation or oversaturation with Ca(OH)₂ and thus no pozzolanic activity at 8 days and 15 days in accordance with BS EN 196-5, (2011). The described, possible filler effect was the main reason to determine the pozzolanic reactivity with the more reliable Frattini method. All the tested samples are plotted in the graph as a relation between the hydroxyl ions [OH⁻] and the calcium ions [CaO] measured in the solution after 8 days, and 15 days.

The results are reported in Figure 4.11 indicates the control samples and the samples containing 80% cement and 20% pozzolan of original CBA and ground (CBA-3000, CBA-5000, CBA-7000) shows pozzolanic activity at 8 days. For control samples showed that non pozzolanic activity materials which plotted above the curve indicated that amount of Ca²⁺ ions located in the portlandite zone and low percentages of limestone at 8 days. As expected, cement being hydraulic showed non-pozzolanic activity, and the mean value after the Frattini test was located on the solubility curve. Furthermore, control

samples containing only cement hydration, which is results in a saturated solution of $\text{Ca}(\text{OH})_2$ and the presence of reactive silicate and aluminate surfaces in test pozzolans ensures removal of dissolved Ca from solution. For other such as original CBA were results above the solubility curve in the regain that represents non pozzolanic characteristics. This is due to the pozzolanic reaction that took place and not initiated in the original CBA. According to study by (Faleschini et al., 2021) was observed that incineration original CBA was found to non-pozzolanic reaction was mentioned the reason due to no other sources of Ca^{2+} is present in the test system, while the negative values of CaO removal implies the presence of calcium in the solution (Donatello et al., 2010). Thus, the CaO was not only consumed, but probably added to the system. The effect could be related to the precipitated portlandite or C-S-H gel passing through the filter.

On the other hand, Figure 4.11 shows Frattini test results for $[\text{CaO}]$ versus $[\text{OH}^-]$ of mechanical grinding of CBA with sizes (CBA-3000, CBA-5000, CBA-7000) at 8 days. For ground (CBA-3000, CBA-5000, CBA-7000) presented positive pozzolanicity at 8 days when 20% of OPC was replaced by ground CBA, according to standard BS EN 196-5, (2011) for pozzolanic cements. The ground (CBA-3000, CBA-5000, CBA-7000) blends cement showed a clear pozzolanic reaction, with both CaO concentration and alkalinity indicating undersaturation with respect to portlandite. Furthermore, the pozzolanic activity of ground CBA slows pozzolanic characteristics which enhance by increased the grinding and decreasing the size of the CBA compared to original CBA and control samples. Moreover, all the ground CBA residues processed contained fairly high amounts of CaO. However, this is the clear evidence that improve the pozzolanic characteristics and reduced the consumption of calcium hydroxide in the pozzolanic reaction. The other reason for ground CBA is due to increase the reactive SiO_2 content by grinding size (Kramar & Ducman, 2018). According to study by Wu et al. (2020) was reported that the pozzolanic reactivity was enhanced for waste magnetite tailing as cement replacement indicates that part of the Ca^{2+} released by cement hydration into solution was removed due to the progress of the pozzolanic reaction, and that the amount of Ca^{2+} that was removed was small.

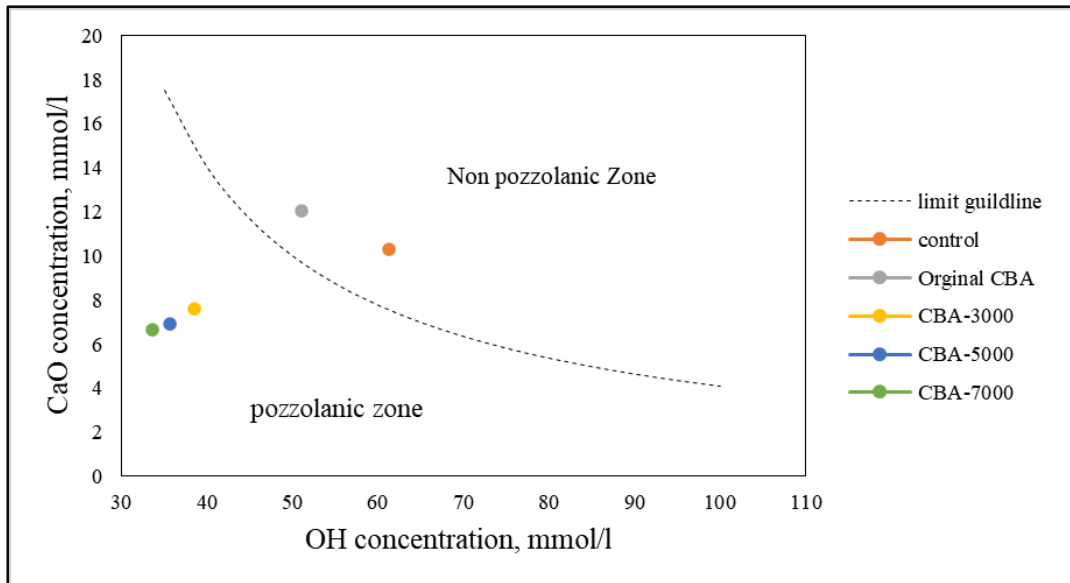


Figure 4.11 Results of the Frattini test for control and various sizes of ground CBA samples at 8 days

Figure 4.12 displays the Frattini test results for $[CaO]$ versus $[OH]^-$ and influence of control samples, original CBA, and ground CBA (CBA-3000, CBA-5000, CBA-7000) at 15 days in accordance with BS EN 196-5, (2011) standard. As shown in Figure 4.12 all of the plotted data for ground CBA (CBA-3000, CBA-5000, CBA-7000) are located underneath the saturation curve of lime, indicating some pozzolanic activity at 15 days. For others such as control and original CBA samples which are located above the saturation curve of lime non pozzolanic activity, which is represented as having insufficient pozzolanic activity. The reason for this is pozzolanic inactivity due to original CBA and control particles and inhibits Ca ions from reacting with amorphous Si surfaces. The second reason contains a high proportion of Ca^{2+} ions, which negatively affects the result of this test.

On the other hand, it is clear that the highest rate of the pozzolanic activity was achieved for ground CBA (CBA-7000) which consumed the lowest of the CaO at 15 days of curing. The enhance in the pozzolanic activity with increase the grinding size of ground CBA due to enhance the process of hydrates and a distinct relationship of the amorphization. Furthermore, for the results of ground CBA (CBA-3000, CBA-5000, CBA-7000) lying below the saturation curve indicates the removal of Ca^{2+} from the solution attributed to the start the hydration process which led to enhance the pozzolanic activity. According to (Rosales et al., 2022) was observed that the reference cements not

being pozzolanic cements, were above the reference line, indicating non-pozzolanicity. Also another study was conducted by (Khan et al., 2022) observed that total amount of calcium hydroxide that react with pozzolanic material is determined by the content of the reactive phases in the pozzolan, the SiO₂ concentration of reactive phases, the calcium hydroxide/pozzolan ratio, and the curing duration.

Overall, according to aforementioned results show that original CBA and control are not pozzolanic at 8 and 15 days of curing while the ground CBA (CBA-3000, CBA-5000, and CBA-7000) as pozzolanic reactivity at 8 and 15 days. The negative value of % CaO removal for original CBA and control samples was surprising as the amount of calcium in solution appears greater than expected. Also, many factors play the important role that can improve the pozzolanic reactivity such as content, reactive phases, pozzolan ratio, and the curing duration.

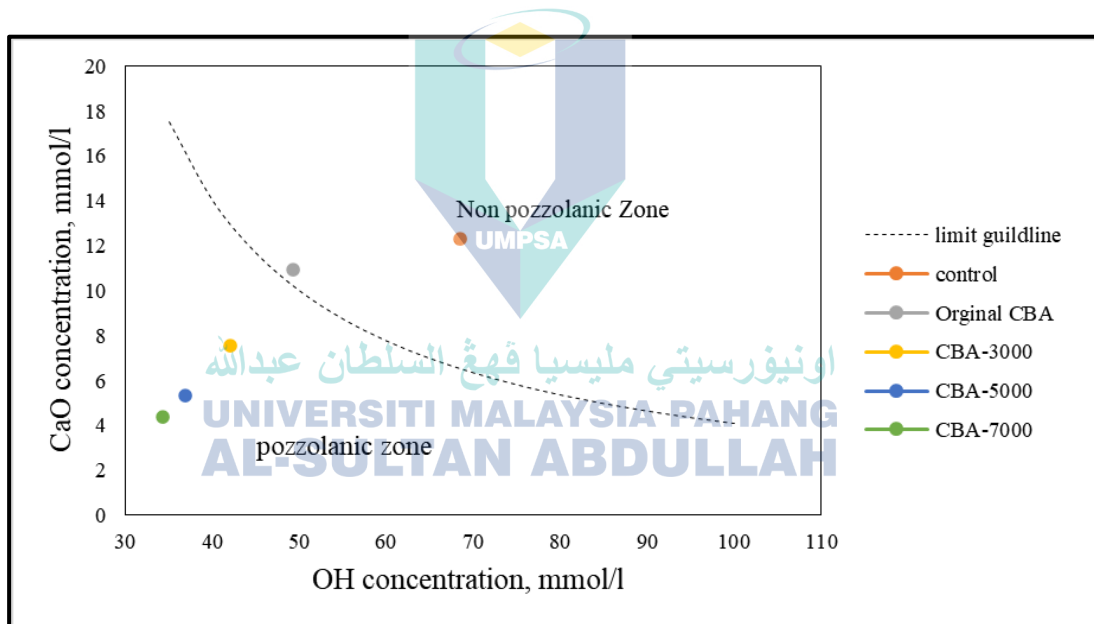


Figure 4.12 Results of the Frattini test for control and various sizes of ground CBA samples at 15 days

4.2.4.3 Compressive strength and Strength Activity Index of Hardened Mortar

The findings related to the compressive strength test for mortars containing various types of ground CBA (CBA-3000, CBA-5000, CBA-7000) as partial cement replacement and different ages of curing 7, 14, 28, 56, 90, and 180 days of curing are presented in Figures 4.13, 4.14, and 4.15 respectively. The compressive strength of CBA-based mortars was enhanced up to CBA 10% than control at the early age of curing in

comparison to conventional samples. However, the findings showed late pozzolanic reaction effect and gained higher compressive strength after 28 days of curing. From these illustrations, the compressive strength at age 7 days shows the mortar with 10% was higher compared to control samples. The strength reduced as larger amounts of CBA in higher percentage were integrated into the mix. However, at 28, 60, and 90 days of age, the other mortar specimens with larger amounts of ground CBA in higher percentage exhibited higher compressive strengths up to 20% compared to that of the reference mortar of 0% CBA. It can be understood that the compressive strength of mortar with various percentage of CBA would continue to increase with increasing curing age. The compressive strength improved with longer curing ages due to the continuous formation of calcium silicate hydrate (C-S-H) gel product (Argiz et al., 2017). Similar trend had been reported by (Ibrahim et al., 2015) integrated ground CBA as partial cement replacement in the mortar mixture.

Figures 4.13, 4.14, and 4.15 illustrates, the compressive strength of hardened mortar with different ratios and with various grinding sizes of CBA (CBA-3000, CBA-5000, CBA-7000) as partial cement replacement. Control specimen, without CBA in the mixture, would act as a benchmark for other mixtures. Other notation used are ground CBA (CBA-3000, CBA-5000, CBA-7000) describes the mixture that contains CBA with various sizes in mortar mixture. Furthermore, the compilation of raw data for strength activity index is included in the Appendices (Appendix B).

In terms of various grinding sizes for CBA, a comparison between ground CBA-3000, CBA-5000, CBA-7000 mortars, it was found that the strength of CBA-7000 mortars recorded higher values compared to that of the CBA-3000, and CBA-5000 mortars as illustrated in Figures 4.13, 4.14, and 4.15. Based on 7, 14, 28, 56, 90, and 180 days, three different fineness levels and five different ratios of CBA were used to determine the optimum combination to be used after that in SCC mixture. At different CBA contents, the compressive strength initially improved up to a cement replacement of 20% and then started to decrease with increasing CBA content. For all CBA types of (CBA-3000, CBA-5000, CBA-7000), the optimal replacement ratio for CBA was 20% at all curing ages. However, due to a pozzolanic reaction occurring between CBA and cement, they are improved at an early age, which is consistent with the results of (Cheah

et al., 2023) reported predicted that C–S–H development from cement hydration results in faster strength increase than C–S–H formation due to the interaction between pozzolan and portlandite (also known as pozzolanic behavior) at an early age. According to (Burhanudin et al., 2023; Cheah et al., 2023) showed that the impact of grinding was examined in terms of the ratio by-weight of CBA retained on a 45 µm sieve. Numerous replacement ratios were used. The findings show the compressive strength values increased by 4% with particle size 4.3µm at all curing periods. All mortar mixes with ground CBA as cement were found to have met the target strength at 28 days.

Figure 4.13 shows a conventional strength development trend of mortar mixture containing ground CBA-3000 as partial cement replacement. In overall, the inclusion of ground CBA-3000 in the mixture as a cement replacement material improved the strength properties up to 10% while the other replacement of ground CBA-3000 file to improve the strength performance. The strength improvements of 3.516% at 10% of ground CBA-3000, while the strength reduction 25.604%, 36.929%, 46.354%, 59.607% was observed in 20%, 30%, 40%, 50% of ground CBA-3000 in mortar mixture, respectively. However, there was strength reduction when curing continued up to 56 days at 20% to 50% of ground CBA-3000 compared to control mortar samples. The same trend could also be seen at 10% of ground CBA-3000 at 56 days and 90 days. Nevertheless, the strength performance of CBA-3000 becomes comparable with the control after 180 days of curing. In summary, CBA 10% of ground CBA-3000 was the optimum replacement for achieving the improvement in the strength value with the control.

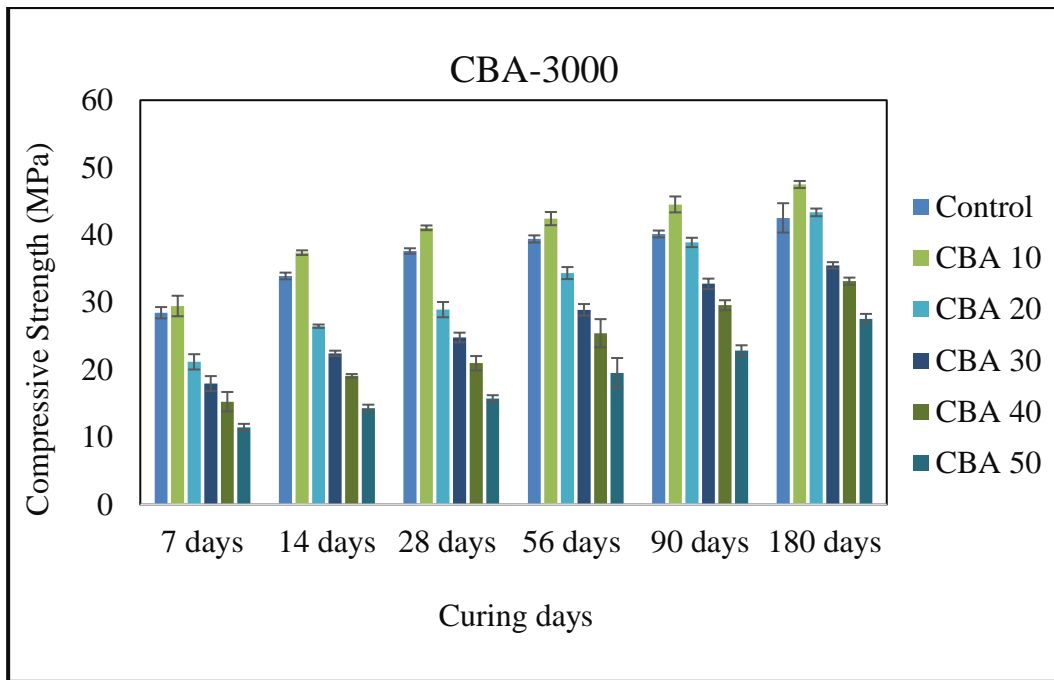


Figure 4.13 Compressive strength results of CBA-3000 as cement replacement in mortar mixture

As shown in Figure 4.14 different replacement level of ground CBA-5000 substitution and curing days had significant effects on the strength of hardened mortars. Conventional strength development also be seen in ground CBA-5000 mortar specimens as shown in Figure 4.14. Strength reduction at the early age of 19.201%, 27.596%, and 59.168%, was observed in 30%, 40%, and 50% specimens of ground CBA-5000 mixture, respectively. However, after 28 days, the substitution of cement with 20% of ground CBA-5000 had accelerated its pozzolanic reaction and increased strength to 13.288% higher than the control. Even though the grinding cycle for CBA-5000 was increased compared to CBA-3000 and other proportions of 30%, 40% and 50% showed a decreasing trend. Nevertheless, the mechanical grinding shows long term effect on compressive strength results, where other replacement ratios 30% 40%, and 50% enhance the strength properties at 180 days in compared to early age curing at 28 days.

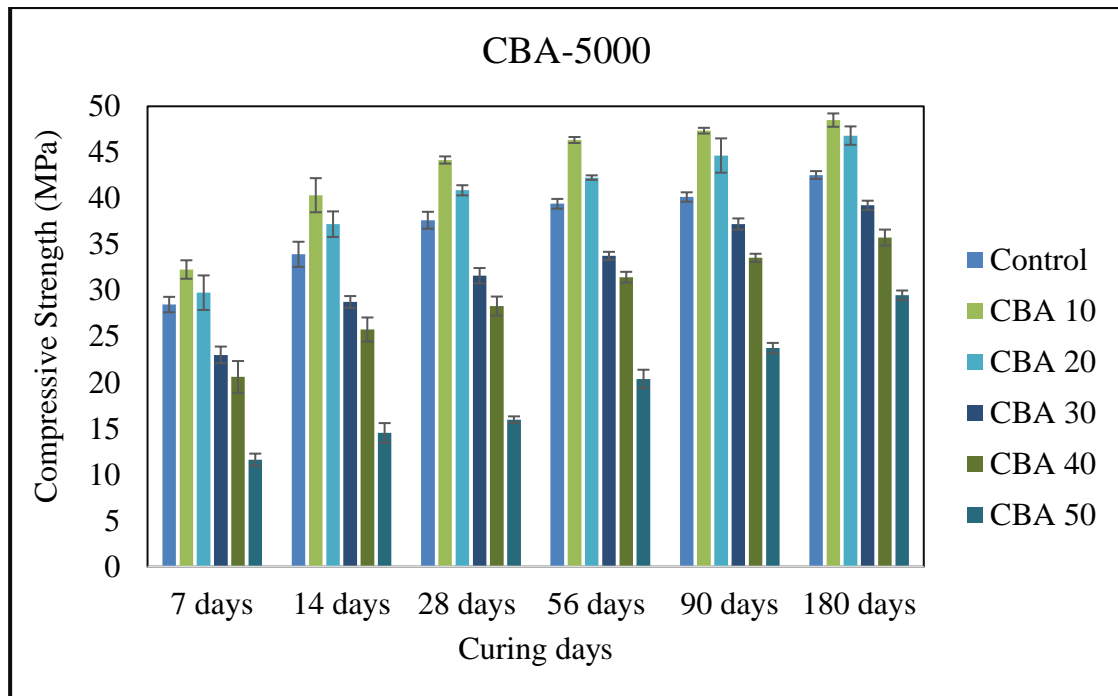


Figure 4.14 Compressive strength results of CBA-5000 as cement replacement in mortar mixture

Lower early strength performance for ground CBA-5000 specimens is related to the pozzolanic reaction had not initiated significantly, so the early strength was due to the presence of CBA in the higher amounts of CBA-5000 as partial cement replacement in mortar mixture. The second reason due to porous structure of ground CBA-5000 which lead to increase the absorptions of CBA particles in comparison to cement particles. Also, the effect of porosity in the CBA-5000 lead to delay for hydration process and the quantity of water required for mixture. These data are supported by the previous studies, which reported that before 14 days of curing, the pozzolanic activity of ground CBA with lime was very low and pozzolanic activity only started after 28 days. Meanwhile, a higher strength value up to CBA 20% after 28 days compared to control samples which was pointed out that pozzolanic activity begun at this stage, which is, due to the consumption of excess $(Ca(OH)_2)$ from the hydration product of cement. Moreover, due to the addition of CBA, the hydration process of the cement-mortar involves the chemical interaction between water and cement, resulting in the formation of a bonding agent. The results of the study demonstrated a steady reduction in compressive strength as the amount of CBA added to the mixture increased at 180 days. The stable strength performance can be seen at late curing ages 180 days compared to CBA-3000 and control samples in the mortar mixture. Nevertheless, the decreasing trend for CBA-5000 at 30% and 40%, 50%

is probably due to finer particles provide an increased the specific surface area and absorbed more available water in the mix, which lowers its pozzolanic reactivity in hydration process of the mortar mixture (Abdulmatin et al., 2018; Loginova et al., 2019).

Figure 4.15 displays the compressive strength performance of mortar specimens containing ground CBA-7000. At different CBA contents, the compressive strength initially improved up to a cement replacement of 20% and then started to decrease with increasing CBA content. However, due to a pozzolanic reaction occurring between CBA and cement, they are improved at an later curing age, which is consistent with the results of (Canpolat et al., 2004) they predicted that C–S–H development from cement hydration results in faster strength increase than C–S–H formation due to the interaction between pozzolan and portlandite (also known as pozzolanic behavior) at an early age. Moreover, the reduction strength at the early age of 11.423%, 30.648%, 41.794% and 67.342% for 20%, 30%,40%, and 50%, respectively at 7 days of curing. The conversion of ground CBA-3000, and ground CBA-5000, the ground CBA-7000 showed a significant improvement of 8.44% and 12.635% for 10% and 20% of the mortar containing ground CBA-7000 with higher strength than the control at 90 days of curing. However, replacement up to 20% remained from the early to the later age. However, adding more than 20% of ground CBA-7000 produced lower strength values of 8.989%, 22.082% and 40.537% for 30%, 40%, and 50%, respectively, compared to the reference mortar.

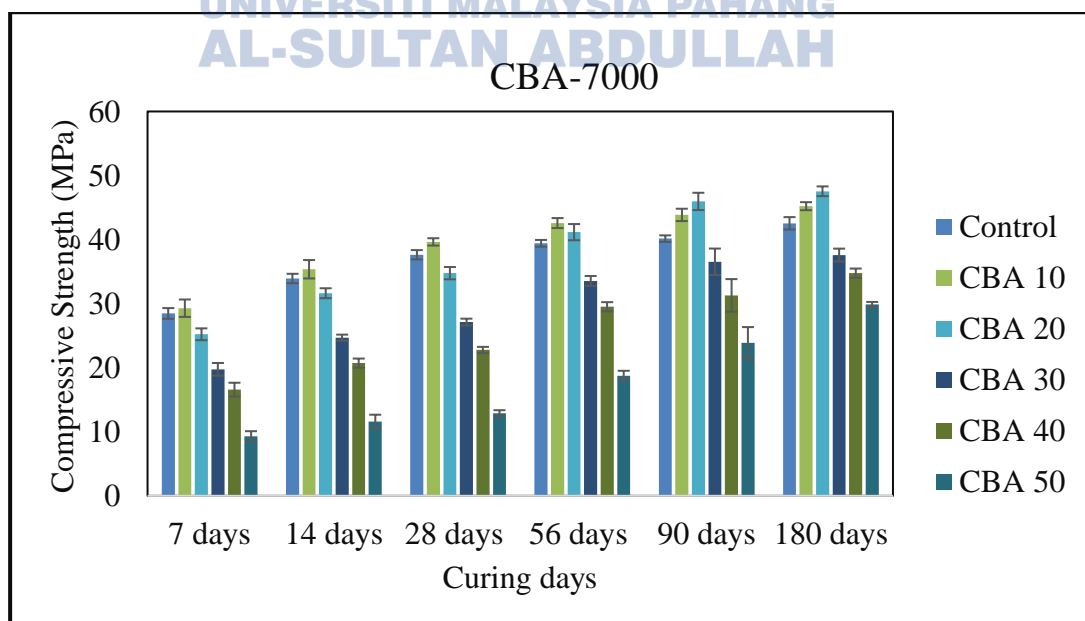


Figure 4.15 Compressive strength results of CBA-7000 as cement replacement in mortar mixture

In overall, late pozzolanic reaction is a general phenomenon in the use of ground (CBA-3000, CBA-5000, and CBA-7000) as a cement replacement material in mortar mixture. This is a common trend when the amount of cement is reduced. Insufficient hydration from the lack of tricalcium silicate compound from cement in the ground CBA (CBA-3000, CBA-5000, and CBA-7000) mixture has generated fewer portlandite to be consumed by additional reactive silica. It diminishes the role of secondary calcium silicate hydrate (C-S-H) framework produced by pozzolanic reaction. However, roles would be exchanged at a later age. Slower hydration produces less primary C-S-H gels, yet the abundance of portlandite provides a critical source for pozzolanic reaction. Hence, secondary C-S-H gels from late pozzolanic reaction give additional support to the mortar in sustaining strength. This situation justifies the slight increment of strength for the mortar containing 10% of ground CBA. Meanwhile, unstable strength performance in this cluster is mainly due to delayed as ground CBA leads to retardation of cement hydration (Chindasiriphan et al., 2023; Chuang et al., 2023). In this sense, additional grinding process to get ultra fine particles should be added in future research to reduce the particles into smaller size and improve the strength properties, thereby will enhances their pozzolanic performance. In short, the amount of cement replacement by ground CBA could be doubled from original CBA.

4.3 Statistical Analysis Pearson Correlation Analysis

Statistical analysis was conducted to justify the obtained results using mathematical inferences for a more solid conclusion. Furthermore, statistical analysis can be used to propagate the measurement error through a mathematical model to estimate the error in the derived quantity. Also, statistical analysis is an important tool in experimental research and is essential for the reliable interpretation of experimental results. The Pearson's correlation compares two average or called as means of data and shows the significant differences between the data sets. In this study, comparison was made to justify the accuracy of the data sets and the significant differences between the data.

The grinding process for various sizes of CBA as pozzolanic material are not well known especially the details of sizes and characteristics to be used as eco-friendly approach. Therefore, one of the most popular correlation methods is Pearson's correlation, which produces a score that can vary from (-1 to +1). However, the Pearson correlation coefficient was adopted to provide analysis in the correlation level between each size of

CBA. The IBM package of statistical program was used to analyze the available data and measure interrelationship between pairs of variables. Table 4.3 presents the complete results of Pearson correlation matrix for each variable. The following equation calculates the Pearson correlation based on the results between two variables. The Pearson correlation results derived from BET Surface Area, Volume of pores BJH (cm^3/g), specific gravity, tests with various sizes of CBA in comparison original CBA as shown in Table 4.3. The analysis on the calculated correlation coefficient was derived from the classification of each of the independent variables, namely, potentially Important, possibly important, not important. However, the rules for classified the variables according to the results and statistics which known as Correlation coefficient between -1.0 and -0.6 or +0.6 and +1.0, Correlation coefficient between -0.6 and -0.2 or +0.2 and +0.6, and Correlation coefficient between -0.2 and +0.2.

Table 4.3 Pearson correlation analysis for various grinding sizes in comparison to Original CBA

Variable	Specific Gravity	BET Surface Area (m^2/g)	BJH Volume of pores (cm^3/g)
Original CBA	1.00	1.00	1.00
CBA -3000	0.884615	0.91766	0.804223
CBA-5000	0.838627	0.96026	0.904263
CBA-7000	0.981980	0.99210	0.916814

According to the results for Pearson correlation was mentioned in the above Table 4.3 was found the range of the data 1.0 and -0.6 or +0.6 and +1.0 and classified as potentially Important. Furthermore the result for correlation coefficient were found in the first break point approximately ± 0.6 based on the fact the 95% confidence level for the correlation coefficient was derived from former statistic literatures in Pearson correlation analysis (Stehlik-Barry & Babinec, 2017). Based on this correlation coefficients, it can be concluded that CBA with size CBA-7000 the features had potentially important correlation to the amount of original CBA to be used in the SCC mixture. Furthermore, it can be concluded that CBA-7000 had potentially important correlations to the original CBA in terms of physical properties such as BET, BJH, and specific gravity. It was expected, because the more fineness of CBA which is suitable to be use as cement

replacement with micro size of CBA that can achieve the standard requirements ASTM C618.

4.4 Summary of Key Findings

Based on the results of this study, the effectiveness of mechanical treatment for CBA with various grinding sizes were tested in the characteristics to improve the pozzolanic properties. The optimum sizes of original CBA and ground CBA (CBA-3000, CBA-5000, CBA-7000) were characterized accordingly by its potential application as pozzolanic material in cementitious system. Furthermore, the optimum sizes of CBA were used in the SCC mixture to investigate their influence in the properties of SCC. The following conclusion were derived based on a comparative study of test results:

- i. Based on the physical properties of CBA were observed the average particle sizes 33.468 μm , also was observed the specific gravity leading to increase by increased the grinding cycle of CBA from CBA-3000 to CBA-7000. Furthermore, the specific surface area of ground CBA with increased the grinding cycles of ground CBA led to produced higher specific surface area compared to cement and original CBA. The colour of CBA change from gray after grinding was found to be darker in color as dark gray or blackish due to mechanical pretreatment process which impact in the change the color of the materials. The CBA performs as reservoir for water with higher surface area which leads to higher the water requirement. The particle size analysis revealed that the CBA particles had diverse porosity textures, and irregular shapes.
- ii. Based on the chemical composition, the XRF test results indicated that chemical oxides composition was observed that CBA and ground CBA are rich in silicon dioxide and achieve the ASTM C618 guideline as pozzolanic replacement materials.
- iii. Based on the XRD analysis indicated that the original CBA and ground CBA (CBA-3000, CBA-5000, CBA-7000) samples consisted primarily of quartz (SiO_2), mullite ($3\text{Al}_2\text{O}_3 \cdot 2\text{SiO}_2$) and iron (Fe_2O_3). Furthermore, the cement sample consisted primarily compounds of tricalcium Silicate (C_3S), dicalcium silicate (C_2S), tricalcium aluminate (C_3A), and Tetracalcium aluminoferrite (C_4AF).
- iv. Based on the SEM, the morphology was observed the cement particles have dense structure and irregular shape it showed also fine particles and the most of particles

small angular in shape. The original CBA, and ground CBA (CBA-3000, CBA-5000, CBA-7000) that the particles had a porous, irregular, and sharp shape.

- v. Based on the FTIR spectral analysis, indicated that the CBA samples have main functional bond Si–O–Si due to high amount of silica for original and ground CBA which increased with increased the grinding cycles and lead to reduce the size of ground CBA. Furthermore, the main functional bond for cement contains Si-O, which makes the CBA suitable materials to be used as partial cement replacement.
- vi. Based on the TGA, the total weight loss for cement was around 5.0wt% due to the evaporation of surface adsorbed water. For the original CBA the total weight loss around 16wt% and for ground CBA the total weight loss of around 30wt% corresponds to the moisture absorbed during preparation and grinding process of ground CBA (CBA-3000, CBA-5000, CBA-7000).
- vii. Based on pozzolanic characteristics, the binder reactions in mortar mixture and cement paste can be enhanced by replacement of ground CBA up to 20%. Larger replacement levels rather delay the hydration reactions. This can be due to the dilution of the clinker content in the paste, to the limited pozzolanic activity of the ground CBA at early ages. Assessment of the pozzolanic activity using the Chapelle test and Frattini test indicates the enhance the pozzolanic activity with increases the grinding cycles and decreases the size of the ground CBA which leads to increase the specific surface area. The compressive strength at early age at 7 days for the mixtures with ground CBA10% (CBA-3000, CBA-5000, CBA-7000) higher than for the control with OPC. At late curing ages, showed enhanced the strengths are obtained for mixes with up to 20% ground CBA compared to control samples. By increasing the fineness of the ground CBA, somewhat improve the compressive strengths until reach 20% in CBA-7000 in the late curing ages. However, due to the late pozzolanic reaction which affects the strength development.
- viii. The CBA-7000 is an optimal mechanical pretreatment method that involves grinding. The optimum grinding size for mechanical pretreatment method physical properties based on BET surface area (m^2/g), volume of pores BJH (cm^3/g), specific surface area (m^2/g). The mechanical pretreatment method significantly enhances the pozzolanic characteristics in terms of strength activity index, and Frattini test. The optimal

mechanical pretreatment has been effectively used in the manufacturing of SCC with various substitution ratios. The impact of a substantial increase in silica content in ground CBA-7000 is precisely validated by the findings of Chappelle analysis, strength activity index, and Frattini test. The greater utilization of Ca(OH)_2 by silica content in ground CBA-7000 compared to other sizes of ground CBA-3000 and CBA-5000, as well as the original CBA, suggests the potential development of (C-S-H) phase during the hydration process.



اونيورسيتي مليسيا قهغ السلطان عبدالله
**UNIVERSITI MALAYSIA PAHANG
AL-SULTAN ABDULLAH**

CHAPTER 5

FRESH, MECHANICAL, DURABILITY, AND ELEVATED TEMPERATURE PROPERTIES OF COAL BOTTOM ASH IN SELF COMPACTING CONCRETE

5.1 Introduction

This chapter discusses the influence of ground CBA content towards fresh, mechanical, durability and elevated temperature with 10% to 50% replacement for cement in SCC production. The optimum grinding size CBA-7000 was used to investigate the influence of the SCC mixture. The beginning of this chapter discusses the results for fresh properties of SCC namely (Slump flow, L-box, V-funnel and J-Ring) containing ground CBA as partial cement replacement with various replacement ratios (10% to 50%). The performance of mechanical properties of ground CBA as cement replacement such as namely compressive strength, flexural strength, splitting tensile strength and ultrasonic pulse velocity (UPV). Furthermore, the relationships between mechanical properties of the ground CBA content and curing age, and their effects on compressive strength, flexural strength, splitting tensile strength and UPV a of the SCC were analyzed in this chapter. Furthermore, the optimum replacement ratio was presented and discussed in this chapter. All specimens were subjected to water curing at early and late curing ages. Analysis on the microstructural properties such as TGA, and FESEM were performed on the representative from higher and lower replacement ratios (10%, 20%, 50%) for ground CBA as cement replacement in SCC production at 7, 28, 56 days of curing compared to conventional samples. Moreover, this chapter presents and discusses the durability performance of ground CBA as partial cement replacement with various ratios on durability testing namely acid resistance, sulphate resistance and water absorption. The influence of ground CBA as partial cement replacement subjected to low and high elevated temperatures based on visual observation, mass loss, and strength loss were presented in this chapter. Finally, the chapter ends with a summary of the key findings.

5.2 Fresh Properties of Optimum Mechanically Treated Ground CBA Based on SCC

In order to evaluate the fresh concrete properties of SCC mixes in terms of flowability, passing ability, and viscosity in accordance with the specifications established by (EFNARC, 2005), various workability experiments were conducted. The flow test was used to investigate the flowability of the prepared SCC mixture. The viscosity of SCC mixtures was measured.

5.2.1 Slump Flow of Optimum Mechanically Treated Ground CBA Based on SCC

Evaluation of fresh SCC properties was achieved by the utilization of slump flow test. This test was carried out to identify the effect of ground CBA content on the workability of SCC mixture. Figure 5.1 presents the slump flow of SCC specimen for control sample and ground CBA as partial cement replacement. The recommended range as mentioned in the standard guidelines (EFNARC, 2005) for slump flow is 550–850 mm. The control specimen has a slump flow of 674 mm as adopted from the selected mix design of trail mixes. The slump flow of SCC specimen decrease steadily as ground CBA was used to replace cement in the mixture. The reduction in the slump flow due to the porosity of CBA in SCC, thus absorbed more fluid with higher content of CBA in SCC mixture. According to the EFNARC (EFNARC, 2005) standard, slump flow results range from 550–850 mm. However, segregation may occur in SCC mixes with a slump of more than 700 mm, while in SCC mixes with a slump of less than 500 mm, the slump is insufficient to pass through densely packed reinforcement. The second reason for the slump flow of more than 700 is the possibility that the concrete mix could segregate during flow. The second explanation for the slump flow of more than 700 is the possibility that the SCC mixture segregates during flow. The error bars represent one standard deviation from the mean (3 replicates)

Figure 5.1 shows the results of the slump flow test, indicating the range of values given in the EFNARC specification (EFNARC, 2005). The slump flow varies between 675 and 585 mm for SCC containing ground CBA in a ratio of 10% to 50% as a substitute for partial cement. Nevertheless, the result of the slump flow was within the range considered by the standard as slump flow (SF2). The results of the slump flow test showed that the flow rate decreased with an increasing percentage of ground CBA used as cement

replacement in the SCC mix. The observed reduction in slump flow can be attributed to the presence of pores in the SCC mix containing ground CBA, resulting in greater absorption of fluid associated with a higher percentage of ground CBA. The second explanation given was the irregular structure of ground CBA, which leads to less interaction between particles.

The findings showed that the addition of ground CBA reduced the slump flow diameter, whereas replacing cement increased it. CBA consists of finer particles and has a large surface area. The use of CBA in the manufacturing of SCC leads to an increased water requirement. In these recent findings, the water content was maintained consistent but the quantity of SP was raised to 1.8% in order to meet the specifications for the SCC. This fresh property of ground CBA leads to a decrease in the viscosity of SCC mixes. The optimum flow ratios for (SCC) can be achieved by adding 10% cement replacement with ground CBA. This phenomenon has been confirmed by several other researchers (Aswathy & Paul, 2015; Keerio et al., 2021; Siddique et al., 2012a). These results proved that the ground CBA with fine particle size and porosity could be decreased the workability as reported by (Burhanudin et al., (2018; Mangi et al., (2019). Many studies reported that the ground CBA in concrete mixture decrease the workability remarkably (Al-Fasih et al., 2019; Cheah et al., 2023; Jamaluddin et al., 2016).

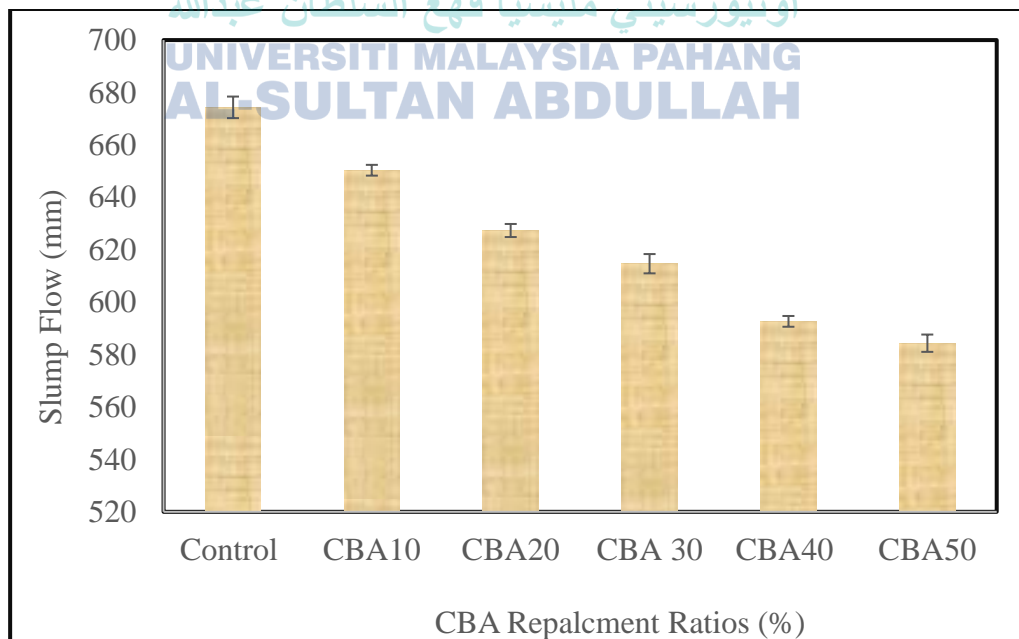


Figure 5.1 Slump flow of SCC mixes containing different replacement levels of ground CBA

5.2.2 L-Box of Optimum Mechanically Treated Ground CBA Based on SCC

The height ratio of the L-box was also determined using the H2/H1 ratio to calculate the suitability of the SCC mixture to pass through the bar. The test uses a three-bar L-box that simulates the scenario of a larger amount of reinforcement. This test is conducted to understand the effect of pozzolanic material on SCC mixture. The finding of the L-box was found to be decreased as CBA ratio increased in SCC mixture. Figure 5.2 shows the findings of the L-box test, which is the range of the EFNARC standard (EFNARC, 2005), and the results for L-box ranges from 0.83 to 0.71 for SCC containing ground CBA range 10% to 50 as partial cement replacement. The error bars represent one standard deviation from the mean (3 replicates).

As illustrated in the Figure 5.2, the difference in higher ΔH shown is higher in SCC mixture containing CBA as partial cement replacement with various replacement ratio. The reduction in the L-box due to porous ground CBA which lead to more interaction between particles. The second reason due to irregular shape of particle clusters and the distribution of coarse aggregate particles play a crucial factor in determining the likelihood of blockages occurring. The increased fineness and density of the CBA particles result in a higher absorption and porous of CBA lead to decreased the L-box flow of the SCC mix, in comparison to the control mix. It is reasonable to suppose that the velocity of the L-Box flow might result in a reduction in the flow of L-box of CBA substitution when compared to control samples.

However, the paste matrix with the aggregate provides a smooth transportation effect through the paste phase and an air passage for the passing ability performance of the SCC mixture. The passing ability of the different mixes satisfy the standard requirement range for passing ability of fresh SCC mixture. This trend in agreement with previous studies by (Jamaluddin et al., 2016; Zainal Abidin et al., 2014). According to study by Meena et al., (2023) it was reported that the blocking index ratio in the L-box was between 0.89 and 0.95 when the CBA with FA was replaced in SCC mixture. In agreement another author Ibrahim et al., (2021b) was reported that the blocking ratio in the L-box was 0.8–0.9 when the CBA was substituted.

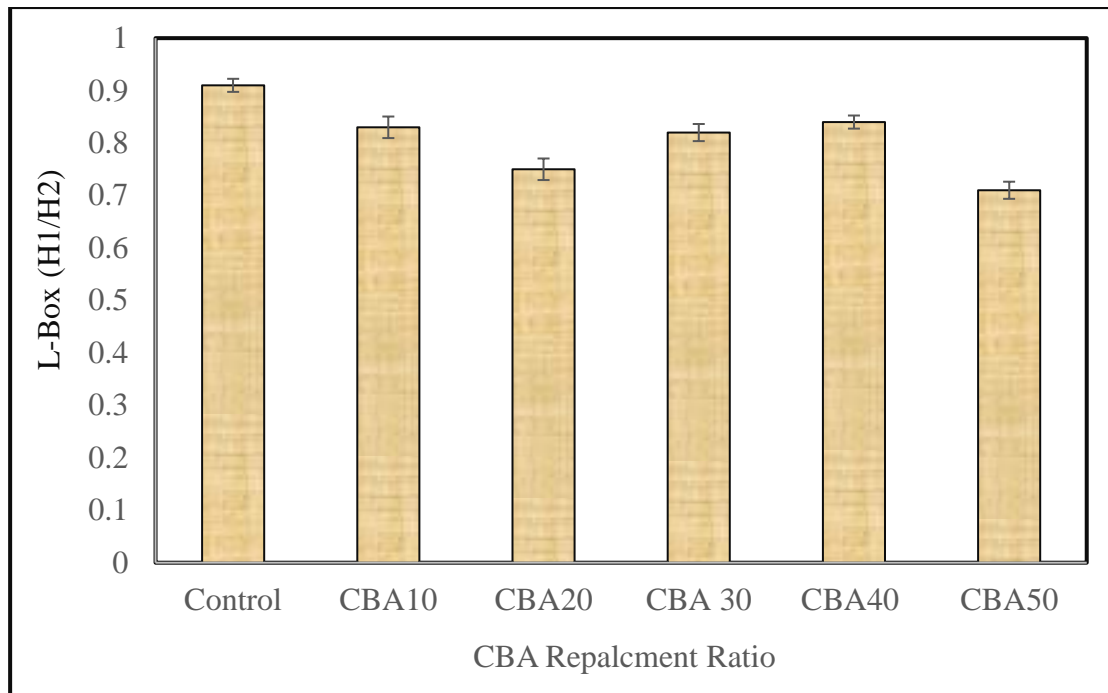


Figure 5.2 L-box of SCC mix containing different replacement levels of ground CBA

5.2.3 V-Funnel of Optimum Mechanically Treated Ground CBA Based on SCC

Though the test is designed to measure flowability, the result is affected by SCC properties other than flow. The V funnel is filled with concrete and the time taken by it to flow through the apparatus measured. This test gives account of the filling capacity (flowability). V-funnel flow time is the elapsed time in seconds between the opening of the bottom outlet depending upon the time after which opened. The error bars represent one standard deviation from the mean (3 replicates).

Figure 5.3 shows the findings of the V-funnel test, which is the range of the EFNARC standard (EFNARC, 2005), and the V-funnel ranges from 19 to 24 second for SCC mixture containing CBA range 10% to 50 as partial cement replacement. As the replacement ratios of ground CBA increased from 10% to 50%, the V-funnel has been increased owing to the porosity of CBA contrasted with the control mix. CBA saturates more water demand with a higher content of CBA. The data results achieved suggested the CBA structure, which has a rough form that decreases interparticle abrasion among aggregates and showed that the excessive inclusion of CBA has declined the viscosity of SCC mixtures.

According to (Khayat, 1999) the V-funnel time, which is between 9 to 25 second, is recommended for mixture to qualify as a SCC in confirm with EFNARC specification. Siddique et al., (2012a) reported that the v-funnel time for CBA as replacement in SCC was in the range of the standard from 9 to 25 seconds and was observed. The test results indicate that all SCC mixes meet the requirements of allowable flow time. The maximum size of coarse aggregate was kept as 16 mm in order to avoid blocking effect in the SCC mixture. This trend in agreement with previous studies by (Keerio et al., 2021; Siddique & Kunal, 2015)

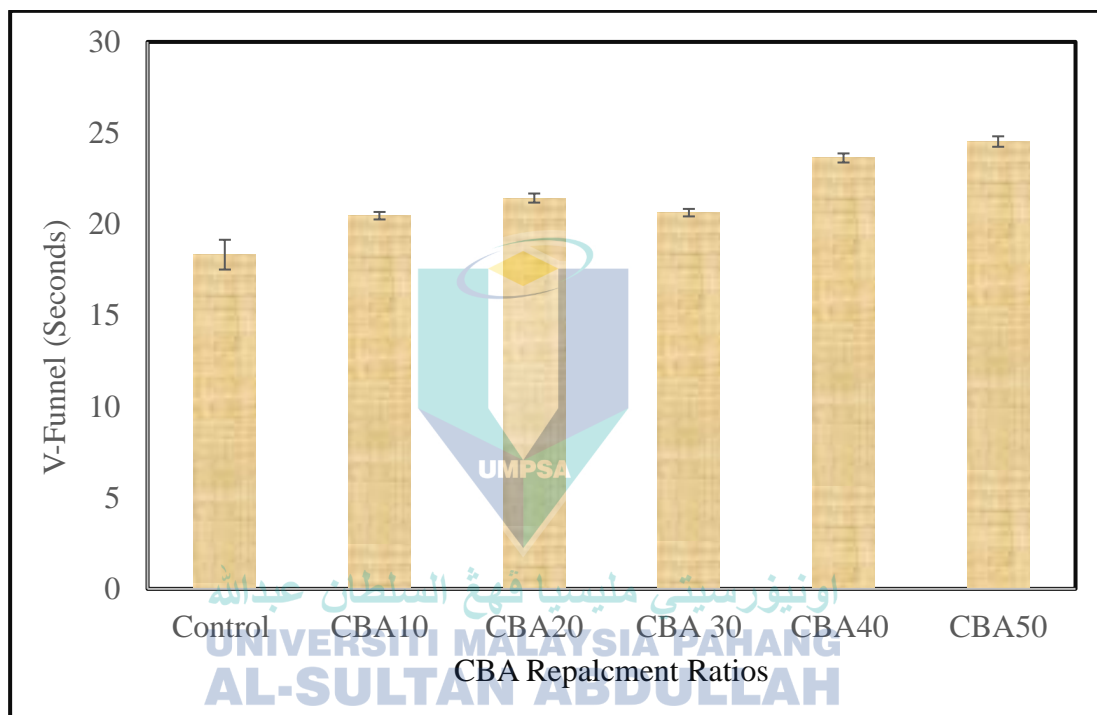


Figure 5.3 V-Funnel of SCC mix containing different replacement levels of ground CBA

5.2.4 J-Ring of Optimum Mechanically Treated Ground CBA Based on SCC

The J-ring test, in parallel to the L-box test, can be applied in conjunction with the test of slump flow to ascertain that concrete mixture can pass-through bars, as per EFNARC (EFNARC, 2005). According to another standard as mentioned in the ASTM C1621 (ASTM C1621, 2014), J-ring can be defined as a method of testing concrete's mixture capacity of passing through under its weight, thereby filling spaces, and getting a blocking evaluation. The error bars represent one standard deviation from the mean (3 replicates). The J-ring test to measure passage capacity of SCC mixture through bars.

Fresh ground CBA in SCC mixture was poured into the slump flow cone, elevated to the top, and the spread of the ground CBA in SCC was then gauged in two perpendicular directions. The ability of concrete to pass through a J-shaped circular reinforcement with reinforcing bars 48 mm apart in diameter was tested by filling a cone with SCC, lifting it upward, and allowing the ground CBA in SCC to flow through.

Figure 5.4 shows the findings of the J-ring flow test, which is the range of the EFNARC standard (EFNARC, 2005). The J-ring flow ranges from 650 mm to 570 mm for control samples and those made of CBA replacement ratios from 10% to 50% respectively. The results of the J-ring flow test showed that the flow rate decreased with an increasing percentage of ground CBA used as cement replacement in the SCC mixture as shown in Figure 5.4. It is clear that as replacement level of ground CBA was increased water content need to be increased in order to maintain SCC at the required level of workability, this attribute to ground CBA ability to absorb water due to the high surface area compared to cement for control samples. Generally, demand for water increased as the amount of CBA increased. This was mostly because of the larger surface area and higher amount of unburned carbon present in the CBA. The use of CBA significantly increased the demand for water. The increase in water usage was attributable to the decreased flocculation caused by the interaction between the CBA particles and the cement particles in compared to control mix.

According to study by Siddique & Kunal, (2015) it was reported that the J-Ring diameter and difference in concrete height inside and outside J-Ring were in the range of 527–627 mm, and the difference in height was less than 40 mm. The reduction in the J-Ring due to the presence of pores of CBA which lead to require more water content for SCC mixture. In agreement with this another study by Meena et al. (2023) was reported that adding CBA in the SCC mixture has significantly shortened the flow and irregularity in shape and porosity in texture CBA particles offer higher inter particle friction, resulting in decreased workability characteristics of SCC mixture.

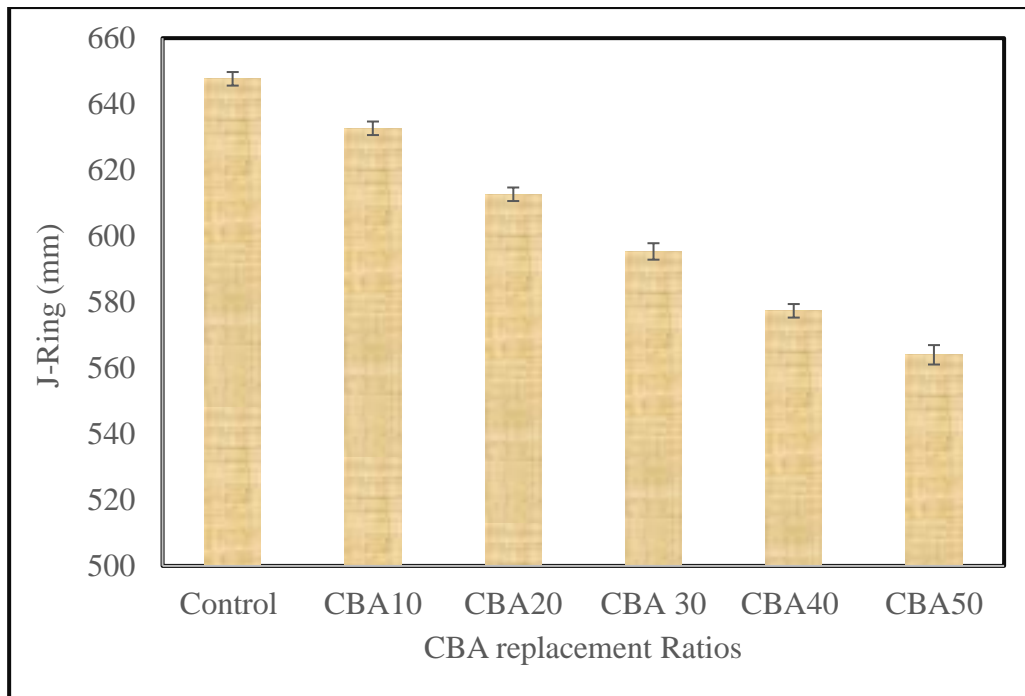


Figure 5.4 J-Ring of SCC mix containing different replacement levels of ground CBA

5.3 Mechanical Properties of Optimum Mechanically Treated Ground CBA Based on SCC

This section presents the sub sections for the mechanical properties of SCC. Mechanical properties of concrete are evaluated based on the compressive strength, flexural strength, tensile strength, and ultrasonic pulse velocity (UPV) of SCC specimen. The influence of ground CBA as replacement for cement on mechanical properties is discussed.

5.3.1 Compressive Strength of Optimum Mechanically Treated Ground CBA Based on SCC

Figure 5.5 demonstrates the compressive strength of SCC with CBA as an alternative for cement with various replacement ratios (10%, 20%, 30%, 40%, and 50%) at (7, 14, 28, 56, 90, and 180) days of curing as shown in Figure 5.5. The error bars represent one standard deviation from the mean (3 replicates). The compressive strength of ground CBA with various replacement ratios based on SCC mixture was lower than control at the early age of curing at 7 days, yet certain mixtures due to late pozzolanic reaction effect and gained enhance in the compressive strength at 28 days. For instance, it can be seen from these illustrations that the compressive strength at age 7 days shows

that SCC mixture with 0% ground CBA (control) exhibited the highest strength; Nevertheless, the strength became reduced as larger amounts of ground CBA in higher percentage were integrated into the mixture. However, at other curing ages for ground CBA for SCC specimens with larger amounts of ground CBA in higher percentage (CBA 20%) exhibited higher compressive strengths compared to that of the SCC of 0% ground CBA (control). The range of measured values for compressive strength ranged from 39 MPa to 21 MPa for control specimens to 50% CBA after 28 days of curing. The results show that the differences in the compressive strength values of different substitution ratios depend to some extent on the amount of CBA contained in the SCC mixture. The control specimens of SCC exhibited a range of values ranging from 36.329 MPa to 39.599 MPa at the corresponding curing ages of 7 and 28 days. In addition, it was shown that the optimum amount of CBA as a cement replacement is CBA20% compared to conventional specimens, which had values ranging from 36.893 MPa to 40.2133 MPa after 7 and 28 days of curing, correspondingly. This could be because of ground CBA has a late pozzolanic reaction, which is important to make the material denser and thus improve the compressive strength. According to Argiz et al. (2017) reported that the pozzolanic properties of fine particles CBA cause a late pozzolanic reaction that affects the strength properties. According to previous study Oruji et al. (2017) it is shown that concrete mixtures containing 20% finer CBA achieve adequate strength. The results of the current study are consistent with the results of previous research studies (Singh & Siddique, 2014; Soofinajafi et al., 2016).

However, the inclusion of ground CBA in the SCC mixture as cement replacement enhanced the strength up to 20% at late curing ages (56, 90 days). Moreover, there was strength reduction when curing continued up to 90 days, when increase the replacement ratios (CBA30%, CBA40%, CBA50%) compared to control samples. Nevertheless, it becomes comparable with the control after 180 days of curing. The reduction in the strength properties of 30.083%, 35.291%, and 46.738% was observed in CBA 30%, CBA 40%, and CBA 50% of SCC mixture, respectively at 7 days of curing. Nevertheless, after 28 days, up to CBA20% specimens had accelerated their pozzolanic reaction and gained 1.55% higher strength than control specimens in the SCC mixture. At above 56, 90, and 180 days of ages, SCC mixture specimens with 20% ground CBA as cement replacement recorded the highest strength value as compared to that of the other mixes. The strength yielded a rise of 8.76% compared to that of the control SCC at

90 days of curing age. The used of ground CBA which size is fine and increase the fineness compared to cement which contribute towards strength increment of SCC mixture. According to studies by (Brake et al., 2018; Cheriaf et al., 1999; Mangi et al., 2019) enhancements in compressive strength of SCC at 90 days incorporating ground CBA as an alternative. This is due to the pozzolanic reaction which started after 28 days of curing indicated that a higher production of hydration at later ages enhanced the compressive strength. Furthermore, the inclusion of finer grinding CBA, demonstrated an increase in compressive strength due to natural pore refinement action, as finer particles filled the pores in the mixture that led to increased hydration of paste generated during the pozzolanic processes. All SCC mixes with ground CBA as partial cement replacement in the present study were found to have met the target strength and above (35 MPa) at above 28, 56, 90 and 180 days of curing.

On overall, the investigation of the influence of the CBA alternative as cement in SCC on its strength characteristics revealed that the incorporation of CBA as a replacement material at levels of up to 20 % yielded a significant improvement relative to traditional SCC mixture. Previous research Singh, Mithulraj, et al., (2019) has shown that the incorporation of a modest amount of CBA in SCC has resulted in notable improvements in mechanical parameters, including compressive strength. These enhancements have been seen to reach up to 20% at several ages of curing, as illustrated in the results of the study. The increase in strength may be described to the pore refinement effect resulting from the pozzolanic activity of CBA. The use of CBA as a replacement material leads to an enhanced level of porosity. However, it is worth noting that the presence of silica in ground CBA particles plays a crucial role in facilitating the synthesis of calcium-silicate-hydrate (C-S-H), a gel-like substance that significantly contributes to the development of strength in materials. The observed increase in strength may be attributed to the higher concentration of calcium silicate hydrate (C-S-H) in the SCC samples mixed with ground CBA. This increase in C-S-H is a consequence of the reaction between the calcium hydroxide produced during cement hydration and the reactive silica present in the ground CBA.

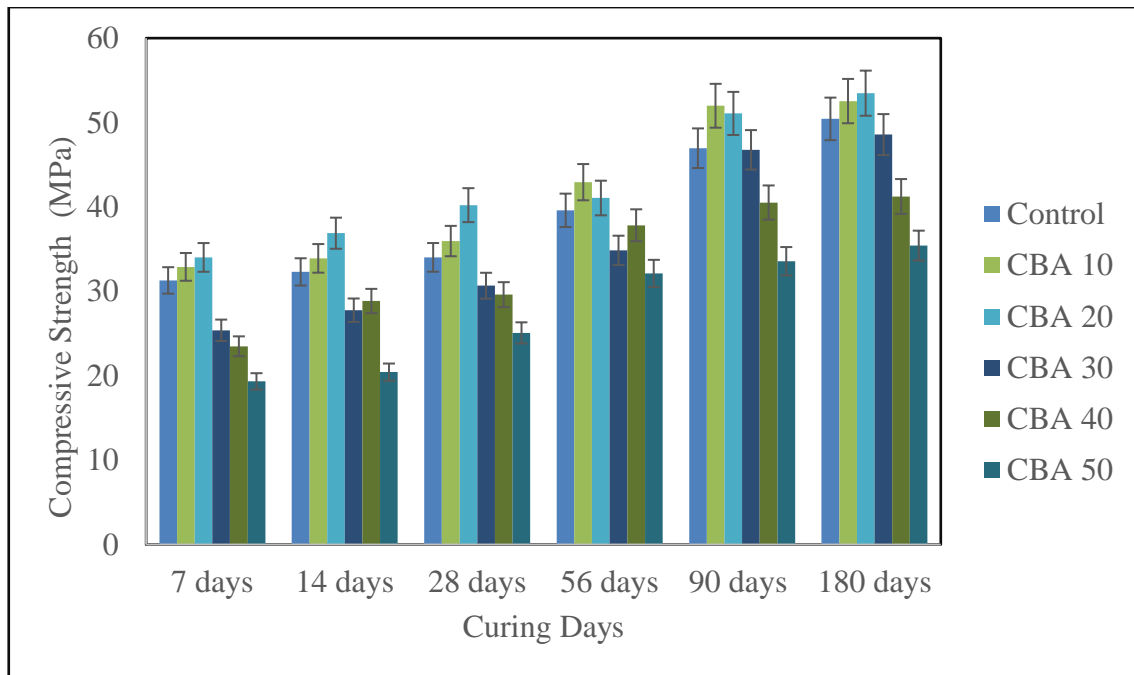


Figure 5.5 Compressive strength results of SCC containing ground CBA-7000 with various replacement ratios at different curing ages

5.3.2 Flexural Strength of Optimum Mechanically Treated Ground CBA Based on SCC

Flexural strength is also known as bend strength or modulus of rupture or fracture strength. It is an important measure in order to investigate the concrete beams to resist failure in bending. This can be identified by maximum bending stress applied for the materials before it yields. Flexural strength is evaluated with beam (prismatic) samples undergoing a bending moment by applying a load through upper and lower rollers. Generally, flexural strength shows the force and stress that are examined in the samples of unreinforced concrete to bear the bending failure, as mentioned in ASTM C78, (2010). Figure 5.6 illustrates the flexural strength of ground CBA in SCC mixture at 7, 14, 28, 56, 90, and 180 days of age. The error bars represent one standard deviation from the mean (3 replicates).

Overall, the SCC mixes exhibited continuous strength increment with increasing curing age. These results indicated that ground CBA as partial cement replacement had an influence on the flexural strength of the SCC mixture. The results indicated that the flexural strength is growing at curing period of 7, 14, 28, 60, 90, and 180 days of age. At 7 days of curing, for the flexural strength for SCC mixture of CBA10%, CBA20%,

CBA30%, CBA40%, and CBA50% gained flexural strength 4.381MPa, 3.896 MPa, 3.894 MPa, 3.432 MPa, 2.869 MPa respectively. At 28-day flexural strength of control mix CBA0 was observed as 5.399 MPa, whereas mixes CBA10%, CBA20%, CBA30%, CBA40%, and CBA50% achieved 5.146MPa, 4.553MPa 4.047MPa, 3.959MPa. and 3.431MPa, respectively. The decrease in CBA substitution ratios resulting from the effective pozzolanic reaction forming (C-S-H) in the mixture was not complete before 28 days of curing, delaying the process of hydration. The experimental results of this study show comparability with the results of previous studies (Kurama & Kaya, 2008; Mangi, et al., 2019). It was observed that the flexural strength for all series of ground CBA in SCC mixture were in the range of 5.399 to 3.431 MPa at 28 days of curing age from 0% control without CBA to 50% ground CBA. Furthermore, the finding shows that decreased as replacement ratio of ground CBA increased for flexural strength in SCC mixture at 28 days of curing. The reduction in the flexural strength due to the delay in hydration process and slow pozzolanic activity of CBA at 28 curing period. The same result had been acquired by other researchers (Aydin, 2016; Kurama & Kaya, 2008; Sachdeva & Sharma, 2018) in which concrete mixture containing CBA showed the reduction flexural strength compared than control specimen, and the reduction in the early ages up to 28 day due to the finer particle sizes of CBA in the concrete need more water to enhance the strength development of the specimen. The second reason is the inside structure of CBA with pores, as well as delay in the hydration, along with a slower pozzolanic activity at the early ages of 7 days and 28 days.

However, at ages 56, 90 and 180 days of curing age, it was the SCC mixes with CBA 10, CBA20 of ground CBA that recorded the highest flexural strength value. At 56 days the flexural strength result was observed of control mix CBA0 was observed as 5.609 MPa, whereas mixes CBA10%, CBA20%, CBA30%, CBA40%, and CBA50% achieved 5.963MPa, 5.892MPa 4.751MPa, 4.431MPa, and 4.324MPa, respectively. These findings also indicate that the flexural strength of ground CBA20% rose around 4% SCC samples compared to control samples SCC at 90 days. Research done by (Targan et al., 2003) late curing time, such as 60 and 90 days, leads to an increase in flexural strength of concrete containing CBA in the mixture. This is due to the (C-S-H) gel distribution, which was the result of cement and CBA pozzolanic reactivity in the hydration process.

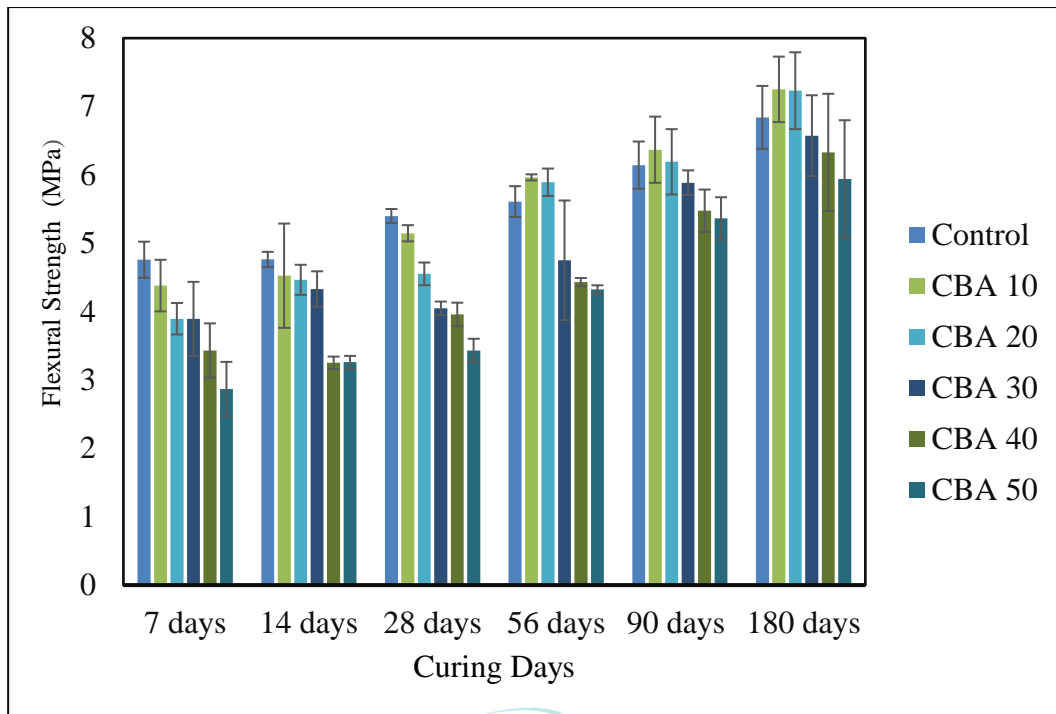


Figure 5.6 Flexural strength results of SCC containing ground CBA-7000 with various replacement ratios at different curing ages

5.3.3 Splitting Tensile Strength of Optimum Mechanically Treated Ground CBA Based on SCC

It is defined as an indirect technique of assessing concrete splitting tensile strength using a cylinder sample across a vertical diameter. Moreover, the tensile strength for concrete samples is the tensile stresses developed due to applying a compressive load, at which the concrete samples might crack, as mentioned by ASTM C469, (2011). Splitting tensile strength mainly draws upon the binder efficiency. Various mechanical characteristics of concrete can be assessed using one of the fundamental and significant characteristics. The splitting tensile strength of the concrete structures significantly affects the cracking development and size. Concrete is weak under tension and, therefore, it is essential to conduct a preliminary assessment of the concrete's splitting tensile strength (Khayat & De Schutter, 2014).

Figure 5.7 illustrates the tensile strength of ground CBA in SCC mixture at 7, 14, 28, 56, 90, and 180 days of age. The error bars represent one standard deviation from the mean (3 replicates). Overall, the SCC mixes exhibited continuous strength increment with increasing curing age. These results indicate that ground CBA had an influence on the splitting tensile strength of the SCC mixture. At 7 days of curing, for the splitting tensile

strength for SCC mixture of CBA10%, CBA20%, CBA30%, CBA40%, and CBA50% gained splitting tensile strength 3.219 MPa, 3.095MPa, 2.675MPa, 2.491MPa, 1.791MPa respectively, compared to control SCC was 3.621MPa. It can be seen from these illustrations that the splitting tensile strength at age 7 days and 14 days (early ages) shows that SCC mixes with 0% ground CBA exhibited the highest strength. Nevertheless, the strength became reduced as larger amounts of ground CBA replacement ratios in the SCC mixture. The reduction in the splitting tensile strength due to the increase in the volume of pores which is lead to CBA particles absorb large amounts of water in the concrete gained by replacing CBA in the mixes (Hasim et al., 2022; Yang et al., 2020). The second reason to reduction of splitting tensile strength at early ages due to the addition of ground CBA, and the pozzolanic reaction was not yet initiated at this time of curing ages.

However, at ages 28, 56 ,90 and 180 days showed the enhance in the splitting tensile strength at CBA 10% and CBA 20% on the SCC mixture. At 28 days the splitting tensile strength result of control mix CBA0% was observed as 5.135MPa, whereas mixes CBA10%, CBA20%, CBA30%, CBA40%, and CBA50% achieved 5.504MPa, 5.699MPa 4.047MPa, 3.794MPa. and 3.292MPa, respectively. At 56 days the splitting tensile strength result was observed of control mix CBA0% was observed as 6.342 MPa, whereas mixes CBA10%, CBA20%, CBA30%, CBA40%, and CBA50% achieved 6.837MPa, 6.976MPa 4.941MPa, 4.1663MPa. and 3.5197MPa, respectively. At 90 days the splitting tensile strength result of control mix CBA0 was observed as 7.205 MPa, whereas mixes CBA10%, CBA20%, CBA30%, CBA40%, and CBA50% achieved 7.560MPa, 7.678MPa 5.247MPa, 4.455MPa. and 3.866MPa, respectively. At 180 days the splitting tensile strength result of control mix CBA0 was observed as 7.469 MPa, whereas mixes CBA10%, CBA20%, CBA30%, CBA40%, and CBA50% achieved 7.634MPa, 7.718MPa 6.041MPa, 5.189MPa, and 4.099MPa, respectively. From the aforementioned that late curing ages showed the improvement in the splitting tensile strength of ground CBA up to 20 % replacement in the SCC mixture. From the results was observed that ground CBA which has pozzolanic properties contribute towards pozzolanic reaction thus produces higher strength. Through pozzolanic reaction in the concrete structure, secondary C-S-H gels were produced and improving the aggregate-cement interface thus the concrete becomes stronger. However, utilization of ground CBA in SCC mixture of more than 20% would decrease the concrete strength significantly. Due to larger amount of ground CBA inclusion, it leads to less cement that

resulted in aggregate could not bind perfectly with cement paste. The poorest splitting tensile result was attributed by the inclusion of CBA50% ground CBA, which is the largest amount of cement replacement in SCC mixes. It was observed that the cracks mainly exist at cement paste and aggregate interfaces as illustrated in Figure 5.8 which indicates that the aggregate has loose connection with cement paste. However, the result is still in the range for structural SCC application.

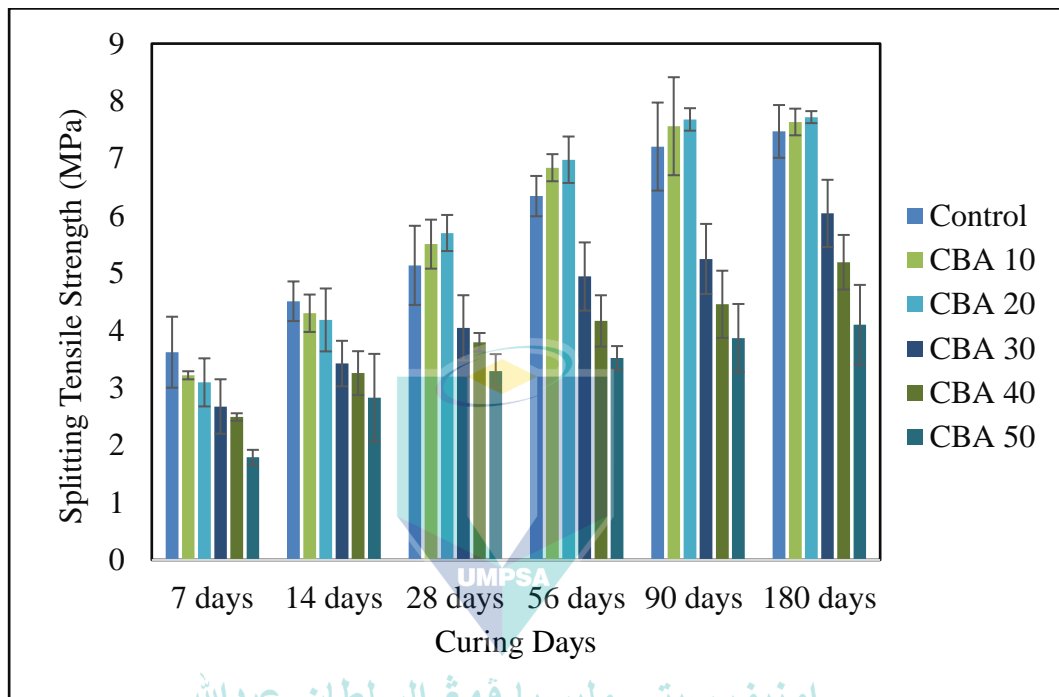


Figure 5.7 Splitting tensile strength results of SCC containing ground CBA-7000 with various replacement ratios at different curing ages



Figure 5.8 Failure occurs through coarse aggregate of SCC mixes containing ground CBA with various replacement ratios

5.3.4 Ultrasonic Pulse Velocity of Optimum Mechanically Treated Ground CBA Based on SCC

Figure 5.9 illustrates the UPV of ground CBA in SCC mixture at 7, 14, 28, 56, 90, and 180 days of age. The error bars represent one standard deviation from the mean (3 replicates). Overall, the SCC mixes exhibited continuous UPV increment with increasing curing age. These results indicate that ground CBA had an influence on the UPV of the SCC mixture. Generally, the inclusion of ground CBA produced lower UPV values compared to normal SCC mixture. The results show that UPV of ground CBA for control sample is 4133m/s whereas mixes CBA10%, CBA20%, CBA30%, CBA40%, and CBA50% achieved 4020m/s, 3890m/s, 3725m/s, 3640m/s, and 3155m/s respectively at 7 days of curing. The reduction in the UPV for SCC containing ground CBA due to the increase of voids in SCC mixture samples when increased the replacement ratio of ground CBA as partial cement replacement compared to control samples. The results show that mixture with ground CBA 50% as cement replacement achieved the lowest UPV value of 3155 m/s at 7 days, which falls in the range between 3000 – 3500 m/s, that is classified as good quality. The low concrete quality could be owing to porous properties of ground CBA. The lack of interlocking between aggregates generates voids and that results in a lower UPV travel rate. Nevertheless, the remaining SCC mixtures at 14 and 28 days of

curing fall between good and very good quality because it falls in the range of 3000 m/s – 3500 m/s and 3500 m/s – 4500 m/s. Baite et al., (2016) stated that the existence of industrial waste such as CBA as cement replacement materials showed decrease the UPV values with increased the replacement ratio of CBA in the concrete mixture.

However, at long curing period of 56, 90 and 180 days, it showed the results of UPV for SCC containing ground CBA as partial cement replacement found to be lower than that of control SCC mixes. The UPV through the SCC mixtures CBA10%, CBA20%, CBA 30%, CBA40% and CBA50% were lower by 1.42%, 4.59%, 9.40%, 11.83%, and 12.87% respectively in comparison to the control mix CBA0 at 180 days of curing. Overall, the reduction in the late curing ages clearly proved that they are highly influenced by the presence of cracks (joints) or cavities and the porous CBA which effect in the UPV test for SCC mixture. The second reason since UPV values depend directly on the interfacial transition zone (ITZ) characteristics of the mixture, hence presence of weak ITZ and higher porosity leads to decrease in these values. This result matches with the previous (Saxena et al., 2023; Singh, Arya, et al., 2019; Yang et al., 2020). Those studies conducted who concluded that the UPV decreased with increasing CBA content in the concrete mixture. Siddique, (2013) reported that the UPV value decreases gradually when the replacement level of CBA increased in the SCC mix.

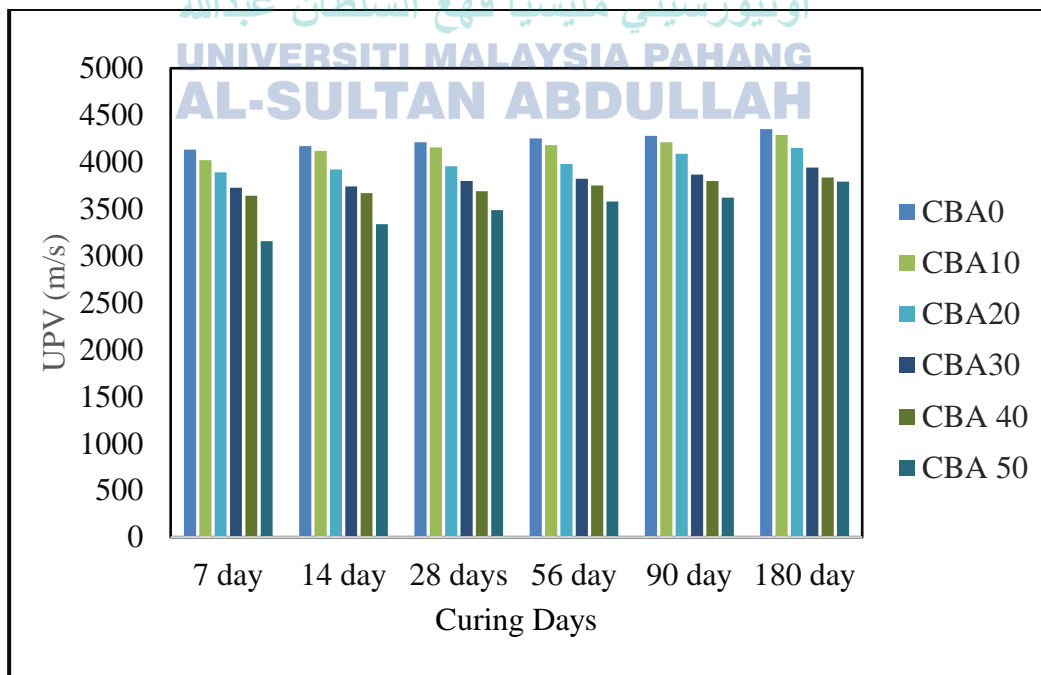


Figure 5.9 UPV results of SCC containing ground CBA-7000 with various replacement ratios at different curing ages

5.4 Co-Relationships Between Mechanical Properties of Self-Compacting Concrete

In this study, to examine the relationship between the different mechanical properties of concrete containing of ground CBA, a regression analysis was performed. In the regression analysis, the coefficient of determination (R^2), normally ranging from 0 to 1, represents the goodness of a model fit. An R^2 value close to 1 indicates that the regression accurately fits the data and vice versa. Regression analysis was performed based on the mechanical properties and different curing ages at early curing age 7 days and late curing age at 180 days for SCC samples.

The relationship between the compressive strength and flexural strength of ground CBA in SCC mixture samples under two different curing (7, and 180 days) ages is demonstrated in Figures 5.10 and 5.11. Moreover, the relationship between the compressive strength and flexural strength of ground CBA in SCC mixture samples, which are based on the test results in this study, is derived by the following equation:

$$y = 0.0773x + 1.626, R^2 = 0.7138 \text{ for 7 days} \quad 5.1$$

$$y = 0.0696x + 3.4267, R^2 = 0.9236 \text{ for 180 days} \quad 5.2$$

Where, y = flexural strength MPa, and x = Compressive strength in MPa

A regression value, R^2 greater than 0.85, indicates a strong relationship between the parameters for the properties. It can be seen from the results showed the $R^2=0.7138$ at 7 days, which is developed at 180 days to $R^2= 0.9236$. Furthermore, the coefficient of determination R^2 points showed a positive relationship between the regression curve and the data outcomes between compressive strength and flexural strength. Furthermore, the result indicated that as the curing age increased, the compressive strength also increased. Moreover, longer curing time would allow better hydration process, which then would aid in SCC mixture densification and load bearing capability. However, it became clear that as the ground CBA content in SCC mixture increased, the compressive strength decreased in the high replacement ration as shown in the Figures 5.10 and 5.11. It has been evident in the literature as had been noted by Yang et al., (2020) who reported the relationship between flexural strength and compressive strength and showed the influence at early and long curing ages. The finding indicated that flexural strength of the

CBA concrete increased as the compressive strength increased, which is in agreement with this experimental data.

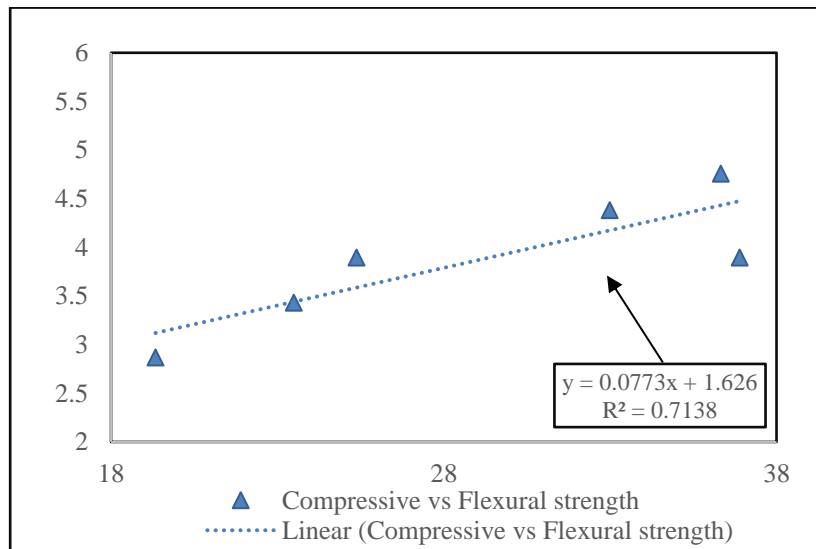


Figure 5.10 Co-relation compressive strength vs flexural strength of SCC containing ground CBA at 7 days

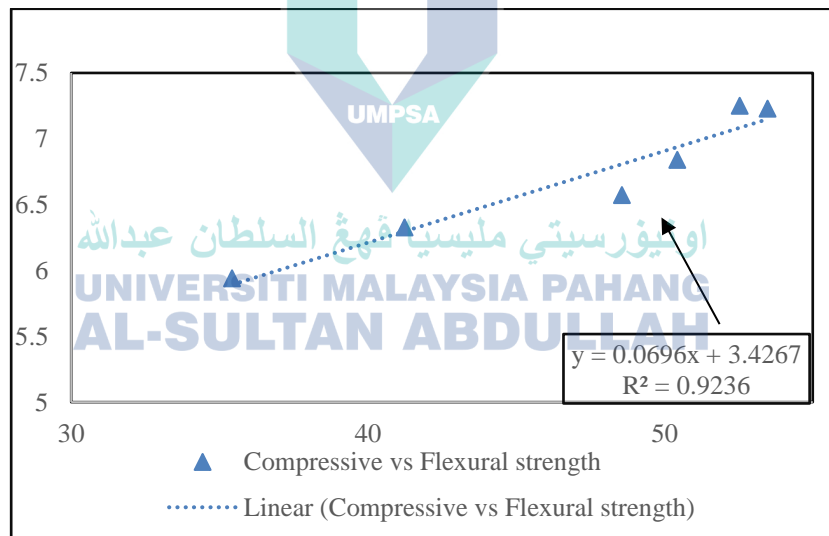


Figure 5.11 Co-relation compressive strength vs flexural strength of SCC containing ground CBA at 180 day

Figures 5.12 and 5.13 demonstrates the relationship between splitting tensile strength and compressive strength of ground CBA in SCC mixtures. The equations showing the relationships between compressive strength and splitting tensile strength together with the coefficients of determination R^2 derived from the test results of the present study is given in the equations 5.3 and 5.4. It can be noticed from the relationship

that R^2 increased for the long curing ages. The result indicates that improvement for the strength from early to long curing ages. The equation showing the relationships between compressive strength (X) and splitting tensile strength (Y).

$$y = 0.0816x + 0.4442, R^2 = 0.8658 \text{ for 7 days} \quad 5.3$$

$$y = 0.2049x - 3.263, R^2 = 0.9461 \text{ for 180 days} \quad 5.4$$

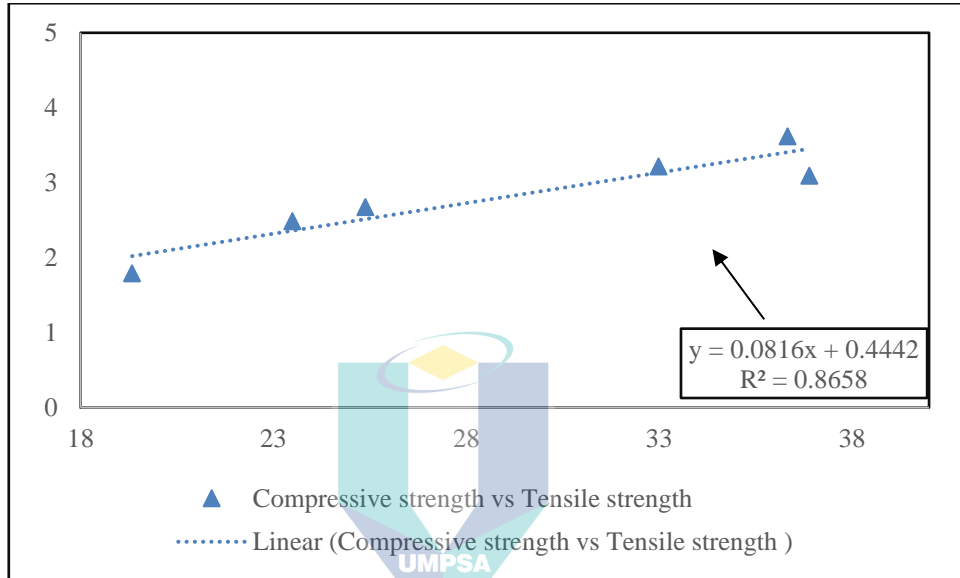


Figure 5.12 Co-relation Compressive strength vs Tensile strength of SCC containing ground CBA at 7 days

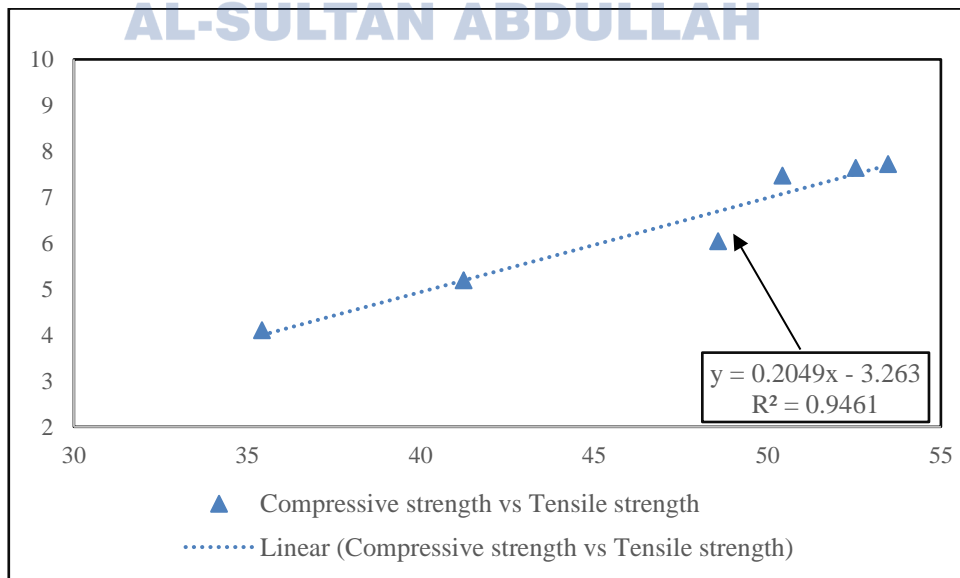


Figure 5.13 Co-relation Compressive strength vs Tensile strength of SCC containing ground CBA at 180 days

Figures 5.14 and 5.15 shows the relationship between UPV and compressive strength of ground CBA in SCC mixture obtained from the present study at 7 days and 180 days. The equation shows the relationships between compressive strength (X) and the UPV (Y), together with the coefficients of determination (R^2) derived is given in equations 5.5 and 5.6. The empirical parameters of the equation obtained from the present study are almost similar to that reported by (Nash't et al., 2005; M. Singh & Siddique, 2015; Turgut, 2004).

$$y = 0.125x, R^2 = 0.9761 \text{ for 7 days} \quad 5.5$$

$$y = 0.0278x + 2.7526 R^2 = 0.6982 \text{ for 180 days} \quad 5.6$$

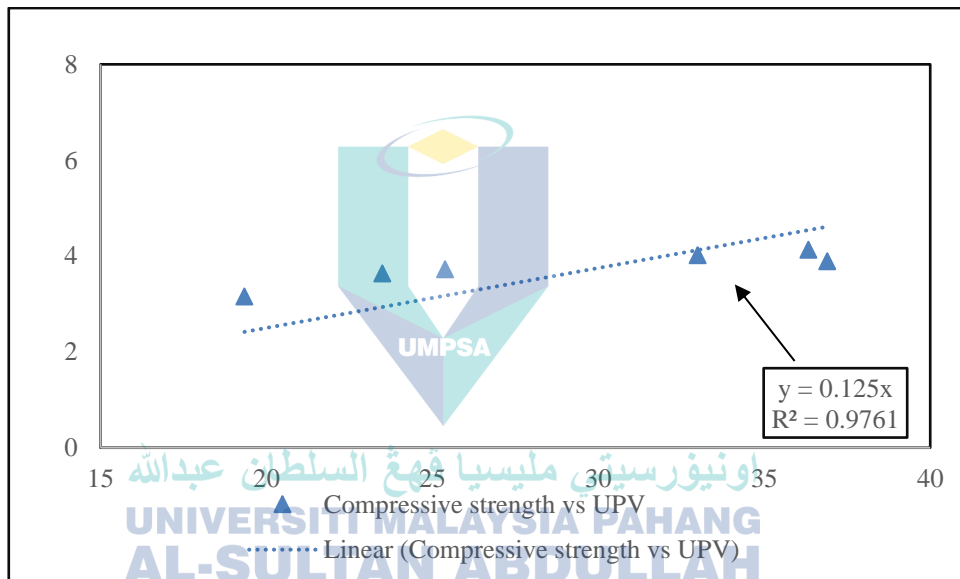


Figure 5.14 Co-relation Compressive strength vs UPV of SCC containing ground CBA at 7 days

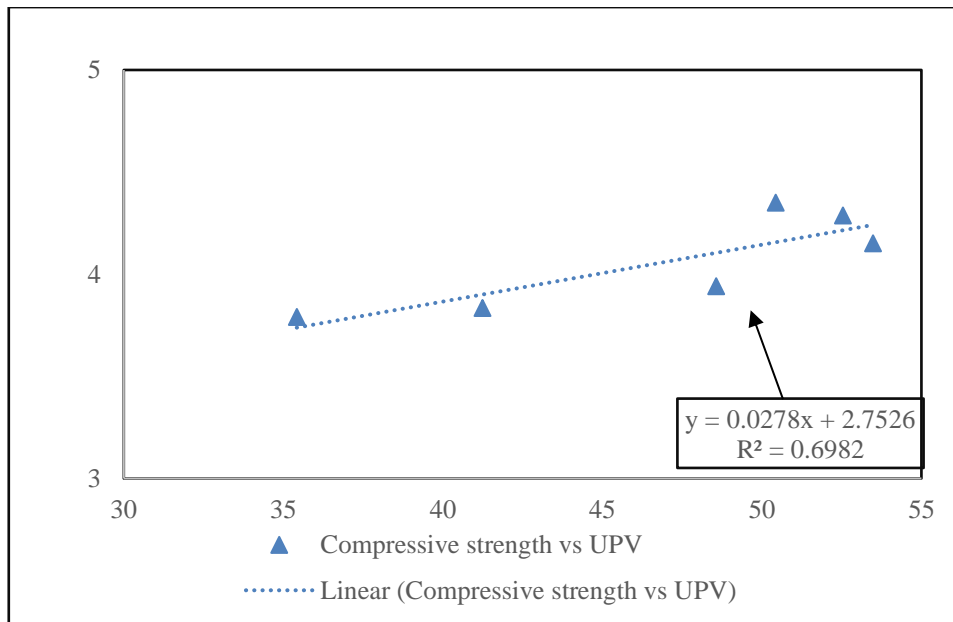


Figure 5.15 Co-relation Compressive strength vs UPV of SCC containing ground CBA at 180 days

Figures 5.16 and 5.17 showed the relationship between the flexural strength and the UPV of SCC mixture containing ground CBA at 7 days and 180 days. In this study was observed that The CBA SCC mixture for flexural strength was closely related to the ultrasonic pulse velocity. Furthermore, the range of data for UPV between 4.13 to 3.15 Km/s from 0% to 50% of ground CBA, while the range of data for flexural strength 4.759 to 2.869 MPa at 7 days respectively. The equation showing the relationships between flexural strength and (X) and the UPV (Y), together with the coefficients of determination (R^2) derived is given c 5.7 and 5.8. The empirical parameters of the equation obtained from the present study are almost similar to that reported by Park et al. (2021) who observed the influence of relationship between flexural and UPV containing CBA in concrete mixture.

$$y = 0.9598x, R^2 = 0.9938 \text{ for 7 days} \quad 5.7$$

$$y = 0.388x + 1.4611, R^2 = 0.7123 \text{ for 180 days} \quad 5.8$$

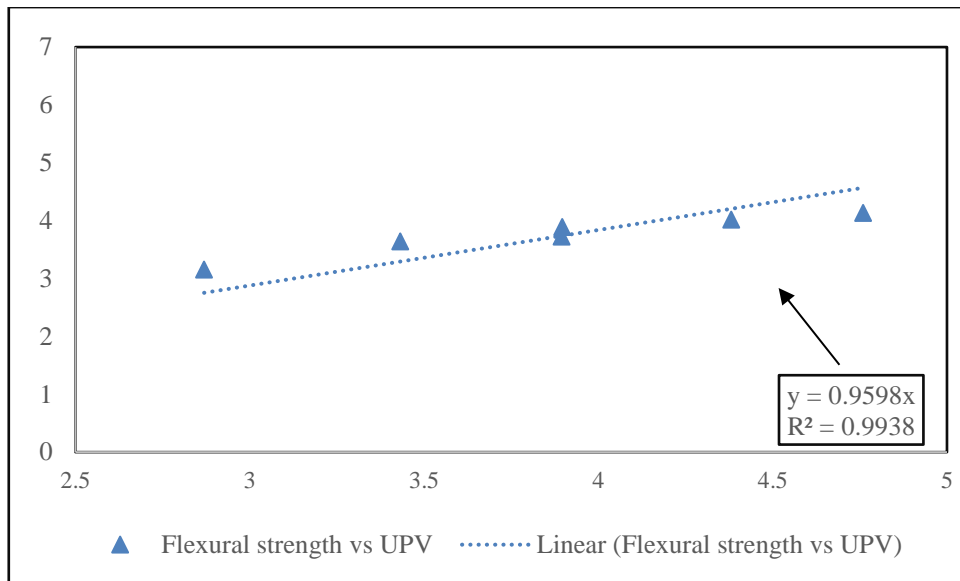


Figure 5.16 Co-relation Flexural strength vs UPV of SCC containing ground CBA at 7 days

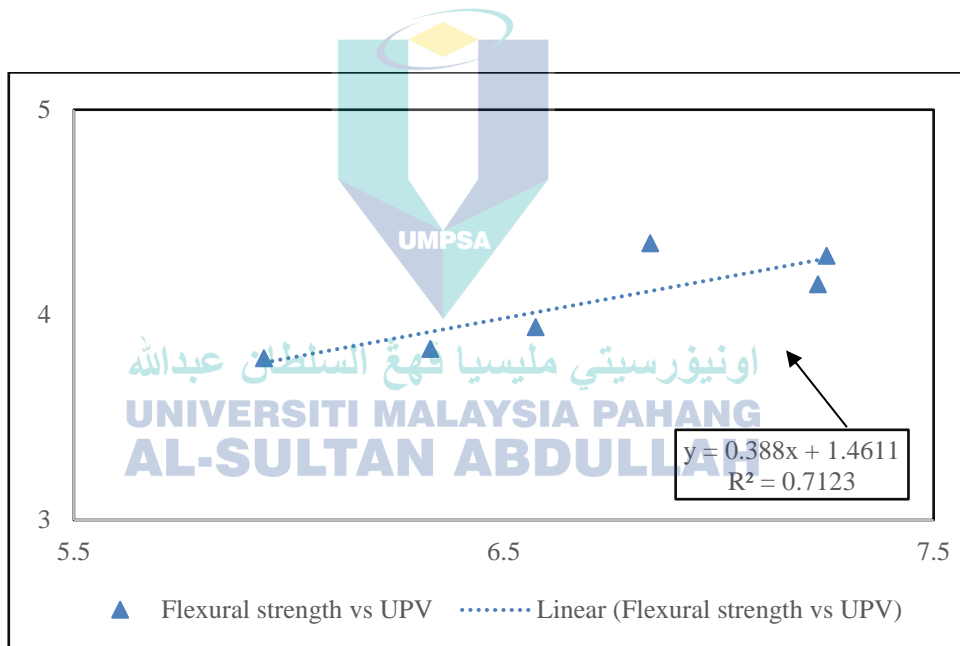


Figure 5.17 Co-relation Flexural strength vs UPV of SCC containing ground CBA at 180 days

The relationship between the flexural strength and splitting tensile strength of SCC mixture containing ground CBA under two different curing ages at 7 days and 180 days as shown in Figures 5.18 and 5.19. The equation showing the relationship between flexural strength and splitting tensile strength together with the coefficients of determination R^2 derived from test results of the present research is given in equations 5.9 and 5.10. The equation showing the relationships between splitting tensile strength

(X) and flexural strength (Y). The coefficient of R^2 values for the co-relationships was found comparable with those obtained by the previous researcher (Mangi et al., 2019).

$$y = 0.932x - 0.7933, R^2 = 0.9453 \text{ for 7 days} \quad 5.9$$

$$y = -1.0437x^2 + 16.684x - 58.331, R^2 = 0.9636 \text{ for 180 days} \quad 5.10$$

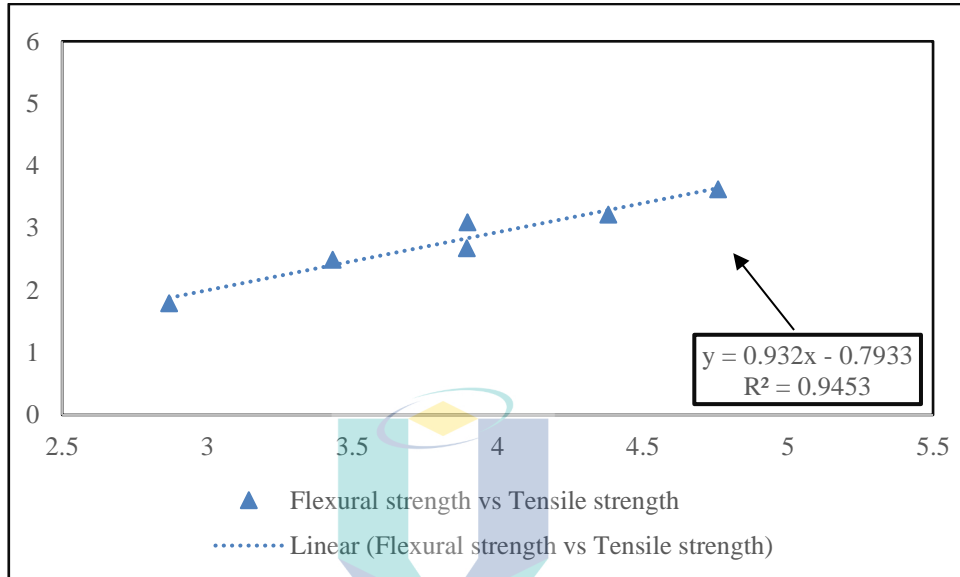


Figure 5.18 Co-relation Flexural strength vs Tensile strength of SCC containing ground CBA at 7 days

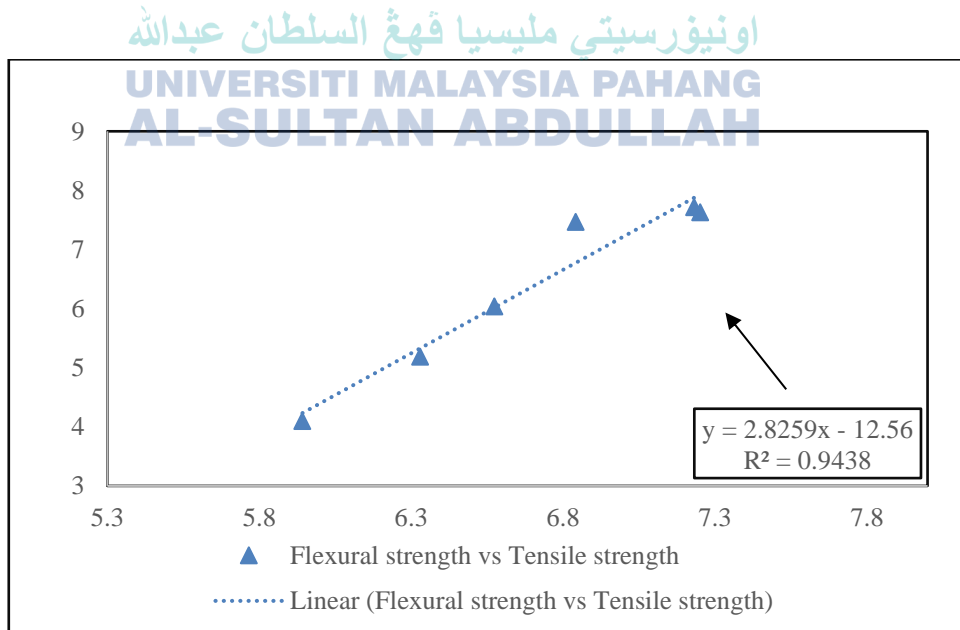


Figure 5.19 Co-relation Flexural strength vs Tensile strength of SCC containing ground CBA at 180 days

Figures 5.20 and 5.21 shows the relationship between the UPV and splitting tensile strength of SCC mixture containing ground CBA obtained in the study at 7 days and 180 days. As the UPV increased, both the compressive strength and the splitting tensile strength of SCC mixture containing ground CBA increased with increased the curing ages up to 180 days. The equation showing the relationship between UPV and splitting tensile strength together with the coefficients of determination R^2 derived from test results of the present research is in equations 5.11 and 5.12. The equation showing the relationships between UPV (X) and splitting tensile strength (Y). The result indicates the reduction in UPV leading to a decrease in UPV values. This finding is consistent with the findings by (Yang et al., 2020).

$$y = 0.5356x + 2.2531, R^2 = 0.9776 \text{ for 7 days} \quad 5.11$$

$$y = 0.1459x + 3.1316, R^2 = 0.8517 \text{ for 180 days} \quad 5.12$$

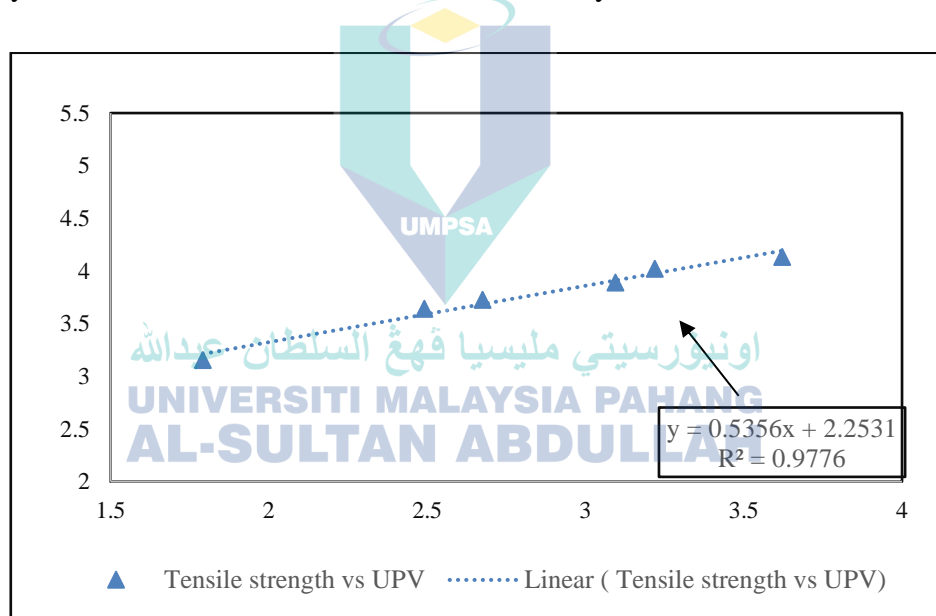


Figure 5.20 Co-relation UPV vs Tensile strength of of SCC containing ground CBA at 7 days

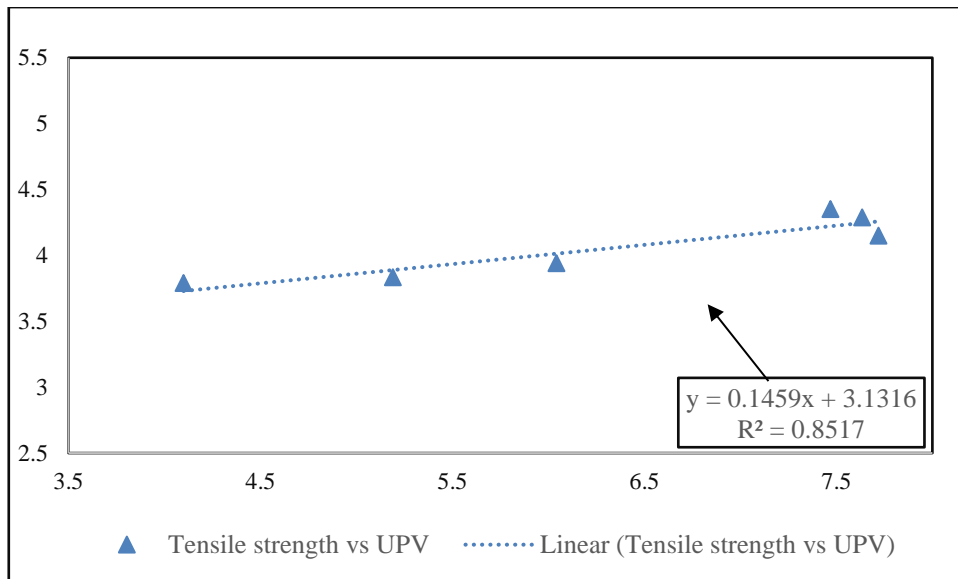


Figure 5.21 Co-relation UPV vs Tensile strength of SCC containing ground CBA at 180 days

5.5 Thermogravimetry Analysis (TGA) on Cement Pastes Samples and optimum mechanically treated Ground CBA

Thermogravimetric analysis (TGA) was performed on cement paste for control and cement paste containing ground CBA (CBA10%, CBA20%, and CBA50%) to determine the rate of pozzolanic reactivity of the materials compared to those of control samples. Figures 5.22, 5.23 and 5.24 shows the TGA results of control and those contained ground CBA at 7, 28, and 56 days of curing. Based on the observation, at 7 days of curing it can be observed that all mixtures showed significant weight loss up to 800°C. Based on the Figure 5.22, all the pastes showed that three transitions of mass loss in the TGA as the following: the first occurred between 0 to 200°C, the second point between 400°C to 600°C, and the third point between 600°C to 800°C. The first point (0 to 200°C) of mass loss curves indicating the removal of moisture on the outer surface of the particle and dehydration C-S-H gels. Meanwhile, the second point (400°C to 600°C) indicates the decomposition of hydrated compounds, mainly C-S-H gels and an amount of CaOH that has been released from structural water and the third point (600°C to 800°C) indicates the decomposition of organic compounds and calcite. This result shows the same pattern with previous study conducted by Rocca et al. (2013). It is evident that Ca(OH)₂ takes part in chemical reaction with CBA based on mass loss difference between early and later age of specimens. Overall, it was observed that the total loss weight was around 35% for the highest loss weight. Furthermore, the highest loss weight was

observed for CBA 20% at 7 days compared to control and other replacement ratios. A major weight loss is observed from 400°C to 750°C attributed to oxidation and burning of the organic particles entrapped inside the ground CBA.

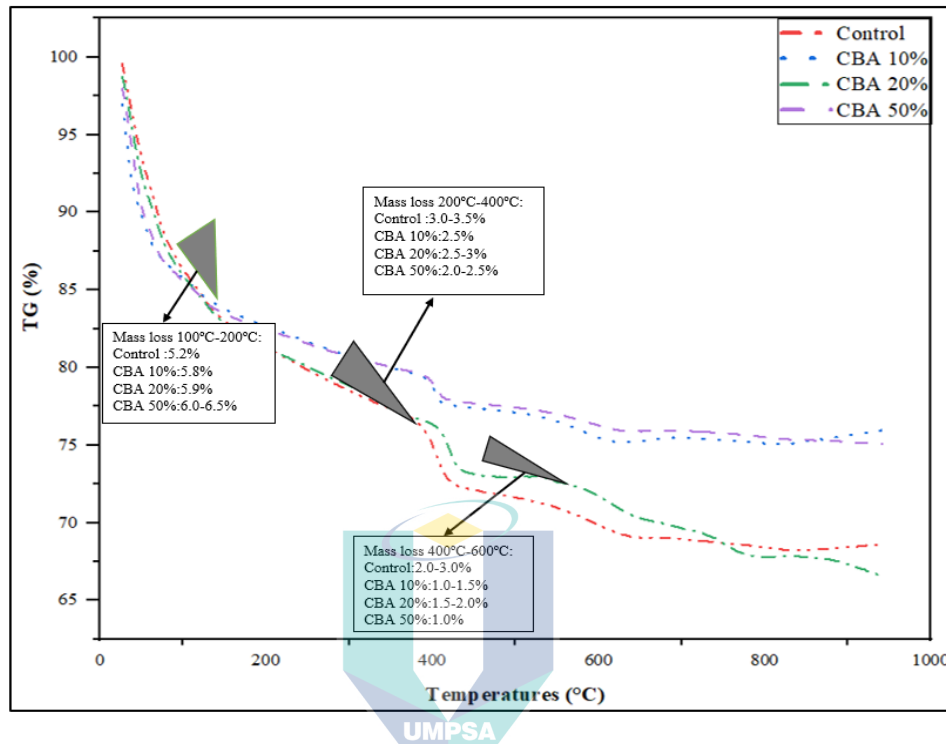


Figure 5.22 Thermogravimetry analysis at 7 days for control cement paste and those contained various replacement ratios of ground CBA

At 28 days of curing the mass loss curves for control was higher than the those contained ground CBA (CBA10%, CBA20%, CBA50%) as shown in Figure 5.23. The highest loss weight was observed for control 30% compared to those made of other replacement ratios. This is due to the evaporation of moisture on voids and the dehydration of calcium silicate hydrates was lower compared to early days of curing. The hydration products have filled the void in both control and ground CBA specimens with a constant curing process. The dehydrolaxation of $\text{Ca}(\text{OH})_2$ at 28 days of curing explained the pozzolanic reactivity of ground CBA. Further hydration process at later age showed the higher consumption of $\text{Ca}(\text{OH})_2$ by ground CBA to produce secondary calcium silicate hydrates and promoted denser and stronger matrix, thus higher strength for ground CBA cement paste. Previous research conducted by Velázquez et al., (2016) mentioned that the mass loss due to $\text{Ca}(\text{OH})_2$ for assessing the pozzolanic activity of fluid catalytic cracking catalyst residue blended cement pastes are different at according to

curing ages. Most of researchers agreed that the higher mass loss difference was observed at later curing age which confirms the participation of $\text{Ca}(\text{OH})_2$ in chemical reaction with amorphous SiO_2 from ground CBA compared to control specimen.

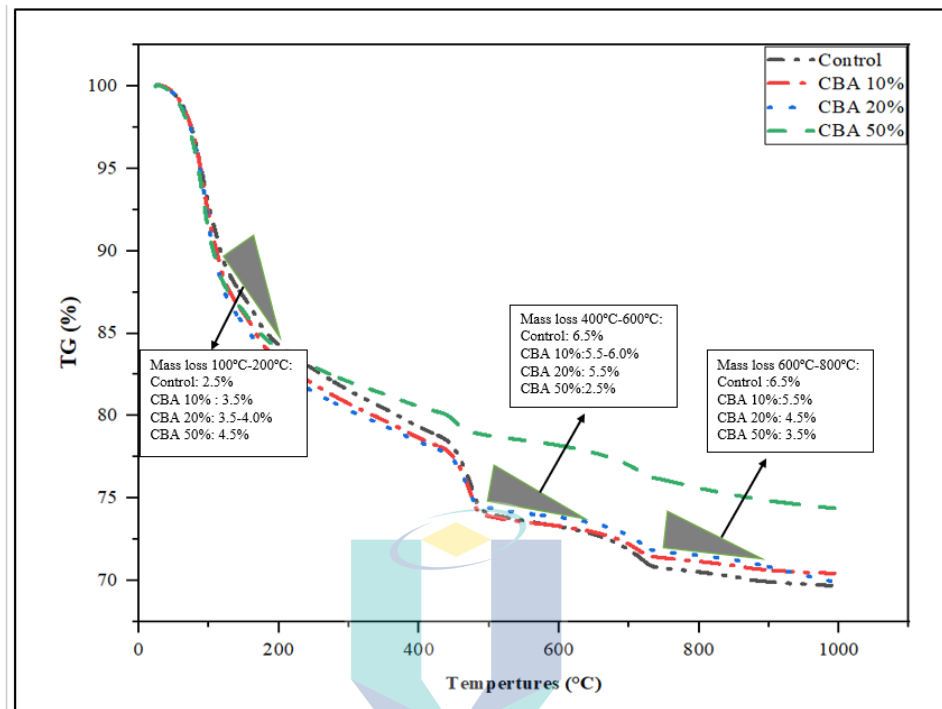


Figure 5.23 Thermogravimetric analysis at 28 days for control cement paste and those contained various replacement ratios of ground CBA

However, based on the observation at 56 days of curing, it showed that the control and CBA 10% was continues the same pattern for weight losses as shown in Figure 5.24. Meanwhile, other replacement ratios for pastes showed that additional mass loss for various points. The mass loss prior to 200°C was mostly attributed to the dehydration of C-S-H, ferroluminate hydrate. Apart from that, this finding in the agreement of the previous studies by Lu et al., (2018); Rostami et al., (2012). The mass loss of pastes containing ground CBA20% and CBA 50% exhibited a lower content than other pastes between 400°C to 600°C, which was attributed to the lower existence of C-H. Overall, the main weight loss for CBA is due to the removal of moisture from the samples. Moreover, the weight loss of CBA at a higher temperature after burning carbon is very low. This showed that CBA was thermally stable and can be used in thermal applications.

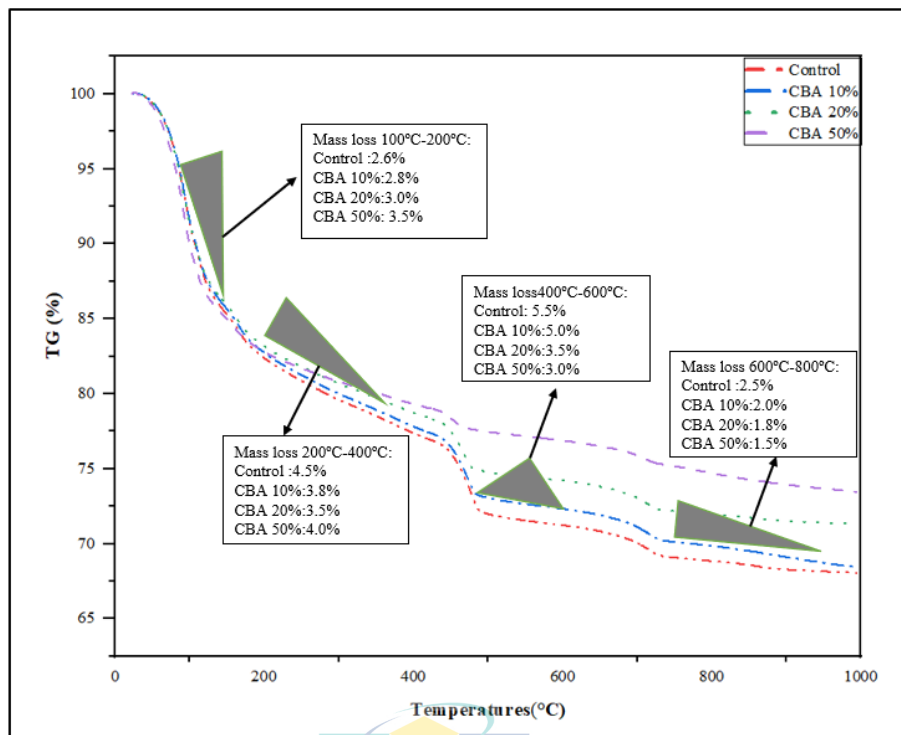


Figure 5.24 Thermogravimetry analysis at 56 days for control cement paste and those contained various replacement ratios of ground CBA

5.6 FESEM of Hardened SCC Samples and those made of optimum mechanically treated Ground CBA (ITZ)

Microstructure analysis on SCC specimens was carried out to investigate the interface between aggregate and bulk paste called interfacial transition zone (ITZ). Larger size of voids and pores makes ITZ was more porous than bulk paste, thus more crystalline compounds such as calcium hydroxide were present. Analysis of the hydration products was performed by using FESEM at 7, 28, and 56 days as shown in Figure 5.25 to determine the main compounds identified in thermal analysis for SCC control and SCC with CBA10% and CBA20%. At the beginning at 7 days of curing, Figure 5.25 a) for control and CBA10%, and CBA20% shows various phases using (FESEM) morphologies for SCC samples. For control samples at 7 days showed more homogenous and dense which lead to agglomeration particles for main ingredients. This is due to inhibiting the mechanism of cement hydration, contributing to weak zones within the matrix. Moreover, for CBA10% and was observed pores and voids for particles, which is due to ground CBA high porosity, and, thus, high absorption rate to these aggregate materials. For SCC contain CBA20%, it showed the crystallization of new products such

as calcium silicate hydrates in the cracks form of the ITZ is directly contributing to the strength of the SCC, besides reducing the amount of calcium hydroxide in the ITZ.

Figure 5.25 b) observed more Ca(OH)_2 crystals, which were large hexagonal plates with massive C-S-H shapes. A large amount of Ca(OH)_2 was produced from cement hydration due to the high amount of CaO present in ordinary Portland cement. These crystals are the source of strength for the cement paste. Various ratios (CBA10%, CBA20%) of ground CBA were used as cement replacement at 28 days of curing (as shown in Figure 5.25 b) and was observed that the C-S-H gel formulation that was developed which lead to improve the pozzolanic properties of the samples. Moreover, the interaction between calcium, sulphate, aluminate, and hydroxyl ions of cement hydration formed needle-shaped prismatic crystal of calcium trisulfoaluminate hydrate. Nevertheless, the shape of the CBA20% prismatic crystals of calcium hydroxide and fibrous crystals of calcium silicate hydrates began to fill the void occupied by water previously and the dissolving cement particles. Also, ettringite may decompose into hexagonal-plate known as monosulfoaluminate hydrate due to its unstable state depending on the alumina/sulphate ratio in Portland cement with ground CBA.

Figure 5.25 c) at 56 days for control samples showed the formulation of C-S-H gel consists of different shapes of fibrous and voids in the SCC samples. Also as shown figure 5.25c) for ground CBA 10% showed the particles were contain C-S-H and contain some of voids and porous in the samples. As shown in Figure c) for ground CBA 20% showed the granular particles with dense structure, which led to participation in the hydration process to generate C-S-H through reacting with ground CBA particles in the SCC samples. Overall, the results of the FESEM showed that the substitute of ground CBA in the SCC mixture had a greater number of C-S-H crystals than the control SCC mixture samples. This was because the cement hydration caused a pozzolanic activity between the silica and the Ca(OH)_2 that came from the cement hydration. Another reason is that SCC with a low water-cement ratio has little cracking. In addition, pozzolanic substances help to achieve the best compatibility and the treatment affects the final strength of the SCC samples.

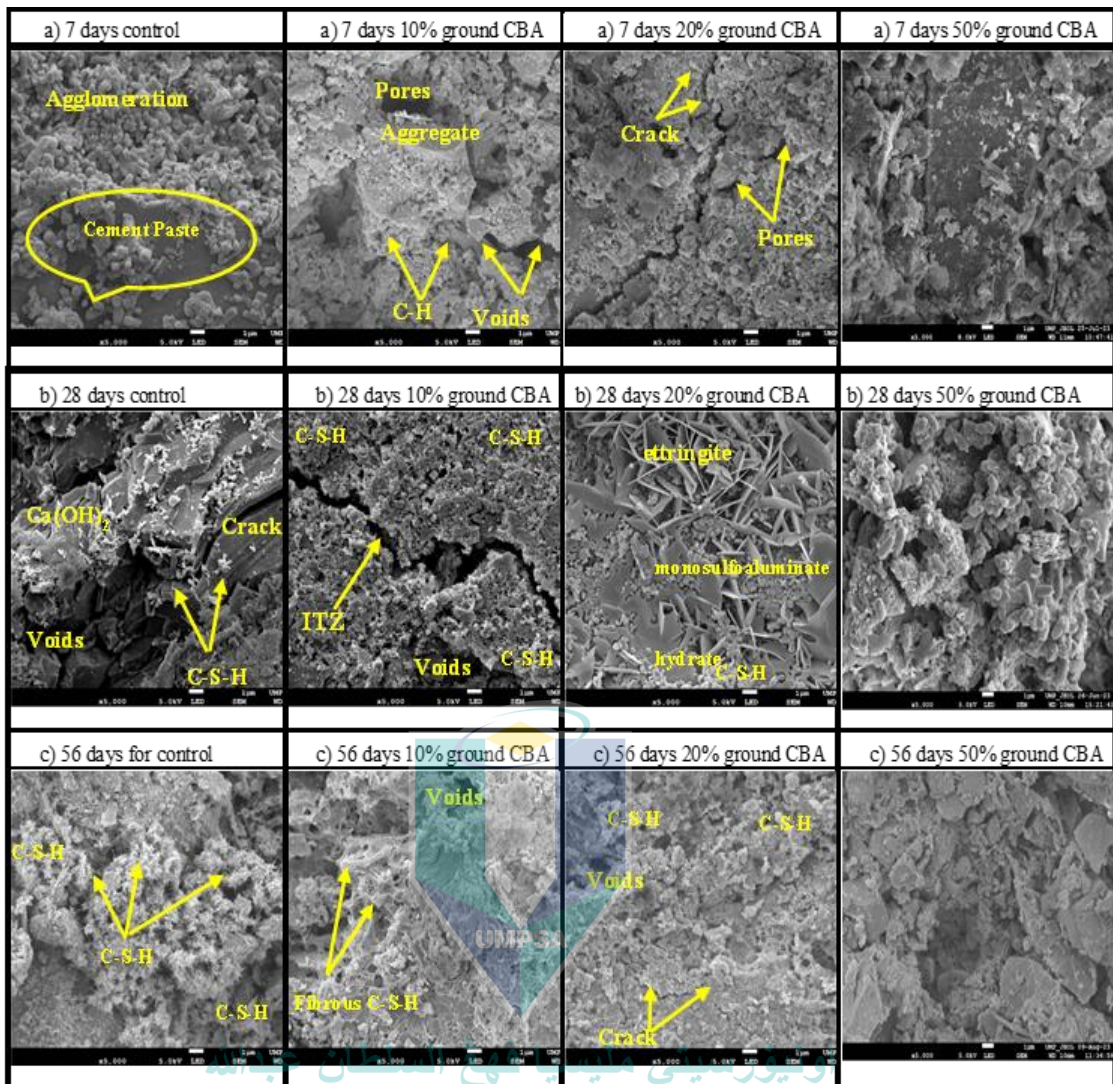


Figure 5.25 FESEM micrographs of SCC specimens at a) 7 days, b) 28 days, and c) 56 days for control and ground CBA 10%, 20%, 50 % of SCC samples at X5000 magnification

5.7 Durability Properties of optimum mechanically treated Ground CBA Based on SCC

This section presents and discusses the results of the testing stated in terms of the durability of SCC containing ground CBA as cement replacement. At the early part of the sub sections start with water absorption test result is presented followed by findings and discussions from this test. After that, the data obtained from acid resistance test and sulphate resistance test are presented.

5.7.1 Water Absorption of optimum mechanically treated Ground CBA Based on SCC

The water absorption test is necessary, and it identifies the concrete durability. In this study, influence of the replacement of ground CBA as partial cement replacement on water absorption of the SCC mixtures were measured at the age of 7, 14, 28, 56, 90, and 180 days of curing as shown in Figure 5.26. The effect of CBA towards water absorption of SCC mixture containing ground CBA under different curing ages. It can be seen from the illustration that the use of ground CBA influenced the water absorption of SCC samples. Control specimens with 0% CBA as partial cement replacement exhibited the decrease percentage of water absorption amongst all curing ages mixes with increased the curing ages up to 180 days. (Khan & Ganesh, 2016) stated that water absorption of concrete containing CBA is influenced by curing ages which is showed decrease the water absorption with increased the curing ages up to 90 days. Furthermore, the result shows that with increase the replacement ratios of CBA lead to increase in the water absorption rate. According to (A. Neville, 2012) stated that the concrete water absorption of ratio not more than 10% is classified as high-quality concrete. In this study, the water absorption of SCC with 0% CBA and with replacement ratio from 10% to 50% as partial cement replacement in all curing ages less than 10% water absorption as in agreement with (Neville, 2012) book guidelines for water absorption for concrete samples. Interestingly, the water absorption for all specimens was in the range of 9.9% higher water absorption ratio to 50% ground CBA at 7 days and lower water absorption ratio 3.1% from 0% without CBA (control) respectively as shown in Figure 5.26 which is within the range for high-quality concrete samples.

However, at 7 days of curing, the water absorption results showed that increased with increased the replacement ratio in SCC mixture as shown in Figure 5.26. The range of water absorption value was from 8.561% to 9.915% for control and CBA50%. Amat et al. (2023); Singh & Siddique, (2015) stated that water absorption increased with increasing replacement ratios of ground CBA, which is due to the greater number and size of voids in ground CBA-SCC mixtures resulting to higher water absorption. Furthermore, at 14 and 28 days of curing, showed continuous increase in the water absorption of ground CBA samples in SCC mixture. Khan & Ganesh, (2016) stated that the water absorption of concrete containing CBA was increased as replacement ratio

increased at 28 days. This was explained due to porous structure of CBA and the voids generated in the mixture after evaporation of free water in SCC samples (Baite et al., 2016).

At 56 curing ages, the results for the water absorption of ground CBA showed increased in the CBA with increase the replacement ratios compared to control samples, and the other replacement ratios showed increased as the CBA replacement ratios increased in the SCC mixture samples. The water absorption results showed the increased in other replacement ratio compared to control samples CBA10%, CBA20%, CBA30%, CBA40%, and 50 % with absorption rate, 5.714%, 5.8753%, 6.134%, 6.837%, 6.99 with control 5.138%, respectively compared to control samples in SCC mixture samples. The increased in the water absorption due to the CBA fineness and the particles' porosity, which allowed the SCC samples to be more absorbed (Balasubramaniam & Thirugnanam, 2015; Mangi et al., 2019).

On the other hand, for long term water absorption results at 90 days showed an decreased in the absorption rate for ground CBA up to 20 % compared to conventional samples in SCC mixture. It can be seen the results for water absorption for CBA10 % and CBA20% of ground CBA with 3.277% and 3.335% respectively, compared to control samples with 3.476% in SCC mixture samples. For the other replacement ratios, it was found to be increased of the water absorption rate for ground CBA with various replacement ratios compared to control samples for CBA30% and CBA40%, CBA50% of ground CBA with 3.687%, 3.754%, 4.3385% compared to control with 3.476%.

At 180 days, the results for water absorption of ground CBA showed that increased as the replacement ratios increased compared to control samples with increase replacement ratios. The decrease of water absorption of ground CBA in the long curing ages among all curing ages. The increased in replacement ratios due to indicates that the continuity of porous in concrete increased with the progress in curing age and the increase in CBA concrete mixtures was significant (Singh & Siddique, 2014a). Overall, it was evident in the present study that the water absorption of ground CBA with various replacement for cement increased as the replacement ratio increased due to high porous particles which lead to absorb more water and influenced in the water absorption rate for ground CBA. FESEM images in Figures 5.27 shows that SCC with 0% ground CBA

consisted of larger sized of voids while SCC with 10%, 20, and 50% showed less voids appeared to be more compact.

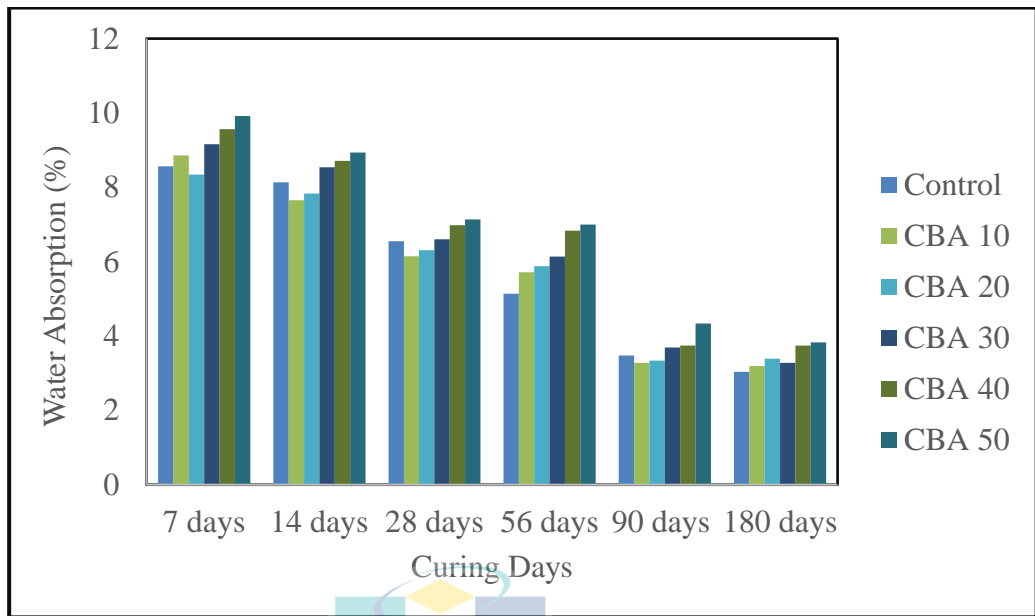


Figure 5.26 Water absorption ratio results of ground CBA with various replacement ratios at different curing ages

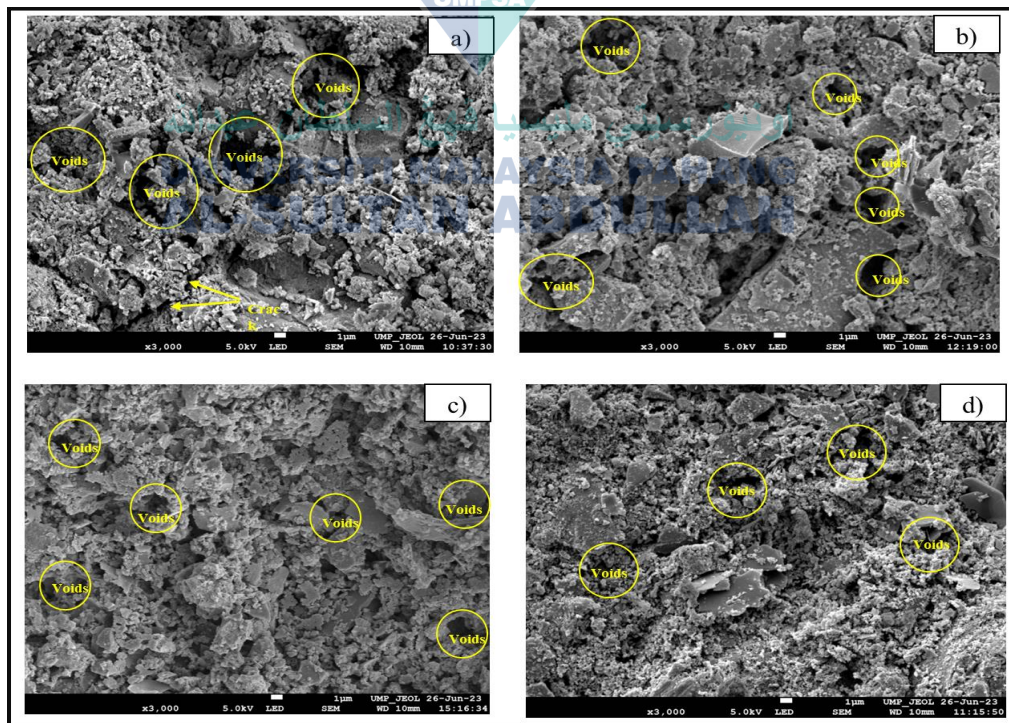


Figure 5.27 FESEM images of a) control, b) ground CBA 10%, c) ground CBA20%, and d) ground CBA50% in SCC at 3000x magnification

5.7.2 Acid Resistance of Optimum Mechanically Treated Ground CBA SCC

SCC is very vulnerable towards acid attack. However, pozzolanic material is well-known mineral admixture that assist towards minimizing the acid intrusion into the concrete mixture. In this experimental study, the effectiveness of ground CBA replacement as partial cement replacement towards acid resistance of SCC are discussed. The investigation on the resistance of ground CBA in the SCC specimens towards acid attack was carried out through specimen weight loss measurement, strength loss of the specimens and visual observation. The specimens have been continuously immersed in sulfuric acid (H_2SO_4) solution curing at 7, 28, 56, 90 days.

5.7.2.1 Visual Observation

Visual observation is one of the experiments made in determining the rate of acid attack on the durability of SCC containing ground CBA as partial cement replacement. This visual observation is very important to indicate the levels of acid attack from time to time as well as to carry out early prevention rather than being attacked by acid. After the acid attack, a visual inspection was also conducted on the specimens ASTM C1898–20, (2020). In the early stages of immersion, all SCC samples containing ground CBA including control specimens showed small erosion indication which is increased with increase the immersed time in the solution.

Figures 5.28, 5.29, 5.30, and 5.31 show images of the physical appearance of the control SCC and SCC containing 10% and 50 ground CBA as cement replacement after having been exposed to 5% of H_2SO_4 solution at 7, 28, 56 and 90 days. At 7 and 28 days of immersion, small signs of detrimental effect were spotted for all specimens. Moreover, it is seen that all the SCC mixture specimens containing ground CBA from 10%, and 50% were structurally intact with only minor damages at the surface after the acid exposures as shown in Figure 5.28, and 5.29. For all the specimens, the surface deterioration of specimens increased with the increase of exposure duration. At 56 days was observed whitish color precipitate was observed on the surface of the SCC specimens containing ground CBA as partial cement as shown in Figure 5.30. At the end of the exposure, more whitish precipitate was observed on the surface of the SCC specimens. A larger quantity of whitish precipitate was detected on the surface of the control SCC compared to that of the SCC containing ground CBA. The pozzolanic effect caused by the presence of CBA

increases the denseness of the concrete internal structure which enhances its durability to acid attack. The enhanced acid resistances of concrete with certain amount of CBA were reported by previous studies (Mangi et al., 2021; Muthusamy et al., 2021).

However, at 56 days and 90 days white precipitation was observed increased more on the surface of SCC specimens, with increased the curing ages up to 90 days for those made of 10 % and 50 % of ground CBA. Moreover, SCC specimens showed severe corrosion, characterized by significant expansion and large areas in which the ground CBA and aggregates in the surface spalled, leading to a very porous surface structure as shown in Figure 5.31. This explains the ingress of the acidic solution into the pores of the immersed SCC specimens containing ground CBA, the removal of calcium salts presents in the samples, and on reaction with carbon-dioxide the deposition of the resulting efflorescence on the outer surface of the SCC specimens. Furthermore, one is the holding salts and the second is the formation of C-S-H gel. The visual inspection of SCC samples caused by less formation of C-S-H gel (Siddique et al., 2012b). Nevertheless, the formation of C-S-H gel is retarded due to salt of acidic environment (Babajide Olabimtan & Mosaberpanah, 2023).

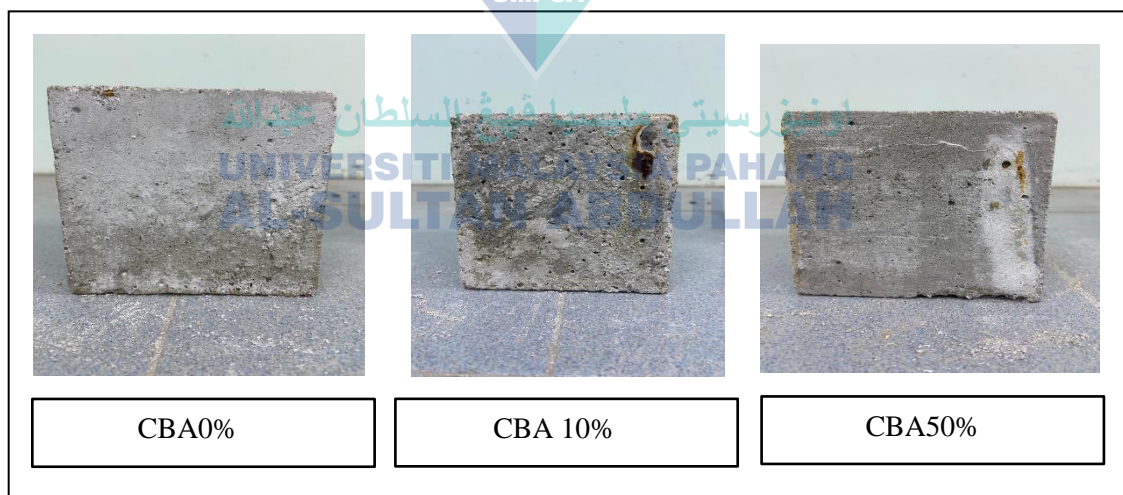


Figure 5.28 SCC specimens containing CBA after being immersed in (H_2SO_4) solution for 7 days

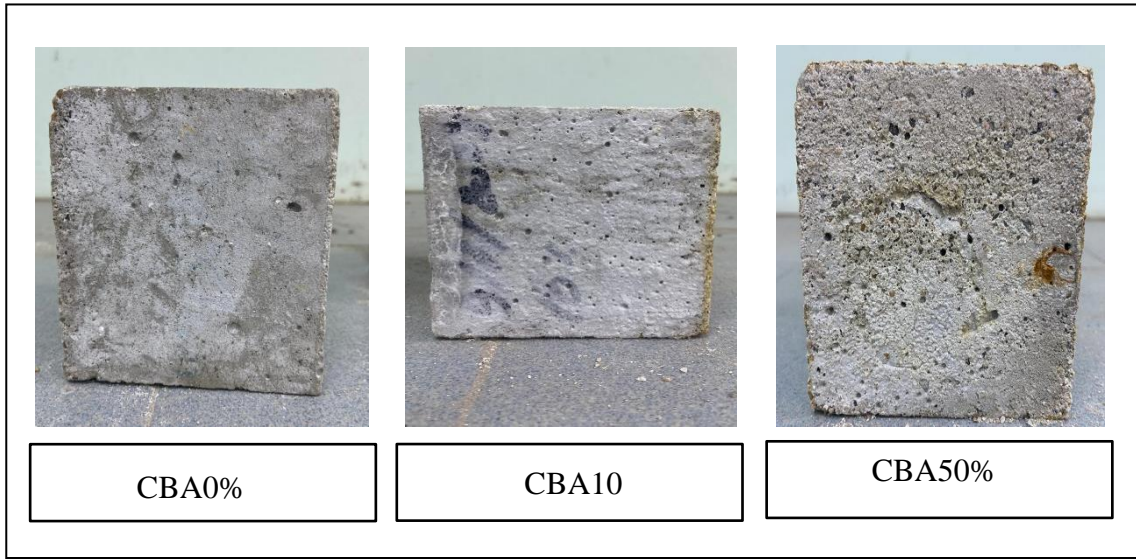


Figure 5.29 SCC specimens containing CBA after being immersed in (H₂SO₄) solution for 28 days.

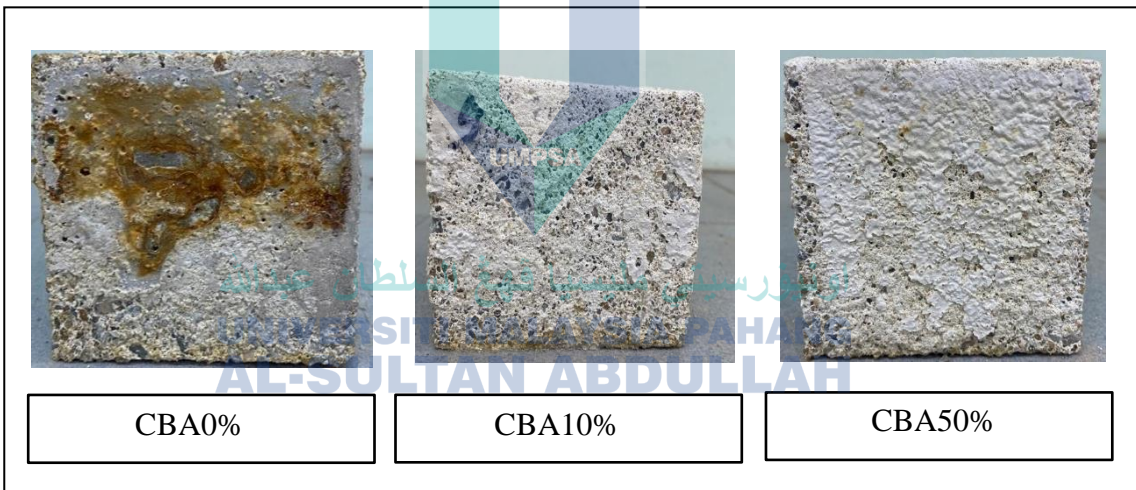


Figure 5.30 SCC specimens containing CBA after being immersed in (H₂SO₄) solution for 56 days.

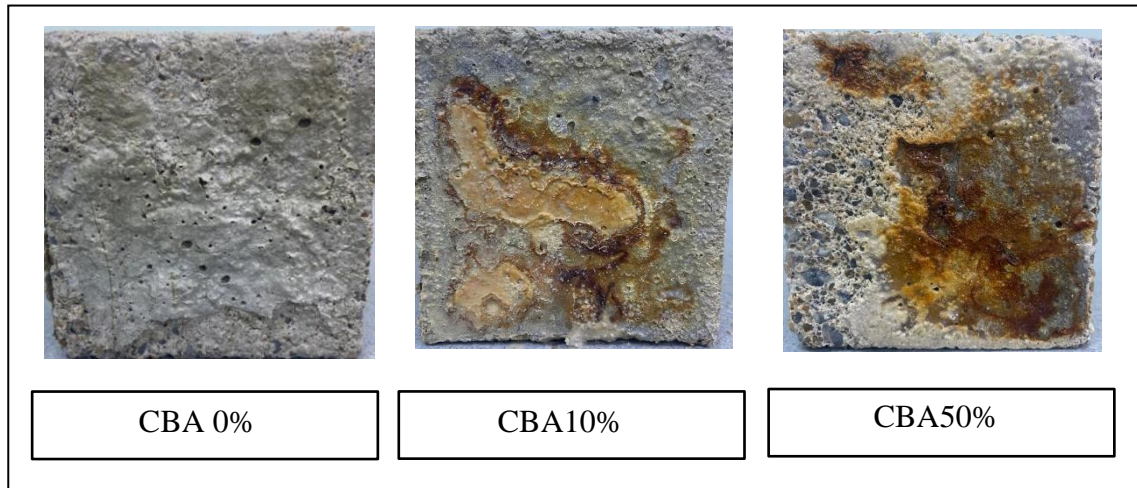


Figure 5.31 SCC specimens containing CBA after being immersed in (H_2SO_4) solution for 90 days

5.7.2.2 Mass Loss

The acid resistance testing was carried out by measuring the specimen's weight loss in H_2SO_4 solution for the total immersion period of 7, 28, 56, and 90 days. The percentage of mass loss for SCC mixture comprises of 0%, 10%, 20%, 30%, 40% and 50% of ground CBA as partial cement replacement specimens as shown in the Figure 5.32. From the Figure 5.32, it appears that the mass loss ratio for all specimens increased gradually by increasing H_2SO_4 immersion period. Evidently, the mass loss of the SCC mixes indicates an upward trend as the duration of immersion in the acid solution H_2SO_4 became longer, which is findings agree with the results of this study by (Senhadji et al., 2014). At the immersion period all specimens were observed to have exhibited higher mass loss from early ages up to long ages 90 days. The mass loss occurred resulting from the attack caused by the reaction of H_2SO_4 with calcium hydroxide, $Ca(OH)_2$, resulting in leaching of the formed salt. In addition, it is also evident that the total mass losses for all specimens were in the range of 3.5% to 5.9% after 90 days of immersion ages in the H_2SO_4 solution. These results indicate that SCC containing CBA shows high durability against acid attack, as most CBA in concrete incorporating pozzolan from previous researches (Singh et al., 2016; Singh & Siddique, 2014b) shows a mass loss between 2.5% to 13.01% within 7 and 90 days of exposure in H_2SO_4 solution.

However, at 28 days of immersion period, the weight loss of SCC containing CBA10%, CBA20%, CBA30%, CBA40%, and CBA50% was 4.374%, 4.318%, 4.067%,

3.924%, and 3.753% respectively as compared to 4.256% weight loss of the control SCC samples. Percentages of weight loss for ground CBA in SCC specimens decreased with increase in CBA content higher than CBA20% replacement of ground CBA in SCC specimens. On the other hand, the weight loss of SCC containing CBA up to 20 % showed less mass loss compared to control SCC specimens.

Moreover, at long immersion period 56 days of H_2SO_4 , weight loss of SCC containing showed the mass loss for 10%, CBA 20%, CBA30%, CBA40%, and CBA50% were 5.428%, 5.326%, 5.171%, 4.888%, and 4.819% respectively as compared to 5.124% weight loss of the control SCC samples. At 90 days of immersion period in H_2SO_4 , the weight loss of CBA-SCC showed the mass loss for 10%, CBA 20%, CBA 30%, CBA40%, and CBA50% was 5.944%, 5.734%, 5.394%, 5.731%, and 5.607%, respectively as compared to 5.394% weight loss of the control SCC specimens. However, replacement of cement by optimum amount of pozzolanic materials such as ground CBA would reduce significantly the amount of $Ca(OH)_2$ that is vulnerable towards acid attack. In addition, $Ca(OH)_2$ produced during hydration process would be consumed by silica in ground CBA converting it into C-S- H gel. Nevertheless, this is essential as the resistance of SCC matrix towards acid attack depends primarily on its pore structure characteristics. The more porous structure as well as higher water absorption of ground CBA than natural sand and gravel is the main reason for this issue for mass losses. Other researchers (Karthik et al., 2021; Natarajan et al., 2023; Senhadji et al., 2014) are also working towards influencing the SCC durability properties in terms of acid resistance by adding pozzolans materials.

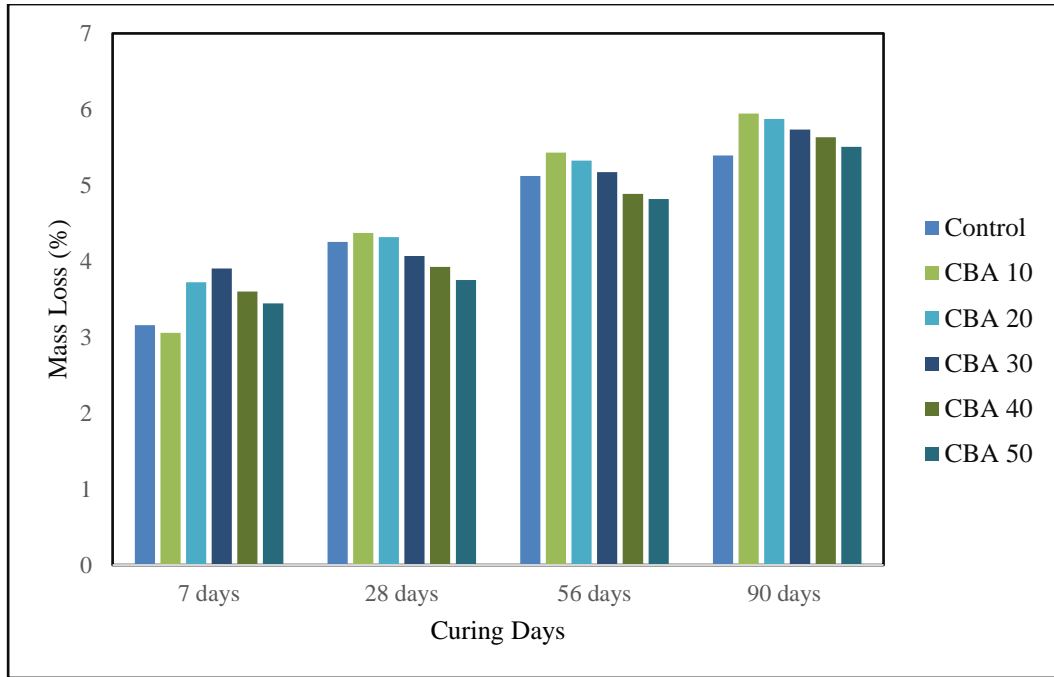


Figure 5.32 Mass loss of SCC containing ground CBA as cement replacement immersed in H_2SO_4 for various curing ages

5.7.2.3 Strength Loss

The strength loss of SCC containing ground CBA as partial cement specimens immersed in 5% H_2SO_4 solution for a period of 7, 28, 56 and 90 days are shown in Figure 5.33. Approximately, 6.5 % to 37.15 % of the total strength deteriorates for all specimens, respectively. These results are in line with the previous research (Singh & Siddique, 2014b) which is within 19.84% to 28% compared to control sample with reduction value 25.94%. after 7 days of immersion in the H_2SO_4 solution. However, in this experimental study, it showed that at early curing age 7 days of immersion in H_2SO_4 the strength loss /deterioration of ground CBA in SCC decreased with increase in replacement level of cement. At 7 days the strength loss /deterioration of ground CBA in SCC containing CBA 10%, CBA20%, CBA30%, CBA40%, and CBA50% was 6.590%, 6.797%, 6.405%, 6.847 and 6.288% respectively lower than that of control SCC. The reduction in the strength ratio of ground CBA-SCC after immersion in H_2SO_4 is due to increased porosity of SCC. However, existence of pores in SCC mixture samples allow the acidic solution H_2SO_4 to seep in easily and fasten the deterioration process. Less dense hydrated cement paste having larger amount of pores would cause the calcium to be dissolved. Similar trend is observed in the works of (Samimi et al., 2018) in which the loss strength was indicated by SCC samples containing optimum quantity of pozzolanic materials. These reactions

influence the produce of secondary C-S-H gel, which increases the voids that are present in the SCC Nagaratnam et al. (2019). The generation of low amount of C-S-H in SCC with ground CBA led to decreased and delay in the hydration process. Pozzolanic reaction makes this SCC mixture samples affected by acid solution (H_2SO_4) also decreased in the strength for SCC containing ground CBA.

At 28 days of immersion in H_2SO_4 the results showed that the strength loss /deterioration of ground CBA in SCC containing CBA10%, CBA20%, CBA30%, CBA40%, and CBA50% was 13.006%, 12.669%, 11.256%, 10.976% and 10.297% respectively lower than that of control SCC. Evidently, the strength loss of the SCC mixes indicates an upward trend as the duration of immersion in the acid solution (H_2SO_4) became longer. Furthermore, at 56 days of immersion in H_2SO_4 , the results showed that the strength loss /deterioration of ground CBA in SCC containing CBA 10%, CBA20%, CBA30%, CBA40%, and CBA50% was 20.828%, 22.062%, 21.382%, 21.778% and 23.870%. It can be seen that the loss strength of all replacement ratios of ground CBA become increased compared to control SCC samples. At the end of the immersion period (i.e., 90 days), all specimens were observed to have exhibited strength loss more than control samples. Overall, the results showed that the loss strength increased with increase the replacement ratio of ground CBA as the pores in SCC samples increases. The absorption capacity and pores of SCC samples with ground CBA and without retains the acidic solution and enhances the reaction between acids and the hydrated materials of SCC. This was confirmed by the increasing loss ratios (%) in compressive strength. (Shariati et al., 2023) had reported that the increase in acid immersion duration would cause the internal voids and pores which lead to increase the loss strength ratio of the concrete specimens to increase as well.

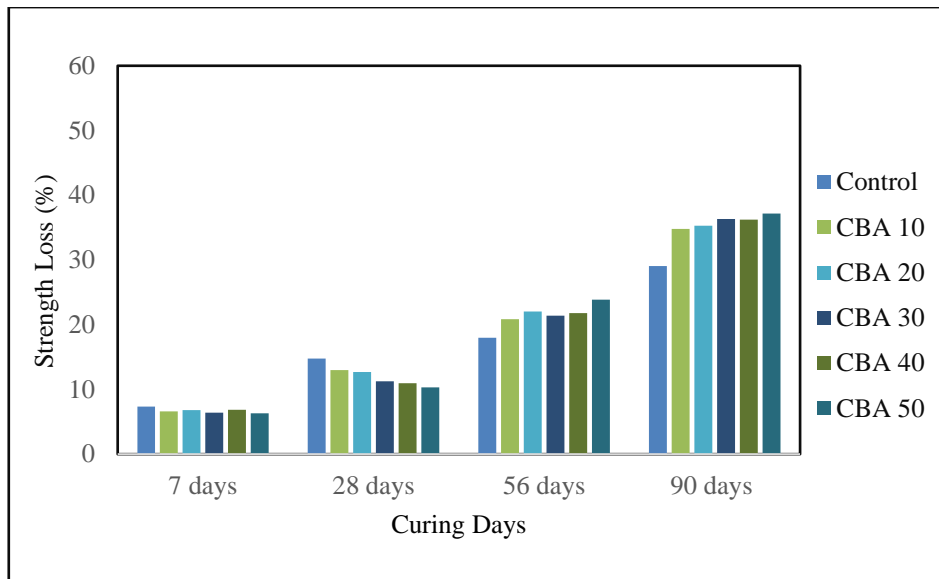


Figure 5.33 Strength deterioration of SCC containing ground CBA as cement replacement immersed in H_2SO_4 for various curing ages

5.7.3 Sulphate Resistance of optimum mechanically treated Ground CBA Based on SCC

Permeability of concrete plays an important role in protecting against external sulphate attack. Sulphate attack can take the form of expansion, loss in compressive strength and loss in mass of concrete (Elahi et al., 2021). The sulphate solution (Na_2SO_4) related expansion of concrete is associated with the formation of ettringites and gypsum (Nanda & Rout, 2021; Ramezaniipour & Riahi Dehkordi, 2017). Since Na_2SO_4 attack is more severe on concrete, the concrete specimens were immersed in a 5% solution of (Na_2SO_4) (Wan Ibrahim et al., 2021a). Exposure to sulphate (Na_2SO_4) is well known to affect the durability of concrete materials in marine environments. This section discusses the analysis conducted on the sulphate attack resistance behaviour of SCC containing different percentages of ground CBA as partial cement replacement with ratios 10% to 50%. Performance of this concrete towards sulphate attack in terms of visual observation and mass loss of the specimens was determined. Other studies (Hamzah et al., 2020; Hamzah et al., 2017) also focused on concrete expansion, mass change and strength deterioration when investigating the damage process of concrete under sulphate attack. The deterioration levels of all specimens were recorded for visual observation, mass loss and strength loss at 7, 28, 56, 90 days of immersion to sulphate solution.

5.7.3.1 Visual Observation

Visual observation is one of the experiments made in determining the rate of sulphate attack on the durability of SCC containing ground CBA as partial cement replacement. This visual observation is very important to indicate the levels of sulphate attack from time to time as well as to carry out early prevention rather than being attacked by sulphate attack. After the sulphate attack, a visual inspection was also conducted on the specimens in accordance with ASTM C267-01 guidelines. In order to investigate the physical effect of SCC mixture containing ground CBA as partial cement replacement when subjected to sulphate solution (Na_2SO_4), visual observation was carried out at 7, 28, 56, 90 days. In the early stage at 7 days of immersion, all SCC samples containing ground CBA including control specimens showed no sign of detrimental effect was spotted in the Na_2SO_4 solution as shown in Figure 5.34. After 28 days of immersion period in the Na_2SO_4 , it showed that small pores occurred and start change in color for control and CBA 10 %, CBA 50% specimens. Furthermore, a small white salt was observed on the surface of the SCC specimens as shown in Figures 5.35. The observation in line with previous studies (Caneda-Martínez et al., 2021; Wan Ibrahim et al., 2021a) also observed that the change in color and cracks appear in the edges of the samples when subjected to sulphate solution at early ages.

At 56 days of immersion in the Na_2SO_4 solution, ground CBA-SCC showed that the expanding concrete started to burst out leaving holes at the surface of the SCC specimens. The SCC samples experience expansive deformation during sulphate attack due to internal expansive stress. Sulphate ions enter concrete pores, react with the pore solution, and produce ettringite. The production of ettringite explains the internal expansive stress that reduces the durability of SCC samples as in Figure 5.36. Moreover, at the end of immersion 90 days in the Na_2SO_4 solution, ground CBA-SCC showed that more whitish precipitate was observed on the surface of the SCC specimens as shown in Figure 5.37. A larger quantity of whitish precipitate was detected on the surface of the SCC control samples compared to that of the SCC samples containing ground CBA 10% and CBA 50%. According to (Cohen & Mather, 1991; Marchand et al., 2001) this physical type of deterioration worsens as the concrete permeability increases. The same observation has been recognized by other researchers, i.e., that sulphate attack results in expansion as well as samples cracking in the samples.

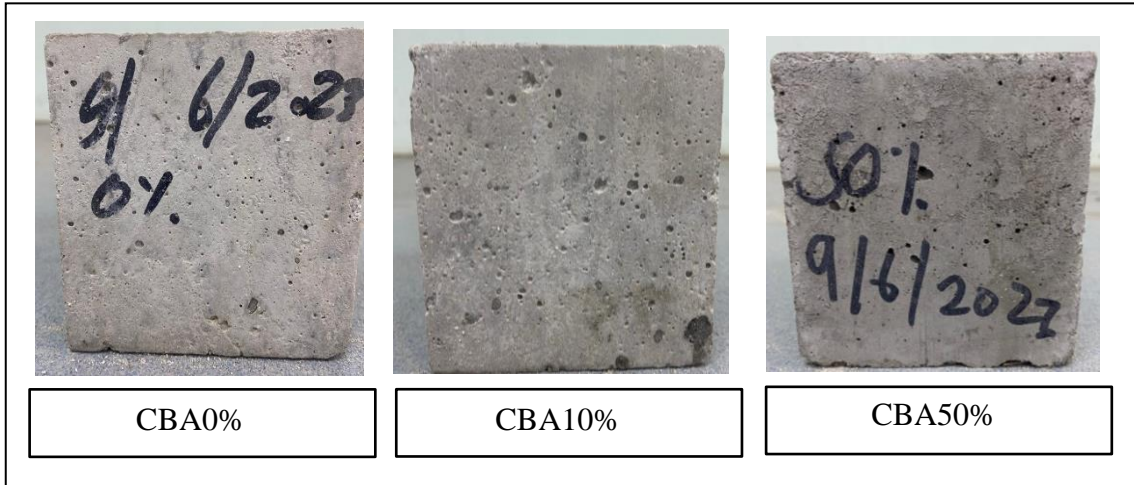


Figure 5.34 SCC specimens containing CBA after being immersed in Sodium sulphate (Na_2SO_4) solution for 7 days.

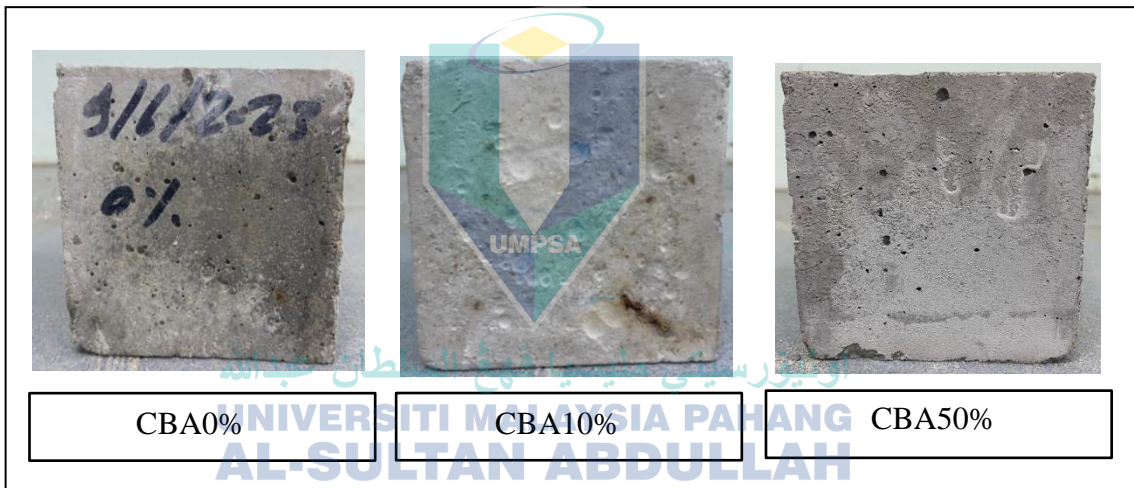


Figure 5.35 SCC specimens containing CBA after being immersed in Sodium sulphate (Na_2SO_4) solution for 28 days

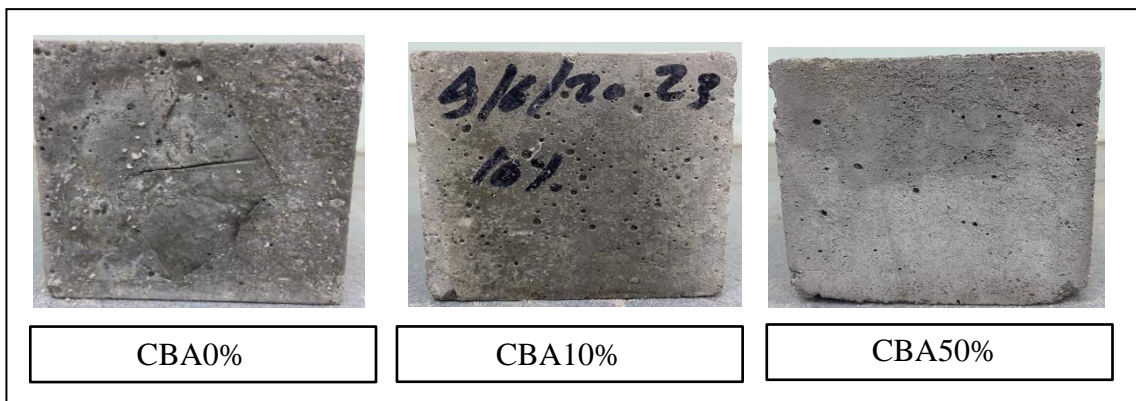


Figure 5.36 SCC specimens containing CBA after being immersed in Sodium sulphate (Na_2SO_4) solution for 56 days

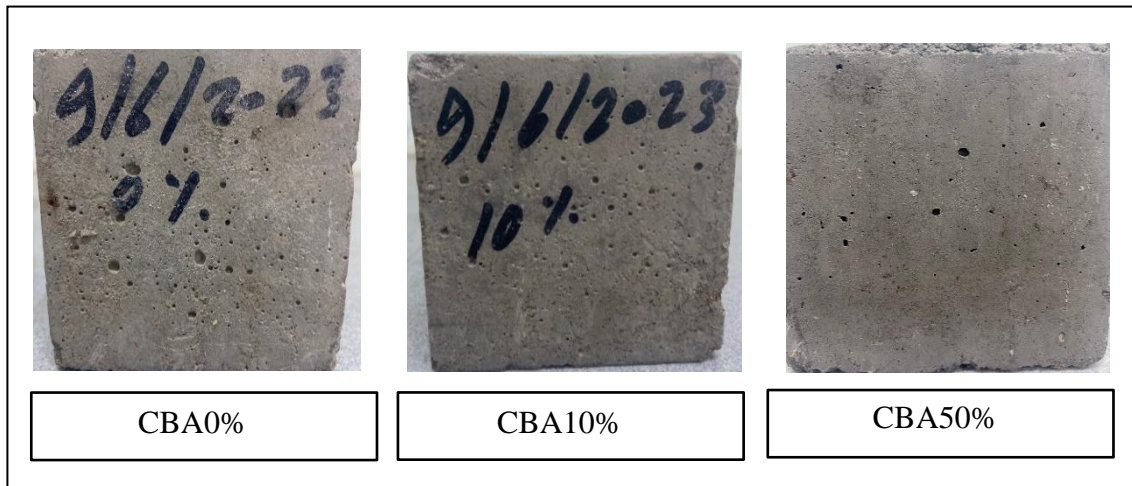


Figure 5.37 SCC specimens containing CBA after being immersed in Sodium sulphate (Na_2SO_4) solution for 90 days

5.7.3.2 Mass Loss

The sulphate resistance testing was carried out by measuring the specimen's weight loss in Na_2SO_4 solution for the total immersion period of 7, 28, 56, and 90 days. The percentage of mass loss for SCC containing 0%, 10%, 20%, 30%, 40% and 50% of ground CBA as partial cement replacement specimens as shown in Figure 5.38. From the Figure 5.38, it appears that the mass for all specimens increased gradually by increasing (Na_2SO_4) immersion period. Evidently, the mass loss of the SCC mixes indicates an upward trend as the duration of immersion in the sulphate solution (Na_2SO_4) became longer. At 7 days of immersion in the sulphate solution Na_2SO_4 it was observed that when used ground CBA as partial cement replacement the weight losses increased as the replacement ratios increased from 10% to 50% compared to control samples. Similar finding had been observed by Kasaniya et al. (2021) in their study in which the mass loss of the concrete immersed in sulphate solution Na_2SO_4 had exhibited an increment in the weight loss when increased the replacement ratios of ground CBA in concrete. This was mainly because these materials did not undergo a chemical reaction with lime to produce more calcium-silicate-hydrate (C-S-H) and other hydrates. These hydrates would have helped improve the pore structure and enhance the ability to resist the entry of harmful sulphate ions. The ground of the raw CBA to a finer particle size greatly enhanced its pozzolanic reactivity and resistance to sulphate ions.

At 28 days of immersion in the sulphate solution Na_2SO_4 it was observed that the weight losses continuously increased when increased the replacement ratios for ground CBA from 10% to 50 % compared to control samples in SCC. In addition, it is also evident that the total mass losses for all mixes were in the range of 1.06 to 1.8 for control and CBA50% respectively. In agreement with our experimental study another research by Aydin, (2016) reported that standard specification of weight loss for sulphate attack between 6% and 16%. Who mentioned that the CBA as cement replacement with various ratios high resistance to sulphate attack at 28 days. Furthermore, the increase in the weight losses due to pore connectivity, and the sulfate solution is easily absorbed by the composites, thereby deteriorating the paste structure containing a high amount of CBA. On the other hand, the weight loss of SCC containing CBA 50 % showed higher mass loss compared to control SCC samples and those contained other replacement ratios.

Moreover, at long immersion period 56 days of Na_2SO_4 weight loss of SCC containing CBA 10%, CBA20%, CBA30%, CBA40%, and CBA50% were 1.925%, 1.931%, 2.184%, 2.230%, and 2.471% respectively as compared to 1.713% weight loss of the control SCC samples. As noted by Mangi et al. (2019) reported that the weight loss for SCC containing ground CBA was increased with increase the replacement ratios and the ages of immersion in Na_2SO_4 solution. The finding showed that the ranges of weight losses was 2.0% to 2.5% under Na_2SO_4 at 56 days. At 90 days of immersion period in Na_2SO_4 , the weight loss of SCC containing CBA were showed the mass loss for 10%, CBA20%, CBA 30 %, CBA 40 %, and CBA 50 % was 1.925%, 1.931%, 2.184%, 2.230%, and 2.471% respectively as compared to 1.713% weight loss of the control SCC samples. It is evidently the increased in the weight losses with increased the replacement ratios and immersion in Na_2SO_4 solution period due to formation of more hydration products and consequently higher quantities of sulphate ions and the reaction products, ettringite and gypsum. This indicated that in the presence of ground CBA in other replacement ratios less than CBA50 % could reduce the hydration process and reduces the salts penetrability in SCC, therefore less weight gain in compared to conventional SCC samples. Overall, the performance of SCC containing ground CBA was noticed that to be adequate under 5% Na_2SO_4 and could significantly improve the durability of SCC samples. Also, the ground CBA is highly effective for reducing sulphate-induced damage or enhancing the sulphate resistance of SCC samples.

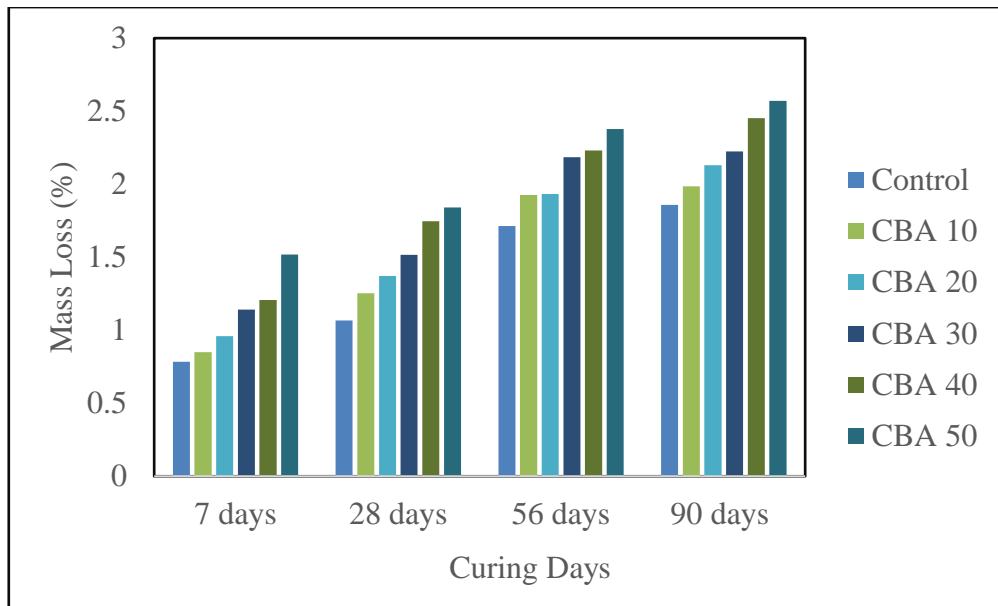


Figure 5.38 Mass loss of SCC containing ground CBA as cement replacement immersed in Na_2SO_4 for various curing ages

5.7.3.3 Strength Loss

The strength loss of SCC containing ground CBA as partial cement specimens immersed in 5% Sodium sulfate (Na_2SO_4) solution for a period of 7, 28, 56 and 90 days are shown in Figure 5.39. At 7 days of immersion in Na_2SO_4 , the compressive strength of control SCC and SCC with 10% and 20% of ground CBA as cement replacement increased by about 1.09% to 1.48%, respectively. On the other hand, the compressive strength of SCC was decreased by about 0.90%, 0.75%, 0.65% for CBA30%, CBA 40%, and CBA50% respectively. Other researchers Mangi et al. (2019) observed strength deterioration of ground CBA as partial cement replacement between 4.72% to 8.04% of immersion in sulphate solution. From the graph, it is also apparent that the incorporation of optimum amount of ground CBA decreases the negative impact of sodium sulphate solution on SCC. Furthermore, the increase in the compressive strength of the SCC specimens exposed to sodium sulphate solution could be attributed to the formation of ettringite, which leads to a more closed pore structure and slight increase in compressive strength. At 28 days of immersion in the observed that continuously recorded improvement in the for compressive strength of SCC containing CBA with up to 20% CBA and the other replacement ratios showed decreased as CBA increased compared to SCC control samples. Similar finding had been observed by Saribas & Cakir (2017) in their study in which the strength loss of the concrete immersed in sulphate solution for 28

days had exhibited an increment due to the presence of voids in the concrete samples structures being filled up with the sulfate ion which lead to filled in the gaps of the specimens.

On the other hand, at long term of curing in at 56 to 180 days of immersion in Na_2SO_4 , it was observed that all specimens continuously recorded a decreases in the strength which lead to increase in the strength loss of SCC samples for control and SCC contain ground CBA. A similar phenomenon was observed by Jiang & Niu, (2014) when they revealed that the compressive strength of specimens subjected to aggressive sulphate solution showed a reduction after long term at 90 days of immersion. The same concept was also reported by Dayarathne et al., (2013) who stated that the presence of more voids in the pore structure of cement matrix are able to accommodate the expansive ettringite during the early stages of immersion. Consequently, the continuous formation of ettringite, that has a relatively large volume, caused internal cracks due to continuous expansion and resulted in a decrease in the compressive strength after long term of immersion. However, the hydration products can be reduced by using ground CBA due to the pozzolanic reaction, which prevents the diffusion of sulphate ions throughout the cement matrix. Amine et al., (2017); Limbachiya et al., (2012) pointed out that the inclusion of pozzolanic material in concrete would decrease the reactive aluminates (C_3A) content, hence reducing the formation of ettringite. According to Demir et al., (2018) they investigated on OPC replacement with FA, CBA, and blast-furnace slag as a partial cement replacement under (Na_2SO_4) solution for the exposure period up-to 360 days and They declared that the compressive strength of blended cement exposed to Na_2SO_4 for 360 days was around 2% greater than that of OPC mortar. According to Tangchirapat et al., (2009) concluded that the concrete specimens incorporating 10% and 20% of pozzolanic materials had higher compressive strength than those without pozzolanic materials, even after soaking in sulphate solution for period up to 180 days, due to the pore refinement process that occurred as a result of pozzolanic reaction. Overall, it was formerly concluded that the pozzolanic reaction consumed calcium hydroxide, making the matrix denser while the product of sulphate attack, ettringite, hard to develop. However, (CBA) has less amount of calcium oxide due to that it could reduce the sulphate attack. Hence, it was experimentally found that concrete containing ground CBA gives the adequate compressive strength and found to be unaffected under Na_2SO_4 solution.

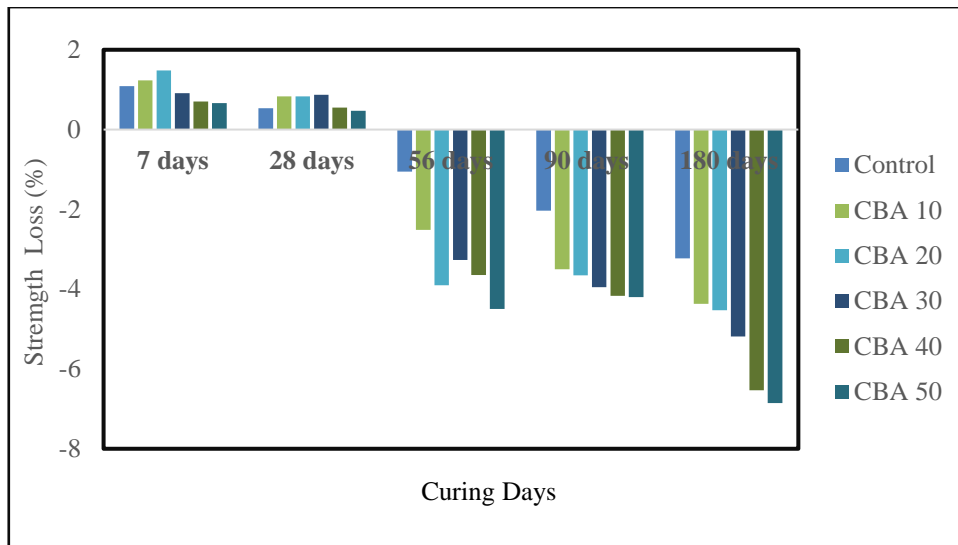


Figure 5.39 Strength deterioration of SCC containing ground CBA as cement replacement immersed in Na_2SO_4 for various curing ages

5.8 Elevated Temperature of Optimum Mechanically Treated Ground CBA Based on SCC

The behaviour of concrete structures at elevated temperatures is non-trivial in predicting the safety of structures in response to certain accidents or particular service conditions. Elevated temperatures affect concrete structure and may result in surface deterioration, spalling, loss of strength and loss of SCC mass. Thus, this section discusses the performance of SCC containing different percentages of ground CBA from 10% to 50% when tested for elevated temperature (200°C, 400°C, 600°C, and 800°C). All the specimens visually observed, tested for mass loss and compressive strength test at the age of 28 days of curing.

5.8.1 Visual Observations

Visual observation is one of the indicators in determining the resistance of SCC containing various percentages of ground CBA towards elevated temperature. Changes on the SCC samples with and without ground CBA observation after exposed to elevated temperature included discoloration, surface spalling, and crack formation presented in figure. SCC specimens underwent color changes and damage after being exposed to various elevated temperatures (200°C, 400°C, 600°C, and 800°C). These observation techniques were commonly employed by other researchers (AzariJafari et al., 2019; Mello et al., 2020; Mujedu et al., 2021; Saif et al., 2023) in investigating the effect of

pozzolanic materials as cement replacement at high temperatures on SCC samples. This is explained by considering that, the mineral admixtures can fill in cracks and pores of the concrete internal structure, as well as react with Ca(OH)_2 to form C-S-H gel. In this study, the SCC samples for control and SCC with ground CBA were exposed at 200°C, no physical changes or visible damage were observed. However, the characteristics and visual appearance were maintained up to a temperature of 200°C. When the temperature was increased to 400°C, the specimen's color was change with black smoke color for the control samples in edges and for CBA 10% and CBA 50% was in all surfaces of the samples as shown in Figures 5.40, and 5.41. Furthermore, no visible crack on all specimens were observed at 200°C and 400°C of SCC samples for control and SCC containing ground CBA samples.

When the temperature increased to 600°C, the SCC control samples observed the intensity of beige and smoke black color increased with more rough edges. Moreover, SCC containing ground CBA 10%, and CBA50% showed that cracks started to appear when the temperature reached 600°C as shown in Figure 5.42. At the temperature 800°C develop more cracks on their surfaces than other specimens exposed to 200°C, 400°C and 600°C as shown in Figure 5.43. This is due to the escape of chemically bounded water in the C-S-H leading to the failure of SCC samples at temperatures over 600°C. This explained due to the formation of the cracks attributed to the decomposition of calcium hydroxide (Ca(OH)_2) into lime (CaO) and its consequent reaction with the moisture from the surrounding air during cooling seems to cause cracks due to the volume increase related with these reactions. Furthermore, this can be explained the degradation of concrete samples when subjected to elevated temperatures is caused by the thermal mismatch resulting from the expansion of siliceous aggregate and the contraction of the concrete. The decomposition of hydrates occurs as a consequence of the decomposition of Portlandite (CH) and C-S-H (calcium-silicate-hydrate). This leads to the coarsening of the pore structure owing to the production of voids caused by the loss of bound water. Additionally, cracking develops when lime is rehydrated.

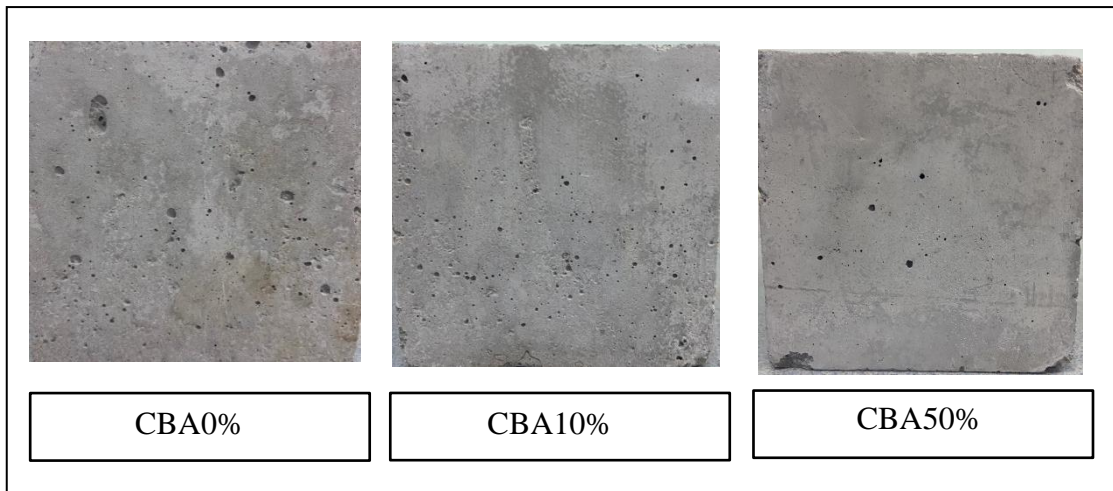


Figure 5.40 Visual observation for surface texture of the SCC specimens exposed to 200°C.

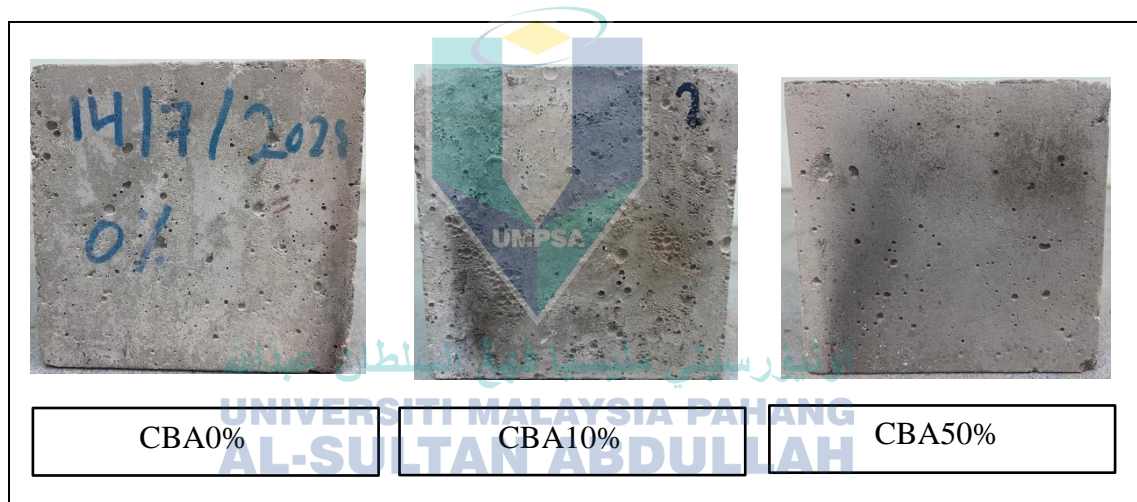


Figure 5.41 Visual observation for surface texture of the SCC specimens exposed to 400°C.

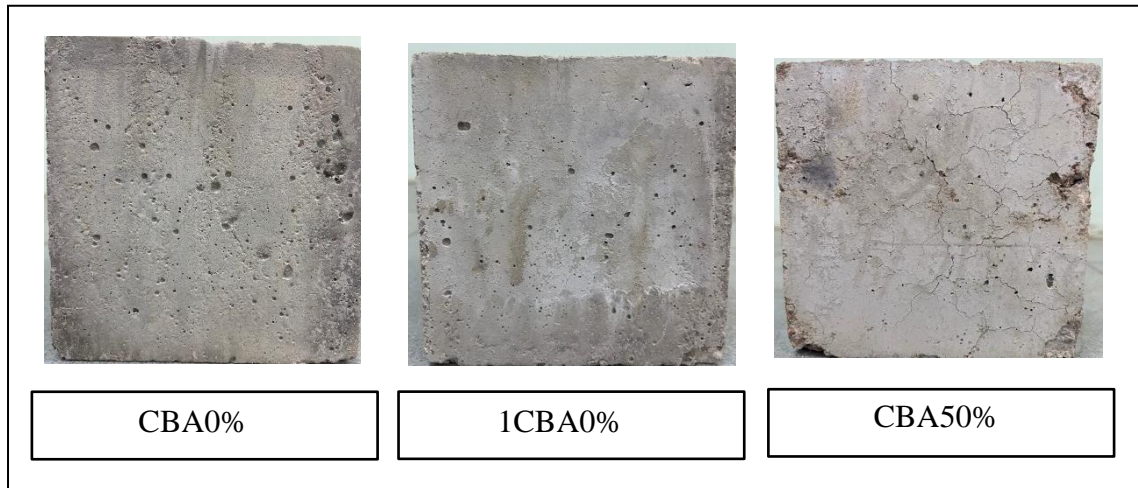


Figure 5.42 Visual observation for surface texture of the SCC specimens exposed to 600°C

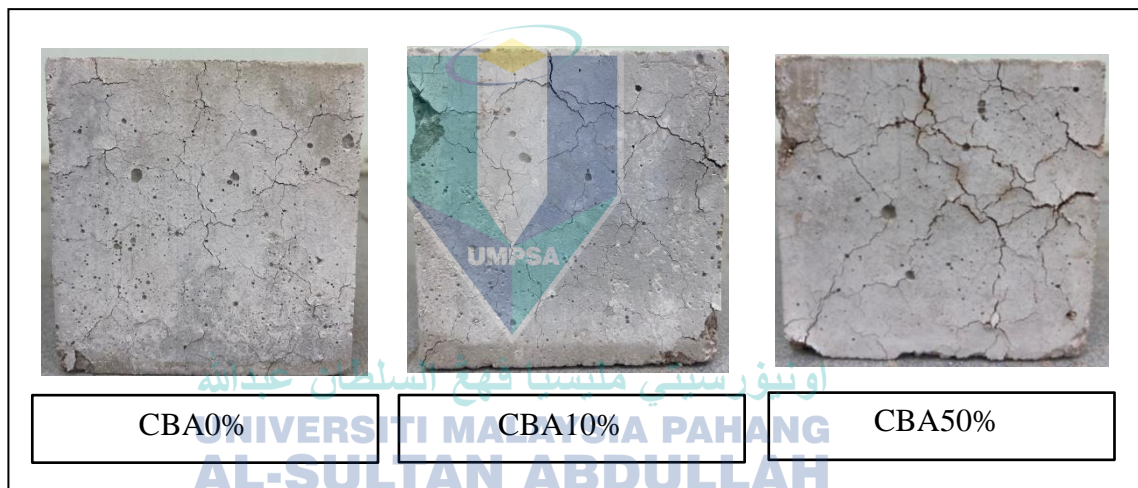


Figure 5.43 Visual observation for surface texture of the SCC specimens exposed to 800°C

5.8.2 Mass Loss

The analysis demonstrates the mass loss of SCC containing ground CBA as partial cement replacement when exposed to different elevated temperatures (i.e., 200°C, 400°C, 600°C and 800°C) for one hour after reaching specific temperature as shown in Figure 5.44. The mass loss at 200°C, 400°C, 600°C, and 800°C showed increment with increase the temperatures for all seen of SCC specimens. It is indicated that mass of the SCC specimen significantly reduced with an increase in temperature compared to mass for samples before exposure to elevated temperatures. The mass loss of the specimens was

around 6.928 to 10.533% when subjected to 200°C, 400°C, 600°C and 800°C. According to Nathe & Patil, (2022) it was observed that the influence of CBA there was significant reduction in the weight of the specimen when subjected to elevated temperature from 100°C to 800°C. Furthermore, the ranges of mass losses between 1.540% to 2.850% majorly due to moisture loss from the concrete samples.

However, on this study at 200°C showed that the highest mass losses was at CBA10% with mass loss ratio 6.99% compared to control samples with mass loss ratio 6.92% in SCC. The other replacement ratios (20%, 30%,40% and 50% of ground CBA) showed that influence in the weight loss was 5.81%, 6.90%, 6.52%, 6.21%, respectively for SCC samples when subjected to 200°C. The weight loss in the SCC samples containing ground CBA showed the weight losses close to each other due to the removal of moisture content after heating at 200°C. When temperature rose up to 400°C, it was observed that the mass loss was increased for SCC containing ground CBA and control samples without CBA. The increase in weight loss is due to the release of both capillary water and gel water from the samples when subjected to 400°C. According to Kanagaraj et al., (2023) it was reported that the mass loss due the evaporation of free and chemically bound water is responsible for weight loss up to 60 minutes when exposure to elevated temperature. When the heating continued beyond 600 °C the mass loss showed only slight increment for SCC with ground CBA and control samples. It was observed that the highest percentage of mass loss of the SCC containing CBA and control samples occurred at 800°C compared to other elevated temperatures. The levels of percentage of mass loss of mortars containing 0% and CB10%, CBA20%, CBA30%, CBA40%, CBA50% at 800°C were 9.87%,10.09%, 9.64%, 10.37%, 10.41%, 10.53% respectively. Results clearly indicated that the mass loss of SCC specimens containing CBA was higher compared to that of the control SCC.

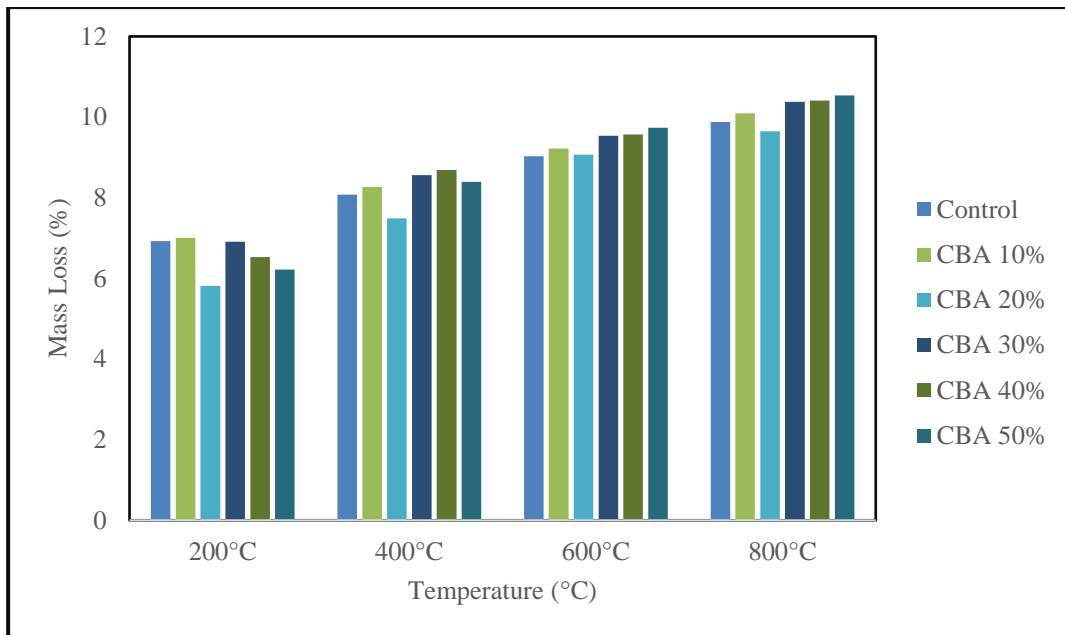


Figure 5.44 Mass loss of SCC specimens containing ground CBA and control exposed to elevated temperatures

5.8.3 Strength loss

The residual strength or strength losses values of the SCC specimens after exposure to high temperatures (i.e., 200°C, 400°C, 600°C and 800°C) as presented in Figure 5.45. The results also revealed that the strength of SCC decreased as the exposing temperature increased from 200°C to 800°C. According to Ahn et al., (2016a), one of the main effects of high temperatures on concrete structures is the reduction in compressive strength of concrete containing coal ashes. Similar to the results of the current study Yüksel et al., (2011) observed a strength deterioration was increased when temperature is increased up to 500°C. The increase in the strength losses of concrete containing CBA could be attributed to the dehydration of the (C-S-H) in hardened cement paste due to high temperature. As a conclusion, it was observed that the reduction in strength is substantial, if concrete samples is heated up to 800°C.

At temperature 200°C, the compressive strength of SCC for ground CBA decreased compared to the compressive strength of SCC for control ground CBA with various replacement before exposure to elevated temperature. The levels of percentage of Strength loss of SCC containing ground CBA as partial cement replacement CBA0%, CBA10%, CBA20%, CBA30%, CBA40%, and CBA50 at 200°C were 8.311%, 10.79%, 9.32% 13.733%, 16.611%, and 14.377%, respectively. According to Mello et al., (2020) strength losses were observed in the SCC with higher contents of additives, which is

related to the lower contents or absence of C-H in their compositions, and higher strength losses associated to $\text{Ca}(\text{OH})_2$ dissociation at temperatures at 200°C . When temperature increased up to 400°C , it was observed that the strength decreased which led to increase in the strength loss for SCC containing ground CBA with various replacement ratios CBA10% to CBA50% and SCC control samples. Rafieizonooz et al., (2017) has reported the influence of CBA as a replacement materials in concrete when exposed to elevated temperatures at 400°C . It was shown that increased in the strength loss when increase the temperatures up to 400°C , which lead to decrease the compressive strength could be attributed to the steady dehydration and decomposition of the cement paste in the concrete samples. When the heating continued beyond 600°C , it was also observed continuously increased in the strength loss for SCC containing ground CBA and control samples. Moreover, it was shown that the highest strength loss of SCC occurred at 800°C . The level of strength loss of SCC contained CBA0%, CBA10%, CBA20%, CBA30%, CBA40%, and CBA50 were 44.5%, 40.61%, 46.05%, 50.01% 62.43%, and 65.08%, respectively. Form the results clearly indicated that the strength loss of SCC specimens containing ground CBA was higher compared to that of the control SCC. This is due to the decomposition of ground CBA at high temperatures, resulting in the formation of pores and cracks in the matrix. The same researchers have also reported that the pores would help in heat dissipation and that the pores cause crack patterns.

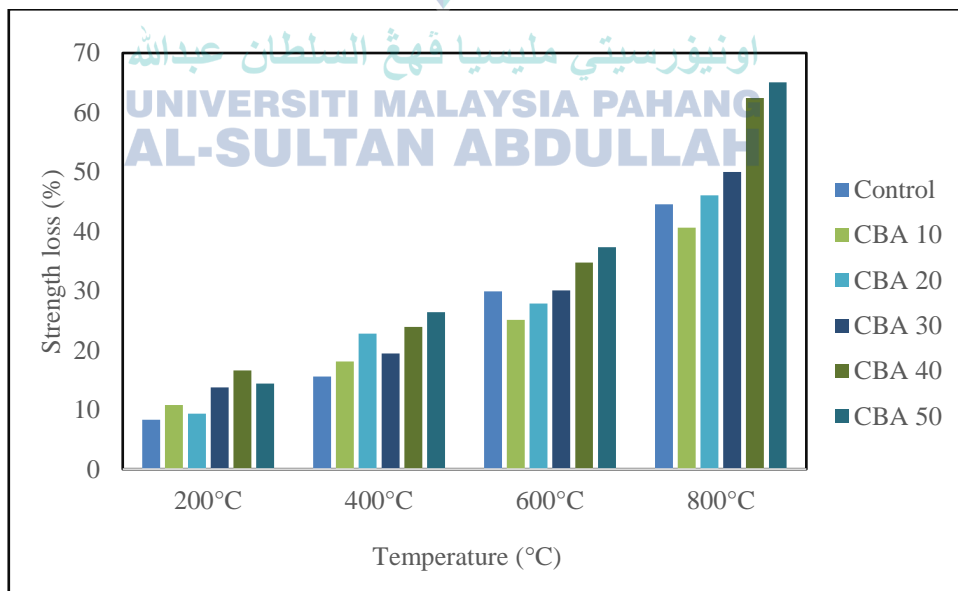


Figure 5.45 Effect of temperature towards strength loss of SCC containing ground CBA when subjected to elevated temperature

5.9 Summary of Key Findings

From the results, it can be concluded that, the utilization of ground CBA quantity as partial cement replacement in SCC showed the influence in the fresh, mechanical and durability as well as subjected to elevated temperatures. Firstly, for the fresh properties the slump flow of CBA was found to be in the range of 675 to 588 mm, which decreased with increasing proportion of CBA in the mix. The V-funnel was observed in the range of 19 to 24 seconds, which is within the range of the standard. The L-box ratio was in the range of 0.9 to 0.71. The J-Ring flow was found in the range of 650 to 570 mm. All fresh properties of SCC with ground CBA as cement replacement were in the range of EFNARC standard.

In terms of the mechanical properties, the present experimental study found evidence that up to CBA20% as cement replacement resulted the optimum strengths such as compressive, flexural, and tensile strengths as well as UPV. This was due to the ground CBA particles used in this study contributes towards the presence of silica in ground CBA particles plays a crucial role in facilitating the synthesis of (C-S-H) gel-like substance that significantly contributes to the development of strength in SCC. Moreover, the hydration process aided in the improvement of the mechanical characteristics such as the (C-S-H) gel filling in the pore structures of the SCC. On overall, the integration ground CBA 20% in SCC production able to produce hardened SCC with highest strengths value of all SSC mixes.

From an experimental study conducted which provided evidence that ground CBA as cement replacement influenced the durability properties of SCC. The utilization of optimum level of percentage of the ground CBA as cement replacement was found to have increased in the water absorption with increased the replacement levels and curing ages. This is due to high porous particles which lead to absorb more water for SCC samples. However, in terms of sulphate resistance of SCC containing ground CBA was observed to have exhibited more resistance which was indicated the loss strength and mass loss were in the acceptable ranges for durability properties. Nevertheless, in terms of acid attack of SCC containing ground CBA exhibited to higher mass loss and strength losses this due to the reaction of H_2SO_4 with calcium hydroxide, $Ca(OH)_2$, resulting in leaching of the formed salt. The second reason is due to the increased porosity of SCC

mixture samples. However, the existence of pores in SCC mixture samples allows the acidic solution H_2SO_4 to seep in easily and fasten the deterioration process.

Regarding high temperatures, it was observed that using ground CBA as a partial cement replacement in SCC samples considerably heightened both the weakening of strength and mass loss as temperatures rose from $200^{\circ}C$ to $400^{\circ}C$. Moreover, at $600^{\circ}C$, all samples underwent decay due to the increased temperature; however, SCC containing 10% ground CBA exhibited less deterioration in comparison to other samples, including the control specimens. The combination of CBA and calcium hydroxide ($Ca(OH)_2$), released during cement hydration in the presence of water, results in the formation of stable compounds such as C-S-H gel. This contributes to the improvement of long-term durability and strength.



اونيورسيتي مليسيا قهغ السلطان عبدالله
UNIVERSITI MALAYSIA PAHANG
AL-SULTAN ABDULLAH

CHAPTER 6

CONCLUSION AND RECOMMENDATIONS

6.1 Introduction

In this chapter, the conclusions of this study were drawn from the findings and discussion obtained from Chapters Four and Five based on the objectives listed in Chapter One. In this study, experimental runs were conducted to study the effect of ground CBA as cement replacement on the properties of SCC. The chemical composition and physical properties, and pozzolanic properties, and microstructural characterization of ground CBA as partial cement replacement have been examined. From the results obtained, it is clear that the used of ground CBA up to 20% as partial cement replacement to produce SCC has achieve and improved the properties. The use of CBA as cement replacement has an acceptable compressive strength of more than 35 MPa the target strength. Therefore, industrial by-products ground CBA can be used to obtain SCC with accepted engineering properties. Recommendations for future research are also given in the final chapter of this thesis.

6.2 Conclusions

Based on experimental investigation, and analysis were conducted to provide substantial justification and support the potential of ground CBA as partial cement replacement material in SCC mixture. Based on this study results and analysis, the conclusion can be drawn to conclude the finding. The conclusions of this research study are in subsection as follows:

6.2.1 Characteristics of Ground CBA in Physical and Chemical and Microstructure Properties as Pozzolanic Materials

Based on the physical properties of CBA, it was observed that the average particle sizes was decreased as the grinding cycles increases. It was also observed the specific gravity leading to increase by increased the grinding cycles of CBA from CBA-3000 to CBA-7000, while specific surface area of ground CBA with increased the grinding cycles of ground CBA led to produced smaller specific surface area compared to cement and

original CBA. The color of CBA change from gray after grinding was found to be darker in color as dark gray or blackish due to mechanical pretreatment process. In terms of chemical composition, it was observed that original CBA and ground CBA are fundamentally composed of SiO_2 , Al_2O_3 , and Fe_2O_3 which is the most important indication of the pozzolanic properties of the materials. These components are the main factors in improving the properties of SCC due to assist to be a pozzolanic materials. The mechanical pre-treatment of CBA has enhanced its microstructural characteristics, making it a viable option as an alternative cementitious material. The microstructure characteristics exhibit a compact structure with tiny particles, mostly small and angular in form. The original CBA, as well as the ground CBA models (CBA-3000, CBA-5000, CBA-7000), exhibited particles with a porous, uneven, and sharp morphology.

6.2.2 Pozzolanic Characteristics of Ground CBA in Cementitious Composite Particles as Pozzolanic Materials

Pozzolanic properties of the binder reactions in the mixture and cement paste can be enhanced by replacement of ground CBA up to 20%. Larger replacement levels rather delay the hydration reactions. This can be due to the dilution of the clinker content in the paste, to the limited pozzolanic activity of the ground CBA at early ages. Assessment of the pozzolanic activity using the Chapelle test and Frattini test indicates the enhance the pozzolanic activity with increases the grinding cycles and decreases the size of the ground CBA which leads to increase the BET specific surface area. In addition, the process of mechanically grinding CBA enhances the pozzolanic characteristics across different grinding sizes of CBA. The CBA-7000 is an optimal mechanical pretreatment method that involves grinding. This method significantly enhances the pozzolanic characteristics in terms of strength activity index, and Frattini tests. The optimal mechanical pretreatment has been effectively used in the manufacturing of SCC with various substitution ratios. The impact of a substantial increase in silica content in ground CBA-7000 is precisely validated by the findings of Chapelle analysis, strength activity index, and Frattini test. The greater utilization of $\text{Ca}(\text{OH})_2$ by silica content in ground CBA-7000 compared to other sizes of ground CBA-3000 and CBA-5000, as well as the original CBA, suggests the potential development of (C-S-H) phase during the hydration process.

6.2.3 Fresh and Mechanical Properties of Optimum Mechanically Treated Ground CBA Based on SCC

All fresh properties of SCC with ground CBA as cement replacement were in the range of EFNARC standard guidelines. In terms of the mechanical properties, the present experimental study, it was found evidence that up to CBA20% as cement replacement resulted the optimum strengths such as compressive, flexural, and tensile strengths. This was due to the ground CBA particles used in this study contributes towards the presence of silica in ground CBA particles plays a crucial role in facilitating the synthesis of (C-S-H) gel-like substance that significantly contributes to the development of strength up to CBA 20% in SCC. Moreover, the hydration process aided in the improvement of the mechanical characteristics such as the (C-S-H) gel filling in the pore structures of the SCC. On overall, the integration ground CBA 20% in SCC production able to produce hardened SCC with highest strength.

6.2.4 Durability Properties of SCC Containing Ground CBA and Subjected to Elevated Temperatures

Utilizing ground CBA as a partial substitute for cement in SCC contributes to a decrease in thermal cracking caused by excessive heat elevation up to 400°C. Satisfactory performance is displayed by SCC containing 10% ground CBA across all replacement levels when exposed to elevated temperatures. When exposed to temperatures of 600°C or higher, all samples underwent deterioration. In terms of durability of (SCC) with varying amounts of ground CBA was examined in relation to acid attack, sulfate resistance, and water absorption. For acid and sulfate attacks, durability evaluations were based on visual assessments, weight loss, and strength reduction. In the case of acid attacks, the presence of differing proportions of ground CBA in SCC demonstrated a notable impact on the specimens. Despite the decrease in mass and strength that correlated with longer immersion periods, there was minimal deterioration observed. Conversely, regarding sulfate attacks, incorporating an optimal level of up to 20% ground CBA resulted in superior resistance by reducing deterioration effects as well as mass loss and residual strength. Experimental analysis on water absorption in SCC containing ground CBA indicated higher absorption rates compared to the control group during early curing stages; however, at later curing ages showed that above CBA20%, absorption rates were lower than control. Additionally, water absorption levels for all SCC specimens with ground CBA remained within acceptable standards, below 10%.

6.3 Recommendations For Future Studies

In the investigation conducted, evidence was presented to demonstrate the positive effect of mechanical pretreatment of ground CBA as a source material and its role within the SCC framework. For future advancements, various recommendations and proposals can be taken into account. These insights will assist future researchers in achieving enhanced findings and more precise outcomes. It is suggested that further studies investigate related subject areas as outlined below:

- i. The research found that the highest performance was achieved by grinding CBA and using it as a partial substitute for cement in SCC. Therefore, it is recommended to include ultrafine and nano particles of ground CBA in order to improve its mechanical and durability characteristics.
- ii. The current research indicates that using ground CBA as a partial cement substitute results in self-compacting concrete (SCC) displaying improved strength and durability. However, further investigation into the impact of CBA on SCC's thermal properties, chloride resistance, and corrosion is necessary. This should also be applied to various structural elements, such as walls and slabs.
- iii. Additionally, the microstructure characteristics of SCC with ultrafine CBA as a cement substitute under varying curing conditions could be more comprehensively comprehended to determine the performance of SCC incorporating Ultrafine CBA.
- iv. Using ground CBA as a partial substitute for cement leads to the creation of eco-friendly (SCC). This SCC could be even more environmentally friendly if ground CBA were employed not only as a cement replacement but also to reduce the consumption of primary resources needed for SCC production.

REFERENCES

- Aali, P., Ramana, G. V., Datta, M., & Gupta, S. K. (2019). Coal combustion residue as structural fill material for reinforced soil structures. *Journal of Cleaner Production*, 232, 417–426. <https://doi.org/10.1016/j.jclepro.2019.05.354>
- Abba, S. I., Ma'aruf, A., & Nuruddeen, M. M. (2017). Sulfate Attack''A Theoretical Review Approach I. *International Journal of Advance Technology in Engineering and Science*, 3(1), 643–651.
- Abbas, S., Arshad, U., Abbass, W., Nehdi, M. L., & Ahmed, A. (2020). Recycling untreated coal bottom ash with added value for mitigating alkali–silica reaction in concrete: A sustainable approach. *Sustainability*, 12(24), 10631.
- Abdullah, M. H., Rashid, A. S. A., Anuar, U. H. M., Marto, A., & Abuelgasim, R. (2019). Bottom ash utilization: A review on engineering applications and environmental aspects. *IOP Conference Series: Materials Science and Engineering*, 527(1), 12006.
- Abdulmatin, A., Tangchirapat, W., & Jaturapitakkul, C. (2018). An investigation of bottom ash as a pozzolanic material. *Construction and Building Materials*, 186, 155–162. <https://doi.org/10.1016/j.conbuildmat.2018.07.101>
- Abed, M. A. (2019). *Green Self-compacting High-performance Concrete* (Doctoral dissertation, Budapest University of Technology and Economics (Hungary)).
- Abubakar, A. U., & Baharudin, K. S. (2012). Properties of concrete using tanjung bin power plant coal bottom ash and fly ash. *International Journal of Sustainable Construction Engineering and Technology*, 3(2), 56–69.
- Adesina, A., & Awoyera, P. (2019). Overview of trends in the application of waste materials in self-compacting concrete production. *SN Applied Sciences*, 1(9), 1–18.
- Aggarwal, P., Siddique, R., Aggarwal, Y., & Gupta, S. M. (2008). Self-compacting concrete-procedure for mix design. *Leonardo Electronic Journal of Practices and Technologies*, 7(12), 15–24.
- Aggarwal, Y., & Siddique, R. (2014). Microstructure and properties of concrete using bottom ash and waste foundry sand as partial replacement of fine aggregates. *Construction and Building Materials*, 54, 210–223. <https://doi.org/10.1016/j.conbuildmat.2013.12.051>
- Ahmad, R., Yasufuku, N., Omine, K., & Tsuji, K. (2010). Utilization of coal ash as recycling material options in view point of geoenvironment. In *Advances in Environmental Geotechnics* (pp. 715–720). Springer.
- Ahn, Y. B., Jang, J. G., & Lee, H.-K. (2016a). Mechanical properties of lightweight concrete made with coal ashes after exposure to elevated temperatures. *Cement and Concrete Composites*, 72, 27–38.
- Ahn, Y. B., Jang, J. G., & Lee, H. K. (2016b). Mechanical properties of lightweight concrete made with coal ashes after exposure to elevated temperatures. *Cement and*

- Aiken, T. A., Gu, L., Kwasny, J., Huseien, G. F., McPolin, D., & Sha, W. (2022). Acid resistance of alkali-activated binders: A review of performance, mechanisms of deterioration and testing procedures. *Construction and Building Materials*, 342, 128057.
- Akhshah, M. F. I., Azam, S. N. S. H. N., & Rahim, A. (2023). Delayed ettringite formation in the marine environment and its relationship to sulphate attack. *AIP Conference Proceedings*, 2719(1).
- Al-Amoudi, O. S. B., Ahmad, S., Maslehuddin, M., & Khan, S. M. S. (2022). Lime-activation of natural pozzolan for use as supplementary cementitious material in concrete. *Ain Shams Engineering Journal*, 13(3), 101602.
- Al-Fasih, M. Y. M., Ibrahim, M. H. W., Basirun, N. F., Jaya, R. P., & Sani, M. S. H. M. (2019). Influence of Partial Replacement of Cement and Sand with Coal Bottom Ash on Concrete Properties. *Carbon (C)*, 3, 0–10.
- Al Biajawi, M. I., Embong, R., Muthusamy, K., Ismail, N., & Obiany, I. I. (2022). Recycled coal bottom ash as sustainable materials for cement replacement in cementitious Composites: A review. *Construction and Building Materials*, 338, 127624.
- Al Biajawi, M. I., Embong, R., & Shubbar, A. (2023). Engineering properties of self-compacting concrete incorporating coal bottom ash (CBA) as sustainable materials for green concrete: a review. *Journal of Building Pathology and Rehabilitation*, 8(2), 105.
- Al Biajawi, M. I., Johari, I., Embong, R., Muthusamy, K., & Udi, U. J. (2023). Impact of concrete containing shredded latex gloves and silicone catheter on the fresh and mechanical properties at room and elevated temperatures. *AIP Conference Proceedings*, 2688(1).
- Al Biajawi, M. I. Y., & Embong, R. (2023). The Impact of Varying Ratios of Water-to-Cement Content on the Fresh and Strength Properties of Self-Compacting Concrete. *Construction Technologies and Architecture*, 4, 69–80.
- Alexander, M., Bentur, A., & Mindess, S. (2017). *Durability of concrete: design and construction* (Vol. 20). CRC Press.
- Alexandra, C., Bogdan, H., Camelia, N., & Zoltan, K. (2018). Mix design of self-compacting concrete with limestone filler versus fly ash addition. *Procedia Manufacturing*, 22, 301–308.
- Amat, R. C., Rahim, N. L., Mohamed, S. A., Ibrahim, N. M., Matagi, A. B. H., Muhamad, N., Raischi, M., & Bahatin, M. (2023). Effect of Incorporating Coal Bottom Ash on The Properties of Concrete. *IOP Conference Series: Earth and Environmental Science*, 1216(1), 12024.

- American Coal Ash Association. (2018). *production and use of coal Forecast I Market Forecast Through 2033 prepared by: american road & Transportation builders association prepared for: american coal ash association june 2015 combustion products in the u.s.* <https://www.acaa-usa.org/Portals/9/Files/PDFs/ReferenceLibrary/ARTBA-final-forecast.compressed.pdf>
- Amine, Y., Leklou, N., & Amiri, O. (2017). Effect of supplementary cementitious materials (scm) on delayed ettringite formation in heat-cured concretes. *Energy Procedia*, *139*, 565–570.
- Amran, M., Debbarma, S., & Ozbakkaloglu, T. (2021). Fly ash-based eco-friendly geopolymer concrete: A critical review of the long-term durability properties. *Construction and Building Materials*, *270*, 121857.
- Amran, M., Huang, S.-S., Onaizi, A. M., Murali, G., & Abdelgader, H. S. (2022). Fire spalling behavior of high-strength concrete: A critical review. *Construction and Building Materials*, *341*, 127902.
- Ankur, N., & Singh, N. (2021). Performance of cement mortars and concretes containing coal bottom ash: A comprehensive review. *Renewable and Sustainable Energy Reviews*, *149*, 111361. <https://doi.org/10.1016/j.rser.2021.111361>
- Aragón, P., Robayo-Salazar, R. A., & Mejía de Gutiérrez, R. (2020). Alkali-activated concrete based on natural volcanic pozzolan: Chemical resistance to sulfate attack. *Journal of Materials in Civil Engineering*, *32*(5), 4020106.
- Ardalan, R. B., Joshaghani, A., & Hooton, R. D. (2017). Workability retention and compressive strength of self-compacting concrete incorporating pumice powder and silica fume. *Construction and Building Materials*, *134*, 116–122.
- Argiz, C., Moragues, A., & Menéndez, E. (2018). Use of ground coal bottom ash as cement constituent in concretes exposed to chloride environments. *Journal of Cleaner Production*, *170*, 25–33. <https://doi.org/10.1016/j.jclepro.2017.09.117>
- Argiz, C., Sanjuán, M. Á., & Menéndez, E. (2017). Coal bottom ash for Portland cement production. *Advances in Materials Science and Engineering*, *2017*(1), 6068286.
- Arickx, S., De Borger, V., Van Gerven, T., & Vandecasteele, C. (2010). Effect of carbonation on the leaching of organic carbon and of copper from MSWI bottom ash. *Waste Management*, *30*(7), 1296–1302.
- Ashish, D. K., & Verma, S. K. (2019). An overview on mixture design of self-compacting concrete. *Structural Concrete*, *20*(1), 371–395.
- Aslani, F., & Samali, B. (2015). Constitutive relationships for self-compacting concrete at elevated temperatures. *Materials and Structures*, *48*, 337–356.
- Asokbunyarat, V., Van Hullebusch, E. D., Lens, P. N. L., & Annachhatre, A. P. (2015). Coal bottom ash as sorbing material for Fe(II), Cu(II), Mn(II), and Zn(II) removal from aqueous solutions. *Water, Air, and Soil Pollution*, *226*(5), 1–17. <https://doi.org/10.1007/s11270-015-2415-5>.

- ASTM C 597. (2016). ASTM C597-16, Standard Test Method for Pulse Velocity Through Concrete. *ASTM International, West Conshohocken, PA.*
- ASTM C1012. (2018). *Standard test method for length change of hydraulic-cement mortars exposed to a sulfate solution.* ASTM International West Conshohocken, PA.
- ASTM C127. (2012). Standard test method for density, relative density (specific gravity), and absorption of aggregate. *ASTM International West Conshohocken, PA.*
- ASTM C136-06. (2006). Standard test method for sieve analysis of fine and coarse aggregates. *ASTM International West Conshohocken, PA.*
- ASTM C136. (2012). *Annual book of ASTM standards, ASTM C136-06 standard test method for sieve analysis of fine and coarse aggregates.* ASTM International West Conshohocken, PA.
- ASTM C150/C150M. (2016). standard specification for Portland cement. In *ASTM International West Conshohocken, PA.* ASTM International West Conshohocken, Pennsylvania.
- ASTM C1621. (2014). *Standard test method for passing ability of self-consolidating concrete by J-ring.* ASTM C 1621, West Conshohocken, PA, USA.
- ASTM C1723-10. (2010). ASTM C1723 - 10 Standard Guide for Examination of Hardened Concrete Using Scanning Electron Microscopy. *ASTM International, West Conshohocken, PA.*
- ASTM C1898. (2020). Standard Test Methods for Determining the Chemical Resistance of Concrete Products to Acid Attack. *ASTM International West Conshohocken, PA,*
- ASTM C31. (2016). Standard practice for making and curing concrete test specimens in the laboratory, ASTM C-192. *American Society for Testing Materials, 8.*
- ASTM C33. (2003). Standard specification for concrete aggregates. *Philadelphia, PA: American Society for Testing and Materials.*
- ASTM C39. (2020). ASTM C39/C39M-20 Standard Test Method for Compressive Strength of cylindrical Concrete Specimens. *West Conshohocken, PA.*
- ASTM C469. (2011). C496/C496M-17, Standard test method for splitting tensile strength of cylindrical concrete specimens ASTM C-496. *West Conshohocken: ASTM International.*
- ASTM C566-19. (2019). Standard Test Method for Total Evaporable Moisture Content of Aggregate by Drying. *ASTM International West Conshohocken, PA.*
- ASTM C618. (2019). ASTM C618-19, Standard Specification for Coal Fly Ash and Raw or Calcined Natural Pozzolan for Use in Concrete. *Annual Book of ASTM Standards,*
- ASTM C642, A. (2013). Standard test method for density, absorption, and voids in hardened concrete. *ASTM, ASTM International.*

- ASTM C78. (2010). Standard test method for flexural strength of concrete (using simple beam with third-point loading). *American Society for Testing and Materials*, 100, 12959–19428.
- ASTM D388-18a. (2018). *ASTM D388 - 18a Standard Classification of Coals by Rank*. <https://www.astm.org/DATABASE.CART/HISTORICAL/D388-18A>.
- ASTM D4326-13. (2013). *ASTM D4326 - 13 Standard Test Method for Major and Minor Elements in Coal and Coke Ash By X-Ray Fluorescence*.
- ASTM E1131. (2020). Standard Test Method for Compositional Analysis by Thermogravimetry. *ASTM International West Conshohocken, PA*.
- Aswathy, P. U., & Paul, M. M. (2015). Behaviour of self compacting concrete by partial replacement of fine aggregate with coal bottom ash. *Behaviour*, 2(10).
- Aydin, E. (2016). Novel coal bottom ash waste composites for sustainable construction. *Construction and Building Materials*, 124, 582–588. <https://doi.org/10.1016/j.conbuildmat.2016.07.142>
- AzariJafari, H., Amiri, M. J. T., Ashrafiyan, A., Rasekh, H., Barforooshi, M. J., & Berenjjan, J. (2019). Ternary blended cement: An eco-friendly alternative to improve resistivity of high-performance self-consolidating concrete against elevated temperature. *Journal of Cleaner Production*, 223, 575–586.
- Babajide Olabimtan, S., & Mosaberpanah, M. A. (2023). The Implementation of a Binary Blend of Waste Glass Powder and Coal Bottom Ash as a Partial Cement Replacement toward More Sustainable Mortar Production. *Sustainability*, 15(11), 8776.
- Babalola, O. E., Awoyera, P. O., Le, D.-H., & Romero, L. M. B. (2021). A review of residual strength properties of normal and high strength concrete exposed to elevated temperatures: Impact of materials modification on behaviour of concrete composite. *Construction and Building Materials*, 296, 123448.
- Bai, J., Li, W., & Li, B. (2008). Characterization of low-temperature coal ash behaviors at high temperatures under reducing atmosphere. *Fuel*, 87(4–5), 583–591.
- Baite, E., Messan, A., Hannawi, K., Tsohnang, F., & Prince, W. (2016). Physical and transfer properties of mortar containing coal bottom ash aggregates from Tefereyre (Niger). *Construction and Building Materials*, 125, 919–926.
- Bakhtyar, B., Kacemi, T., & Nawaz, M. A. (2017). A review on carbon emissions in Malaysian cement industry. *International Journal of Energy Economics and Policy*, 7(3), 282–286.
- Balakrishnan, B., Awal, A., Abdullah, A. B., & Hossain, M. Z. (2017). Flow properties and strength behaviour of masonry mortar incorporating high volume fly ash. *International Journal of GEOMATE*, 12(31), 121–126.

- Balasubramaniam, T., & Thirugnanam, G. S. (2015). Durability studies on bottom ash concrete with manufactured sand as fine aggregate. *Journal of Industrial Pollution Control*, 31(1).
- Becerra-Duitama, J. A., & Rojas-Avellaneda, D. (2022). Pozzolans: A review. *Engineering and Applied Science Research*, 49(4), 495-504.
- Bernal, J., Reyes, E., Massana, J., León, N., & Sánchez, E. (2018). Fresh and mechanical behavior of a self-compacting concrete with additions of nano-silica, silica fume and ternary mixtures. *Construction and Building Materials*, 160, 196–210.
- Bijen, J. (2003). *Durability of engineering structures: Design, repair and maintenance*. Elsevier.
- Bouziani, T. (2013). Assessment of fresh properties and compressive strength of self-compacting concrete made with different sand types by mixture design modelling approach. *Construction and Building Materials*, 49, 308–314.
- Brake, N. A., Oruji, S., & Haselbach, L. (2018). Increasing Compressive Strength of Recycled Aggregate Concrete Using High Fineness Bottom Ash Blended Cement. *International Conference on Transportation and Development 2018: Airfield and Highway Pavements - Selected Papers from the International Conference on Transportation and Development 2018*, 401–410.
- Brunauer, S., Emmett, P. H., & Teller, E. (1938). Adsorption of gases in multimolecular layers. *Journal of the American Chemical Society*, 60(2), 309–319.
- BS EN 196-5. (2011). Methods of testing cement. Part 5: Pozzolanicity test for pozzolanic cement. *British Standards Institution*.
- Bui, V. K., Akkaya, Y., & Shah, S. P. (2002). Rheological model for self-consolidating concrete. *Materials Journal*, 99(6), 549–559.
- Burhanudin, M. K., Ibrahim, M. H. W., Jaya, R. P., & Umniati, B. S. (2023). Characterisation of Ground Coal Bottom Ash With Different Grinding Times. *International Journal of Sustainable Construction Engineering and Technology*, 14(3), 49–56.
- Burhanudin, M. K., Ibrahim, M. H. W., Sani, M., Juki, M. I., Jamaluddin, N., Jaya, R. P., Shahidan, S., Basirun, N. F., & Bosro, M. Z. M. (2018). Influence of ground coal bottom ash with different grinding time as cement replacement material on the strength of concrete. *Malaysian Construction Research Journal*, 4(2), 93–102.
- Cabrera, M., Martínez-Echevarria, M. J., López-Alonso, M., Agrela, F., & Rosales, J. (2021). Self-compacting recycled concrete using biomass bottom ash. *Materials*, 14(20), 6084.
- Caneda-Martínez, L., Kunther, W., Medina, C., de Rojas, M. I. S., & Frías, M. (2021). Exploring sulphate resistance of coal mining waste blended cements through experiments and thermodynamic modelling. *Cement and Concrete Composites*, 121, 104086.

- Canpolat, F., Yilmaz, K., Köse, M. M., Sümer, M., & Yurdusev, M. A. (2004). Use of zeolite, coal bottom ash and fly ash as replacement materials in cement production. *Cement and Concrete Research*, 34(5), 731–735. [https://doi.org/10.1016/S0008-8846\(03\)00063-2](https://doi.org/10.1016/S0008-8846(03)00063-2)
- Caviglia, C., Destefanis, E., Bernasconi, D., Pastero, L., Confalonieri, G., Corazzari, I., Turci, F., Bonadiman, C., Tassinari, R., Pavese, A., Caviglia, C., Destefanis, E., Bernasconi, D., Pastero, L., Confalonieri, G., Corazzari, I., Turci, F., Bonadiman, C., Tassinari, R., & Pavese, A. (2020). Environmental managing of bottom ashes from municipal thermovalorization waste for civil applications, as a function of particle size, based on steam washing. *EGUGA*, 17649. <https://ui.adsabs.harvard.edu/abs/2020EGUGA..2217649C/abstract>
- Cewep. (2017). *BOTTOM ASH FACT SHEET*. www.apec.org
- Chambua, S. T., Jande, Y. A. C., & Machunda, R. L. (2021). Strength and durability properties of concrete containing pumice and scoria as supplementary cementitious material. *Advances in Materials Science and Engineering*, 2021, 1–13.
- Chandru, P., Natarajan, C., & Karthikeyan, J. (2018). Influence of sustainable materials in strength and durability of self-compacting concrete: a review. *Journal of Building Pathology and Rehabilitation*, 3(1), 1–16.
- Cheah, C. B., Liew, J. J., Kevin, K. L. P., Siddique, R., & Tangchirapat, W. (2023). Influence of milling parameters on the properties of ground coal bottom ash and its blended cement. *Construction and Building Materials*, 363, 129745.
- Cheriaf, M., Rocha, J. C., & Pera, J. (1999). Pozzolanic properties of pulverized coal combustion bottom ash. *Cement and Concrete Research*, 29(9), 1387–1391.
- Chindasiriphan, P., Meenyut, B., Orasutthikul, S., Jongvivatsakul, P., & Tangchirapat, W. (2023). Influences of high-volume coal bottom ash as cement and fine aggregate replacements on strength and heat evolution of eco-friendly high-strength concrete. *Journal of Building Engineering*, 65, 105791.
- Choi, Y. W., Kim, Y. J., Shin, H. C., & Moon, H. Y. (2006). An experimental research on the fluidity and mechanical properties of high-strength lightweight self-compacting concrete. *Cement and Concrete Research*, 36(9), 1595–1602.
- Chuang, C.-W., Chen, T.-A., & Huang, R. (2023). Effect of Finely Ground Coal Bottom Ash as Replacement for Portland Cement on the Properties of Ordinary Concrete. *Applied Sciences*, 13(24), 13212.
- Cleaner Coal Ash Disposal Gets Bipartisan Support in Virginia - Circle of Blue*. (2019). U.S. Fish and Wildlife Service Southeast. <https://www.circleofblue.org/2019/world/cleaner-coal-ash-disposal-gets-bipartisan-support-in-virginia/>.

- Coal Combustion By products. (2018). *Coal Combustion Byproducts*, Kentucky Geological Survey, University of Kentucky. <https://www.uky.edu/KGS/coal/coal-for-combustionbyproducts.php>
- Cohen, M. D., & Mather, B. (1991). Sulfate attack on concrete: research needs. *Materials Journal*, 88(1), 62–69.
- Criado, M., Fernández-Jiménez, A., & Palomo, A. (2007). Alkali activation of fly ash: Effect of the SiO₂/Na₂O ratio: Part I: FTIR study. *Microporous and Mesoporous Materials*, 106(1–3), 180–191.
- Danchuwa, I. M., Abatcha, M. Z., Aliyu, Y., Yawale, M. B., Abubakar, W. H., & Abubakar, A. U. (2022). Characterization of Some Portland Limestone Cements in Nigeria Using Fourier-Transform Infrared Spectroscopy (FTIR). *Journal of Structural Monitoring and Built Environment*, 2(1), 49–58.
- Danish, P., & Ganesh, G. M. (2020). Self-compacting Concrete—Optimization of Mix Design Procedure by the Modifications of Rational Method. *International Conference on Innovative Technologies for Clean and Sustainable Development*, 369–396.
- Das, S., Lee, S.-H., Kumar, P., Kim, K.-H., Lee, S. S., & Bhattacharya, S. S. (2019). Solid waste management: Scope and the challenge of sustainability. *Journal of Cleaner Production*, 228, 658–678.
- Dayarathne, W., Galappaththi, G. S., Perera, K. E. S., & Nanayakkara, S. M. A. (2013). Evaluation of the potential for delayed ettringite formation in concrete. *National Engineering Conference, Sri Lanka*.
- De Silva, P., Sagoe-Crenstil, K., & Sirivivatnanon, V. (2007). Kinetics of geopolymerization: role of Al₂O₃ and SiO₂. *Cement and Concrete Research*, 37(4), 512–518.
- Demir, İ., Güzelkücük, S., & Sevim, Ö. (2018). Effects of sulfate on cement mortar with hybrid pozzolan substitution. *Engineering Science and Technology, an International Journal*, 21(3), 275–283.
- Deonaraine, A., Schwartz, G. E., & Ruhl, L. S. (2023). Environmental Impacts of Coal Combustion Residuals: Current Understanding and Future Perspectives. *Environmental Science & Technology*, 57(5), 1855–1869.
- Diaz Caselles, L., Hot, J., Cassagnabère, F., & Cyr, M. (2021). External sulfate attack: comparison of several alternative binders. *Materials and Structures*, 54, 1–23.
- Dinakar, P., Sethy, K. P., & Sahoo, U. C. (2013). Design of self-compacting concrete with ground granulated blast furnace slag. *Materials & Design*, 43, 161–169.
- Domone, P. (2009). *Proportioning of self-compacting concrete—the UCL method*.
- Domone, P. L. (2006). Self-compacting concrete: An analysis of 11 years of case studies. *Cement and Concrete Composites*, 28(2), 197–208.

- Domone, P. L. (2007). A review of the hardened mechanical properties of self-compacting concrete. *Cement and Concrete Composites*, 29(1), 1–12.
- Donatello, S., Tyrer, M., & Cheeseman, C. R. (2010). Comparison of test methods to assess pozzolanic activity. *Cement and Concrete Composites*, 32(2), 121–127.
- Dou, X., Ren, F., Nguyen, M. Q., Ahamed, A., Yin, K., Chan, W. P., & Chang, V. W. C. (2017). Review of MSWI bottom ash utilization from perspectives of collective characterization, treatment and existing application. In *Renewable and Sustainable Energy Reviews* (Vol. 79, pp. 24–38). Elsevier Ltd. <https://doi.org/10.1016/j.rser.2017.05.044>
- Durgun, M. Y., & Sevinç, A. H. (2022). Determination of the effectiveness of various mineral additives against sodium and magnesium sulfate attack in concrete by Taguchi method. *Journal of Building Engineering*, 57, 104849.
- Duxson, P., Provis, J. L., Lukey, G. C., Mallicoat, S. W., Kriven, W. M., & Van Deventer, J. S. J. (2005). Understanding the relationship between geopolymer composition, microstructure and mechanical properties. *Colloids and Surfaces A: Physicochemical and Engineering Aspects*, 269(1–3), 47–58.
- Edamatsu, Y., Nishida, N., & Ouchi, M. (1999). A rational mix-design method for self-compacting concrete considering interaction between coarse aggregate and mortar particles. *Self-Compacting Concrete (Stockholm, 13-14 September 1999)*, 309–320.
- EFNARC. (2005). Specification and guidelines for self-compacting concrete. *European Federation of Specialist Construction Chemicals and Concrete System*.
- EFNARC, (2002). Guidelines for self-compacting concrete. *London, UK: Association House*, 32, 34.
- Elahi, M. M. A., Shearer, C. R., Reza, A. N. R., Saha, A. K., Khan, M. N. N., Hossain, M. M., & Sarker, P. K. (2021). Improving the sulfate attack resistance of concrete by using supplementary cementitious materials (SCMs): A review. *Construction and Building Materials*, 281, 122628.
- Elemam, W. E., Abdelraheem, A. H., Mahdy, M. G., & Tahwia, A. M. (2020). Optimizing fresh properties and compressive strength of self-consolidating concrete. *Construction and Building Materials*, 249, 118781.
- Eliche-Quesada, D., Felipe-Sesé, M. A., & Fuentes-Sánchez, M. J. (2021). Biomass bottom ash waste and by-products of the acetylene industry as raw materials for unfired bricks. *Journal of Building Engineering*, 38, 102191.
- Embong, R. B. (2019). Pozzolanic and Strength Properties of Mortar Containing Chemically Pre-Treated Coal Bottom Ash. In *Doctor of Philosophy*. Faculty of Engineering Technology, Universiti Malaysia Pahang Malaysia.

- Embong, R., Kusbiantoro, A., Muthusamy, K., & Ismail, N. (2021). Recycling of coal bottom ash (CBA) as cement and aggregate replacement material: a review. *IOP Conference Series: Earth and Environmental Science*, 682(1), 12035.
- Embong, R., Kusbiantoro, A., Shafiq, N., & Nuruddin, M. F. (2016). Strength and microstructural properties of fly ash based geopolymer concrete containing high-calcium and water-absorptive aggregate. *Journal of Cleaner Production*, 112, 816–822.
- Embong, R., Shafiq, N., Kusbiantoro, A., & Nuruddin, M. F. (2016). Effectiveness of low-concentration acid and solar drying as pre-treatment features for producing pozzolanic sugarcane bagasse ash. *Journal of Cleaner Production*, 112, 953–962. <https://doi.org/10.1016/j.jclepro.2015.09.066>
- EN, BS. (2013). 1097-6. Tests for Mechanical and Physical Properties of Aggregates Part 6: Determination of Particle Density and Water Absorption. *BSI Standards Ltd.: Brussels, Belgium*.
- Esmailkhanian, B., Khayat, K. H., Yahia, A., & Feys, D. (2014). Effects of mix design parameters and rheological properties on dynamic stability of self-consolidating concrete. *Cement and Concrete Composites*, 54, 21–28.
- Faleschini, F., Toska, K., Zanini, M. A., Andreose, F., Settini, A. G., Brunelli, K., & Pellegrino, C. (2021). Assessment of a municipal solid waste incinerator bottom ash as a candidate pozzolanic material: comparison of test methods. *Sustainability*, 13(16), 8998.
- Feng, Q., Yamamichi, H., Shoya, M., & Sugita, S. (2004). Study on the pozzolanic properties of rice husk ash by hydrochloric acid pretreatment. *Cement and Concrete Research*, 34(3), 521–526. *اونيورسيتي مليسيا فهد الساس*
- Ferrara, L., Park, Y.-D., & Shah, S. P. (2007). A method for mix-design of fiber-reinforced self-compacting concrete. *Cement and Concrete Research*, 37(6), 957–971. *UNIVERSITI MALAYSIA PAHANG*
- Ferraz, E., Andrejkovicova, S., Hajjaji, W., Velosa, A. L., Silva, A. S., & Rocha, F. (2015). Pozzolanic activity of metakaolins by the French standard of the modified Chapelle test: a direct methodology. *Acta Geodynamica et Geomaterialia*, 12(3), 289–298.
- Feys, D. (2009). *Interactions between rheological properties and pumping of self-compacting concrete*. Ghent University.
- Flewitt, P. E. J., & Wild, R. K. (2017). *Physical methods for materials characterisation*. CRC Press.
- Gagatek, D., & Hooton, R. D. (2019). Assessing performance of sulfate-resistant Portland cements. *ACI Materials Journal*, 116(6), 227–233.
- Ganesan, H., Sachdeva, A., Petrounias, P., Lampropoulou, P., Sharma, P. K., & Kumar, A. (2023). Impact of Fine Slag Aggregates on the Final Durability of Coal Bottom Ash to Produce Sustainable Concrete. *Sustainability*, 15(7), 6076.

- Ghafoori, N., & Bucholc, J. (1996). Investigation of lignite-based bottom ash for structural concrete. *Journal of Materials in Civil Engineering*, 8(3), 128–137.
- Ghoddousi, P., & Saadabadi, L. A. (2017). Study on hydration products by electrical resistivity for self-compacting concrete with silica fume and metakaolin. *Construction and Building Materials*, 154, 219–228.
- Glushkov, D., Paushkina, K., Shabardin, D., Strizhak, P., & Gutareva, N. (2019). Municipal solid waste recycling by burning it as part of composite fuel with energy generation. *Journal of Environmental Management*, 231, 896–904.
- Gorme, J. B., Maniquiz, M. C., Kim, S.-S., Son, Y.-G., Kim, Y.-T., & Kim, L.-H. (2010). Characterization of Bottom Ash as an Adsorbent of Lead from Aqueous Solutions. *Environmental Engineering Research*, 15(4), 207–213.
- Guo, Z., Jiang, T., Zhang, J., Kong, X., Chen, C., & Lehman, D. E. (2020). Mechanical and durability properties of sustainable self-compacting concrete with recycled concrete aggregate and fly ash, slag and silica fume. *Construction and Building Materials*, 231, 117115.
- Hakeem, I. Y., Amin, M., Zeyad, A. M., Tayeh, B. A., Agwa, I. S., & Abu el-hassan, K. (2023). Properties and durability of self-compacting concrete incorporated with nanosilica, fly ash, and limestone powder. *Structural Concrete*, 24(5), 6738–6760.
- Hammoud, O., Blanc, D., Lupsea-Toader, M., & de Brauer, C. (2017). Influence of Chemical Pre-treatment on the Leaching Behaviour of Bottom Ash. *5th International Conference on Sustainable Solid Waste Management*.
- Hamzah, A. F. (2017). *Durability of self-compacting concrete with coal bottom ash as sand replacement—Material under aggressive environment* (Doctoral dissertation, PhD Thesis UTM).
- Hamzah, A. F., Ibrahim, M. H. W., Jamaluddin, N., Jaya, R. P., Arshad, M. F., & Abidin, N. E. Z. (2015). Fresh characteristic and mechanical compressive strength development of self-compacting concrete integrating coal bottom ash as partial fine aggregates replacement. *Int. J. of Mechanical and Mechatronics Engineering*, 15(4), 61–67.
- Hamzah, A. F., Ibrahim, M. H. W., Jamaluddin, N., Jaya, R. P., Arshad, M. F., Zainal Abidin, N. E., Manan, E. A., & Omar, N. A. (2016). Nomograph of self-compacting concrete mix design incorporating coal bottom ash as partial replacement of fine aggregates. *Journal of Engineering and Applied Sciences*, 11(7), 1671–1675.
- Hamzah, A. F., Ibrahim, M. H. W., & Manan, E. A. (2020). Carbonation and strength of self-compacting concrete with coal bottom ash exposed to seawater by wetting-drying cycle. *IOP Conference Series: Earth and Environmental Science*, 476(1), 12032.
- Hamzah, A. F., Jamaluddin, N., Mangi, S. A., & Ramadhansyah, P. J. (2020). Influence of bottom ash as a sand replacement material on durability of self-compacting concrete exposed to seawater. *Journal of Engineering Science and Technology*, 15(1), 555–571.

- Hamzah, A. F., Wan Ibrahim, M. H., Jamaluddin, N., Jaya, R. P., & Zainal Abidin, N. E. (2015). Cementitious materials usage in self-compacting concrete: A review. *Advanced Materials Research*, *1113*, 153–160.
- Hanjitsuwan, S., Phoo-ngernkham, T., & Damrongwiriyanupap, N. (2017). Comparative study using Portland cement and calcium carbide residue as a promoter in bottom ash geopolymer mortar. *Construction and Building Materials*, *133*, 128–134. <https://doi.org/10.1016/j.conbuildmat.2016.12.046>
- Hannan, N. I. R. R., Shahidan, S., Ali, N., Bunnori, N. M., Zuki, S. S. M., & Ibrahim, M. H. W. (2020). Acoustic and non-acoustic performance of coal bottom ash concrete as sound absorber for wall concrete. *Case Studies in Construction Materials*, *13*, e00399.
- Hannan, N. I. R. R., Shahidan, S., Ali, N., & Maarof, M. Z. (2017). A comprehensive review on the properties of coal bottom ash in concrete as sound absorption material. *MATEC Web of Conferences*, *103*, 1005.
- Hashemi, S. S. G., Mahmud, H. Bin, Djobo, J. N. Y., Tan, C. G., Ang, B. C., & Ranjbar, N. (2018). Microstructural characterization and mechanical properties of bottom ash mortar. *Journal of Cleaner Production*, *170*, 797–804. <https://doi.org/10.1016/j.jclepro.2017.09.191>
- Hasim, A. M., Shahid, K. A., Ariffin, N. F., Nasrudin, N. N., & Zaimi, M. N. S. (2022). Properties of high volume coal bottom ash in concrete production. *Materials Today: Proceedings*, *48*, 1861–1867.
- Heidrich, C., Feuerborn, H. J., & Weir, A. (2013, April). Coal combustion products: a global perspective. In *World of coal ash conference* (Vol. 22, p. 25)..
- Heirman, G., & Vandewalle, L. (2003). The influence of fillers on the properties of self-compacting concrete in fresh and hardened state. *Proc. of the 3rd Int. Symp. on Self-Compacting Concrete (SCC2003)*, 606–618.
- Ho, L. S., & Huynh, T.-P. (2023). Long-term mechanical properties and durability of high-strength concrete containing high-volume local fly ash as a partial cement substitution. *Results in Engineering*, *18*, 101113.
- Hodhod, O. A., & Salama, G. (2013). Developing an ANN model to simulate ASTM C1012-95 test considering different cement types and different pozzolanic additives. *HBRC Journal*, *9*(1), 1–14.
- Hopkins, D. S., & Oates, D. B. (1998). *Cementitious composition containing bottom ash as pozzolan and concretes and mortars therefrom*. Google Patents.
- Huda, B. N., Wahyuni, E. T., & Mudasir, M. (2021). Eco-friendly immobilization of dithizone on coal bottom ash for the adsorption of lead (II) ion from water. *Results in Engineering*, *10*, 100221.
- Hwang, C., & Tsai, C. (2005). The effect of aggregate packing types on engineering properties of self-consolidating concrete. *SCC*.

- Hwang, S.-D., & Khayat, K. H. (2008). Effect of mixture composition on restrained shrinkage cracking of self-consolidating concrete used in repair. *ACI Materials Journal*, 105(5), 499.
- Ibrahim, A. H., Choong, K. K., Megat Johari, M. A., Md Noor, S. I., Zainal, N. L., & Ariffin, K. S. (2015). Effects of Coal Bottom Ash on the Compressive Strength of Portland Cement Mortar. *Applied Mechanics and Materials*, 802, 149–154. <https://doi.org/10.4028/www.scientific.net/amm.802.149>
- Ibrahim, M. H. B. W., Shahidan, S., Algaifi, H. A., Hamzah, A. F. Bin, & Jaya, R. P. (2021a). CBA Self-compacting Concrete Exposed to Water Curing. In *Properties of Self-Compacting Concrete with Coal Bottom Ash Under Aggressive Environments* (pp. 9–31). Springer.
- Ibrahim, M. H. B. W., Shahidan, S., Algaifi, H. A., Hamzah, A. F. Bin, & Jaya, R. P. (2021b). *Properties of Self-Compacting Concrete with Coal Bottom Ash Under Aggressive Environments*. Springer.
- Ibrahim, M. H. W., Hamzah, A. F., Jamaluddin, N., Ramadhansyah, P. J., & Fadzil, A. M. (2015). Split Tensile Strength on Self-compacting Concrete Containing Coal Bottom Ash. *Procedia - Social and Behavioral Sciences*, 195, 2280–2289. <https://doi.org/10.1016/j.sbspro.2015.06.317>
- IEA. (2020). *Key World Energy Statistics 2020 – Analysis - IEA*. <https://www.iea.org/reports/key-world-energy-statistics-2020>
- Jamaluddin, N., Hamzah, A. F., Wan Ibrahim, M. H., Jaya, R. P., Arshad, M. F., Abidin, N. E. Z., & Dahalan, N. H. (2016). Fresh properties and flexural strength of self-compacting concrete integrating coal bottom ash. *MATEC Web of Conferences*, 47, 01010. <https://doi.org/10.1051/mateconf/20164701010>
- Jang, J. G., Kim, H. J., Kim, H. K., & Lee, H.-K. (2016). Resistance of coal bottom ash mortar against the coupled deterioration of carbonation and chloride penetration. *Materials & Design*, 93, 160–167.
- Jarusiripot, C. (2014). Removal of reactive dye by adsorption over chemical pretreatment coal based bottom ash. *Procedia Chem*, 9, 121–130.
- Jaturapitakkul, C., & Cheerarot, R. (2003). Development of bottom ash as pozzolanic material. *Journal of Materials in Civil Engineering*, 15(1), 48–53.
- Jawahar, J. G., Sashidhar, C., Reddy, I. V. R., & Peter, J. A. (2012). A simple tool for self compacting concrete mix design. *International Journal of Advances in Engineering & Technology*, 3(2), 550.
- Jiang, L., & Niu, D. (2014). Damage Evolution of Concrete Exposed to Sulfate Attack Under Drying-Wetting Cycles. *The Open Construction & Building Technology Journal*, 8(1).
- Kadir, A. A., Hassan, M. I. H., & Abdullah, M. (2016). Investigation on leaching behaviour of fly ash and bottom ash replacement in self-compacting concrete. *IOP Conference Series: Materials Science and Engineering*, 133.

- Kalaw, M. E., Culaba, A., Hinode, H., Kurniawan, W., Gallardo, S., & Promentilla, M. A. (2016). Optimizing and characterizing geopolymers from ternary blend of Philippine coal fly ash, coal bottom ash and rice hull ash. *Materials*, 9(7), 580.
- Kalaw, M. E. L., Culaba, A. B., Nguyen, H. T., Nguyen, K., Hinode, H., Kurniawan, W., Gallardo, S. M., & Promentilla, M. A. B. (2015). Mechanical and thermal properties of geopolymers from mixtures of coal ash and rice hull ash using water glass solution as activator. *ASEAN Journal of Chemical Engineering*, 15(2), 51–61.
- Kaminskas, R., Cesnauskas, V., & Barauskas, I. (2020). Influence of Biomass Fly Ash on Sulfate Attack of Cement Stone. *Journal of Materials in Civil Engineering*, 32(9), 4020246.
- Kanaan, D., Soliman, A. M., & Suleiman, A. R. (2022). Zero-cement concrete resistance to external sulfate attack: a critical review and future needs. *Sustainability*, 14(4), 2078.
- Kanagaraj, B., Anand, N., Andrushia, A. D., Kiran, T., & Lubloy, E. (2023). Pull-Out behavior and microstructure characteristics of binary blended self-compacting geopolymer concrete subjected to elevated temperature. *Alexandria Engineering Journal*, 76, 469–490.
- Kanyal, K. S., Agrawal, Y., & Gupta, T. (2021). Properties of Sustainable Concrete Containing Red Mud: A Review. *Journal of Scientific Research and Reports*, 15–26.
- Karthik, D., Nirmalkumar, K., & Priyadharshini, R. (2021). Characteristic assessment of self-compacting concrete with supplementary cementitious materials. *Construction and Building Materials*, 297, 123845.
- Kasaniya, M., Thomas, M. D. A., & Moffatt, E. G. (2021). Efficiency of natural pozzolans, ground glasses and coal bottom ashes in mitigating sulfate attack and alkali-silica reaction. *Cement and Concrete Research*, 149, 106551.
- Kasemchaisiri, R., & Tangtermsirikul, S. (2008). Properties of self-compacting concrete in incorporating bottom ash as a partial replacement of fine aggregate. *Science Asia*, 34, 87–95.
- Keerio, M. A., Saand, A., Kumar, A., Bheel, N., & Ali, K. (2021). Effect of Local Metakaolin Developed from Natural Material Soorh and Coal Bottom Ash on Fresh, Hardened Properties and Embodied Carbon of Self-Compacting Concrete. *Environmental Science and Pollution Research*, 28, 60000–60018.
- Khaleel, O. R., & Razak, H. A. (2014). Mix design method for self compacting metakaolin concrete with different properties of coarse aggregate. *Materials & Design*, 53, 691–700.
- Khan, A., Sikandar, M. A., Bashir, M. T., Shah, S. A. A., Zamin, B., & Rehman, K. (2022). Assessment for utilization of tobacco stem ash as a potential supplementary cementitious material in cement-based composites. *Journal of Building Engineering*, 53, 104531.

- Khan, A. U., Kumar, N. S., Kumar, C., Anjum, G., NU, S., & LK, A. (2023). A Micro Structural Study of Passive Confined Self-Compacting Concrete under Compression at Elevated Temperatures. *Tuijin Jishu/Journal of Propulsion Technology*, 44(4), 2166–2190.
- Khan, M. I., & Siddique, R. (2011). Utilization of silica fume in concrete: Review of durability properties. *Resources, Conservation and Recycling*, 57, 30–35.
- Khan, R. A., & Ganesh, A. (2016). The effect of coal bottom ash (CBA) on mechanical and durability characteristics of concrete. *Journal of Building Materials and Structures*, 3(1), 31–42. <https://doi.org/10.5281/zenodo.242470>
- Khan, Z., Yusup, S., Ahmad, M. M., & Rashidi, N. A. (2014). Integrated catalytic adsorption (ICA) steam gasification system for enhanced hydrogen production using palm kernel shell. *International Journal of Hydrogen Energy*, 39(7), 3286–3293.
- Khaskheli, Z. H., Buriro, A., Noor, N. B. M., Mangi, S. A., & Zuhairuddin, G. N. S. (2020). Coal bottom ash as supplementary cementitious material in concrete with and without paper pins. *J Eng Sci Technol*, 15(3), 2040–2050.
- Khayat, K. H. (1999). Workability, testing, and performance of self-consolidating concrete. *Materials Journal*, 96(3), 346–353.
- Khayat, K. H., & De Schutter, G. (2014). *Mechanical properties of self-compacting concrete* (Vol. 14). Springer.
- Khayat, K. H., Ghezal, A., & Hadriche, M. S. (1999). Factorial design model for proportioning self-consolidating concrete. *Materials and Structures*, 32, 679–686.
- Kheder, G. F., & Al Jadiri, R. S. (2010). New method for proportioning self-consolidating concrete based on compressive strength requirements. *ACI Materials Journal*, 107(5), 490.
- Khongpermgon, P., Abdulmatin, A., Tangchirapat, W., & Jaturapitakkul, C. (2019). Evaluation of compressive strength and resistance of chloride ingress of concrete using a novel binder from ground coal bottom ash and ground calcium carbide residue. *Construction and Building Materials*, 214, 631–640.
- Khongpermgon, P., Boonlao, K., Ananthanet, N., Thitithananon, T., Jaturapitakkul, C., Tangchirapat, W., & Ban, C. C. (2020). The mechanical properties and heat development behavior of high strength concrete containing high fineness coal bottom ash as a pozzolanic binder. *Construction and Building Materials*, 253.
- Kim, G. M., Jang, J. G., Khalid, H. R., & Lee, H.-K. (2017). Water purification characteristics of pervious concrete fabricated with CSA cement and bottom ash aggregates. *Construction and Building Materials*, 136, 1–8.
- Kim, G. M., Jang, J. G., Naeem, F., & Lee, H. K. (2015). Heavy Metal Leaching, CO₂ Uptake and Mechanical Characteristics of Carbonated Porous Concrete with Alkali-Activated Slag and Bottom Ash. *International Journal of Concrete Structures and Materials*, 9(3), 283–294. <https://doi.org/10.1007/s40069-015-0111-x>

- Kim, H. K., Ha, K. A., & Lee, H. K. (2016). Internal-curing efficiency of cold-bonded coal bottom ash aggregate for high-strength mortar. *Construction and Building Materials*, 126, 1–8. <https://doi.org/10.1016/j.conbuildmat.2016.08.125>
- Kim, H. K., Jang, J. G., Choi, Y. C., & Lee, H. K. (2014). Improved chloride resistance of high-strength concrete amended with coal bottom ash for internal curing. *Computers and Chemical Engineering*, 71, 334–343. <https://doi.org/10.1016/j.conbuildmat.2014.08.069>
- Kim, H. K., & Lee, H. K. (2015). Coal bottom ash in field of civil engineering: A review of advanced applications and environmental considerations. *KSCCE Journal of Civil Engineering*, 19(6), 1802–1818. <https://doi.org/10.1007/s12205-015-0282-7>
- Kim, H. K., & Lee, H. K. (2016). Autogenous shrinkage reduction with untreated coal bottom ash for high-strength concrete. *ACI Materials Journal*, 113(3), 277–285. <https://doi.org/10.14359/51688700>
- Kizgut, S., Cuhadaroglu, D., & Samanli, S. (2010). Stirred grinding of coal bottom ash to be evaluated as a cement additive. *Energy Sources, Part A: Recovery, Utilization, and Environmental Effects*, 32(16), 1529–1539.
- Kodur, V., Kumar, P., & Rafi, M. M. (2020). Fire hazard in buildings: review, assessment and strategies for improving fire safety. *PSU Research Review*, 4(1), 1–23.
- Kopp, O. C. . C. (2018). *Coal - Problems associated with the use of coal* | Britannica. <https://www.britannica.com/science/coal-fossil-fuel/Problems-associated-with-the-use-of-coal>
- Kramar, S., & Ducman, V. (2018). Evaluation of ash pozzolanic activity by means of the strength activity index test, frattini test and DTA/TG analysis. *Tehnički Vjesnik*, 25(6), 1746–1752.
- Kravchenko, J., & Lysterly, H. K. (2018). The impact of coal-powered electrical plants and coal ash impoundments on the health of residential communities. *North Carolina Medical Journal*, 79(5), 289–300.
- Kumar, P., & Singh, N. (2020). Influence of recycled concrete aggregates and Coal Bottom Ash on various properties of high volume fly ash-self compacting concrete. *Journal of Building Engineering*, 32, 101491. <https://doi.org/10.1016/j.jobbe.2020.101491>
- Kurama, H., & Kaya, M. (2008). Usage of coal combustion bottom ash in concrete mixture. *Construction and Building Materials*, 22(9), 1922–1928. <https://doi.org/10.1016/j.conbuildmat.2007.07.008>
- Kusbiantoro, A., Hanani, A., & Embong, R. (2019). Pozzolanic reactivity of coal bottom ash after chemically pre-treated with sulfuric acid. *Materials Science Forum*, 947 MSF, 212–216. <https://doi.org/10.4028/www.scientific.net/MSF.947.212>
- Latifi, N., Marto, A., Rashid, A. S. A., & Yii, J. L. J. (2015). Strength and physico-chemical characteristics of fly ash–bottom ash mixture. *Arabian Journal for Science and Engineering*, 40(9), 2447–2455.

- Lawrence, C. D. (1990). Sulphate attack on concrete. *Magazine of Concrete Research*, 42(153), 249–264.
- Lehne, J., & Preston, F. (2018). Making concrete change. *Innovation in Low-Carbon Cement and Concrete*.
- Li, J., & Wang, J. (2019). Comprehensive utilization and environmental risks of coal gangue: A review. *Journal of Cleaner Production*, 239, 117946.
- Li, J., Yin, J., Zhou, S., & Li, Y. (2005). Mix proportion calculation method of self-compacting high performance concrete. *SCC'2005-China: 1st International Symposium on Design, Performance and Use of Self-Consolidating Concrete*, 199–205.
- Li, J., Zhang, J., Ni, S., Liu, L., & Walubita, L. F. (2021). Mechanical performance and environmental impacts of self-compacting concrete with recycled demolished concrete blocks. *Journal of Cleaner Production*, 293, 126129.
- Li, P., Li, W., Sun, Z., Shen, L., & Sheng, D. (2021). Development of sustainable concrete incorporating seawater: A critical review on hydration, microstructure and mechanical strength. *Cement and Concrete Composites*, 104100.
- Limbachiya, M., Meddah, M. S., & Ouchagour, Y. (2012). Use of recycled concrete aggregate in fly-ash concrete. *Construction and Building Materials*, 27(1), 439–449.
- Lin, K. L., & Lin, D. F. (2006). Hydration characteristics of municipal solid waste incinerator bottom ash slag as a pozzolanic material for use in cement. *Cement and Concrete Composites*, 28(9), 817–823. <https://doi.org/10.1016/j.cemconcomp.2006.03.003>
- Liu, Y., Sidhu, K. S., Chen, Z., & Yang, E. H. (2018). Alkali-treated incineration bottom ash as supplementary cementitious materials. *Construction and Building Materials*, 179, 371–378. <https://doi.org/10.1016/j.conbuildmat.2018.05.231>
- Loginova, E., Volkov, D. S., Van De Wouw, P. M. F., Florea, M. V. A., & Brouwers, H. J. H. (2019). Detailed characterization of particle size fractions of municipal solid waste incineration bottom ash. *Journal of Cleaner Production*, 207, 866–874.
- Lu, B., Shi, C., Zhang, J., & Wang, J. (2018). Effects of carbonated hardened cement paste powder on hydration and microstructure of Portland cement. *Construction and Building Materials*, 186, 699–708.
- Luna, Y., Arenas, C. G., Cornejo, A., Leiva, C., Vilches, L. F., & Fernández-Pereira, C. (2014). Recycling by-products from coal-fired power stations into different construction materials. *International Journal of Energy and Environmental Engineering*, 5(4), 387–397. <https://doi.org/10.1007/s40095-014-0120-6>
- Ma, S.-H., Xu, M.-D., Qiqige, X., Wang, H., & Zhou, X. (2017). Challenges and developments in the utilization of fly ash in China. *Int J Environ Sci Develop*, 8, 781–785.

- Ma, Z., Fang, G., Liang, Z., & Jin, D. (2021). Experimental study on Mechanical Properties of green and environmental friendly self-compacting recycled concrete. *IOP Conference Series: Earth and Environmental Science*, 787(1), 12029.
- Maekawa, K., & Ozawa, K. (1999). Development of SCC's prototype. *Written in Japanese*, *Self-Compacting High-Performance Concrete*, Social System Institute, 20–32.
- Malik, M., Bhattacharyya, S. K., & Barai, S. V. (2021). Thermal and mechanical properties of concrete and its constituents at elevated temperatures: A review. *Construction and Building Materials*, 270, 121398.
- Mangi, S. A., Ibrahim, M. H. W., Jamaluddin, N., Arshad, M. F., Khahro, S. H., & Jaya, R. P. (2021). *Influence of Coal Ash on the Concrete Properties and Its Performance Under Sulphate and Chloride Conditions*.
- Mangi, S. A., Ibrahim, M. H. W., Jamaluddin, N., Arshad, M. F., Memon, F. A., Jaya, R. P., & Shahidan, S. (2018). A review on potential use of coal bottom ash as a supplementary cementing material in sustainable concrete construction. *International Journal of Integrated Engineering*, 10(9), 127–135. <https://doi.org/10.30880/ijie.2018.10.09.006>
- Mangi, S. A., Ibrahim, M. H. W., Jamaluddin, N., Arshad, M. F., Memon, S. A., Shahidan, S., & Jaya, R. P. (2019). Coal bottom ash as a sustainable supplementary cementitious material for the concrete exposed to seawater. *AIP Conference Proceedings*, 2119(July). <https://doi.org/10.1063/1.5115361>
- Mangi, S. A., Ibrahim, M. H. W., Jamaluddin, N., Arshad, M. F., & Mudjanarko, S. W. (2019). Recycling of coal ash in concrete as a partial cementitious resource. *Resources*, 8(2), 7–9. <https://doi.org/10.3390/resources8020099>
- Mangi, S. A., Ibrahim, M. H. W., Jamaluddin, N., Shahidan, S., Arshad, M. F., Memon, S. A., Jaya, R. P., Mudjanarko, S. W., & Setiawan, M. I. (2018). Influence of ground coal bottom ash on the properties of concrete. *International Journal of Sustainable Construction Engineering and Technology*, 9(2), 26–34.
- Mangi, S. A., Wan Ibrahim, M. H., Jamaluddin, N., Arshad, M. F., Memon, S. A., & Shahidan, S. (2019). Effects of grinding process on the properties of the coal bottom ash and cement paste. *Journal of Engineering and Technological Sciences*, 51(1), 1–13. <https://doi.org/10.5614/j.eng.technol.sci.2019.51.1.1>
- Mangi, S. A., Wan Ibrahim, M. H., Jamaluddin, N., Arshad, M. F., & Putra Jaya, R. (2019). Short-term effects of sulphate and chloride on the concrete containing coal bottom ash as supplementary cementitious material. *Engineering Science and Technology, an International Journal*, 22(2), 515–522. <https://doi.org/10.1016/j.jestch.2018.09.001>
- Mangi, S. A., Wan Ibrahim, M. H., Jamaluddin, N., Arshad, M. F., & Ramadhansyah, P. J. (2019). Effects of ground coal bottom ash on the properties of concrete. *Journal of Engineering Science and Technology*, 14(1), 338–350.

- Mangi, S. A., Wan Ibrahim, M. H., Jamaluddin, N., Arshad, M. F., & Shahidan, S. (2019). Performances of concrete containing coal bottom ash with different fineness as a supplementary cementitious material exposed to seawater. *Engineering Science and Technology, an International Journal*, 22(3), 929–938. <https://doi.org/10.1016/j.jestch.2019.01.011>
- Mansour, A. M., & Al Biajawi, M. I. (2022). The effect of the addition of metakaolin on the fresh and hardened properties of blended cement products: A review. *Materials Today: Proceedings*.
- Marchand, J., Odler, I., & Skalny, J. P. (2001). *Sulfate attack on concrete*. CRC Press.
- Martín-Garrido, M., Martínez-Ramírez, S., Pérez, G., & Guerrero, A. M. (2020). Study of C-S-H dehydration due to temperature increase during fires. *Journal of Raman Spectroscopy*, 51(11), 2318–2327.
- Marto, A., Kassim, K. A., Makhtar, A. M., Wei, L. F., & Lim, Y. S. (2010). Engineering characteristics of Tanjung Bin coal ash. *Electronic Journal of Geotechnical Engineering*, 15, 1117–1129.
- Massazza, F. (2003). Pozzolana and Pozzolanic Cements. In *Lea's Chemistry of Cement and Concrete* (pp. 471–635). Elsevier Ltd. <https://doi.org/10.1016/B978-075066256-7/50022-9>
- Mastali, M., & Dalvand, A. (2018). The impact resistance and mechanical properties of fiber reinforced self-compacting concrete (SCC) containing nano-SiO₂ and silica fume. *European Journal of Environmental and Civil Engineering*, 22(1), 1–27.
- Mathews, M. E., Anand, N., Kodur, V. K. R., & Arulraj, P. (2021). The bond strength of self-compacting concrete exposed to elevated temperature. *Proceedings of the Institution of Civil Engineers-Structures and Buildings*, 174(9), 804–821.
- McLennan, A. R., Bryant, G. W., Stanmore, B. R., & Wall, T. F. (2000). Ash formation mechanisms during pf combustion in reducing conditions. *Energy & Fuels*, 14(1), 150–159.
- Meena, A., Singh, N., & Singh, S. P. (2023). High-volume fly ash Self Consolidating Concrete with coal bottom ash and recycled concrete aggregates: Fresh, mechanical and microstructural properties. *Journal of Building Engineering*, 63, 105447.
- Mello, L. C. de A., dos Anjos, M. A. S., de Sá, M. V. V. A., de Souza, N. S. L., & de Farias, E. C. (2020). Effect of high temperatures on self-compacting concrete with high levels of sugarcane bagasse ash and metakaolin. *Construction and Building Materials*, 248, 118715.
- Menéndez, E., Álvaro, A. M., Hernández, M. T., & Parra, J. L. (2014). New methodology for assessing the environmental burden of cement mortars with partial replacement of coal bottom ash and fly ash. *Journal of Environmental Management*, 133, 275–283. <https://doi.org/10.1016/j.jenvman.2013.12.009>.

- Menéndez, E., Argiz, C., & Sanjuán, M. Á. (2019). Chloride induced reinforcement corrosion in mortars containing coal bottom ash and coal fly ash. *Materials*, 12(12), 1933.
- Mertens, G., Snellings, R., Van Balen, K., Bicer-Simsir, B., Verlooy, P., & Elsen, J. (2009). Pozzolanic reactions of common natural zeolites with lime and parameters affecting their reactivity. *Cement and Concrete Research*, 39(3), 233–240.
- Miraldo, S., Lopes, S., Pacheco-Torgal, F., & Lopes, A. (2021). Advantages and shortcomings of the utilization of recycled wastes as aggregates in structural concretes. *Construction and Building Materials*, 298, 123729.
- Morse, E., Turgeon, A. (2012). *Coal* | National Geographic Society. <https://www.nationalgeographic.org/encyclopedia/coal/>
- Mousa, A. (2023). Utilization of coal bottom ash from thermal power plants as a cement replacement for building: A promising sustainable practice. *Journal of Building Engineering*, 74, 106885.
- Mujedu, K. A., Ab-Kadir, M. A., Sarbini, N. N., & Ismail, M. (2021). Microstructure and compressive strength of self-compacting concrete incorporating palm oil fuel ash exposed to elevated temperatures. *Construction and Building Materials*, 274, 122025.
- Muthusamy, K., Hafizuddin Rasid, M., Nabilah Isa, N., Hanis Hamdan, N., Atikah Shafika Jamil, N., Mokhtar Albshir Budiea, A., & Wan Ahmad, S. (2021). Mechanical properties and acid resistance of oil palm shell lightweight aggregate concrete containing coal bottom ash. *Materials Today: Proceedings*, 41, 47–50. <https://doi.org/10.1016/j.matpr.2020.10.1001>
- Muthusamy, K., Rasid, M. H., Jokhio, G. A., Budiea, A. M. A., Hussin, M. W., & Mirza, J. (2020). Coal bottom ash as sand replacement in concrete: A review. *Construction and Building Materials*, 236, 117507.
- Nadeem, A., Memon, S. A., & Lo, T. Y. (2014). The performance of fly ash and metakaolin concrete at elevated temperatures. *Construction and Building Materials*, 62, 67–76.
- Nadir, H. M., & Ahmed, A. (2022). The mechanisms of sulphate attack in concrete—A review. *Modern Approaches on Material Science*, 5(2), 658–670.
- Nagamoto, N., & Ozawa, K. (1999). Mixture properties of self-compacting, high-performance concrete. *Special Publication*, 172, 623–636.
- Naganathan, S., Mohamed, A. Y. O., & Mustapha, K. N. (2015). Performance of bricks made using fly ash and bottom ash. *Construction and Building Materials*, 96, 576–580.
- Nagaratnam, B. H., Mannan, M. A., Rahman, M. E., Mirasa, A. K., Richardson, A., & Nabinejad, O. (2019). Strength and microstructural characteristics of palm oil fuel ash and fly ash as binary and ternary blends in Self-Compacting concrete. *Construction and Building Materials*, 202, 103–120.

- Nanda, B., & Rout, S. (2021). Properties of concrete containing fly ash and bottom ash mixture as fine aggregate. *International Journal of Sustainable Engineering*, 1–11.
- Nash't, I. H., A'bour, S. H., & Sadoon, A. A. (2005). Finding an unified relationship between crushing strength of concrete and non-destructive tests. *Middle East Nondestructive Testing Conference & Exhibition*, 27–30.
- Natarajan, K. S., Ashokan, M., & Vellaipandian, K. (2023). Durability performance of self-compacting concrete using binary and ternary blended pozzolanic and waste material. *Innovative Infrastructure Solutions*, 8(10), 271.
- Nathe, D. N., & Patil, Y. D. (2022). Performance of coal bottom ash concrete at elevated temperatures. *Materials Today: Proceedings*, 65, 883–888.
- Neville, A. (2012). *Properties of Concrete 5th edition (Harlow)*. Pearson Education.
- Neville, A. M. (2011). Properties of concrete fifth edition. *Green Technology an A-to-Z Guide*. SAGE Publication, California.
- NF P18-513. (2012). Addition for concrete - Metakaolin - Specifications and conformity criteria. *AFNOR-Association Française de Normalisation-Standard*. <https://www.boutique.afnor.org/standard/nf-p18-513/addition-for-concrete-metakaolin-specifications-and-conformity-criteria/article/760894/fa175740>
- Ngohpok, C., Sata, V., Satiennam, T., Klungboonkrong, P., & Chindaprasirt, P. (2018). Mechanical Properties, Thermal Conductivity, and Sound Absorption of Pervious Concrete Containing Recycled Concrete and Bottom Ash Aggregates. *KSCE Journal of Civil Engineering*, 22(4), 1369–1376. <https://doi.org/10.1007/s12205-017-0144-6>
- Okamura, H. (1997). Self-compacting high-performance concrete. *Concrete International*, 19(7), 50–54.
- Okamura, H., Maekawa, K., & Ozawa, K. (1993). High performance concrete. *Gihoudou Pub, Tokyo*, 125–128.
- Okamura, H., Maekawa, K., & Ozawa, K. (1995). Development of self-compacting high performance concrete. *Doboku Gakkai Ronbunshu*, 1995(522), 23–26.
- Okamura, H., & Ouchi, M. (2003). Self-compacting concrete. *Journal of Advanced Concrete Technology*, 1(1), 5–15.
- Oruji, S., Brake, N. A., Nalluri, L., & Guduru, R. K. (2017). Strength activity and microstructure of blended ultra-fine coal bottom ash-cement mortar. *Construction and Building Materials*, 153, 317–326.
- Ozbay, E., Oztas, A., Baykasoglu, A., & Ozbebek, H. (2009). Investigating mix proportions of high strength self compacting concrete by using Taguchi method. *Construction and Building Materials*, 23(2), 694–702.
- Page, C. L., & Page, M. M. (2007). *Durability of concrete and cement composites*. Elsevier.

- Park, J.-H., Bui, Q.-T., Jung, S.-H., & Yang, I.-H. (2021). Selected strength properties of coal bottom ash (CBA) concrete containing fly ash under different curing and drying conditions. *Materials*, *14*(18), 5381.
- Pathak, N., & Siddique, R. (2012). Properties of self-compacting-concrete containing fly ash subjected to elevated temperatures. *Construction and Building Materials*, *30*, 274–280.
- Pei, C. S. (1993). *Coal as an energy resource in Malaysia*.
- Petersson, O., Billberg, P., & Van, B. K. (2004). A model for self-compacting concrete. In *Production methods and workability of concrete* (pp. 495–504). CRC Press.
- Phutthananon, C., Tippracha, N., Jongpradist, P., Tunsakul, J., Tangchirapat, W., & Jamsawang, P. (2023). Investigation of Strength and Microstructural Characteristics of Blended Cement-Admixed Clay with Bottom Ash. *Sustainability*, *15*(4), 3795.
- Pipilikaki, P., & Beazi-Katsioti, M. (2009). The assessment of porosity and pore size distribution of limestone Portland cement pastes. *Construction and Building Materials*, *23*(5), 1966–1970. <https://doi.org/10.1016/j.conbuildmat.2008.08.028>
- Pisciotta, M., Pilorgé, H., Davids, J., & Psarras, P. (2023). Opportunities for cement decarbonization. *Cleaner Engineering and Technology*, 100667.
- Promsawat, P., Chatveera, B., Sua-iam, G., & Makul, N. (2020). Properties of self-compacting concrete prepared with ternary Portland cement-high volume fly ash-calcium carbonate blends. *Case Studies in Construction Materials*, *13*, e00426.
- Qian, Y., Yang, D., Liu, M., Guo, Z., Xiao, Z., & Ma, Z. (2023). Performance recovery of high-temperature damaged ultra-high-performance concrete under different curing environments. *Developments in the Built Environment*, 100274.
- Quarcioni, V. A., Chotoli, F. F., Coelho, A. C. V., & Cincotto, M. A. (2015). Indirect and direct Chapelle's methods for the determination of lime consumption in pozzolanic materials. *Revista IBRACON de Estruturas e Materiais*, *8*, 1–7.
- Rafieizonooz, M., Khankhaje, E., & Rezaia, S. (2022). Assessment of environmental and chemical properties of coal ashes including fly ash and bottom ash, and coal ash concrete. *Journal of Building Engineering*, 104040.
- Rafieizonooz, M., Mirza, J., Salim, M. R., Hussin, M. W., & Khankhaje, E. (2016). Investigation of coal bottom ash and fly ash in concrete as replacement for sand and cement. *Construction and Building Materials*, *116*, 15–24. <https://doi.org/10.1016/j.conbuildmat.2016.04.080>
- Rafieizonooz, M., Salim, M. R., Mirza, J., Hussin, M. W., Salmiati, Khan, R., & Khankhaje, E. (2017). Toxicity characteristics and durability of concrete containing coal ash as substitute for cement and river sand. *Construction and Building Materials*, *143*, 234–246. <https://doi.org/10.1016/j.conbuildmat.2017.03.151>
- Rahman, M. M., & Bassuoni, M. T. (2014). Thaumassite sulfate attack on concrete: Mechanisms, influential factors and mitigation. *Construction and Building*

Materials, 73, 652–662.

- Raisi, E. M., Amiri, J. V., & Davoodi, M. R. (2018). Mechanical performance of self-compacting concrete incorporating rice husk ash. *Construction and Building Materials*, 177, 148–157.
- Ramezaniapour, A. A., & Riahi Dehkordi, E. (2017). Effect of combined sulfate-chloride attack on concrete durability-A review. *AUT Journal of Civil Engineering*, 1(2), 103–110.
- Ranjbar, N., Behnia, A., Alsubari, B., Birgani, P. M., & Jumaat, M. Z. (2016). Durability and mechanical properties of self-compacting concrete incorporating palm oil fuel ash. *Journal of Cleaner Production*, 112, 723–730.
- Rantung, D., Supit, S. W. M., & Nicolaas, S. (2019). Effects of different size of fly ash as cement replacement on self-compacting concrete properties. *Journal of Sustainable Engineering: Proceedings Series*, 1(2), 180–186.
- Reddy, C. S., Mohanty, S., & Shaik, R. (2018). Physical, chemical and geotechnical characterization of fly ash, bottom ash and municipal solid waste from Telangana State in India. *International Journal of Geo-Engineering*, 9, 1–23.
- Richardson, M. G. (2002). *Fundamentals of durable reinforced concrete*. CRC Press.
- Robl, T., Oberlink, A., & Jones, R. (2017). *Coal Combustion Products (CCPs): Characteristics, Utilization and Beneficiation*. Woodhead Publishing.
- Rocca, S., van Zomeren, A., Costa, G., Dijkstra, J. J., Comans, R. N. J., & Lombardi, F. (2013). Mechanisms contributing to the thermal analysis of waste incineration bottom ash and quantification of different carbon species. *Waste Management*, 33(2), 373–381.
- Rosales, M., Rosales, J., Agrela, F., de Rojas, M. I. S., & Cabrera, M. (2022). Design of a new eco-hybrid cement for concrete pavement, made with processed mixed recycled aggregates and olive biomass bottom ash as supplementary cement materials. *Construction and Building Materials*, 358, 129417.
- Rostami, V., Shao, Y., Boyd, A. J., & He, Z. (2012). Microstructure of cement paste subject to early carbonation curing. *Cement and Concrete Research*, 42(1), 186–193.
- Ruhl, L., Vengosh, A., Dwyer, G. S., Hsu-Kim, H., Deonaraine, A., Bergin, M., & Kravchenko, J. (2009). Survey of the potential environmental and health impacts in the immediate aftermath of the coal ash spill in Kingston, Tennessee. *Environmental Science & Technology*, 43(16), 6326–6333.
- Ruhl, L., Vengosh, A., Dwyer, G. S., Hsu-Kim, H., Schwartz, G., Romanski, A., & Smith, S. D. (2012). The impact of coal combustion residue effluent on water resources: a North Carolina example. *Environmental Science & Technology*, 46(21), 12226–12233.

- Saak, A. W., Jennings, H. M., & Shah, S. P. (2001). New methodology for designing self-compacting concrete. *Materials Journal*, 98(6), 429–439.
- Sachdeva, A., & Sharma, A. (2018). Utilization of Alccofine and Bottom Ash in Cement Concrete. *International Conference on Sustainable Waste Management through Design*, 233–240.
- Sadon, S. N., Beddu, S., Naganathan, S., Kamal, N. L. M., & Hassan, H. (2017). Coal bottom ash as sustainable material in concrete—a review. *Indian Journal of Science and Technology*, 10(36), 1–10.
- Saif, M. S., Shanour, A. S., Abdelaziz, G. E., Elsayad, H. I., Shaaban, I. G., Tayeh, B. A., & Hammad, M. S. (2023). Influence of blended powders on properties of ultra-high strength fibre reinforced self compacting concrete subjected to elevated temperatures. *Case Studies in Construction Materials*, 18, e01793.
- Samimi, K., Kamali-Bernard, S., & Maghsoudi, A. A. (2018). Durability of self-compacting concrete containing pumice and zeolite against acid attack, carbonation and marine environment. *Construction and Building Materials*, 165, 247–263.
- Sandhya, B., & Reshma, E. K. (2013). A study on mechanical properties of cement concrete by partial replacement of fine aggregates with bottom ash. *International Journal of Students Research in Technology & Management*, 1(4), 416–430.
- Sani, M. S. H. M., Muftah, F., & Muda, Z. (2010). The properties of special concrete using washed bottom ash (WBA) as partial sand replacement. *International Journal of Sustainable Construction Engineering and Technology*, 1(2), 65–76.
- Sanjuán, M. Á., Quintana, B., & Argiz, C. (2019). Coal bottom ash natural radioactivity in building materials. *Journal of Radioanalytical and Nuclear Chemistry*, 319(1), 91–99.
- Saribas, İ., & Cakir, Ö. (2017). Short-term effects of sodium sulfate and sodium chloride solutions on the strength and durability properties of hardened mortars. *Avrupa Bilim ve Teknoloji Dergisi*, 6(10), 38–47.
- Saxena, A., Sulaiman, S. S., Shariq, M., & Ansari, M. A. (2023). Experimental and analytical investigation of concrete properties made with recycled coarse aggregate and bottom ash. *Innovative Infrastructure Solutions*, 8(7), 197.
- Sebaibi, N., Benzerzour, M., Sebaibi, Y., & Abriak, N.-E. (2013). Composition of self compacting concrete (SCC) using the compressible packing model, the Chinese method and the European standard. *Construction and Building Materials*, 43, 382–388.
- Sedran, T. de, De Larrard, F., Hourst, F., & Contamines, C. (2004). Mix design of self-compacting concrete (SCC). In *Production methods and workability of concrete* (pp. 451–462). CRC Press.

- Sedran, T., & De Larrard, F. (1999). Optimization of self-compacting concrete thanks to packing model. *Proceedings 1st SCC Symp, CBI Sweden, RILEM PRO7*, 321–332.
- Senhadji, Y., Escadeillas, G., Mouli, M., & Khelafi, H. (2014). Influence of natural pozzolan, silica fume and limestone fine on strength, acid resistance and microstructure of mortar. *Powder Technology*, 254, 314–323.
- Shah, S. N. R., Akashah, F. W., & Shafigh, P. (2019). Performance of high strength concrete subjected to elevated temperatures: a review. *Fire Technology*, 55, 1571–1597.
- Shariati, M., Kamyab, H., Habibi, M., Ahmadi, S., Naghipour, M., Gorjinezhad, F., Mohammadirad, S., & Aminian, A. (2023). Sulfuric acid resistance of concrete containing coal waste as a partial substitute for fine and coarse aggregates. *Fuel*, 348, 128311.
- Shetty, M. S., & Jain, A. K. (2019). *Concrete Technology (Theory and Practice)*, 8e. S. Chand Publishing.
- Shi, C., & Day, R. L. (2000). Pozzolanic reaction in the presence of chemical activators: Part I. Reaction kinetics. *Cement and Concrete Research*, 30(1), 51–58.
- Shi, C., Wu, Z., Lv, K., & Wu, L. (2015). A review on mixture design methods for self-compacting concrete. *Construction and Building Materials*, 84, 387–398.
- Shi, C., & Yang, X. (2005). Design and application of self-consolidating lightweight concretes. *1st International Symposium on Design Performance and Use of Self-Compacting Concrete-SCC*, 55–64.
- Shrestha, S. L. (2018). Characterization of Some Cement Samples of Nepal Using FTIR Spectroscopy. *International Journal of Advanced Research in Chemical Science (IJARCS)*, 5(7), 19–23.
- Siddique, R. (2013). Compressive strength, water absorption, sorptivity, abrasion resistance and permeability of self-compacting concrete containing coal bottom ash. *Construction and Building Materials*, 47, 1444–1450. <https://doi.org/10.1016/j.conbuildmat.2013.06.081>
- Siddique, R. (2014). Utilization of industrial by-products in concrete. *Procedia Engineering*, 95, 335–347. <https://doi.org/10.1016/j.proeng.2014.12.192>
- Siddique, R. (2019). *Self-compacting concrete: materials, properties and applications*. Woodhead Publishing.
- Siddique, R., Aggarwal, P., & Aggarwal, Y. (2012a). Influence of water/powder ratio on strength properties of self-compacting concrete containing coal fly ash and bottom ash. *Construction and Building Materials*, 29, 73–81.

- Siddique, R., Aggarwal, P., & Aggarwal, Y. (2012b). Mechanical and durability properties of self-compacting concrete containing fly ash and bottom ash. *Journal of Sustainable Cement-Based Materials*, 1(3), 67–82.
- Siddique, R., & Kunal. (2015). Design and development of self-compacting concrete made with coal bottom ash. *Journal of Sustainable Cement-Based Materials*, 4(3), 225–237. <https://doi.org/10.1080/21650373.2015.1004138>
- Silva, R. V., de Brito, J., Lynn, C. J., & Dhir, R. K. (2019). Environmental impacts of the use of bottom ashes from municipal solid waste incineration: A review. *Resources, Conservation and Recycling*, 140, 23–35.
- Simões, J. R., Silva, P. R. da, & Silva, R. V. (2021). Binary Mixes of Self-Compacting Concrete with Municipal Solid Waste Incinerator Bottom Ash. *Applied Sciences*, 11(14), 6396.
- SINGH, G., KUMAR, S., Mohapatra, S. K., & KUMAR, K. (2017). Comprehensive Characterization of Grounded Bottom Ash from Indian Thermal Power Plant. *Journal of Residuals Science & Technology*, 14(1).
- Singh, M. (2018). Coal bottom ash. In *Waste and Supplementary Cementitious Materials in Concrete: Characterisation, Properties and Applications* (pp. 3–50). Elsevier. <https://doi.org/10.1016/B978-0-08-102156-9.00001-8>
- Singh, M., & Siddique, R. (2014a). Compressive strength, drying shrinkage and chemical resistance of concrete incorporating coal bottom ash as partial or total replacement of sand. *Construction and Building Materials*, 68, 39–48.
- Singh, M., & Siddique, R. (2014b). Compressive strength, drying shrinkage and chemical resistance of concrete incorporating coal bottom ash as partial or total replacement of sand. *Construction and Building Materials*, 68, 39–48. <https://doi.org/10.1016/j.conbuildmat.2014.06.034>
- Singh, M., & Siddique, R. (2015). Properties of concrete containing high volumes of coal bottom ash as fine aggregate. *Journal of Cleaner Production*, 91, 269–278.
- Singh, M., & Siddique, R. (2016). Effect of coal bottom ash as partial replacement of sand on workability and strength properties of concrete. *Journal of Cleaner Production*, 112, 620–630.
- Singh, M., Siddique, R., Ait-Mokhtar, K., & Belarbi, R. (2016). Durability properties of concrete made with high volumes of low-calcium coal bottom ash as a replacement of two types of sand. *Journal of Materials in Civil Engineering*, 28(4), 4015175.
- Singh, N., Arya, S., & Raj, M. M. (2019). Assessing the Performance of Self-Compacting Concrete Made with Recycled Concrete Aggregates and Coal Bottom Ash Using Ultrasonic Pulse Velocity. In *Recycled Waste Materials* (pp. 169–178). Springer.
- Singh, N., & Bhardwaj, A. (2020). Reviewing the role of coal bottom ash as an alternative of cement. *Construction and Building Materials*, 233, 117276.

- Singh, N., Kumar, P., & Goyal, P. (2019). Reviewing the behaviour of high volume fly ash based self compacting concrete. In *Journal of Building Engineering* (Vol. 26, p. 100882). Elsevier Ltd. <https://doi.org/10.1016/j.job.2019.100882>.
- Singh, N., Mithulraj, M., & Arya, S. (2018). Influence of coal bottom ash as fine aggregates replacement on various properties of concretes: A review. *Resources, Conservation and Recycling*, *138*, 257–271.
- Singh, N., Mithulraj, M., & Arya, S. (2019). Utilization of coal bottom ash in recycled concrete aggregates based self compacting concrete blended with metakaolin. *Resources, Conservation and Recycling*, *144*, 240–251.
- Singh, S., Sharma, S. K., & Akbar, M. A. (2023). Heat resistance and sorptivity of an air-entrained concrete containing mineral admixtures and CBA. *Journal of Engineering, Design and Technology*, *21*(2), 527–551.
- Sonebi, M. (2004). Medium strength self-compacting concrete containing fly ash: Modelling using factorial experimental plans. *Cement and Concrete Research*, *34*(7), 1199–1208.
- Song, Q., Guo, M.-Z., & Ling, T.-C. (2022). A review of elevated-temperature properties of alternative binders: Supplementary cementitious materials and alkali-activated materials. *Construction and Building Materials*, *341*, 127894.
- Sousa, V., Bogas, J. A., Real, S., & Meireles, I. (2022). Industrial production of recycled cement: energy consumption and carbon dioxide emission estimation. *Environmental Science and Pollution Research*, 1–12.
- Stehlik-Barry, K., & Babinec, A. J. (2017). *Data analysis with IBM SPSS statistics*. Packt Publishing Ltd.
- Statista.(2023). Production of cement in Malaysia from 2014 to 2023. <https://www.statista.com/statistics/719188/cement-production-malaysia/>
- Stevenson, M., & Sagoe-Crentsil, K. (2005). Relationships between composition, structure and strength of inorganic polymers. *Journal of Materials Science*, *40*(8), 2023–2036.
- Su, N., Hsu, K.-C., & Chai, H.-W. (2001). A simple mix design method for self-compacting concrete. *Cement and Concrete Research*, *31*(12), 1799–1807.
- Sua-Iam, G., & Makul, N. (2015). Utilization of coal-and biomass-fired ash in the production of self-consolidating concrete: a literature review. *Journal of Cleaner Production*, *100*, 59–76.
- Talaei, A., Pier, D., Iyer, A. V, Ahiduzzaman, M., & Kumar, A. (2019). Assessment of long-term energy efficiency improvement and greenhouse gas emissions mitigation options for the cement industry. *Energy*, *170*, 1051–1066.
- Tang, S., Wang, Y., Geng, Z., Xu, X., Yu, W., & Chen, J. (2021). Structure, fractality, mechanics and durability of calcium silicate hydrates. *Fractal and Fractional*, *5*(2), 47.

- Tang, Z., Li, W., Tam, V. W. Y., & Xue, C. (2020). Advanced progress in recycling municipal and construction solid wastes for manufacturing sustainable construction materials. *Resources, Conservation & Recycling: X*, 6, 100036.
- Tangchirapat, W., Jaturapitakkul, C., & Chindaprasirt, P. (2009). Use of palm oil fuel ash as a supplementary cementitious material for producing high-strength concrete. *Construction and Building Materials*, 23(7), 2641–2646.
- Targan, Ş., Olgun, A., Erdogan, Y., & Sevinc, V. (2003). Influence of natural pozzolan, colemanite ore waste, bottom ash, and fly ash on the properties of Portland cement. *Cement and Concrete Research*, 33(8), 1175–1182. [https://doi.org/10.1016/S0008-8846\(03\)00025-5](https://doi.org/10.1016/S0008-8846(03)00025-5)
- Tawfik, T. A., Slaný, M., & Palou, M. T. (2023). Influence of heavyweight aggregate on the fresh, mechanical, durability, and microstructural properties of self-compacting concrete under elevated temperatures. *Journal of Building Engineering*, 80, 108104.
- Tayeh, B. A., AlSaffar, D. M., Askar, L. K., & Jubeh, A. I. (2019). Effect of Incorporating Pottery and Bottom Ash as Partial Replacement of Cement. *Karbala International Journal of Modern Science*, 5(4), 9.
- Tayeh, B. A., Hamada, H. M., Almeshal, I., & Bakar, B. H. A. (2022). Durability and mechanical properties of cement concrete comprising pozzolanic materials with alkali-activated binder: A comprehensive review. *Case Studies in Construction Materials*, e01429.
- Thomas, M., Jewell, R., & Jones, R. (2017). Coal fly ash as a pozzolan. In *Coal Combustion Products (CCP's)* (pp. 121–154). Elsevier.
- Tian, Z.-Y., Mbayachi, V. B., Dai, W.-K., Khalil, M., & Ayejoto, D. A. (2023). Thermal Analysis Methods. In *Advanced Diagnostics in Combustion Science* (pp. 71–109). Springer.
- Ting, M. Z. Y., & Yi, Y. (2023). Durability of cementitious materials in seawater environment: A review on chemical interactions, hardened-state properties and environmental factors. *Construction and Building Materials*, 367, 130224.
- Topçu, İ. B., Toprak, M. U., & Uygunoğlu, T. (2014). Durability and microstructure characteristics of alkali activated coal bottom ash geopolymer cement. *Journal of Cleaner Production*, 81, 211–217.
- Turcry, P., Loukili, A., & Haidar, K. (2002). Mechanical properties, plastic shrinkage, and free deformations of self-consolidating concrete. *First North American Conference on the Design and Use of Self-Consolidating Concrete*, 335–340.
- Turgut, P. (2004). Research into the correlation between concrete strength and UPV values. *NDT. Net*, 12(12), 1–9.
- Haq, E., Padmanabhan, S. K., & Licciulli, A. (2014). Synthesis and characteristics of fly ash and bottom ash based geopolymers—A comparative study. *Ceramics*

International, 40(2), 2965–2971.

- Velázquez, S., Monzó, J., Borrachero, M. V., Soriano, L., & Payá, J. (2016). Evaluation of the pozzolanic activity of spent FCC catalyst/fly ash mixtures in Portland cement pastes. *Thermochimica Acta*, 632, 29–36.
- Viet, D. B., Chan, W.-P., Phua, Z.-H., Ebrahimi, A., Abbas, A., & Lisak, G. (2020). The use of fly ashes from waste-to-energy processes as mineral CO₂ sequestrers and supplementary cementitious materials. *Journal of Hazardous Materials*, 122906.
- Vinai, R., Lawane, A., Minane, J. R., & Pantet, A. (2017). *Utilisation of coal bottom ash for the production of compressed building blocks in Sub-Saharan countries*.
- Wan Ibrahim, M. H., Shahidan, S., Amer Algaifi, H., Bin Hamzah, A. F., & Putra Jaya, R. (2021a). CBA self-compacting concrete exposed to chloride and sulphate. In *Properties of Self-Compacting Concrete with Coal Bottom Ash Under Aggressive Environments* (pp. 33–57). Springer.
- Wan Ibrahim, M. H., Shahidan, S., Amer Algaifi, H., Bin Hamzah, A. F., & Putra Jaya, R. (2021b). CBA Self-compacting Concrete Exposed to Seawater by Wetting and Drying Cycles. In *Properties of Self-Compacting Concrete with Coal Bottom Ash Under Aggressive Environments* (pp. 59–75). Springer.
- Whittaker, M., & Black, L. (2015). Current knowledge of external sulfate attack. *Advances in Cement Research*, 27(9), 532–545.
- Wongkeo, W., Thongsanitgarn, P., Pimraksa, K., & Chaipanich, A. (2012). Compressive strength, flexural strength and thermal conductivity of autoclaved concrete block made using bottom ash as cement replacement materials. *Materials and Design*, 35, 434–439. <https://doi.org/10.1016/j.matdes.2011.08.046>
- Wu, C.-R., Hong, Z.-Q., Yin, Y.-H., & Kou, S.-C. (2020). Mechanical activated waste magnetite tailing as pozzolanic material substitute for cement in the preparation of cement products. *Construction and Building Materials*, 252, 119129.
- Wu, P., Lyu, X., Wang, J., & Hu, S. (2017). Effect of mechanical grinding on the hydration activity of quartz in the presence of calcium hydroxide. *Advances in Cement Research*, 29(7), 269–277.
- Wu, Q., & An, X. (2014). Development of a mix design method for SCC based on the rheological characteristics of paste. *Construction and Building Materials*, 53, 642–651.
- Yang, I.-H., Park, J., Dinh Le, N., & Jung, S. (2020). Strength properties of high-strength concrete containing coal bottom ash as a replacement of aggregates. *Advances in Materials Science and Engineering*, 2020.
- Yankun, Z., Guangzhi, C. A. I., & Dongya, Q. (2021). Review on self compacting concrete with manufactured sand. *IOP Conference Series: Earth and Environmental Science*, 634(1), 12121.
- Yin, K., Ahamed, A., & Lisak, G. (2018). Environmental perspectives of recycling

- various combustion ashes in cement production—A review. *Waste Management*, 78, 401–416.
- Yoon, J. Y., Lee, J. Y., & Kim, J. H. (2019). Use of raw-state bottom ash for aggregates in construction materials. *Journal of Material Cycles and Waste Management*, 21(4), 838–849.
- Yüksel, İ., Siddique, R., & Özkan, Ö. (2011). Influence of high temperature on the properties of concretes made with industrial by-products as fine aggregate replacement. *Construction and Building Materials*, 25(2), 967–972.
- Zaid, O., Althoey, F., Abuhussain, M. A., & Alashker, Y. (2024). Spalling behavior and performance of ultra-high-performance concrete subjected to elevated temperature: A review. *Construction and Building Materials*, 411, 134489.
- Zainal Abidin, N. E., Wan Ibrahim, M. H., Jamaluddin, N., Kamaruddin, K., & Hamzah, A. F. (2014). The effect of bottom ash on fresh characteristic, compressive strength and water absorption of self-compacting concrete. *Applied Mechanics and Materials*, 660, 145–151.
- Zainal Abidin, N. E., Wan Ibrahim, M. H., Jamaluddin, N., Kamaruddin, K., & Hamzah, A. F. (2015). The Strength Behavior of Self-Compacting Concrete incorporating Bottom Ash as Partial Replacement to Fine Aggregate. *Applied Mechanics and Materials*, 773, 916–922.
- Zhang, S., Li, L., & Kumar, A. (2008). *Materials characterization techniques*. CRC press.
- Zhou, H., Bhattarai, R., Li, Y., Si, B., Dong, X., Wang, T., & Yao, Z. (2022). Towards sustainable coal industry: Turning coal bottom ash into wealth. *Science of The Total Environment*, 804, 149985.
- Zhou, X., & Shen, J. (2020). Micromorphology and microstructure of coal fly ash and furnace bottom slag based light-weight geopolymer. *Construction and Building Materials*, 242, 118168.
- Zhu, W., Chen, X., Struble, L. J., & Yang, E.-H. (2018). Characterization of calcium-containing phases in alkali-activated municipal solid waste incineration bottom ash binder through chemical extraction and deconvoluted Fourier transform infrared spectra. *Journal of Cleaner Production*, 192, 782–789.
- Zivica, V., & Bajza, A. (2002). Acidic attack of cement-based materials—a review Part 2. Factors of rate of acidic attack and protective measures. *Construction and Building Materials*, 16(4), 215–222.

LIST OF PUBLICATIONS

1. **Mohammad I. Al Biajawi**, Embong, R., & Shubbar, A. (2023). Engineering properties of self-compacting concrete incorporating coal bottom ash (CBA) as sustainable materials for green concrete: a review. *Journal of Building Pathology and Rehabilitation*, 8(2), 105.
2. **Mohammad I. Al Biajawi**, Embong, R., Kusbiantoro, A., Abdel-Jabbar, H., & Azmi, A. H. (2023). Impact of recycled coal bottom ash as mixing ingredient on fresh and mechanical properties of concrete: A review. *Materials Today: Proceedings*.
3. **Mohammad I. Al Biajawi**, & Embong, R. (2023). Influence of setting time and compressive strength for coal bottom ash as partial cement replacement in mortar. *Maejo International Journal of Energy and Environmental Communication*, 5(3), 1-5.
4. **Mohammad I. Al Biajawi**, Embong, R., Muthusamy, K., & Mohamad, N. (2023, May). Effect of fly ash and coal bottom ash as alternative materials in the production of self compacting concrete: A review. In *AIP Conference Proceedings* (Vol. 2688, No. 1). AIP Publishing.
5. **Mohammad I. Al Biajawi**, & Embong, R. (2023). The Impact of Varying Ratios of Water-to-Cement Content on the Fresh and Strength Properties of Self-Compacting Concrete. *Construction Technologies and Architecture*, 4, 69-80.
6. **Mohammad I. Al Biajawi**, Embong, R., Muthusamy, K., Ismail, N., & Obiany, I. I. (2022). Recycled coal bottom ash as sustainable materials for cement replacement in cementitious Composites: A review. *Construction and Building Materials*, 338, 127624.
7. **Mohammad I. Al Biajawi**, Embong, R., & Muthusamy, K. (2022). An overview of the utilization and method for improving pozzolanic performance of agricultural and industrial wastes in concrete. *Materials Today: Proceedings*, 48, 778-783.
8. **Mohammad I. Al Biajawi**, Embong, R., & Muthusamy, K. (2021). Influence of Mineral Admixtures on the Properties of Self-Compacting Concrete: An Overview. *Construction*, 1(2), 62-75.
9. **Mohammad I. Al Biajawi**, Rahimah Embong, Adli Hilmi Azmi, Norasyikin Ismail, Utilization of Coal Bottom Ash as Lightweight Aggregate in Concrete Production: A Review. *Lecture Notes in Networks and Systems*, VIII, 549, 2367-3370.
10. **Mohammad I. Al Biajawi**, Rahimah Embong, Andri Kusbiantoro, Haneen Abd Al jabbar, Influences of Various Particle Sizes of Coal Bottom Ash as Supplementary Cementitious Material on the Pozzolanic Properties. *Lecture Notes in Networks and Systems*, VIII, 549, 2367-3370.

11. **Mohammad I. Al Biajawi** , Rahimah Embong , Khairunisa Muthusamy, Haneen Abdel Jabar, Nahla Hilal, and Fadzli Mohamed Nazri On the Post-Heat Behavior of Cement Mortar Containing Mechanically Modified Ground Coal Bottom Ash. *Key Engineering Material*. Trans Tech Publications (Accepted).
12. **Mohammad I. Al Biajawi**, Embong, Coal Bottom Ash as an Eco-Friendly Cement Substitute in Self-Compacting Concrete: Properties and Potential. *Journal of Advanced Research in Applied Mechanics*. (Accepted).
13. **Mohammad I. Al Biajawi**, Embong, Mohd Mustafa Al Bakri Abdullah, Effects of Fine Particle Size on the Characteristics of Coal Bottom Ash as an Environmentally Friendly Material in Concrete Production. *Archives of Metallurgy and Materials* (Accepted).
14. Embong, R., **Mohammad I. Al Biajawi**, Bassam A. Tayeh, & Andri Kusbiantoro, Coal Bottom Ash-Based Sustainable Production: A Review on the Durability Properties of Concrete. *Innovative Infrastructure Solutions* (Under review).



اونيورسيتي مليسيا قهغ السلطان عبدالله
UNIVERSITI MALAYSIA PAHANG
AL-SULTAN ABDULLAH

AWARDS

1. Best paper award in World Sustainable Construction Conference Series 2021
2. Silver Medal CITREX 2023
3. Sijil Penghargaan Anugerah Cendekia Bitara 2022 Kategori Penerbitan Jurnal (Cendekia).



اونيورسيتي مليسيا قهغ السلطان عبدالله
UNIVERSITI MALAYSIA PAHANG
AL-SULTAN ABDULLAH



اونيورسيتي مليسيا قهغ السلطان عبدالله
UNIVERSITI MALAYSIA PAHANG
AL-SULTAN ABDULLAH

APPENDIX A: NUMBER OF SAMPLES USED IN THE EXPERIMENTAL WORK

Testing	Details of Specimens	
	CBA Percentage (%)	Number of Specimen
Compressive Strength	0, 10, 20, 30, 40, and 50	108 (18 controls, 90 with CBA)
Flexural Strength	0, 10, 20, 30, 40, and 50	108 (18controls, 90 with CBA)
Splitting Tensile Strength	0, 10, 20, 30, 40, and 50	108 (18 controls, 90 with CBA)
Acid Resistance	0, 10, 20, 30, 40, and 50	72 (12 controls, 60 with CBA)
Sulphate Resistance	0, 10, 20, 30, 40, and 50	72 (12 controls, 60 with CBA)
Water absorption	0, 10, 20, 30, 40, and 50	108 (18 controls, 90 with CBA)
Elevated Temperature	0, 10, 20, 30, 40, and 50	72 (12 controls, 60 with CBA)

UMPSA

اونيورسيتي مليسيا قهغ السلطان عبدالله
UNIVERSITI MALAYSIA PAHANG
AL-SULTAN ABDULLAH

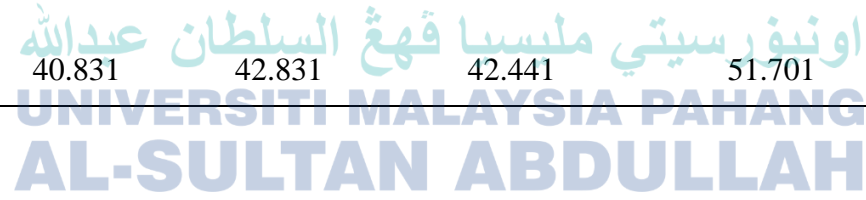
APPENDIX B: STRENGTH ACTIVITY INDEX FOR VARIOUS SIZES OF GROUND CBA

Strength activity index (SAI) of CBA-3000 as cement replacement at 7, 14, 28, 56, 90, and 180 days.

Mix No	Cement Replacement (%)	Strength Activity Index (%)					
		7 days	14 days	28 days	56 days	90 days	180 days
Control	0	100	100	100	100	100	100.
CBA10-3000	10	103.516	110.163	109.1423	107.654	109.963	111.641
CBA20-3000	20	74.395	78.023	76.881	87.152	96.834	101.921
CBA30-3000	30	63.071	66.156	65.88	73.328	81.589	83.416
CBA40-3000	40	55.244	56.269	55.758	64.536	73.669	77.918
CBA50-30000	50	40.217	42.181	41.797	49.578	56.879	64.8127

Strength activity index (SAI) of CBA-5000 as cement replacement at 7, 14, 28, 56, 90, and 180 days.

Mix No	Cement Replacement (%)	Strength Activity Index (%)					
		7 days	14 days	28 days	56 days	90 days	180 days
Control	0	100	100	100	100	100	100
CBA10-5000	10	113.373	118.918	117.392	117.572	118.633	114.008
CBA20-5000	20	104.535	109.647	108.643	107.211	111.225	110.051
CBA30-5000	30	80.799	84.749	83.979	85.651	92.687	92.257
CBA40-5000	40	72.404	75.948	75.236	79.7691	83.539	84.025
CBA50-50000	50	40.831	42.831	42.441	51.701	59.151	69.317

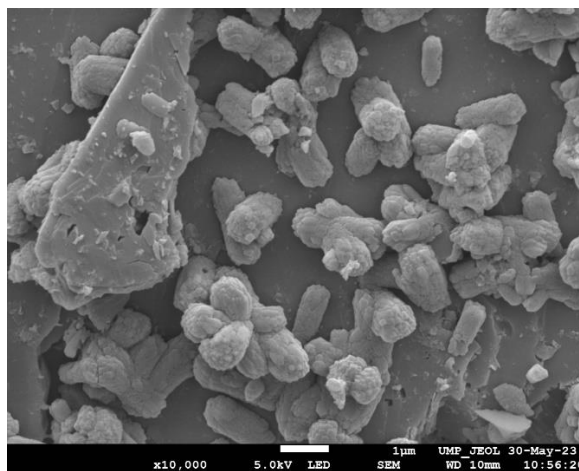
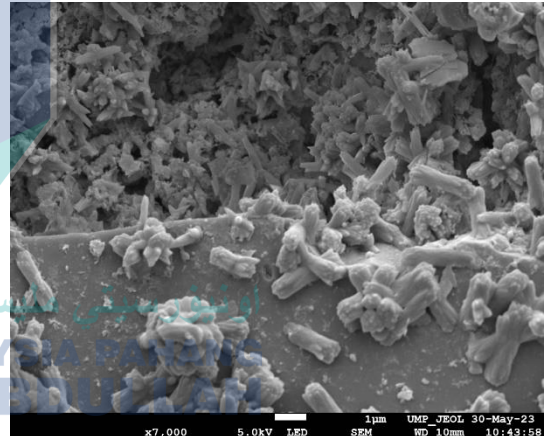
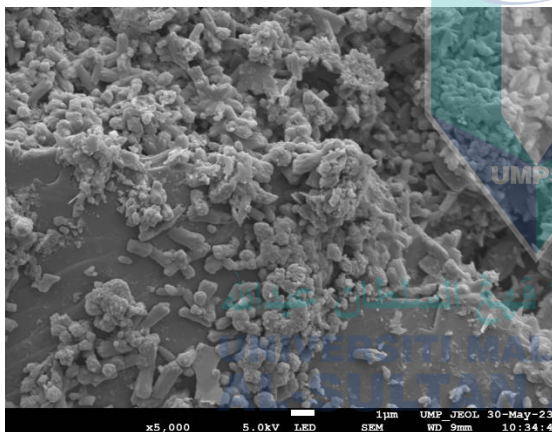
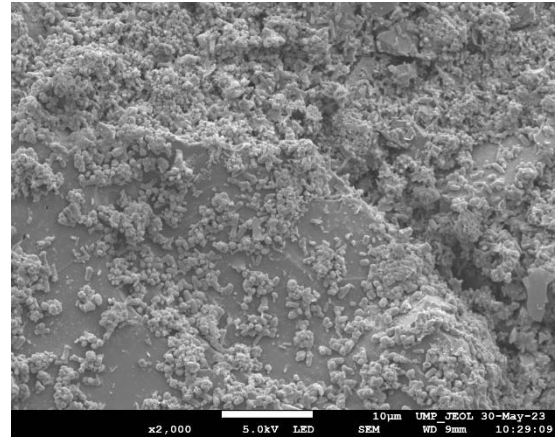
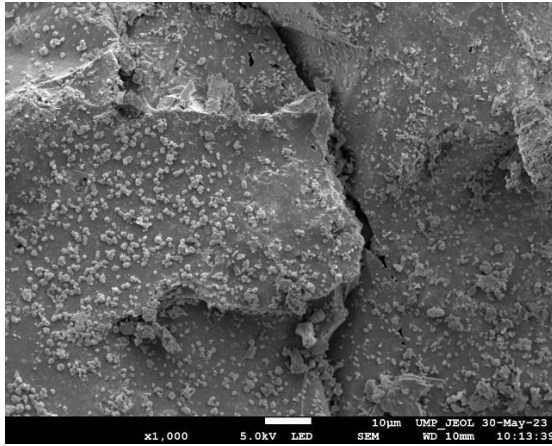


Strength activity index (SAI) of CBA-7000 as cement replacement at 7, 14, 28, 56, 90, and 180 days

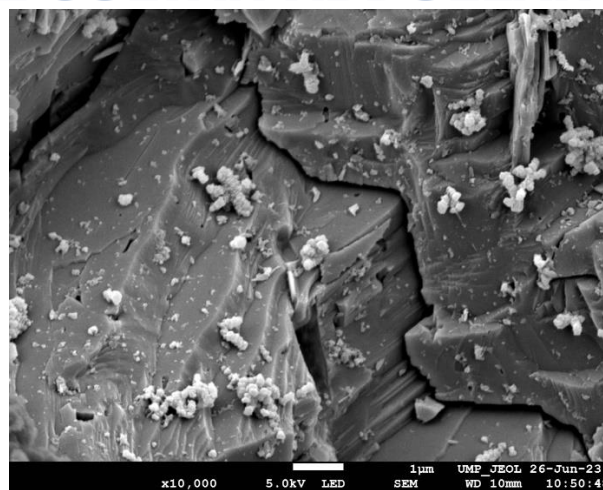
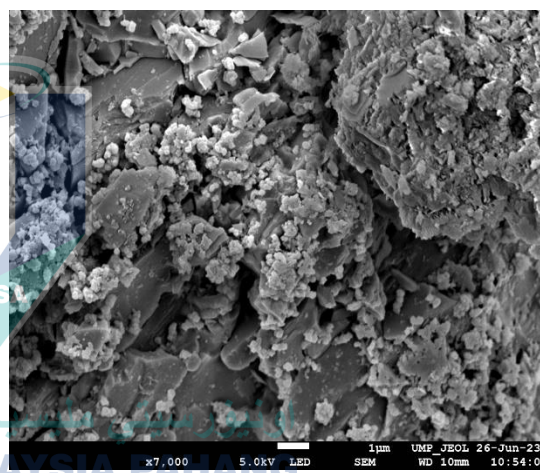
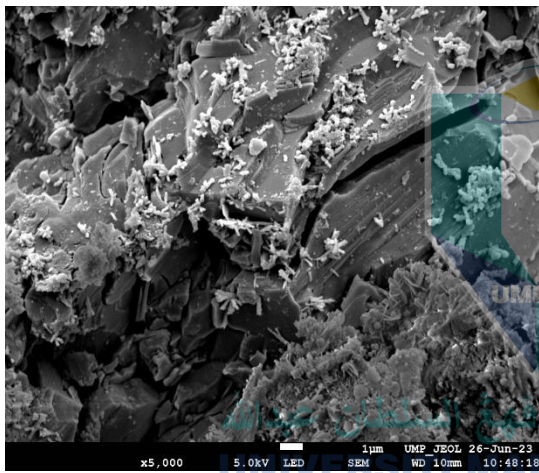
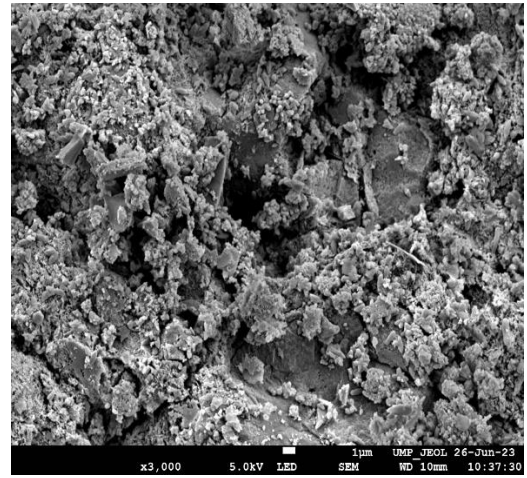
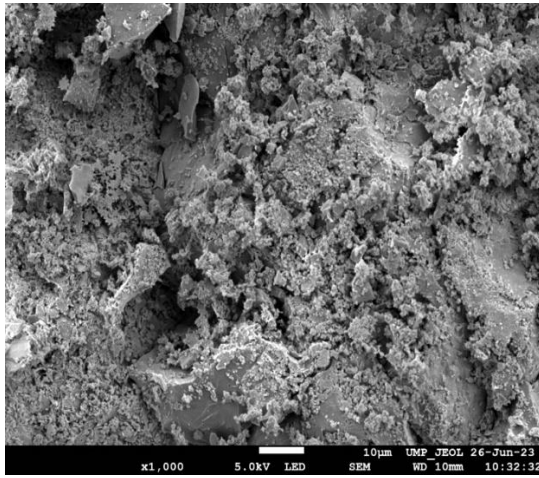
Mix No	Cement Replacement (%)	Strength Activity Index (%)					
		7 days	14 days	28 days	56 days	90 days	180 days
Control	0	100	100	100	100	100	100
CBA10-7000	10	99.37	104.253	105.341	108.025	109.221	106.347
CBA20-7000	20	88.577	93.266	92.378	104.425	114.463	111.753
CBA30-7000	30	69.351	72.744	72.071	85.112	91.011	88.355
CBA40-7000	40	58.206	59.574	60.502	74.881	77.91	81.693
CBA50-7000	50	32.658	34.254	34.236	47.581	59.462	70.219

APPENDIX C: MICROSTRUCTURE IMAGES FOR SCC CONTROL AND SCC WITH VARIOUS RATIOS OF GROUND CBA

MICROSTRUCTURAL IMAGES OF CONTROL 7 DAYS

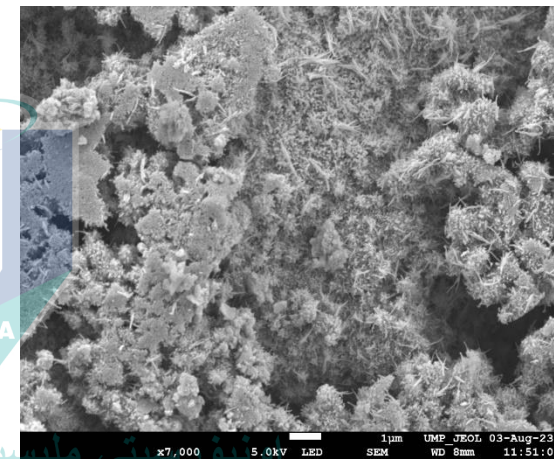
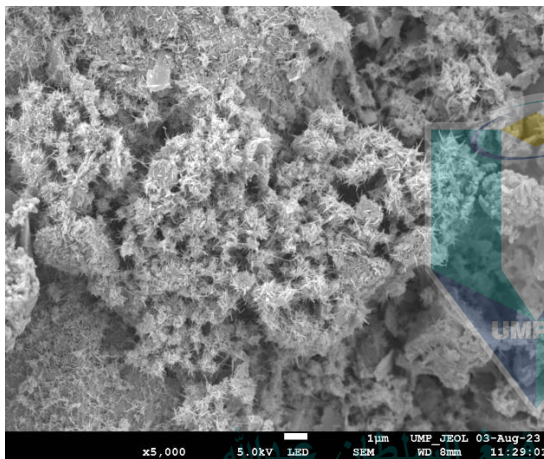
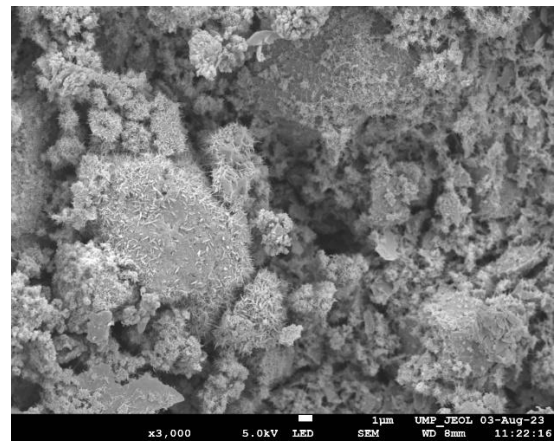
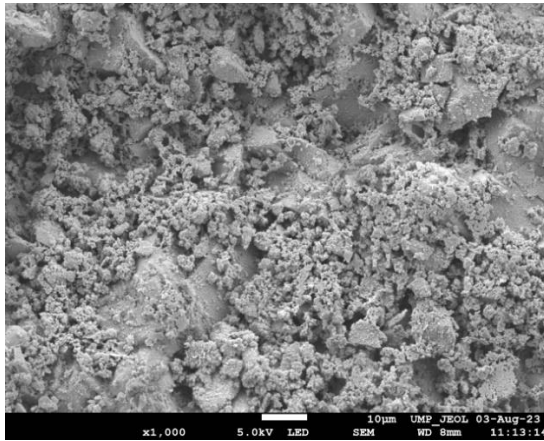


MICROSTRUCTURAL IMAGES OF CONTROL 28 DAYS

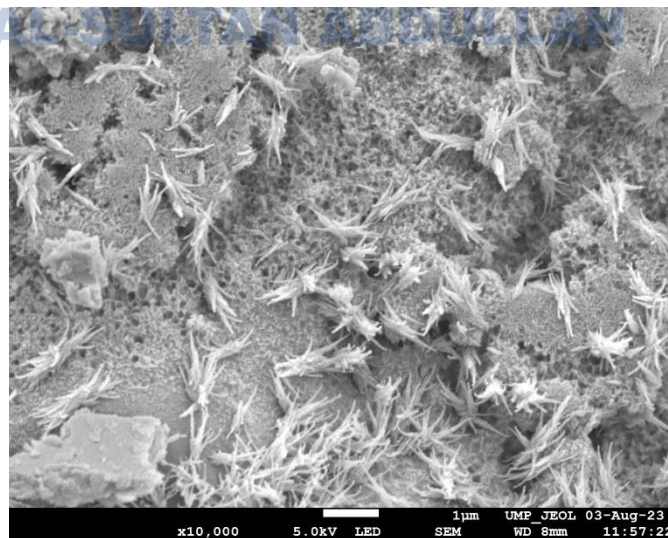


UNIVERSITI MALAYSIA PAHANG
AL-SULTAN ABDULLAH

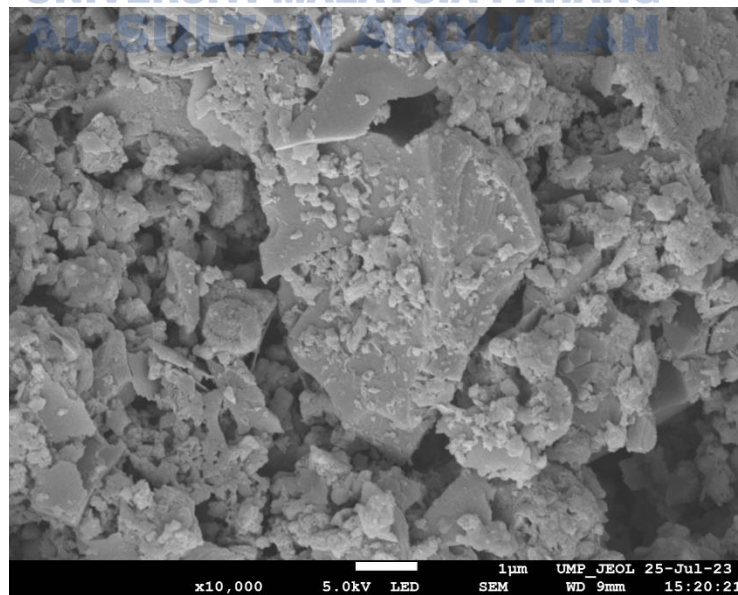
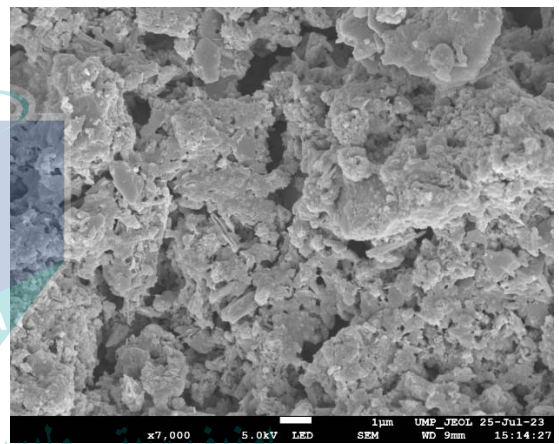
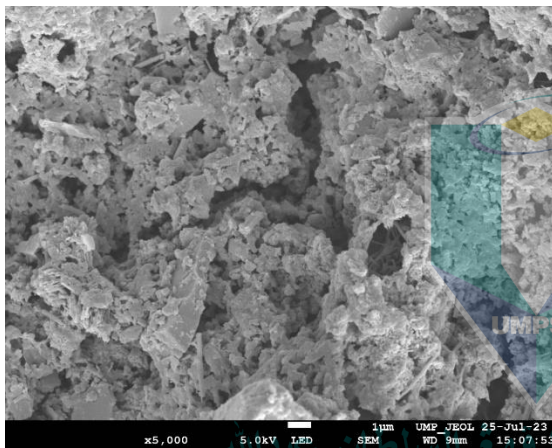
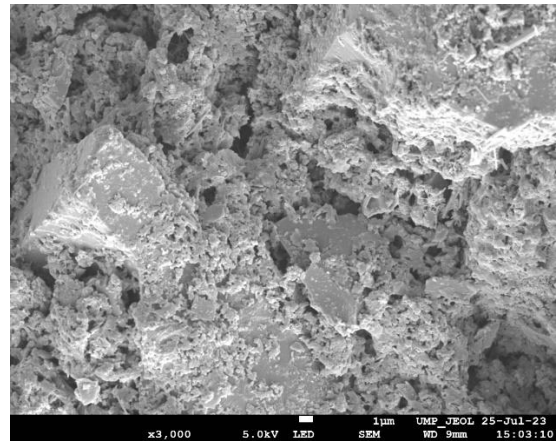
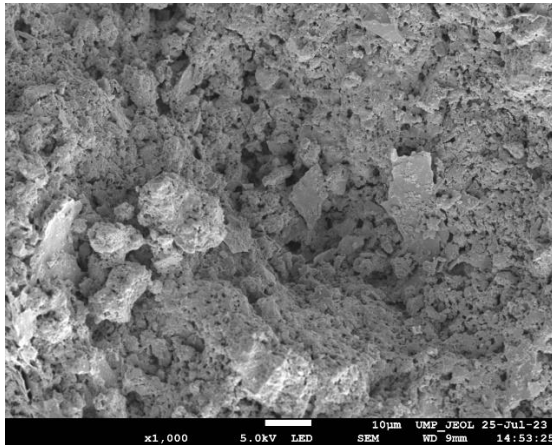
MICROSTRUCTURAL IMAGES OF CONTROL 56 DAYS



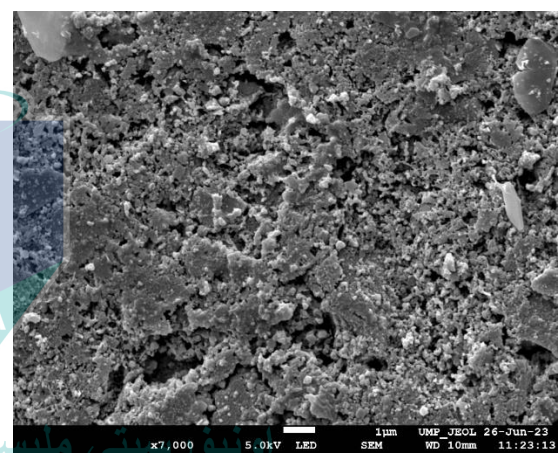
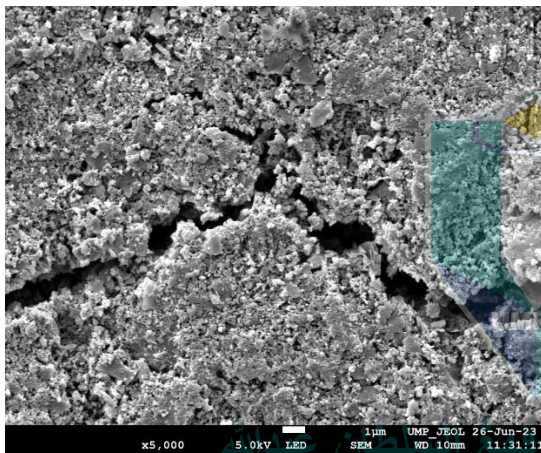
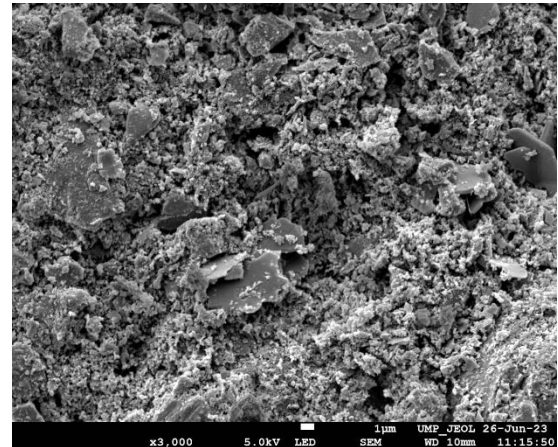
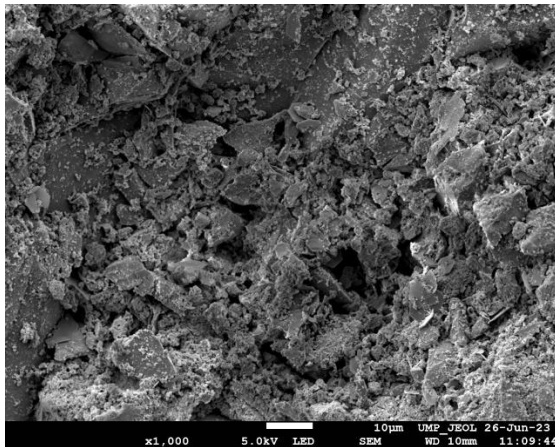
UNIVERSITI MALAYSIA PAHANG
ABDULLAH



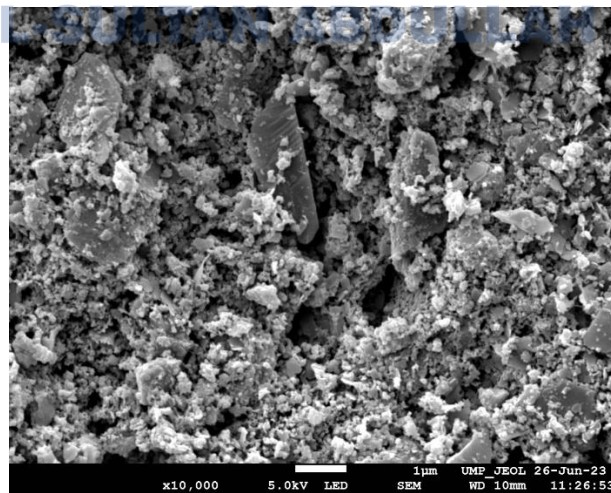
MICROSTRUCTURAL IMAGES OF GROUND CBA10% 7 DAYS



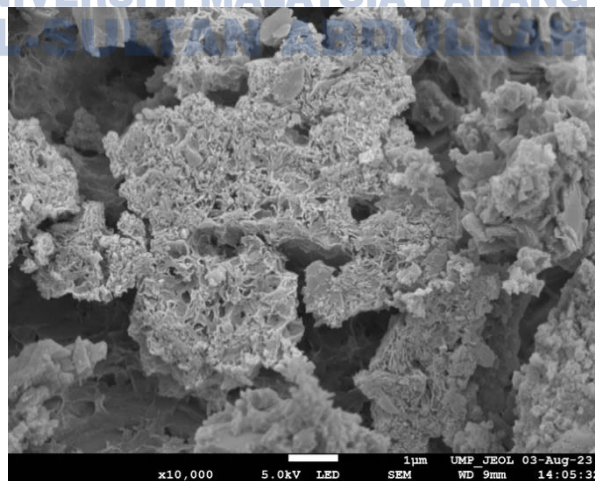
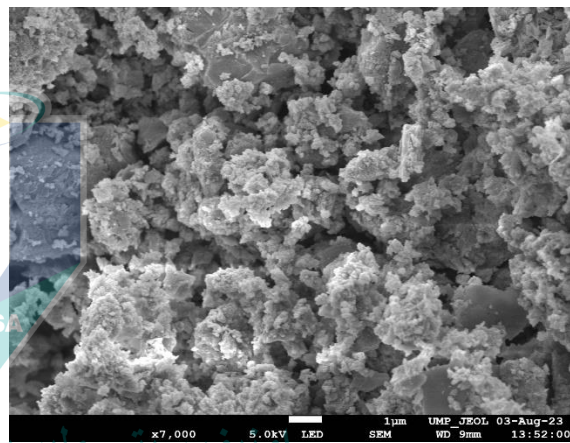
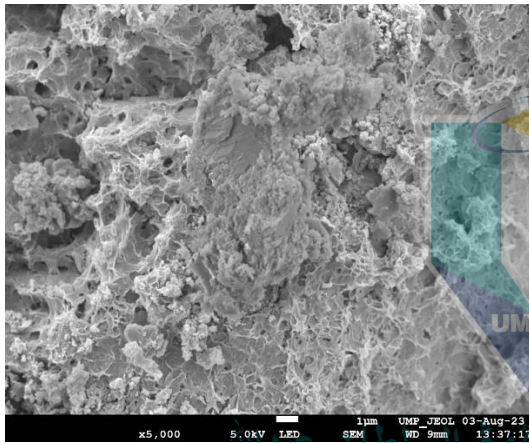
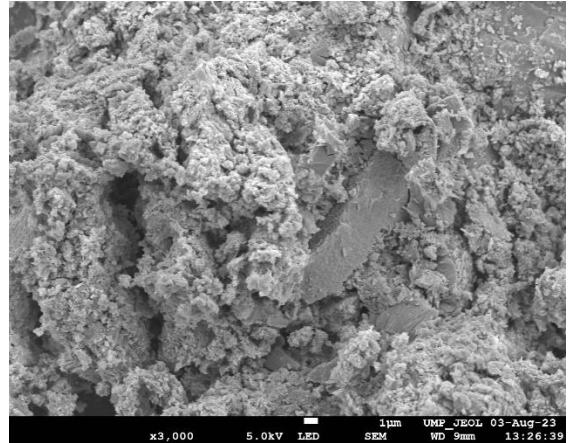
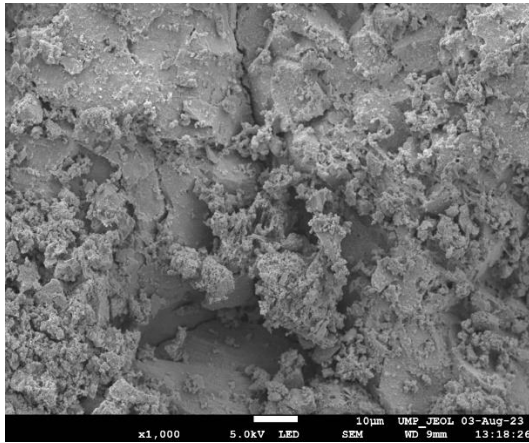
MICROSTRUCTURAL IMAGES OF GROUND CBA10% 28 DAYS



UNIVERSITI MALAYSIA PAHANG
AL

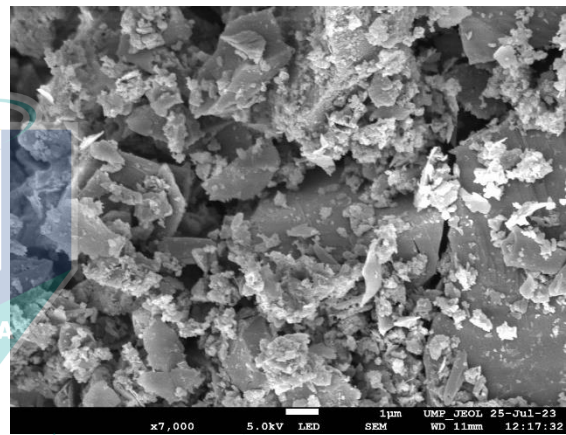
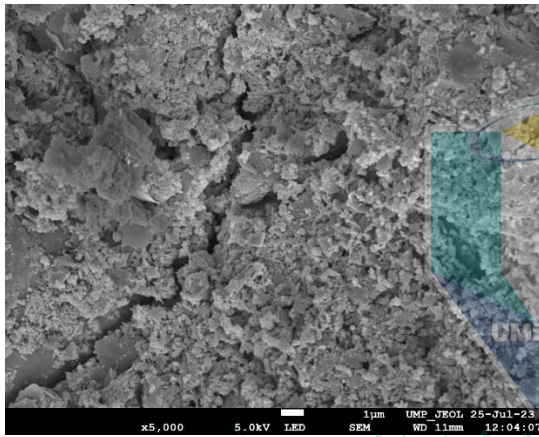
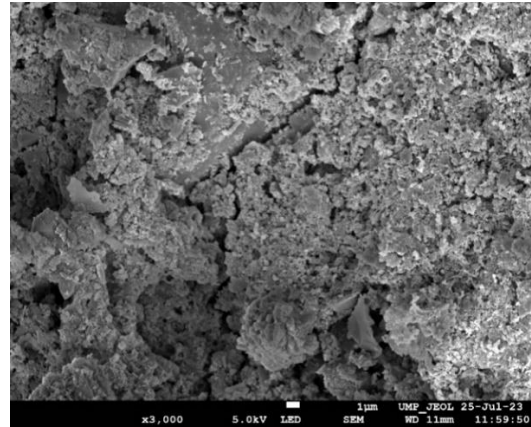
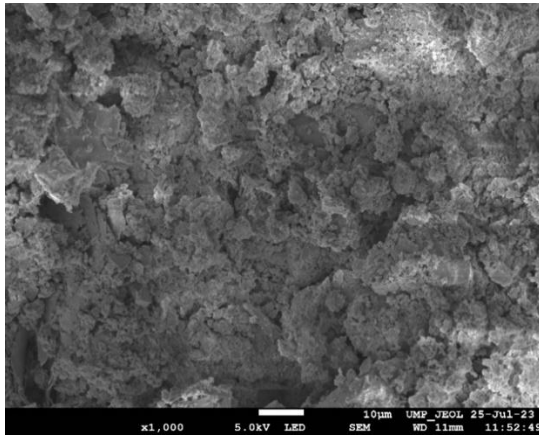


MICROSTRUCTURAL IMAGES OF GROUND CBA10% 56 DAYS

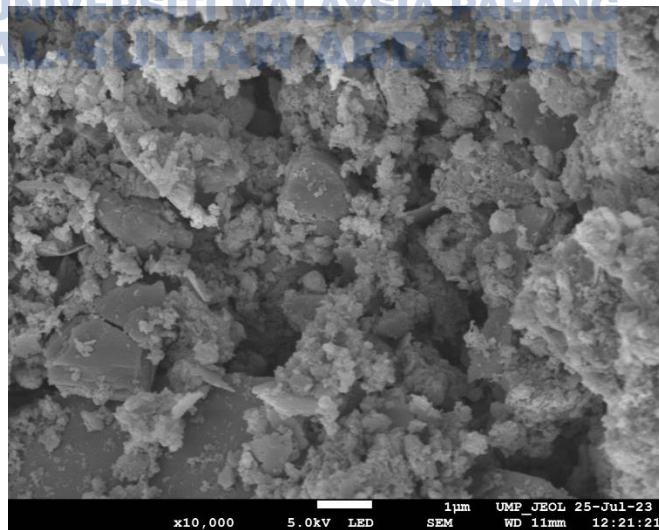


اوپوزميتي مليسيا مع العلم
UNIVERSITI MALAYSIA PAHANG
AL-SULTAN ABDULLAH

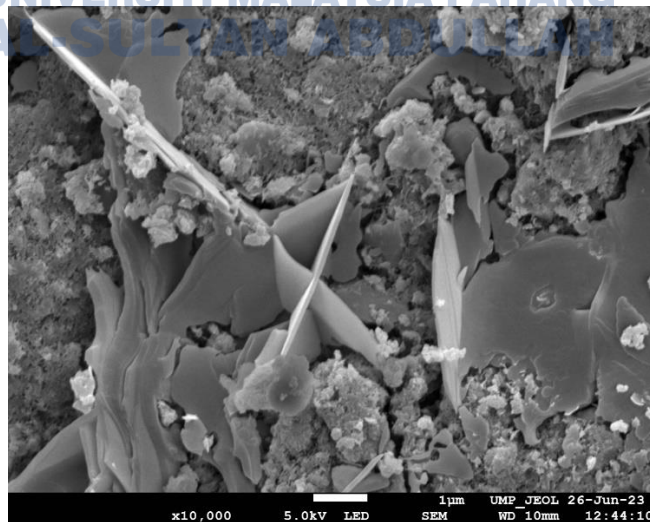
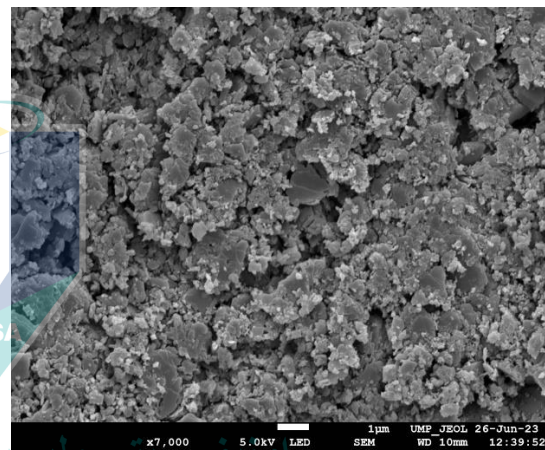
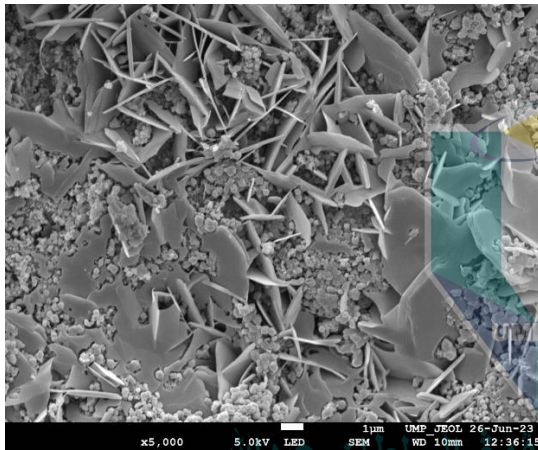
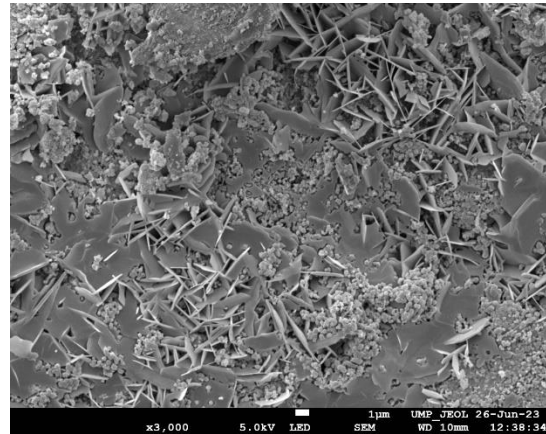
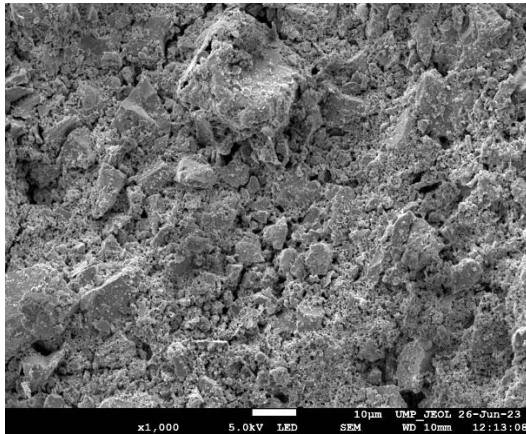
MICROSTRUCTURAL IMAGES OF GROUND CBA20% 7 DAYS



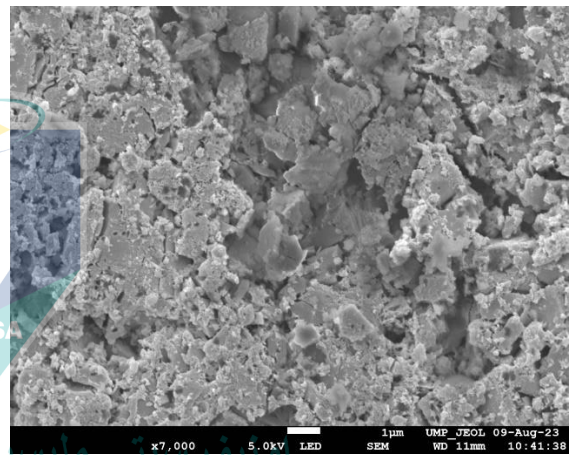
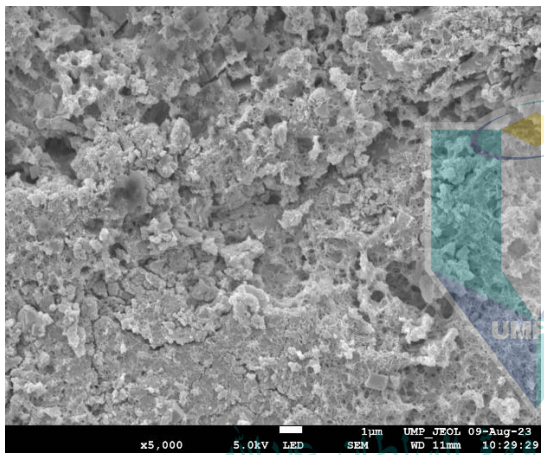
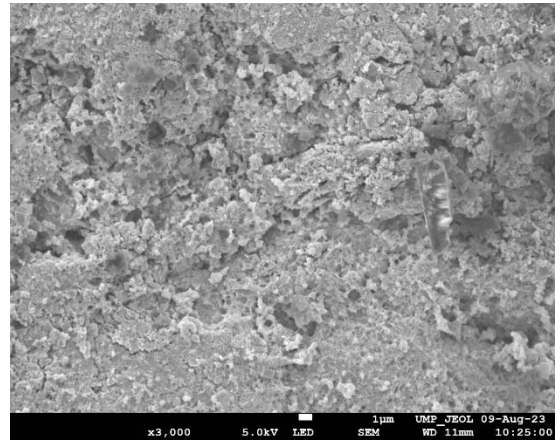
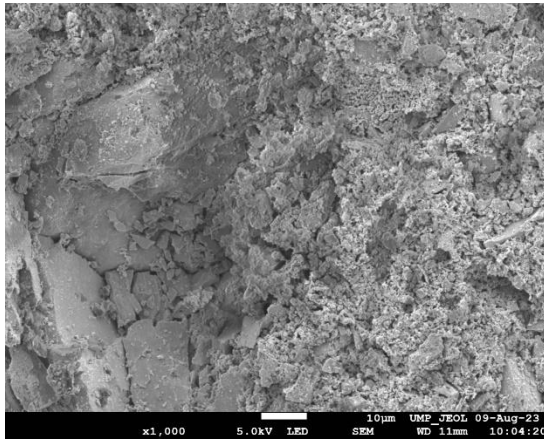
اونیورسیتی ملیسیا فہم السلطان عبداللہ
UNIVERSITI MALAYSIA PAHANG
AL-SULTAN ABDULLAH



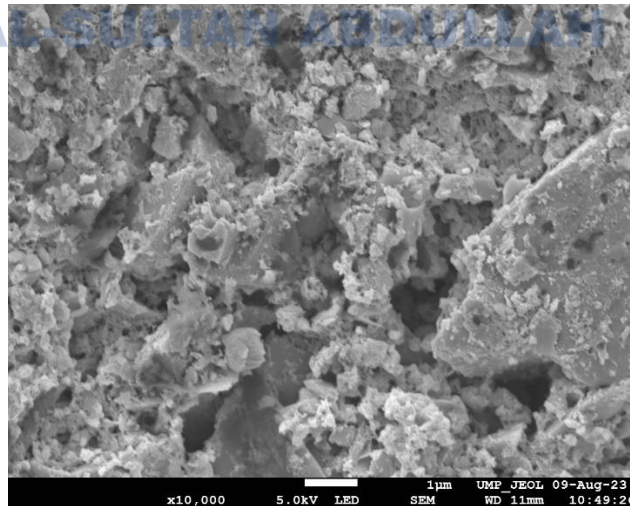
MICROSTRUCTURAL IMAGES OF GROUND CBA20% 28 DAYS



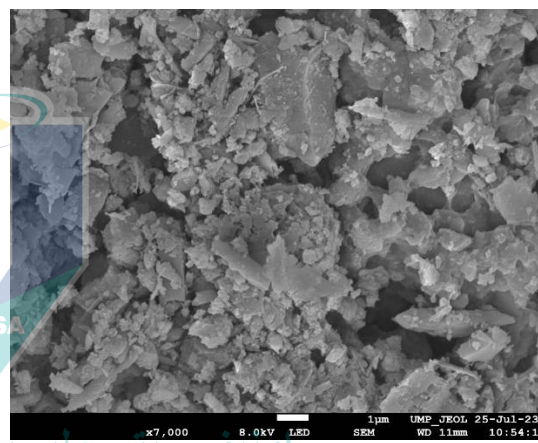
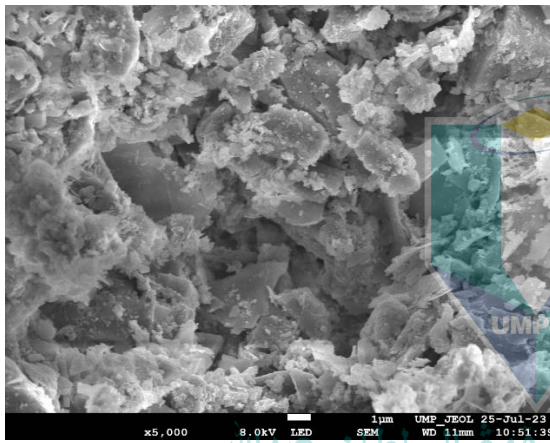
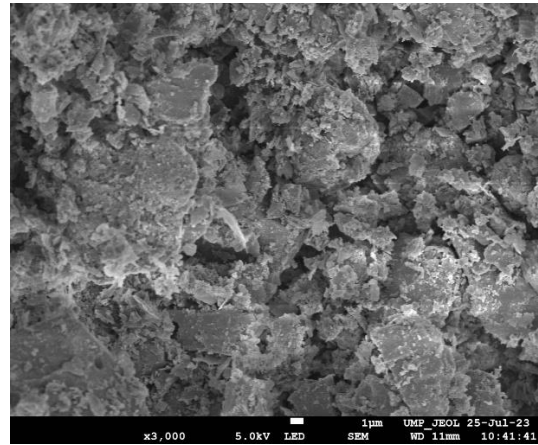
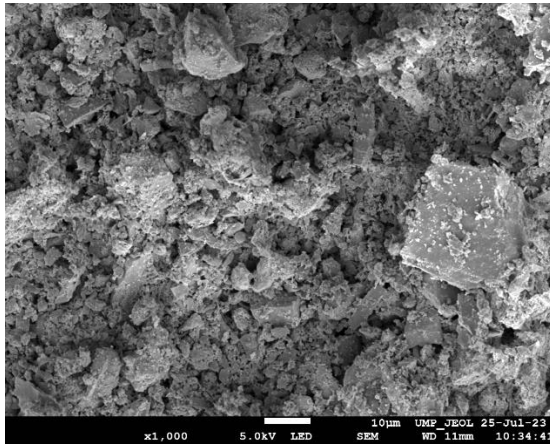
MICROSTRUCTURAL IMAGES OF GROUND CBA20% 56 DAYS



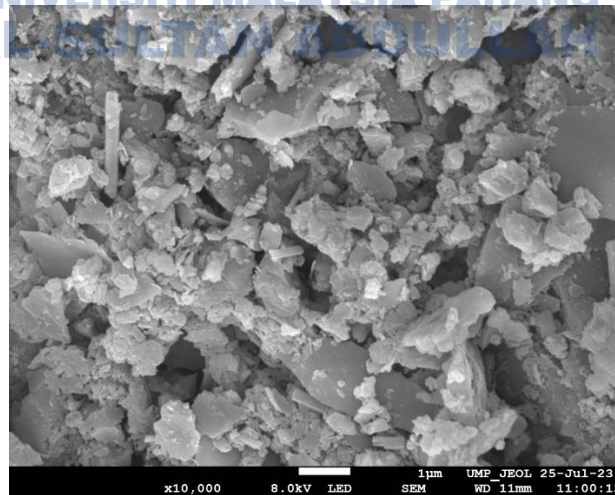
UNIVERSITI MALAYSIA PAHANG
AL-SULTAN ABDULLAH



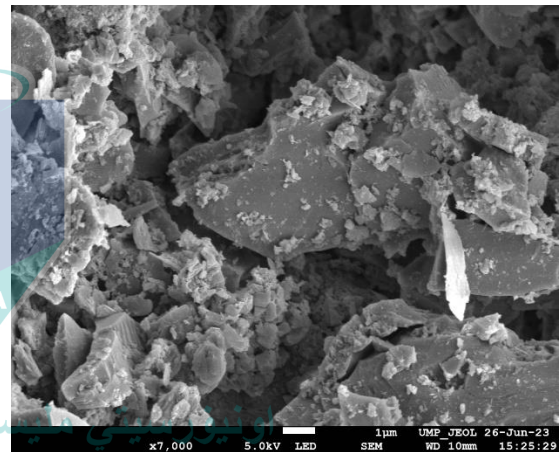
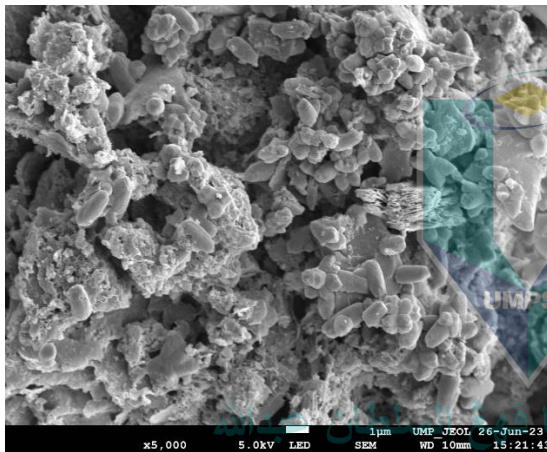
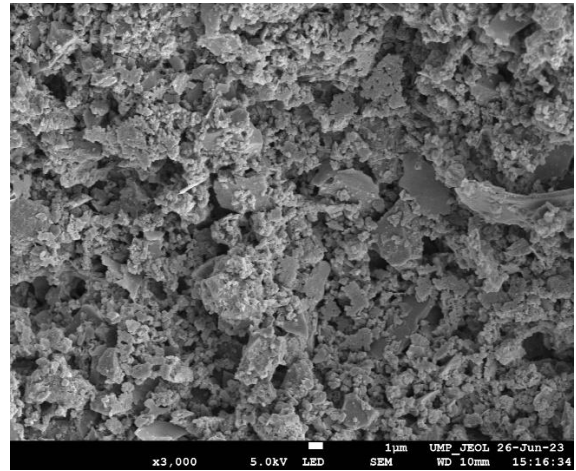
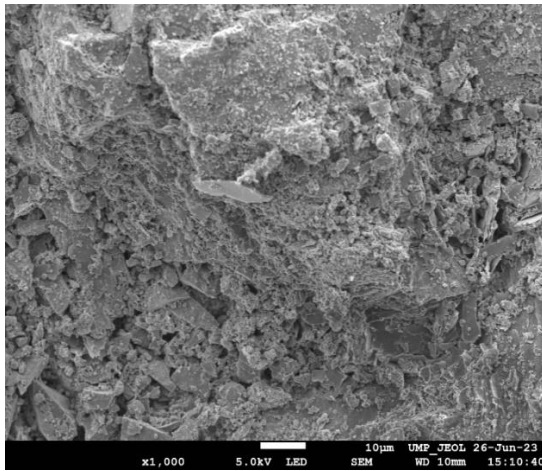
MICROSTRUCTURAL IMAGES OF GROUND CBA50% 7 DAYS



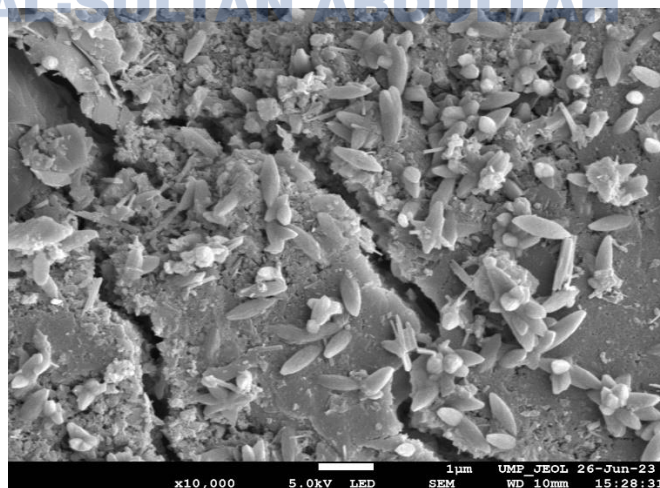
اوتورسيتي مليسيا فتح السلطان عبدالله
UNIVERSITI MALAYSIA PAHANG
AL-SULTAN ABU FUAD



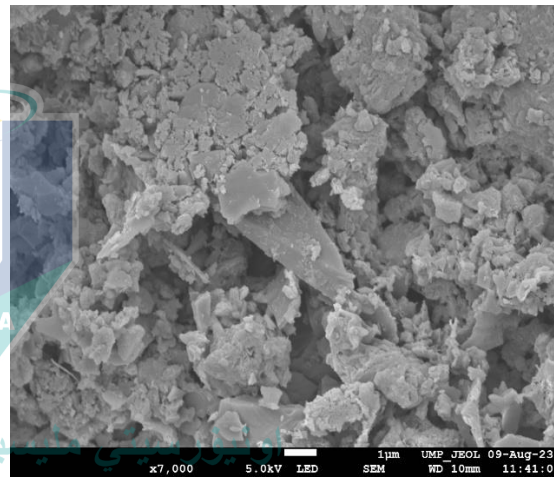
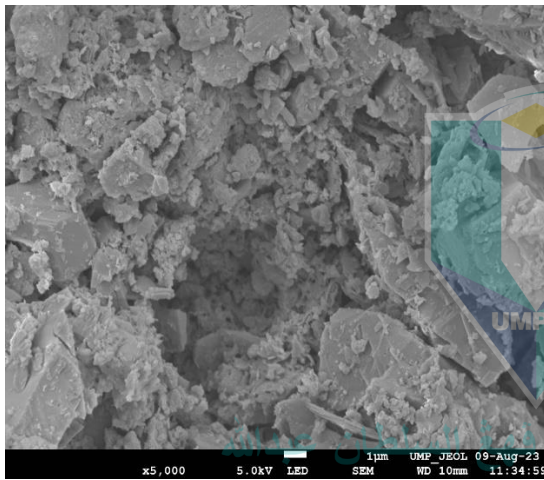
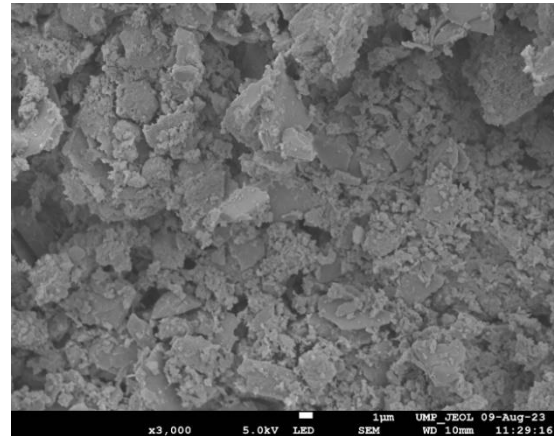
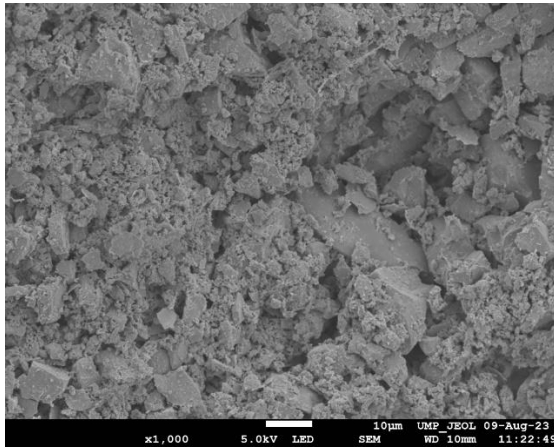
MICROSTRUCTURAL IMAGES OF GROUND CBA50% 28 DAYS



UNIVERSITI MALAYSIA PAHANG
AL-SULTAN ABDULLAH



MICROSTRUCTURAL IMAGES OF GROUND CBA50% 56 DAYS



UNIVERSITI MALAYSIA PAHANG
AL-SULTAN ABDULLAH

